UNIVERSITÀ
DEGLI STUDI
DI BRESCIA

DOTTORATO DI RICERCA IN TECHNOLOGY FOR HEALTH

SSD: ING-INF/04

XXXV CICLO

Automatic Control of General Anesthesia: New Developments and Clinical Experiments

Ph.D. Thesis

Ph.D. Candidate:
Michele Schiavo

Ph.D. Advisor:
Prof. Antonio Visioli
Prof. Nicola Latronico

Academic Year 2021 - 2022

Ai miei genitori.
Grazie per tutto il vostro sostegno e amore.

Abstract

L'anestesia generale è uno stato di coma farmacologicamente indotto, temporaneo e reversibile. Il suo obiettivo consiste nel provocare la perdita totale della coscienza e nel sopprimere la percezione del dolore. Essa costituisce un aspetto fondamentale per la medicina moderna in quanto consente di praticare interventi chirurgici invasivi senza causare ansia e dolore al paziente. Nella pratica clinica dell'anestesia totalmente endovenosa questi effetti vengono generalmente ottenuti mediante la somministrazione simultanea del farmaco ipnotico propofol e del farmaco analgesico remifentanil. Il dosaggio di questi farmaci viene gestito dal medico anestesista basandosi su linee guida farmacologiche e monitorando la risposta clinica del paziente. Recenti sviluppi nelle tecniche di elaborazione dei segnali fisiologici hanno consentito di ottenere degli indicatori quantitativi dello stato anestetico del paziente. Tali indicatori possono essere utilizzati come segnali di retroazione per sistemi di controllo automatico dell'anestesia. Lo sviluppo di questi sistemi ha come obiettivo quello di fornire uno strumento di supporto per l'anestesista.

Il lavoro presentato in questa tesi è stato svolto nell'ambito del progetto di ricerca riguardante il controllo automatico dell'anestesia attivo presso l'Università degli Studi di Brescia. Esso è denominato ACTIVA (Automatic Control of Total IntraVenous Anesthesia) ed è il risultato della collaborazione tra il Gruppo di Ricerca sui Sistemi di Controllo dell'Università degli Studi di Brescia e l'Unità Operativa Anestesia e Rianimazione 2 degli Spedali Civili di Brescia. L'obiettivo del progetto ACTIVA consiste nello sviluppo teorico, nell'implementazione e nella validazione clinica di strategie di controllo innovative per il controllo automatico dell'anestesia totalmente endovenosa. Nel dettaglio, in questa tesi vengono inizialmente presentati i risultati sperimentali ottenuti con strutture di controllo basate sull'algoritmo PID e PID ad eventi per la somministrazione di propofol e remifentanil. Viene poi presentato lo sviluppo teorico e la validazione clinica di strutture di controllo predittivo basate su modello. Successivamente vengono presentati i risultati di uno studio in simulazione riguardante una soluzione di controllo innovativa che consente all'anestesista di regolare esplicitamente il bilanciamento tra propofol e remifentanil. Infine, vengono presentati gli sviluppi teorici ed i relativi studi in simulazione riguardanti soluzioni di controllo personalizzate per le fasi di induzione e mantenimento dell'anestesia.

Abstract

General anesthesia is a state of pharmacologically induced, temporary and reversible coma. Its goal is to cause total loss of consciousness and suppress the perception of pain. It constitutes a fundamental aspect of modern medicine as it allows invasive surgical procedures to be performed without causing anxiety and pain to the patient. In the clinical practice of total intravenous anesthesia, these effects are generally obtained by the simultaneous administration of the hypnotic drug propofol and of the analgesic drug remifentanil. The dosing of these drugs is managed by the anesthesiologist on the basis of pharmacological guidelines and by monitoring the patient's clinical response. Recent developments in physiological signal processing techniques have introduced the possibility to obtain quantitative indicators of the patient's anesthetic state. These indicators can be used as feedback signals for automatic anesthesia control systems. The development of these systems aims to provide a support tool for the anesthesiologist.

The work presented in this thesis has been carried out in the framework of the research project concerning the automatic control anesthesia at the University of Brescia. The project is called ACTIVA (Automatic Control of Total IntraVenous Anesthesia) and is the result of the collaboration between the Research Group on Control Systems of the University of Brescia and the Anesthesia and Intensive Care Unit 2 of the Spedali Civili di Brescia. The objective of the ACTIVA project consists in the theoretical development, implementation, and clinical validation of innovative control strategies for the automatic control of total intravenous anesthesia. In detail, in this thesis the experimental results obtained with control structures based on the PID and on event-based PID controllers for the administration of propofol and remifentanil are initially presented. The theoretical development and clinical validation of model predictive control strategies is then proposed. Next, the results of a simulation study regarding an innovative control solution that allows the anesthesiologist to explicitly adjust the balance between propofol and remifentanil are given. Finally, the theoretical developments and the relative simulation studies concerning personalized control solutions for induction and maintenance phases of anesthesia are explained.

Introduction

In modern clinical practice, the use of technological tools has become part of the standard of care. The introduction of new technologies in medicine is of paramount interest since it allows considerable improvements in the quality of care to be obtained. For example, remarkable results have been obtained with computer-aided diagnostic systems [1], robotic surgery devices [2], robotic rehabilitation systems [3], optimization of pharmacological strategies for cancer therapy [4] and artificial pancreas for the automatic control of insulin delivery [5].
In this framework, closed-loop control of general anesthesia has attracted a considerable research interest in recent years [6, 7]. General anesthesia is a pharmacologically induced, temporary and reversible state that aims to provoke the inhibition of sensitivity, consciousness, and pain. It is a fundamental aspect in modern medicine. Indeed, it allows invasive clinical procedures to be carried out without causing anxiety and pain to the patient and preventing the formation of memory. In the clinical practice of total intravenous anesthesia (TIVA), these effects are obtained by simultaneously administering two drugs, propofol and remifentanil. The first one has a hypnotic effect, while the latter has an analgesic effect. They must be adequately dosed, avoiding over and under dosing that could cause the onset of side effects. Traditionally, the administration of these drugs is manually regulated by the anesthesiologist that decides their dosing depending on many factors such as the type of surgery, the physical characteristics of the patient, recommended infusion patterns and indicators of depth of anesthesia (DoA). These latter, being qualitative, lend themselves to different interpretations that depend on the experience and training of each anesthesiologist. In order to reduce this variability and to assist the anesthesiologists, some measurement devices of the anesthetic status have been introduced. For example, the developments in brain monitoring techniques provided reliable quantitative indexes of the patient hypnotic state. However, the administration of propofol and remifentanil is only a part of the anesthesiologist work that is, in fact, demanding and hence prone to errors due to distraction and fatigue. With the aim of reducing the anesthesiologist workload, the feasibility of automatic control systems for anesthesia has been evaluated by exploiting the aforementioned quantitative indexes of hypnosis as feedback variables. They are not intended to replace the anesthesiologist. Conversely, their goal is to automate the low-level, repetitive task of drug dosing, thus leaving the anesthesiologist free to focus on higher-level clinical tasks and decisions. The availability of monitoring devices for hypnosis has spurred the development of closed-loop control systems for the automatic administration of propofol. Clinical studies have shown the effectiveness of this approach with different control architectures and its benefits with respect to manual control in terms of keeping physiological variables of interest within clinically recommended range, reducing drug consumption and speeding up recovery [8, 9]. Furthermore, these systems can potentially bring numerous other benefits such as the reduction of human errors and the optimization of drug dosing thanks to the continuous monitoring capability offered

by computerized systems. These aspects can contribute to reduce the variability in the quality of care provided to patients, thus promoting the reproducibility and standardization of anesthetic procedures with a significant benefit in the intraoperative and post-operative phase for both medical staff and patients. However, these systems are still research devices and they are not yet commercially available and routinely used in clinical practice. Indeed, they are not fully accepted by clinicians. This is mainly due to the absence of a simple, flexible and complete control system that can be easily understood and used by anesthesiologist in the operating room. Moreover, the automatic regulation of remifentanil is also required to achieve a fully automatic and effective anesthesia control. However, the number of control systems proposals that can automatically administer remifentanil is still limited since reliable indicators of analgesia are not currently available.

The aim of this thesis is to contribute in the development of closed-loop systems for anesthesia that can go beyond the scope of research and that can be used in routine clinical practice. This objective is pursued through theoretical development, implementation and clinical validation of innovative control strategies. For all the control solutions that are developed, particular attention is given to their applicability in the real clinical scenario. To this end, their development must take into account that they has to be intuitive for the anesthesiologist, who operates in any case as supervisor and needs to fully understand the behavior of the controller. In this context, also the implementation of collaborative control strategies that combines the actions of the controller with manual interventions performed by the anesthesiologist plays a key role. Indeed, this allows the behavior of the control system to be better tailored to specific clinical needs by exploiting anesthesiologist's knowledge and expertise.

The thesis is structured as follows. In Chapter 1 the topic of closed-loop anesthesia is introduced. In particular, an overview of general anesthesia and of the tools currently available in the clinical practice is provided. Then, an introduction to the anesthesia control problem is given. In Chapter 2 the state of the art regarding closed-loop control of anesthesia is described. Here the background and the contributions of the thesis are presented. In Chapter 3 the experimental results obtained with a control scheme for propofol and remifentanil coadministration based on proportional-integral-derivative (PID) control are presented. Particular attention is given to the evaluation of the clinical performance of the proposed control solution and to its practical applicability in the operating room. In Chapter 4 the experimental results obtained with an event-based PID controller for propofol and remifentanil coadministration are presented. The aim of this innovative control technique is to mimic the way of operating of the anesthesiologist, who can therefore clearly understand the behavior of the controller and better supervise the system operations. In Chapter 5, model predictive control (MPC) of anesthesia is covered. In particular, an innovative control structure based on the presence of an external predictor is presented. The case of propofol only administration is first considered and the experimental results obtained are presented. Then, the approach is extended to the case of propofol and remifentanil coadministration. Finally, the approach is further extended by introducing the event-based technique. In Chapter 6 a recently proposed open-source patient simulator is used to evaluate the performance of the PID-based and of the event-based PID control schemes when a tuning parameter that regulates the remifentanil/propofol balance is changed. Chapters 7 and 8 focus on the theoretical development of personalized control solutions. In particular, in Chapter 7 a PID tuning methodology that provides a patient individualized selection of the controller parameters is presented. This methodology focuses on the maintenance phase of anesthesia. In Chapter 8 optimization-based strategies that provide a personalized propofol bolus for anesthesia induction are presented.

Contents

CONTENTS

Chapter 1

Introduction to closed-loop anesthesia

This introductory chapter provides the basics to understand the topics covered in this thesis. First, an overview of general anesthesia and of its clinical practice is provided. Then, the tools that are currently available to support the anesthesiologist are reviewed. They include mathematical models, target controlled infusion (TCI) devices and monitoring devices. Finally, closed-loop control of anesthesia is introduced and the control problem is described.

1.1 Overview of general anesthesia

Anesthesia is fundamental in modern medicine as it allows patients to undergo surgical interventions and invasive medical procedures without anxiety, pain and protecting them from physical and psychological traumas. There are three broad categories of anesthesia that differ for depth, duration and part of the body involved:

- *Local/regional anesthesia*: it is obtained by local injection of specific anesthetic drugs (e.g. ropivacaine). These drugs block the transmission of nerve impulses between the targeted body part and the central nervous system, causing loss of sensation in the interested part. With this type of anesthesia the patient remains conscious as it acts only at the level of the peripheral nervous system.
- *Sedation*: it reduces the central nervous system activity to a lesser degree. It reduces anxiety and it inhibits the creation of long-term memories. The brain activity is reduced but the patient is still conscious.
- *General anesthesia*: it is a drug induced loss of consciousness during which patients are not aroused, even by painful stimulation [10]. Thus, it inhibits sensitivity, consciousness and pain. Paralysis can also be induced.

The first two types are suitable for minor and short-termed surgeries. General anesthesia is appropriate for most major surgical procedures which require unconsciousness of the patient, long duration and paralysis. More in detail, general anesthesia provides three main effects on the patient: hypnosis, analgesia and paralysis, as summarized in Figure 1.1. Hypnosis coincides with loss of consciousness, it prevents intra-operative awareness and memorization. Analgesia prevents the patient from perceiving pain by suppressing the physiological responses
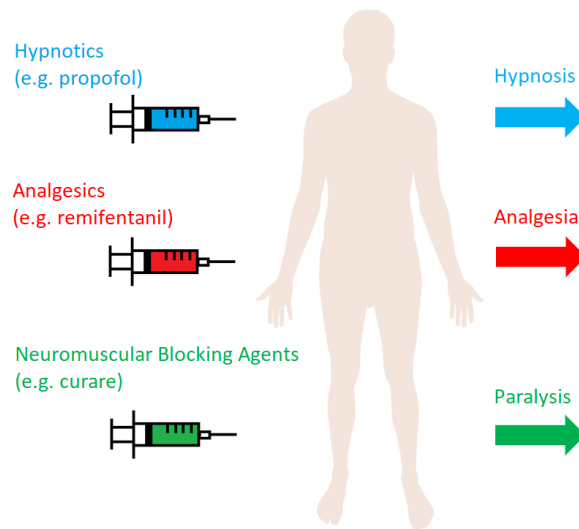
Figure 1.1: *Schematic representation of the drugs administered in TIVA and their clinical effects.*

to nociceptive stimulations. Paralysis prevents the occurrence of involuntary muscle contractions, and it is obtained by blocking the neuromuscular activity. These effects are obtained by means of specific drugs that can be administered by inhalation or by intravenous infusion. This gives rise to two different types of anesthesia: inhalation anesthesia and total intravenous anesthesia (TIVA). The drugs commonly used for inhalation anesthesia are desflurane and sevoflurane. These agents have a combined hypnotic/analgesic effect. Conversely, with TIVA three separate drugs are used to provide the three main effects of anesthesia. The most common drugs are: propofol, remifentanil and rocuronium/atracurium. Propofol is one of the most widely used hypnotic agent because it is potent, it has a fast redistribution and metabolism accounting for rapid onset and short duration of action [11]. It also causes relatively few side effects if properly dosed [12]. Remifentanil is a synthetic opioid with analgesic effects, and it is characterized by a short half-life that minimizes opioid-induced side-effects. The combined use of propofol and remifentanil introduces the problem of the interaction between drugs: there can be an increment or a decrement in the effect of every single drug, strengthening of side effects or the introduction of new ones. In this case, remifentanil increases the effect of propofol as well as its side effects. The study of the interaction between drugs is therefore fundamental to guarantee an adequate level of anesthesia and to properly selecting the dose to administer. Rocuronium and atracurium belongs to the curare drugs which are neuromuscular blocking agents. These drugs act peripherally at the level of the synaptic link between the nerve and the muscle and not centrally in the brain or in the spinal cord. Thus, there is no interaction between curare and hypnotic/analgesic agents.

This thesis focuses on TIVA. Hence, in the rest of this document the term anesthesia always refers to this specific type. The anesthesia procedure is divided into five different phases: premedication, induction, maintenance, emergence and recovery.

- *Premedication*: it consists in the patient's preparation for the surgical procedure. The venous catheter needed for intravenous drugs administration is inserted. Anxiolytic drugs (e.g. midazolam) and/or opioids (e.g. fentanyl) are usually administered in order to increase patient's comfort before entering the operating room. The patient is then

placed on the operating table and all the sensors required for vital signs monitoring are placed like: electrocardiogram electrodes, pulse oximeter sensor, invasive or non-invasive blood pressure sensors and temperature probe. Finally the patient is pre-oxygeneted in order to guarantee an adequate oxygen concentration in the blood before starting anesthesia induction.

- *Induction*: in this phase the patient is driven from consciousness to an anesthetic state suitable for the beginning of the surgical procedure. This is obtained by administering a bolus of propofol in combination with a bolus of fentanyl and/or with an infusion of remifentanil. The administration of analgesic drugs is required in this phase to prevent the patient from feeling pain during airway instrumentation. Indeed, propofol has a respiratory depressant effect and the patients stop breathing autonomously as soon as they lose consciousness. Therefore, mechanical ventilation is required. The instrumentation of the airway can be obtained trough the insertion of a laryngeal mask or an endotracheal tube according to clinical requirements. If the second option is required and intubation is performed a bolus of curare is administered in this phase to suppress reflexes. Anesthesia induction should be fast to preserve the patient from anxiety and to quickly secure patient's airway. The amount of drugs administered in the initial boluses must be adequate in order to provide a fast induction. However, it must not provoke overdosing which can cause hypotension and all the side effects related to it.

- *Maintenance*: it is the phase in which surgery is performed. In this phase it is necessary to maintain an adequate depth of hypnosis (DoH) despite the presence of noxious stimuli related to surgery. The hypnosis and analgesia are maintained by imposing a continuous infusion of propofol and remifentanil by means of specific medical devices called infusion pumps. The infusion rates of these devices are regulated by the anesthesiologist according to alterations of DoH, physiological responses to noxious stimuli, type and phase of surgery to avoid excessively deep or shallow anesthetic states. Boluses of propofol can be administered if the patient shows signs of arousal to avoid awakening. Boluses of propofol and fentanyl can be administered as a preventive measure during phases of strong surgical stimulation. Boluses of curare can be administered in this phase to provide optimal conditions for the surgeon and/or to suppress reflexes. Vasoactive medications (e.g. ephedrine and etilefrine) can be administered in this phase to maintain hemodynamic variables inside recommended ranges.

- *Emergence*: it is the phase in which the patient wakes up. The administration of drugs is stopped during surgical wound medication. The patient usually regains consciousness in 8-10 min. The laryngeal mask or endotracheal tube is removed when the patient starts to breathe autonomously and shows clinical signs of wakefulness.

- *Recovery*: in this phase the patient is moved from the operating room to a recovery room. Here the patient is monitored to assess the stability of vital signs and to check for the onset of side effects such as post-operative nausea and vomiting (PONV), shivering and pain. If necessary, appropriate drugs are administered. After this phase the patient is moved to the ward.

From this description of the anesthesia procedure it is possible to infer that the drug administration task heavily relies on the anesthesiologist ability and experience. Indeed, he or she decides the most appropriate drugs dosing by choosing the sequence and timing of drug boluses and drugs infusion rates. These decisions are based on patient's physical characteristics,

physical status, pathologies, type and phase of surgery. The initial anesthetic plan is based on recommended doses and on anticipated effects given by mathematical models. Then, during the surgery, the anesthetic plan is adjusted on the basis of patient's physiological responses that the anesthesiologist has to continuously monitor. However, the drug dosing task is only a part of the anesthesiologist workload that is, in fact, demanding and hence prone to errors caused by distraction and fatigue. For this reason, in the past years, several tools have been introduced to support the anesthesiologist.

1.2 Tools for general anesthesia

In this section the tools currently available to support the anesthesiologist are described. First the monitoring devices that are commonly used to quantitatively measure the patient's anesthetic state are presented. Then, the mathematical models employed to predict the clinical effect produced by the administration of a certain amount of drug are presented. Finally, Target Controlled Infusion (TCI) system based on the aforementioned models are described.

1.2.1 Monitoring devices for general anesthesia

In the clinical practice, the interpretation of qualitative indicators of DoH is highly subjective and depends on anesthesiologist experience. For this reason in the past decades some quantitative indicators for DoH have been introduced. They are obtained through neuro-monitoring systems that can estimate DoH by analyzing the brain activity through the measurement and elaboration of the electroencephalogram (EEG). The Bispectral Index Scale (BIS, Aspect Medical Systems, Norwood, USA) [13] is one of the most widespread and clinically accepted DoH indicator. Indeed, its clinical efficacy has been widely demonstrated [14, 15, 16, 17, 18, 19]. It is based on the bispectral analysis of a frontal EEG and it provides an estimation of the DoH by means of a dimensionless number which varies from 0 (EEG silence) to 100 (patient fully awake). During anesthesia this index should be kept inside the range from 40 to 60 for most kinds of surgeries [17]. Another indicator of DoH is the NeuroSENSE (WAV_{CNS}) (NeuroWave Systems, Beachwood, USA) [20], that is based on a wavelet decomposition of a frontal EEG. Another index for the DoH is the Patient State index (PSi, Masimo, Irvine, USA). It is based on the analysis of multivariate changes in brain electrical activity [21]. A recently proposed DoH index is the qCON, included in the Conox monitor (Fresenius Kabi, Bad Homburg, DE). The qCON is based on the analysis of EEG spectral ratios and burst suppression (BS) [22].
While for DoH reliable indicators are available and they are routinely used in the clinical practice, the assessment of analgesia is still an open field. Some indicators have been proposed such as ANI [23], NOL [24] and qNOX [22]. In spite of evaluation studies demonstrating their therapeutic significance, these indexes are not fully accepted and routinely used in clinical settings.

1.2.2 Mathematical models for general anesthesia

Pharmacological models describe the relationship between the administration of a certain amount of drug and its clinical effect on the human body. Modern anesthesia relies on these mathematical models to decide how to dose drugs. They can also be exploited in computerized

systems, such as TCI, to perform numerical simulations. In this thesis they are extensively used to design and validate closed-loop control systems for automatic regulation of anesthesia. This thesis is focused on the intravenous administration of propofol and remifentanil and to their desired effect on DoH. A short review of the models used in this work is provided in this section.

All the considered models are Pharmacokinetic/Pharmacodynamic (PK/PD) models with a Wiener structure, i.e., they have a linear part in series with a static nonlinearity as shown in Figure 1.2. The PK describes the dynamic relationship between drug infusion, redistribution and metabolism. The PD describes the relationship between the drug concentration in the blood (plasma concentration) and its clinical effect. It comprises a linear part and a static nonlinearity. The first one describes the relationship between plasma concentration and effect-site concentration. The second one describes the relationship between the drug effect-site concentration and its clinical effect. The linear part of the model is represented with compartmental models. Each compartment represent a group of parts of the human body that have a similar dynamics with respect to drug absorption, redistribution and elimination. Propofol and remifentanil dynamics are well described by a three compartmental PK model plus an effect-site compartment. A schematic representation is shown in Figure 1.3. The overall linear part can be therefore described by the following system of differential equations:

$$\begin{cases} \dot{q}_1(t) = -(k_{10} + k_{12} + k_{13})q_1(t) + k_{21}q_2(t) + k_{31}q_3(t) + u(t) \\ \dot{q}_2(t) = k_{12}q_1(t) - k_{21}q_2(t) \\ \dot{q}_3(t) = k_{13}q_1(t) - k_{31}q_3(t) \\ \dot{C}_e(t) = k_{1e}(q_1(t)/V_1) - k_{e0}C_e(t), \end{cases} \tag{1.1}$$

with:

$$\begin{aligned} k_{10} &= \frac{Cl_1}{60V_1}; \quad k_{12} = \frac{Cl_2}{60V_1}; \; k_{13} = \frac{Cl_3}{60V_1}; \\ k_{21} &= \frac{Cl_2}{60V_2}; \quad k_{31} = \frac{Cl_3}{60V_3}. \end{aligned} \tag{1.2}$$

Here the mass flow of the infused drug is $u(t)$, expressed in mg/s for propofol and in μg/s for remifentanil. The drug masses in the primary, fast and slow compartments are $q_1(t)$, $q_2(t)$ and $q_3(t)$, respectively. They are expressed in mg for propofol and in μg for remifentanil. The drug transfer rates between compartments, expressed in s^{-1}, are k_{12}, k_{13}, k_{21}, k_{31} and k_{1e}. The drug concentration in the effect-site compartment is $C_e(t)$. It is expressed in mg/l for propofol and in μg/l for remifentanil. The drug elimination rate from the primary compartment and from the effect-site compartment, expressed in s^{-1}, are k_{10} and k_{e0}, respectively. The volumes, expressed in l, of the primary, fast and slow compartments are V_1, V_2 and V_3, respectively. The clearances, expressed in l/s, of the primary, fast and slow compartments are Cl_1, Cl_2 and Cl_3, respectively. The plasma concentration represent the drug concentration in the primary compartment and it is calculated as:

$$C_p(t) = \frac{q_1(t)}{V_1}, \tag{1.3}$$

it is expressed in mg/l for propofol and in μg/l for remifentanil.

By defining the state vector as:

$$x(t) = [q_1(t), q_2(t), q_3(t), C_e(t)]^T \in \mathbb{R}^4,$$

the linear system 1.1 can be written in state-space form as:

$$\dot{x}(t) = Ax(t) + Bu(t), \tag{1.4}$$

where:

$$A = \begin{bmatrix} -(k_{10} + k_{12} + k_{13}) & k_{21} & k_{31} & 0 \\ k_{12} & -k_{21} & 0 & 0 \\ k_{13} & 0 & -k_{31} & 0 \\ k_{1e}/V_1 & 0 & 0 & -k_{e0} \end{bmatrix} \in \mathbb{R}^{4\times 4}; \quad B = [1, 0, 0, 0]^T \in \mathbb{R}^4. \tag{1.5}$$

The nonlinear part of the model is a Hill function:

$$y(t) = f(C_e(t)) = E_0 - E_{max} \left(\frac{C_e(t)^\gamma}{C_e(t)^\gamma + C_{e_{50}}^\gamma} \right), \tag{1.6}$$

where $f : \mathbb{R} \to \mathbb{R}$, E_0 is the baseline value of $y(t)$ in the absence of drug, $E_0 - E_{max}$ is the maximum clinical effect on $y(t)$ achievable with drug administration, γ is the maximum steepness of the function, and $C_{e_{50}}$ is the concentration in the effect-site compartment required to reach half of the maximum effect.

Linear PK/PD models for propofol

The Schnider model [25, 26] is among the most widely used PK/PD models for propofol. In the thesis this model is considered since it is widely used in the development of TCI infusion systems (see Section 1.2.3). Moreover, it was successfully exploited to design closed-loop control systems for automatic regulation of propofol anesthesia. This model was developed by collecting blood samples of 24 healthy volunteers with age, weight and height ranging from 26-81 years, 44-123 kg and 155-196 cm, respectively. The model parameters are shown in Table 1.1. Note that the values of some parameters depend on patient's demographic data, which are model covariates. So k_{10}, k_{12} and k_{21} are functions of the patient height, weight, age and gender. In particular $k_{10} = f(weight, height, gender)$, $k_{12} = f(age)$ and $k_{21} = f(age)$.

Linear PK/PD models for remifentanil

In this thesis the Minto [27] PK/PD model for remifentanil is considered. This model was developed by collecting blood samples of 65 healthy volunteers with age, weight and height ranging from 20-85 years, 48-108 kg and 156-192 cm, respectively. The model parameters are shown in Table 1.2. It is worth noting that k_{10}, k_{12}, k_{13} and k_{21} depend on weight, age, height and gender, while k_{31}, k_{e0} and k_{1e} depend on age.
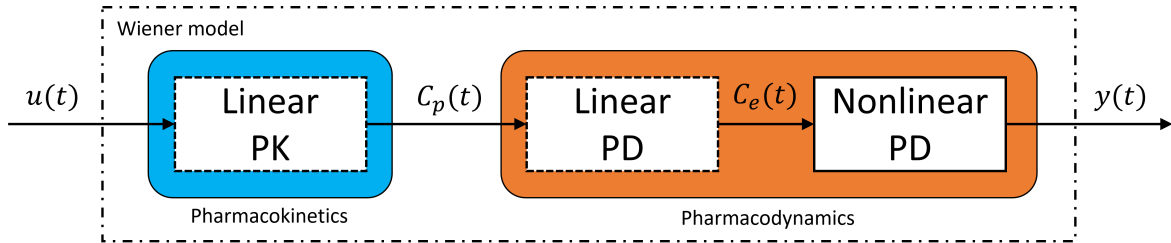
Figure 1.2: *Schematic representation of the Wiener model structure where $u(t)$ is the drug infusion rate, $C_p(t)$ is the plasma concentration, $C_e(t)$ is the effect-site concentration and $y(t)$ is the clinical effect.*
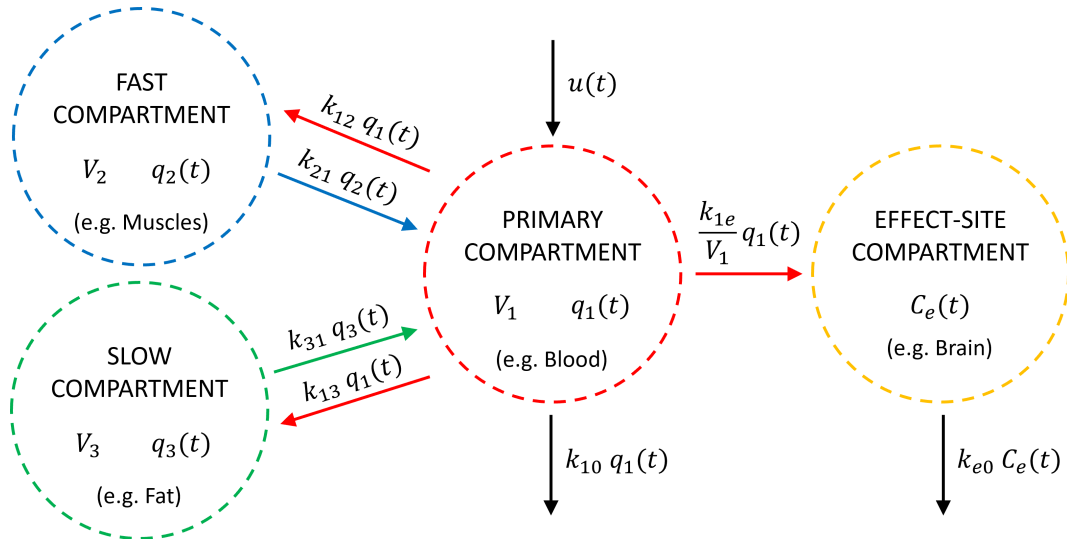
Figure 1.3: *Schematic representation of the linear PK/PD compartmental model where $u(t)$ is the mass flow of the infused drug, $q_1(t)$, $q_2(t)$ and $q_3(t)$ are the drug masses, k_{12}, k_{13}, k_{21}, k_{31} and k_{1e} are the drug transfer rates, $C_e(t)$ is the drug concentration in the effect-site compartment, k_{10} and k_{e0} are the drug elimination rates, V_1, V_2 and V_3 are compartments volumes.*

Parameter	Value
θ_1	4.27
θ_2	18.9
θ_3	238
θ_4	1.89
θ_5	1.29
θ_6	0.836
θ_7	-0.391
θ_8	0.0456
θ_9	-0.0681
θ_{10}	0.0264
θ_{11}	-0.024
LBM $(Males)$	$1.1 * WT - 128 * (WT^2/HT^2)$
LBM $(Females)$	$1.07 * WT - 148 * (WT^2/HT^2)$
V_1 $[l]$	θ_1
V_2 $[l]$	$\theta_2 + \theta_7 * (Age - 53)$
V_3 $[l]$	θ_3
Cl_1 $[l/min]$	$\theta_4 + ((WT - 77) * \theta_8) + ((LBM - 59) * \theta_9) + ((HT - 177) * \theta_{10}))$
Cl_2 $[l/min]$	$\theta_5 + \theta_{11} * (Age - 53)$
Cl_3 $[l/min]$	θ_6
k_{e0} $[1/s]$	$0.456/60$
k_{1e} $[1/s]$	k_{e0}

Table 1.1: *Parameters values of the Schnider PK/PD model for propofol, LBM is the lean body mass, WT is the weight expressed in kg and HT is the height expressed in cm. Age is expressed in years.*

Parameter	Value
LBM $(Males)$	$1.1 * WT - 128 * (WT^2/HT^2)$
LBM $(Females)$	$1.07 * WT - 148 * (WT^2/HT^2)$
V_1 $[l]$	$5.1 - 0.0201 * (Age - 40) + 0.072 * (LBM - 55)$
V_2 $[l]$	$9.82 - 0.0811 * (Age - 40) + 0.108 * (LBM - 55)$
V_3 $[l]$	5.42
Cl_1 $[l/min]$	$2.6 - 0.0162 * (Age - 40) + 0.0191 * (LBM - 55)$
Cl_2 $[l/min]$	$2.05 - 0.0301 * (Age - 40)$
Cl_3 $[l/min]$	$0.076 - 0.00113 * (Age - 40)$
k_{e0} $[1/min]$	$0.0595 - 0.007 * (Age - 40)$
k_{1e} $[1/min]$	k_{e0}

Table 1.2: *Parameters values of the Minto PK/PD model for remifentanil, LBM is the lean body mass, WT is the weight expressed in kg and HT is the height expressed in cm. Age is expressed in years.*

Parameter	E_0	E_{max}	γ	$C_{e_{50}}$ $[mg/l]$
Value	95.9	87.5	2.69	4.92

Table 1.3: *Average parameters values of the Hill function for propofol-BIS relationship proposed in the Vanluchene model.*

Nonlinear PD models for propofol

The relationship between propofol concentration in the effect-site compartment and the DoH, assessed via the BIS, is described by means of the nonlinear Hill function (1.6). The average values of E_0, E_{max}, $C_{e_{50}}$ and γ were identified in the model of Vanluchene [28] and they are shown in Table 1.3. However, the value of E_0 can be assessed for each patient by measuring the baseline value of the BIS before the administration of propofol. With the exception of E_0 the values for the other parameters are not know *a priori*, they do not depend on the patient's demographics and they are subjected to a large variability. Hence, the Hill function is a significant source of uncertainty in the model.

Nonlinear PD models for propofol and remifentanil coadministration

When propofol and remifentanil are coadministered, their linear PK/PD model is not affected. On the contrary, the nonlinear PD model is modified to account for their synergistic effect on the BIS. The following interaction model is considered [28, 29, 30]:

$$BIS(t) = E_0 - E_{max}\left(\frac{\left(\dfrac{U_{prop}(t) + U_{remif}(t)}{U_{50}(\phi)}\right)^{\gamma}}{1 + \left(\dfrac{U_{prop}(t) + U_{remif}(t)}{U_{50}(\phi)}\right)^{\gamma}}\right), \qquad (1.7)$$

where U_{prop} and U_{remif} are the effect-site concentrations of propofol and remifentanil normalized with respect to half of the effect-site concentration required to reach the maximum effect and ϕ is a dimensionless parameter that represents the combination power of propofol and remifentanil:

$$U_{prop}(t) = \frac{C_{e,p}(t)}{C_{e_{50}}}; \quad U_{remif}(t) = \frac{C_{e,r}(t)}{C_{e_{50},r}}; \qquad (1.8)$$

$$\phi = \frac{U_{prop}(t)}{U_{prop}(t) + U_{remif}(t)}, \qquad (1.9)$$

where $C_{e_{50}}$ and $C_{e_{50},r}$ are the $C_{e_{50}}$ values for propofol and remifentanil, respectively, $C_{e,p}(t)$ and $C_{e,r}(t)$ are the effect-site concentrations of propofol and remifentanil, respectively and β describes the synergistic effect of propofol and remifentanil. Finally, $U_{50}(\phi)$ is a term required for the normalization of the drugs combined effect:

$$U_{50}(\phi) = 1 - \beta\phi + \beta\phi^2. \qquad (1.10)$$

The average values of the parameters are shown in Table 1.4. Note that, also in this case, the parameters of the nonlinear interaction model do not depend on the patient's demographics and they are subjected to a large variability. Hence, the nonlinear interaction model for propofol and remifentanil coadministration also represents a significant source of uncertainty.

Parameter	E_0	E_{max}	γ	$C_{e_{50}}$ [mg/l]	$C_{e_{50},r}$ [μg/l]	β
Value	95.9	87.5	2.69	4.92	12.5	1.5

Table 1.4: *Average parameters values of the Hill function for propofol/remifentanil-BIS relationship.*

1.2.3   Target controlled infusion (TCI)

As described in Section 1.1, the goal of anesthetic drugs administration is to achieve and maintain over time a desired clinical effect while minimizing side effects. Traditionally, in TIVA, the anesthesiologist relies on drug dose recommendations and predefined infusion patterns. They are personalized for each patient by scaling them according to patient's weight, that is the only covariate taken into account when determining a dose with these traditional methods. Indeed, the mathematical models presented in Section 1.2.2 are difficult to exploit in the clinical practice because they have intricate mathematical relationships that relates the covariates to drug dose. Hence, for the anesthesiologist it is not straightforward to take them into account when drugs are manually administered. For this reason, computerized systems, known as TCI, were introduced to support the anesthesiologist in drug dosing task [31]. These devices can use the most accurate models available from the literature as they only represent trivial calculations for the computer, thus providing a more precise titration of anesthetics by means of a personalized drug infusion profile [32]. The anesthesiologist gives as reference to the TCI system a desired plasma or effect-site target concentration. The computer determines the necessary dose to reach the desired concentration and drives an infusion pump to deliver it. In particular, by using a PK/PD model of the drug and the patient demographic data, the computer continuously determines the amount of drug in each compartment and how that affects the dose of drug necessary to achieve the desired concentration. Both the induction and maintenance phases of anesthesia can be performed with TCI devices. First, a bolus of drug is administered by the system. Theoretically, this bolus aims to instantly achieve the target concentration. Second, an infusion equal to the elimination rate of the drug is given to maintain the target concentration.
The first commercially available TCI system for propofol administration was the Diprifusor (AstraZeneca, Cambridge, UK) [33]. Then, open TCI systems were introduced, where PK/PD models libraries also for other drugs, like remifentanil, are included. Today, TCI systems are widespread and they are routinely used in the clinical practice [34]. However, it is worth stressing that TCI is an open-loop control architecture and this makes it subject to errors due to unavoidable model uncertainties, thus making manual adjustments necessary. The anesthesiologist needs to provide feedback by adjusting the target concentration based on the observed clinical response that may differ from that foreseen by the model.

1.3   Closed-loop anesthesia

After the introduction of TCI systems, a further step forward in the development of computerized systems for anesthesia consists in closed-loop control systems. The investigation of this kind of systems for TIVA regulation has been stimulated by the introduction of EEG-
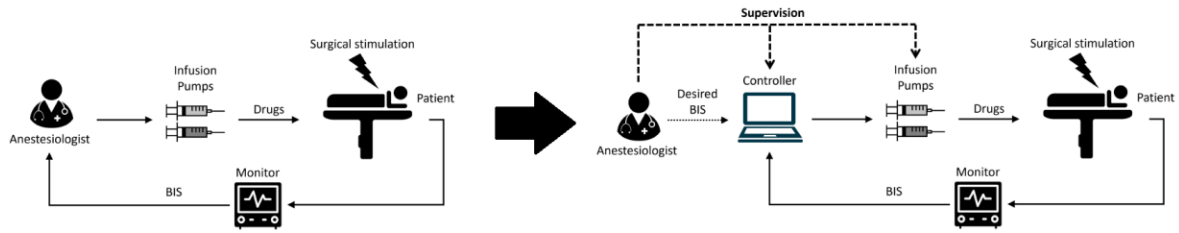
Figure 1.4: *Schematic representation of the transition from manual control to automatic control of anesthesia.*

derived indicators of DoH, such as the BIS, that can be exploited as feedback signals to autonomously regulate drug infusion.

With respect to TCI, closed-loop systems are fully autonomous and, in principle, they do not require any kind of manual intervention. Indeed, the anesthesiologist assumes the role of a system supervisor, as shown in Figure 1.4. As pointed out in Section 1.1, the dosing of anesthetic drugs is only a part of the anesthesiologist workload in the operating room that is demanding and hence prone to errors due to distraction and fatigue. Closed-loop systems have the potential to provide better working conditions for the anesthesiologist and, thus, an improved patient safety. Moreover, since a closed-loop computerized system is not subjected to distraction, fatigue, or emotional reactions in emergency situations, it can provide a standardization in the quality of cares provided to the patients. Moreover, unlike TCI, closed-loop systems do not rely entirely on PK/PD models, which, even if accurate, will always have mismatches. Conversely, they calculate their actions according to the actual state of the patient, assessed through physiological signals measured in real-time. Thus, they provide an additional degree of customization of drug dosing, reducing the risk of overdosing and underdosing. All these aspects can have a positive impact in terms of economic and social costs as they have the potential to reduce the onset of post-operative complications related to anesthesia management, thus improving the quality of patient's recovery and reducing the length of hospitalizations.

Despite the presence of these potential benefits, these systems are still research devices and they are not routinely used in the clinical practice. Indeed, the implementation of this systems is not trivial. For example, their clinical performance strongly depends on the reliability of the signal used as feedback. Moreover, they have to deal with the presence of measurement noise and artifacts, strong nonlinearities, intra- and inter-patient variability and the lack of quantitative measures for analgesia. Their diffusion is also hindered by the mistrust of clinical practitioners. Indeed, it is important for this kind of systems to be safe, intuitive and easy to use. Problems arising from the practical implementation of the control device could also represent a limiting factor.

In this section anesthesia is described from a control system engineering point of view. The control problem is formulated and the control specifications are presented. Finally, a short bibliographic review is proposed. It describes a brief history of closed-loop control systems for anesthesia regulation and the main milestones achieved in their development.

1.3.1 Control problem formulation

A block diagram of a generic closed-loop control system for automatic anesthesia regulation is shown in Figure 1.5. The controlled process is represented by the response of the

patient to drug administration. It represents a particularly challenging process from a control system design point of view. Indeed, as explained in Section 1.2.2, this process is characterized by a strong nonlinear behavior. Moreover, it is subjected to a large variability, that is of two types: intra-patient and inter-patient. The first one represents the fact that the status of a patient, and hence the dynamical behavior, can change throughout a surgical intervention. This can be due, for example, to the concurrent administration of other drugs, to blood losses and to the development of drug tolerance. The second one represents the fact that each patient is different, and hence has a different behavior with respect to drug administration. It is worth stressing that even two patients with exactly the same demographic data can have a completely different reaction to the administration of the same amount of drug. The process is also affected by the dynamics of the infusion pumps. Indeed, they are affected by saturations and slew-rate limitations. Thus, they provide a control action $\overline{u}(t)$ that might differ from the theoretical one $u(t)$. The controlled variables are indicated with $y(t)$. They are measurable physiological variables of interest that are suitable to be used as feedback variables, for example the BIS. They are unavoidably affected by measurement noise $n(t)$ that, if not properly handled, can be detrimental for the performance of the control system. They are also affected by disturbances $d(t)$, that can be caused, for example, by the surgical stimulation. The signal $x(t)$ represents the patient physiological states that are not used as feedback signals but that are nonetheless important and relevant for patient's health. However, they are monitored by the anesthesiologist supervising the system. Basing on that, he/she can decide to intervene by adjusting the set-point values $r(t)$ and/or by carrying out manual interventions $m(t)$ to adjust the drugs infusion rates $u_c(t)$ calculated by the controller.

As described in Section 1.1, anesthesia is essentially a multiple-input-multiple-output (MIMO) control problem as more than one drug must be administered, i.e. propofol and remifentanil, and more than one clinical variable must be controlled, i.e. DoH and analgesia. However, the lack of a reliable quantitative indicator of analgesia hinders the development of MIMO control systems. On the contrary, the wide availability and reliability of DoH monitoring devices allow single-input-single-output (SISO) control systems to be developed. They use an indicator of DoH as feedback variable and the propofol infusion rate as control variable. However, the regulation of remifentanil infusion is fundamental to achieve a fully automated anesthesia control system. To compensate for the lack of feedback variable of analgesia multiple-input-single-output (MISO) control systems, which only exploit a measure of DoH as feedback signal, can be developed. This approach is based on the fact that the DoH variability is correlated with the analgesic coverage in presence of nociceptive stimulation [35, 36]. However, this property cannot be used to control the hypnosis-analgesia balance as it does not provide information on analgesia in the absence of stimulation. This implies that there is a degree of freedom that must be considered in the controller design as the same steady-state value of DoH can be reached with different effect-site concentrations of propofol and remifentanil. This additional degree of freedom is called opioid-hypnotic balance. It must be considered in the design of MISO control systems since different values of this parameter have different clinical effects.

1.3.2 Control specifications

To design anesthesia control systems, the clinical specifications must be translated into appropriate control specifications. In this section the main control specifications are briefly described. Anyway, it is worth noting that they may change depending on patient physical condition, type of surgery and anesthesiologist preferences. There are different control
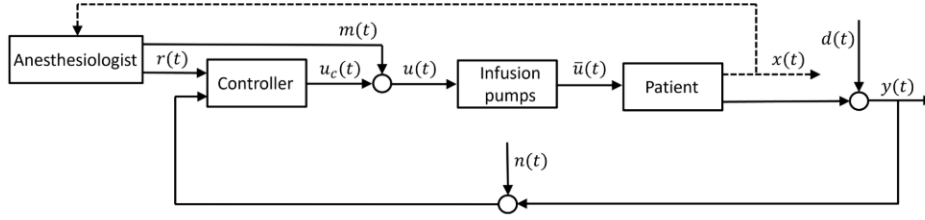
Figure 1.5: *Block diagram of a generic closed-loop system for automatic control of general anesthesia.*

requirements for the induction phase and for the maintenance phase of anesthesia. A fully automated control system for anesthesia regulation should provide satisfactory performance and meet the clinical requirements for both phases. The emergence phase is not relevant for the design of closed-loop systems since it is simply handled by stopping the anesthetic drugs administration. Hence, it depends on patient's own dynamics and not on that of the controller. Anyway, this phase is affected by the quality of control during the induction and maintenance phases as drug overdosing may lead to delayed awakening. From a clinical point of view, during the induction phase it is required that the patient is rapidly brought from wakefulness to an adequate DoH that prevents awareness. Induction should be fast enough to avoid excessive anxiety to the patient and to allow the patient's airway to be safely instrumented. However, a fast induction should not be achieved at the expense of drug overdosing that may lead to excessively low DoH and its related side effects. From a control system design point of view, anesthesia induction can bee seen as a set-point tracking problem, where the DoH must be driven from its initial value to a target value. When the BIS is employed as the feedback variable for DoH, its initial value is close to 100 and the target value is usually 50. In particular, it is required that the BIS drops below 60 since it has been shown that, in general, BIS values below this threshold are associated with a reduced risk of awareness during endotracheal intubation [37]. This should be achieved in less than 5 min while avoiding an excessive BIS undershoot. Values of BIS up to 30 are common in clinical practice and are not considered harmful to the patient health. Conversely, values of BIS below this threshold should be avoided since they are correlated with the onset of BS [38] that has been associated with post-operative delirium [39]. Moreover, it might cause a dangerous hypotension [40]. An adequate analgesic coverage should also be provided during induction to blunt the stimulation related to airway instrumentation. During the maintenance phase, an adequate DoH must be properly maintained despite the presence of surgical stimulation that could provoke an arousal effect on the patient. From a control system design point of view, anesthesia maintenance can be seen as a disturbance rejection control problem where DoH must be maintained at its target value despite the presence of disturbances due to surgical stimulation. The system must rapidly compensate for those disturbances, while avoiding to cause excessive undershoot and overshoot of DoH. When the BIS is employed as the feedback variable for DoH, for most kinds of surgery, it is recommended that it remains as long as possible in the range from 40 to 60 [17]. As it is common in the literature, see e.g., [41, 42], the effect of the surgical stimulation on BIS is modeled as an additive disturbance acting on the BIS signal. In fact, although a nociceptive stimulation affects different vital signs of the patient, this choice represents the worst-case scenario. It is worth noting that different disturbance profiles have been proposed in the literature. The simplest disturbance profile is represented by a double step signal, as shown in Figure 1.6. Although simple, this disturbance profile allows a clear evaluation of

the control performance [42]. More detailed disturbance profiles mimicking the time course of a surgical stimulation profile [43, 44] are shown in Figures 1.7 and 1.8.

As discussed in Section 1.3.1, the BIS is also affected by a significant amount of noise. An example of the noise affecting the BIS signal extracted from real clinical data is shown in Figure 1.9. If not properly handled, the noise can be detrimental for the performance of the control system. For example there can be residual noise in the control action that can provoke mechanical stress to the actuators.

The effect of limitations introduced by the dynamics of the infusion pumps can degrade the performance of control systems [45]. Hence, these limitations should be taken into account during the design phase. One limitation is represented by the saturation on the control action imposed by the minimum and maximum infusion rates of the syringe pumps. For example, the two different models of infusion pumps considered in this work, namely the Graseby 3500 (Smiths Medical, London, UK) and the Alaris GH (Alaris Medical UK Ltd., Basingstoke, Hampshire, UK), can deliver infusion rates that range from 0 ml/h to 1200 ml/h. By expressing the infusion rate of propofol in mg/s and the infusion rate of remifentanil in μg/s it is clear that the lower saturation bound is 0 mg/s for propofol and 0 μg/s for remifentanil. The upper saturation bound depends on the drug dilution. Propofol is commercially available with the dilutions of 10 mg/ml and 20 mg/ml. In the first case the upper saturation bound is:

$$\overline{u}_{p10} = \frac{1200 \text{ ml/h}}{3600 \text{ s/h}} \cdot 10 \text{ mg/ml} = 3.34 \text{ mg/s}, \tag{1.11}$$

while in the second case it is:

$$\overline{u}_{p20} = \frac{1200 \text{ ml/h}}{3600 \text{ s/h}} \cdot 20 \text{ mg/ml} = 6.67 \text{ mg/s}. \tag{1.12}$$

Remifentanil is usually employed with a dilution of 50 μg/ml, hence its upper saturation bound is:

$$\overline{u}_r = \frac{1200 \text{ ml/h}}{3600 \text{ s/h}} \cdot 50 \text{ } \mu\text{g/ml} = 16.67 \text{ } \mu\text{g/s}. \tag{1.13}$$

The dynamic behavior of commercially available infusion pumps is also affected by start-up and update delays which show significant differences between various brands [46, 47].

Another important aspect in the design of this kind of system is represented by the possibility to include manual interventions performed by the anesthesiologist. Indeed, by completely excluding the human intervention from the control loop, the supervision is difficult, since the anesthesiologist cannot adapt the functioning of the system to different clinical situations. This can be perceived as a safety issue thereby precluding the diffusion of such devices in the clinical practice. A step to overcome these limitations consists of collaborative control systems that allow the human operator to intervene (anesthesiologist-in-the-loop) [6]. The first theoretical studies on this kind of systems have been presented in [45, 48], where the effects of both controller and anesthesiologist-in-the-loop for hypnosis regulation have been considered. In these works it is highlighted that, at the current state, automatic systems process only a limited amount of information while the anesthesiologist has a broader view of the overall situation. So, it is important that the anesthesiologist can intervene, for example, with additional drug boluses. Thus, the control system must be adequately tested against such a kind of interventions, in order to demonstrate that they do not lead to instability or, in any case, to a significant degradation of the performance.
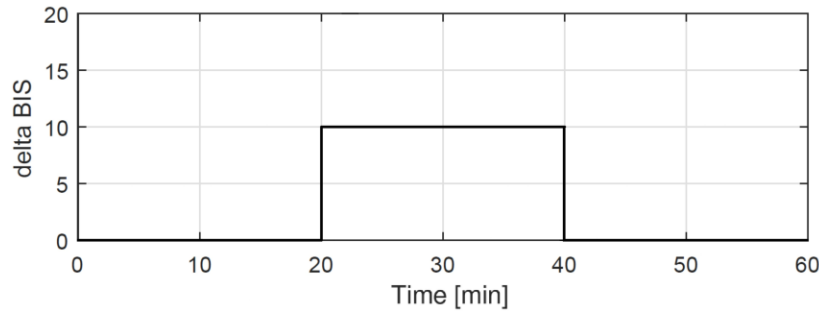
Figure 1.6: *Double step disturbance profile modelling the effect of surgical stimulation.*
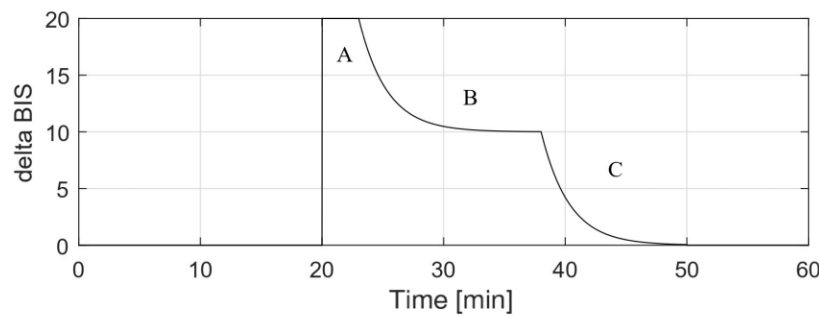
Figure 1.7: *Disturbance profile: (A) arousal due to the first surgical incision; (B) offset slowly decreases but settles at 10% due to continuous normal surgical stimuli; (C) withdrawal of stimuli.*

It is worth noting that, as explained in Section 1.3.1, even if only some physiological variables $y(t)$ are used as feedback signals, other physiological variables $x(t)$ are also important and should be considered in the control system design. To this end, an open-source patient simulator that provides a realistic simulation environment has been recently proposed [49]. It implements both anesthetic and hemodynamic variables and takes into account their interaction. It receives propofol, remifentanil, dopamine, sodium nitroprusside (SNP) and atracurium infusion rates as inputs and gives, as outputs, the BIS, Ramsay Agitation Sedation Score (RASS), the mean arterial pressure (MAP), the cardiac output (CO) and the neuromuscular blockade (NMB), as shown in Figure 1.10. The RASS is used as a surrogate measure of analgesia since a model for more specific indicators is not available yet. Generally, it is recommended to keep the MAP inside the range 65-110 mmHg and the CO inside the range 4-8 l/min. A desirable value for RASS is -5 since it means that the patient is unresponsive to surgical stimulation, while lower values indicates an excessive analgesic dosing.
It is worth stressing that all these specifications must be met for all patients despite the presence of a large intra-patient and inter-patient variability. Hence, controller robustness plays a crucial role.

1.3.3   Performance assessment

A set of performance indexes has been proposed in [41] to theoretically assess the performance of anesthesia control system and verify the fulfilment of the clinical specification. For the induction phase, the indexes are:
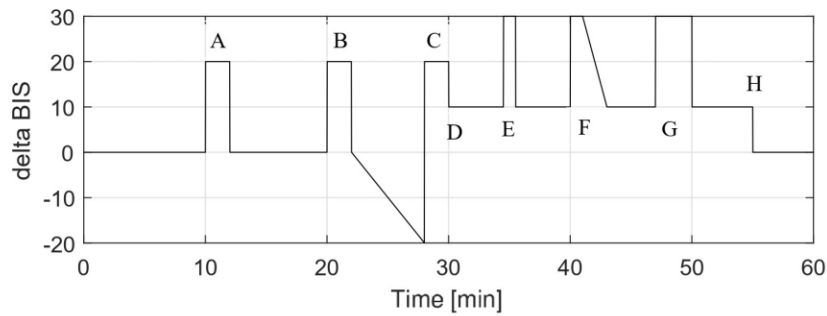
Figure 1.8: *Disturbance profile: (A) intubation; (B) surgical incision followed by no surgical stimulation; (C) abrupt stimulus after a period of low stimulation; (D) onset of a continuous normal surgical stimulation; (E-G) stimulate short-lasting, larger stimuli; (H) withdrawal of stimuli.*
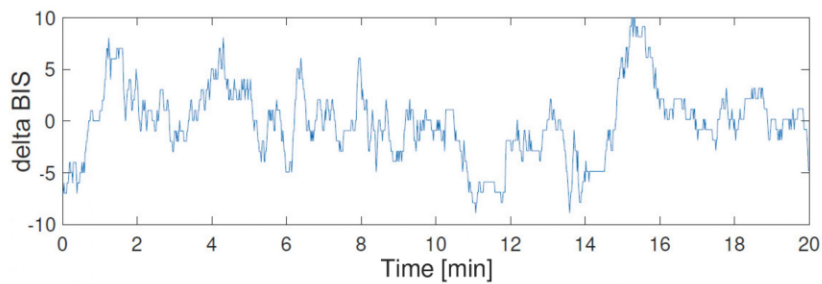
Figure 1.9: *Realistic noise profile extracted from a BIS recording.*
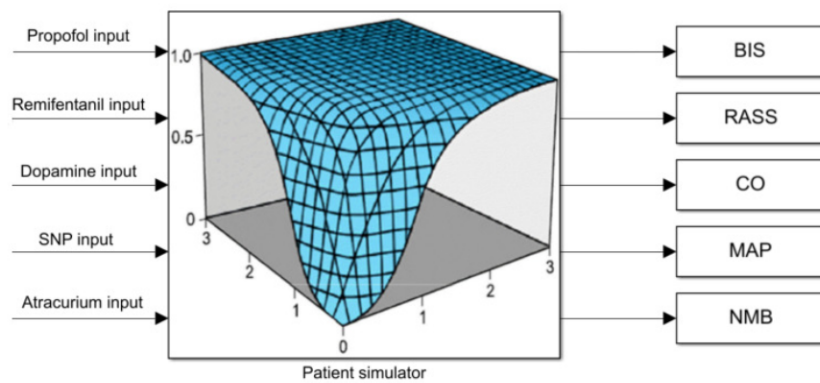
Figure 1.10: *Schematic representation of the open source patient simulator. This figure has been adapted from [49].*

- TT: is the time-to-target, hence the time required for the BIS to reach the value of 55 for the first time;
- ST10: is the settling time at 10%, hence the time required for the BIS to enter and remain between the range from 45 to 55;
- ST20: is the settling time at 20%, hence the time required for the BIS to enter and remain between the range from 40 to 60;
- BIS-NADIR: is the lowest BIS value observed.

Regarding the maintenance phase, the indexes refers to the response obtained when the double step disturbance profile is applied. In this case, only the TT and the $BIS\text{-}NADIR$ indexes are meaningful:

- TT: is the observed time-to-target, which is the time taken by the controller to bring the BIS back in the range from 45 to 55 after the disturbance occurred. This is calculated separately for the positive and for the negative disturbance step, and it is referred to as TTp and TTn, respectively.
- BIS-NADIRp: is the lowest BIS value caused by the controller as a consequence of the disturbance rejection (undershoot).
- BIS-NADIRn: is the highest BIS value after the disturbance ends (overshoot).

To assess the overall control effort the total variation (TV) and the integrated absolute value of the control action (IAU) is used. The first one is defined as:

$$TV = \sum_{k=0}^{\infty} |u_k - u_{k-1}|, \tag{1.14}$$

where u_k is the control action value at time instant k and u_{k-1} is that at time instant $k-1$. The second one is defined as:

$$IAU = \int |u(t)|dt. \tag{1.15}$$

A set of indexes has been presented in [50] to assess the performance of control systems for anesthesia employed in clinical trials. The performance indexes are defined as:

- PE: is the performance error, calculated for each sample j according to the formula

$$PE_j = \frac{BIS_j(t) - \overline{BIS}}{\overline{BIS}} \cdot 100 \quad j = 1, ..., N, \tag{1.16}$$

  where $\overline{BIS}$ is the reference BIS value and BIS is the measured one;
- $MDPE$: is the median performance error, which is a measure of bias and describes whether the measured values are systematically distributed either above or below the BIS reference. It is calculated as:

$$MDPE = Median\{PE_j, \quad j = 1, ..., N\}, \tag{1.17}$$

  where j is the measured sample and N is the number of PE values;
- $MDAPE$: is the median absolute performance error, which reflects the inaccuracy of the control method; it is defined as

$$MDAPE = Median\{|PE_j|, \quad j = 1, ..., N\}, \tag{1.18}$$

- $WOBBLE$, which is an index of time-related changes in the performance and measures the intra-patient variability in performance errors as:

$$WOBBLE = Median|PE_j - MDPE| \quad j = 1, ..., N. \tag{1.19}$$

Other performance indexes useful to evaluate the clinical performance of anesthesia control systems are:

- Induction time: is defined as the time interval between the beginning of infusions and the time when the BIS enters the range from 40 to 60 and remains there for the subsequent 30 s.
- Lowest BIS: is the smallest BIS value observed within the 60 s after the induction time.
- Induction doses: are the anesthetic drug doses administered throughout the induction time.
- Maintenance duration: is the period of time from the end of induction to the time instant at which the automatic control is turned off at the conclusion of surgery.
- BIS 40-60: is the time percentage of BIS inside the range from 40 to 60. The percentage is expressed with respect to the maintenance duration.
- BIS<40: is the time percentage of BIS below 40. The percentage is expressed with respect to the maintenance duration.
- BIS>60: is the time percentage of BIS above 60. The percentages are expressed with respect to the maintenance duration.
- Average drugs infusion rates: indicate the average infusion rates of anesthetics provided within the maintenance duration.
- T awakening: is the time-to-extubation. It is defined as the time that elapses between the end of automatic control and the removal of the endotracheal tube or the laryngeal mask. It has been chosen as an indicator of anesthesia emergence since it is the time that the patient takes to regain the ability to breathe autonomously and to understand the verbal command to open the mouth.

Chapter 2

State of the art

In this chapter the state of the art regarding closed-loop control of anesthesia is described. First, a brief history of the development of these systems is provided. Then, the contribution given by the University of Brescia in the field of closed-loop anesthesia is reviewed. Finally, the contribution that this thesis aims to provide is presented.

2.1 Literature review

Closed-loop control of general anesthesia is a research field that has been widely investigated in the past years [6, 7]. The first attempt dates back in 1950, when an EEG-based automatic regulation of inhalation anesthesia was proposed [51]. Another relevant work based on the automatic regulation of halotane end-tidal concentration was proposed in the middle 1980s [52]. The first work on automatic regulation of propofol infusion guided by the EEG signal was proposed at the end of the 1980s [53] after this drug was approved for clinical use in 1986. Then, from the late 1990s onward the number of proposed closed-loop systems for TIVA increased thanks to the introduction of BIS and WAV_{CNS} monitoring. At first, SISO control solutions that use the BIS as feedback variable and propofol infusion as control variable were proposed. Theoretical solutions and in-silico studies based on proportional-integral-derivative (PID) control [43, 54], μ-synthesis [44], fractional control [43], adaptive bayesian control [55], model predictive control (MPC) [41] and reinforcement learning control [56, 57] were proposed. Experimental results have shown the effectiveness of the SISO approach with different control architectures such as PID control [58, 59, 60, 61, 62, 63], model-based control [64], adaptive bayesian control [65], rule-based control [66], MPC [67, 68], reinforcement learning control [69] and fuzzy control [70, 71]. To obtain an effective control of anesthesia, clinical studies have also pointed out the importance of regulating the infusion of remifentanil [62]. A possible step toward this goal consists in developing MIMO control structures that exploit as feedback signals a measure of DoH to regulate propofol infusion and a measure of analgesia to regulate remifentanil infusion. However, due to the lack of reliable analgesia indexes, closed-loop control of remifentanil has not been widely investigated yet. Some attempts have been made by using non-validated indicators of analgesia. In an in-silico study, an EMG-based surrogate variable has been used in a MPC framework to regulate remifentanil together with BIS that is used to regulate propofol [72]. Experimental results with fuzzy logic control [73] and rule-based control [74, 75] have been performed. In these works the Analgoscore [76], which is an index derived from heart rate (HR) and blood pressure (BP), have been exploited

as feedback variable for remifentanil regulation, while BIS has been exploited for propofol regulation. In [77] experimental results have been obtained by exploiting the PSi and the Analgoscore to regulate propofol and remifentanil, respectively. Although significant results have been obtained, their application is still limited. Indeed, the perceived unsuitability of the currently available analgesia estimations has fostered the investigation of MISO control structures that only exploit a measure of DoH as feedback signal. As pointed out in Section 1.3.1, these structures must deal with the opioid-hypnotic balance issue. The solutions proposed in literature to constrain this additional degree of freedom are based on clinical considerations that are, then, included in the control system design. Therefore, MISO solutions are often preferred over MIMO ones by the clinical practitioners as they often prefer to rely on well-known clinical considerations rather than relying on non-validated indicators of analgesia. For example, simulation results have been presented in [78], where fixed weights in the cost function of a MISO-MPC controller are used to balance the infusions of propofol and remifentanil. In [79] a SISO-MPC has been proposed and a set of *if-then* rules is used to balance the dose of remifentanil according to the dose of propofol. In [80] a mid-ranging controller that exploits the different metabolization times of propofol and remifentanil has been presented. In [81, 82] a positive control strategy has been proposed. Here, the desired proportion between the administered amounts of propofol and remifentanil can be changed during surgery according to clinical criteria without affecting controller performance. Noteworthy clinical results have also been obtained. In [83] a PID-like rule-based controller for the coadministration of propofol and remifentanil has been applied to a population of 83 patients for both the anesthesia induction and maintenance phases. The controller determines the target effect-site concentrations for both drugs that are then given as inputs to two TCI systems. In particular, during the induction phase, the anesthesiologist selects the initial target concentration of propofol, and the controller regulates the target concentration of remifentanil through a predefined set of rules. During the maintenance phase, for small control errors, only the target concentration of remifentanil is updated, while for larger control errors, the values the target concentrations of both drugs are updated. In addition, if the target concentration of remifentanil is increased for more than three consecutive times, then also the propofol target concentration is increased. The system also considers the different metabolization times of the two drugs, hence the minimum interval between two consecutive updates of the target concentration is different for each drug, and it is set equal to the time-to-peak effect. As a consequence, variations of the infusion of remifentanil are more frequent. In this approach, the opioid-hypnotic balance is implicitly managed by the rule-based controller, and the system does not allow the anesthesiologist to explicitly select it. Conversely, the opioid-hypnotic balance is explicitly handled by the anesthesiologist in [84], where a control system based on the habituating control framework for the coadministration of propofol and remifentanil has been tested on a population of 80 patients for both the anesthesia induction and maintenance phases. The infusion of propofol is regulated by a PID controller based on the measured DoH. The infusion of remifentanil is regulated by a specifically designed controller in order to reject disturbances that act on the DoH and to maintain the desired baseline effect-site concentration of remifentanil in absence of stimulation. The anesthesiologist can control the opioid-hypnotic balance by adjusting the baseline effect-site concentration of remifentanil. The mid-raging controller has been tested in [85] on a population of 72 patients. The obtained results show that the MISO control scheme can improve the performance of a SISO control scheme in the same clinical setting, thus highlighting the importance of automatic control of remifentanil.

A great number of studies have demonstrated the feasibility and safety of closed-loop control of anesthesia and randomized controlled trials comparing it to traditional manual control have been performed in a variety of clinically relevant scenarios. They demonstrate the benefits of automatic control in terms of keeping physical variables of interest within clinically recommended ranges, lowering drug dosage, and speeding up recovery [8, 9]. Despite these promising results, automatic control systems are far from having a significant impact on clinical practice and their use is mainly limited to the research community. This is partly due to the lack of cooperation between engineers, clinicians and medical device manufacturers. This hinders the development of simple and complete implementations of automatic controllers for anesthesia that can be easily understood and used by the anesthesiologists. In this context, one of the factors limiting their diffusion is that they are often designed by completely excluding the human intervention from the control loop. This makes their supervision difficult, since the anesthesiologist cannot adapt the functioning of the system to different clinical situations. This can be perceived as a safety issue thereby precluding the diffusion of such devices in the clinical practice. A step to overcome these limitations consists of collaborative control systems that allow the human operator to intervene (anesthesiologist-in-the-loop) [6]. The first theoretical studies on this kind of systems have been presented in [45, 48], where the effects of both controller and anesthesiologist-in-the-loop for hypnosis regulation have been considered. In these works it is highlighted that, at the current state, automatic systems process only a limited amount of information while the anesthesiologist has a broader view of the overall situation. So, it is important that the anesthesiologist can intervene, for example, with additional drug boluses. Thus, the control system must be adequately tested against such a kind of interventions, in order to demonstrate that they do not lead to instability or, in any case, to a significant performance degradation. Problems arising from the practical implementation of the control device could also represent a limiting factor. For example, in [45] the effect of limitations introduced by the dynamics of the infusion pumps is considered. It is shown that this aspect can degrade the performance of the control system and that these limitations should be taken into account during the design phase. The dynamic behavior of commercially available infusion pumps is indeed affected by start-up and update delays which show significant differences between various brands [46, 47]. Solving the aforementioned implementation issues and increasing acceptance by the medical staff are of fundamental importance to spur the diffusion of closed-loop systems in clinical anesthesia.

Another limitation consists in the fact that, usually, closed-loop controllers focus only on the regulation of an indicator of DoH without taking into account the effect on other important clinical variables. However, recently, the combined control of DoH and hemodynamic variables have been considered in in-silico simulations [49, 57, 86, 87] and in clinical experiments [88, 89].

2.2 Thesis background

In this section is given a brief overview of the works that constitute the background of this thesis. They are the results of the research on closed-loop control of anesthesia performed at the University of Brescia in the past years. The research activity focused on the development of SISO and MISO control structures for the automatic regulation of the BIS by controlling propofol and remifentanil infusion rates. In this framework, novel optimization-based techniques for control system design were proposed and event-based control was applied for the

first time for the anesthesia control problem.

2.2.1 The optimization-based approach

The optimization-based design approach will be widely employed in this thesis to tune the parameters of closed-loop control systems. It consists of three phases, as shown in Figure 2.1. The first phase consists in the control structure design. Hence, in the definition of the overall control scheme configuration. The second phase consists in the optimization-based tuning of the control system design parameters. It is performed by numerically solving a min-max optimization problem, in which the optimization function is properly selected to guarantee the fulfillment of the control specifications. In particular, robustness to variability is taken into account by solving the optimization problem on a tuning dataset of thirteen patients that is representative for a wide population. When only propofol is considered, the dataset proposed in [41], and shown in Table 2.1, is used. When also remifentanil is considered, the tuning dataset is enriched by adding the parameters for the remifentanil model that have been randomly generated by using the statistical distributions presented in [30]. The extended tuning dataset is shown in Table 2.2. It is worth noting that, for both datasets, the thirteenth patients is an average patient whose parameters are obtained by calculating the algebraic mean of the parameters of the other twelve patients. To solve the optimization problem, evolutionary algorithms such as genetic algorithms (GA) [90] or particle swarm optimization (PSO) [91] methods are employed. The cost function to be minimized is selected as the worst-case integrated absolute error (IAE) as it has been proved to be an effective performance index for process control. It is defined as:

$$IAE = \int_0^\infty |e(t)|dt, \tag{2.1}$$

where $e(t)$ is the control error, defined as the difference between the controlled variable $y(t)$ and the reference signal $r(t)$. In the context of this thesis $y(t)$ is the patient's BIS and $r(t)$ is the target BIS value. The IAE is evaluated by performing a numerical simulation of the response to drug infusion by exploiting the models presented in Section 1.2.2. For this reason the IAE can not be calculated up to ∞ as in the formal definition. Indeed, it is calculated up to a simulation time that must be properly selected. By defining the vector of the controller parameters as θ, the optimization problem can be formalized as:

$$\min_{\theta} \max_{k \in \{1,...,13\}} \text{IAE}_k, \tag{2.2}$$

where the index k represents each patient of the tuning dataset.
Finally, in the third phase, the robustness of the developed control systems, with the obtained optimal parameters, is verified via a Monte Carlo method by randomly generating a large number of PK/PD models that constitute a testing dataset. To evaluate the robustness with respect to intra-patient variability, for each of the 13 patients of the tuning dataset, a set of 500 perturbed models (thus 6500 models overall) is created, as:

$$\widetilde{P}_i \sim \mathcal{N}(P, \Omega), \tag{2.3}$$

where $\widetilde{P}_i = [\widetilde{V}_{1_i}, \widetilde{V}_{2_i}, \widetilde{V}_{3_i}, \widetilde{Cl}_{1_i}, \widetilde{Cl}_{2_i}, \widetilde{Cl}_{3_i}]^T$ is the ith set of perturbed model parameters drawn from the multivariate normal distribution $\mathcal{N}$. The vector $P = [V_1, V_2, V_3, Cl_1, Cl_2, Cl_3]^T$ con-
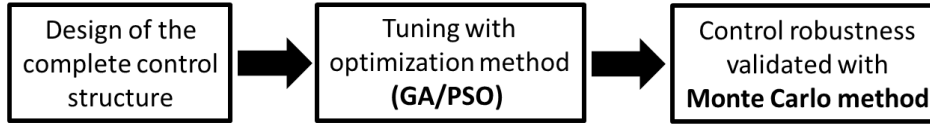
Figure 2.1: *Main phases of the optimization-based approach for control systems design.*

Id	Age	H [cm]	W [kg]	G	$C_{e_{50}}$	γ	E_0	E_{max}
1	40	163	54	F	6.33	2.24	98.8	94.10
2	36	163	50	F	6.76	4.29	98.6	86.00
3	28	164	52	F	8.44	4.10	91.2	80.70
4	50	163	83	F	6.44	2.18	95.9	102.00
5	28	164	60	M	4.93	2.46	94.7	85.30
6	43	163	59	F	12.00	2.42	90.2	147.00
7	37	187	75	M	8.02	2.10	92.0	104.00
8	38	174	80	F	6.56	4.12	95.5	76.40
9	41	170	70	F	6.15	6.89	89.2	63.80
10	37	167	58	F	13.70	1.65	83.1	151.00
11	42	179	78	M	4.82	1.85	91.8	77.90
12	34	172	58	F	4.95	1.84	96.2	90.80
13	38	169	65	F	7.42	3.00	93.1	96.58

Table 2.1: *Demographic data of the patients constituting the tuning dataset for propofol administration (H: heigth, W: weigth, G: gender).*

tains the typical values for each model parameter, that are calculated as shown in Table 1.1 for propofol and in Table 1.2 for remifentanil. The covariance matrix $\Omega = diag(\eta_1, \eta_2, \eta_3, \eta_4, \eta_5, \eta_6)$ contains the random variables that describe the parameters variability. Their values are taken from [25] for propofol and from [27] for remifentanil. The performance is then evaluated in simulation for each perturbed model. To evaluate the robustness with respect to inter-patient variability, another Monte Carlo method is performed. Here, 500 patients are generated by randomly selecting gender, by considering a uniform distribution of age between 20 years and 70 years, of the body mass index (BMI) between 18.5 kg/m^2 and 29.9 kg/m^2, and of the height between 165 cm and 190 cm for males and between 150 cm and 175 cm for females. For each generated patient, the weight has been calculated according to the selected height and BMI to consider only reasonable height and weight combinations. The parameters of the Hill function are also generated by considering the statistical properties of the model considered. In particular, as regards the Hill function parameters related to propofol only administration the perturbed set is obtained from distribution 2.3 with $\widetilde{P}_i = [\widetilde{C}_{e_{50_i}}, \widetilde{\gamma}_i, \widetilde{E}_{0_i}, \widetilde{E}_{max_i}]^T$, $P = [C_{e_{50}}, \gamma, E_0, E_{max}]^T$ that are shown in Table 1.3, while the values of the covariance matrix Ω are taken from [28]. As regards the parameters related to propofol and remifentanil coadministration, which are shown in Table 1.4, the perturbed set is obtained by considering a uniform distribution of $C_{e_{50},r}$ from 7.1 μg/l to 16.7 μg/l and of β from 0.8 to 2.

2.2.2   Proposed control solutions

In this section an overview of the PID-based control schemes that have been developed at University of Brescia in the past years is presented.

Id	Age	H [cm]	W [kg]	G	$C_{e_{50},p}$	$C_{e_{50},r}$	γ	β	E_0	E_{max}
1	40	163	54	F	6.33	12.5	2.24	2.00	98.8	94.10
2	36	163	50	F	6.76	12.7	4.29	1.50	98.6	86.00
3	28	164	52	F	8.44	7.1	4.10	1.00	91.2	80.70
4	50	163	83	F	6.44	11.1	2.18	1.30	95.9	102.00
5	28	164	60	M	4.93	12.5	2.46	1.20	94.7	85.30
6	43	163	59	F	12.00	12.7	2.42	1.30	90.2	147.00
7	37	187	75	M	8.02	10.5	2.10	0.80	92.0	104.00
8	38	174	80	F	6.56	9.9	4.12	1.00	95.5	76.40
9	41	170	70	F	6.15	11.6	6.89	1.70	89.2	63.80
10	37	167	58	F	13.70	16.7	3.65	1.90	83.1	151.00
12	42	179	78	M	4.82	14.0	1.85	1.20	91.8	77.90
12	34	172	58	F	4.95	8.8	1.84	0.90	96.2	90.80
13	38	169	65	F	7.42	10.5	3.00	1.00	93.1	96.58

Table 2.2: *Demographic data of the patients constituting the tuning dataset for propofol and remifentanil coadministration (H: height, W: weight, G: gender).*

PID control for propofol administration

In [92] a SISO control system that uses the BIS as controlled variable and the propofol infusion rate as control variable has been proposed. A schematic representation of the control scheme is shown in Figure 2.2 where $y(t)$ is the measured BIS value and $u(t)$ is the control action that is the propofol infusion rate expressed in mg/s. This value is bounded between 0 mg/s and 6.67 mg/s. The BIS reference value is denoted as $r(t)$ and $e(t)$ is the control error calculated as $e(t) = y(t) - r(t)$. The controller is a standard PID implemented in ideal form:

$$PID(s) = \frac{U(s)}{E(s)} = K_p \left(1 + \frac{1}{sT_i} + sT_d \right), \tag{2.4}$$

where $PID(s)$ is the Laplace transform of the controller, $E(s)$ is the Laplace transform of the error signal, and $U(s)$ is the Laplace transform of the control action. Then, K_p is the proportional gain, T_i is the integral time constant, T_d is the derivative time constant. To deal with the measurement noise issue a second order filter on the PID output has been inserted:

$$PID(s) = \frac{U(s)}{E(s)} = K_p \left(1 + \frac{1}{sT_i} + sT_d \right) \frac{1}{(T_f s + 1)^2}. \tag{2.5}$$

The filter time constant T_f represents an additional tuning parameter. The PID parameters K_p, T_i and T_d have been determined by solving the optimization problem 2.2 by means of GA with a population size of 40 elements and by stopping the optimization when the relative change in the cost function value over the last 50 iterations is less than 0.001. To guarantee good performance for both the induction and maintenance phases, a gain scheduling approach has been adopted. Hence, two different optimization procedure has been carried out and two sets of parameters has been found. The filter time constant T_f is selected with an iterative procedure in such a way that, in simulation, the introduction of noise does not produce an IAE degradation greater than 30 [%]. The tuning parameters for both the induction and maintenance phases are shown in Table 2.3.
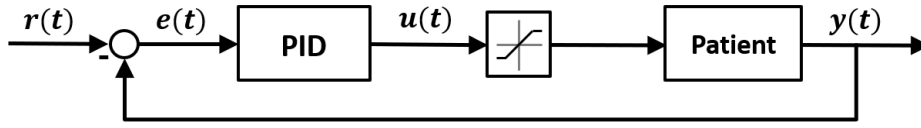
Figure 2.2: *Schematic representation of the SISO control loop for propofol only administration proposed in [92].*

	Induction phase	Maintenance phase
$\mathbf{K_p}$ [mg/s]	0.06	0.44
$\mathbf{T_i}$ [s]	333	1250
$\mathbf{T_d}$ [s]	34	20
$\mathbf{T_f}$ [s]	0.5	0.7

Table 2.3: *Optimal tuning parameters of PID for propofol only administration obtained in [92].*

It is worth noting that this configuration of the PID is subject to the derivative-kick phenomenon when a step is applied to the reference signal $r(t)$. In the context of anesthesia induction this phenomenon can be desirable since it provides an initial propofol bolus that is common in the clinical practice. Anyway, this effect can be avoided by implementing the PID in the following form:

$$U(s) = K_p \left(E(s) + \frac{E(s)}{sT_i} + sT_d Y(s) \right) \frac{1}{(T_f s + 1)^2}, \tag{2.6}$$

where $Y(s)$ is the Laplace transform of the controlled variable. Note that the derivative term is applied to the feedback signal $y(t)$ and not to the error signal $e(t)$ so as to avoid sudden increases in the control variable $u(t)$.

Another option is to implement the PID controller in standard ideal form with filtered derivative term:

$$PID(s) = \frac{U(s)}{E(s)} = K_p \left(1 + \frac{1}{T_i s} + \frac{T_d s}{1 + \frac{T_d}{N} s} \right). \tag{2.7}$$

To obtain a strong filtering effect without significantly affecting the dynamics of the controller a good choice to tune the filter consists in choosing $N = 5$.

PID control for propofol and remifentanil coadministration

In [93] a MISO control system for propofol and remifentanil coadministration has been proposed. The architecture of the control systems is shown in Figure 2.3. The propofol infusion rate, $u_p(t)$ is expressed in mg/s, and it is bounded between 0 and 6.67 mg/s. The remifentanil infusion rate, $u_r(t)$ is expressed in μg/s, and it is bounded between 0 and 16.67 μg/s. The architecture is based on a standard PID controller in form 2.7 A key element of the control scheme is the ratio block that allows the anesthesiologist to explicitly select the desired opioid-hypnotic balance. By expressing the remifentanil infusion rate in μg/s and the propofol infusion rate in mg/s the control system has been designed in such a way that the value of ratio can range from 0.5 to 15. Upper and lower limits have been selected

based on clinical considerations described in [93]. In the clinical practice a good choice of opioid-hypnotic balance is generally obtained with a ratio of 2. This value of the ratio is obtained by applying the infusion pattern proposed in [94]. Its goal is to achieve a balance between the propofol and remifentanil effect-site concentrations that ensures a 50% chance of not responding to surgical stimuli and the quickest return to consciousness after the end of infusions. In clinical practice, different drugs balance could be necessary for each phase of anesthesia, or for each specific surgery procedure. By selecting a lower ratio, the BIS target is obtained with a higher propofol concentration and a lower remifentanil concentration, hence the hypnotic component of anesthesia is predominant. On the contrary, by selecting a higher ratio, the BIS target is obtained with a lower propofol concentration and a higher remifentanil concentration, hence the analgesic component is predominant. For example, the drugs balance is modified depending on the phase of the surgery:

- during intubation it is advisable to select a balance that guarantees the desired DoH associated to a strong analgesic effect, due to the pain induced by the procedure;
- during the preparation of the surgical field, because of the absence of external stimuli, the balance can be changed to decrease the remifentanil administration while maintaining the selected DoH level;
- during surgical incision, a different drug balance might be necessary to compensate for the beginning of the painful stimulation;
- during surgery, the anesthesiologist regulates the balance based on the patient's physiological signs such as hemodynamic variables;
- in some particular cases, in the final phase of the surgery, the drug balance is regulated to maintain the hypnotic level without opioid effect, which is substituted with post-operative analgesic treatment.

General anesthesia can also be performed with the concurrent administration of local anesthetics to satisfy the analgesic requirement. In this case, the drug balance regulation must provide the hypnotic effect with a reduced opioid administration. These examples show that the drugs balance in TIVA is clinically relevant and that the anesthesiologist has to be able to regulate such balance to guarantee a suitable anesthesia. In this context, the controller should provide a satisfactory control performance independently from the selected opioid-hypnotic ratio. The PID tuning parameters K_p, T_i and T_d have been determined by solving the optimization problem 2.2 by means of PSO with a swarm size of 40 particles and by stopping the optimization when the relative change in the cost function value over the last 50 iterations is less than 0.001. The optimization problem has been solved separately for the induction phase and for the maintenance phase, and for all the infusion ratios between 0.5 and 15, thus providing an optimal tuning for each opioid-hypnotic balance. Two sets of tuning rules have been obtained, each one expressing the values of the PID parameters as a function of the ratio, as shown in Table 2.4.

Model-based control for propofol administration

In [95] a model-based SISO control system for propofol administration has been presented. The control scheme is shown in Figure 2.4, it incorporates the PK/PD Schnider model to provide an individualized infusion of propofol, tailoring it to the characteristics of each patient. This strategy falls in the context of personalized medicine that, nowadays, is becoming more
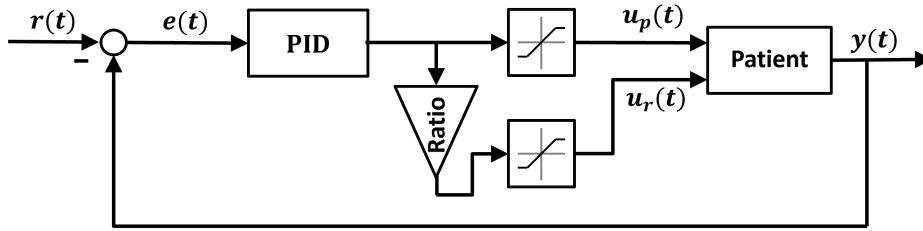
Figure 2.3: *Control architecture for propofol-remifentanil coadministration proposed in [93].*

	Induction phase	**Maintenance phase**
$\mathbf{K_p}$ $[mg/s]$	$0.053(ratio)^{-0.35} - 0.013$	$0.019(ratio)^{-0.38} - 0.0040$
$\mathbf{T_i}$ $[s]$	207	164
$\mathbf{T_d}$ $[s]$	30	15
N	5	5

Table 2.4: *Tuning rules of PID parameters for propofol and remifentanil coadministration obtained in [93].*

and more popular. The linear PK/PD model is referred to as $\tilde{P}$ in the control scheme. Its parameters depend on the demographic data of the patient as shown in Table 1.1. The Hill function is referred to as $\tilde{H}$ in the control scheme. It is computed with the Vanluchene model, whose parameters are shown in Table 1.3. If $\tilde{P}$ and $\tilde{H}$ exactly match the real dynamics of the patient response the behavior of the proposed scheme becomes linear. Indeed, the feedback signal would become the $\tilde{P}$ model output $\tilde{C}_e(t)$ since the innovation signal, $i(t)$, is equal to zero except in the case of external disturbances. However, the models would never be perfect as long as the parameters of $\tilde{P}$ are affected by uncertainties and $\tilde{H}$ is a model calculated on average parameters. Hence, $i(t)$ will be different from zero even in absence of external disturbances and it will be seen as an error that is fed back to the PID controller. To address the presence of noise and to improve robustness, the use of two second order low-pass filters is proposed. The filter F_1, with time constant T_{f1}, pre-filters the BIS so that high noise peaks are removed without affecting the dynamics of the control system. The filter F_2, with time constant T_{f2}, acts on $i(t)$ and handles the trade-off between the contribution of the innovation and the noise filtering action. The controller is a PID (2.7). The tuning parameters K_p, T_i and T_d have been determined by solving the optimization problem (2.2) by means of PSO with a swarm size of 40 particles and by stopping the optimization when the relative change in the cost function value over the last 50 iterations is less than 0.001. In order to guarantee good performance for both the induction and maintenance phases, a gain scheduling approach has been used. Hence, two different optimization procedure has been carried out and two sets of parameters has been found. The filter time constant T_{f2} is selected with an iterative procedure in such a way that, in simulation, the introduction of noise does not produce an IAE degradation greater than 30 [%]. T_{f1} has been determined in an empirical way, so that the filter bandwidth is larger than the process bandwidth and it does not influence the closed-loop dynamics. The tuning parameters for both the induction and maintenance phases are shown in Table 2.5.
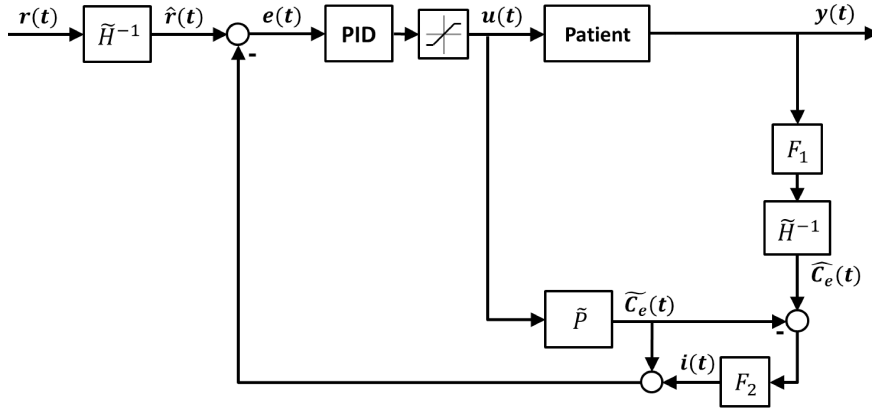
Figure 2.4: *Model-based control architecture for propofol only administration proposed in [95].*

	Induction phase	Maintenance phase
$\mathbf{K_p}$ $[mg/s]$	1	7
$\mathbf{T_i}$ $[s]$	552	608
$\mathbf{T_d}$ $[s]$	27	20
$\mathbf{T_{f1}}$ $[s]$	0.1	0.1
$\mathbf{T_{f2}}$ $[s]$	11	10

Table 2.5: *Optimal tuning parameters for model-based propofol administration obtained in [95].*

Event-based control for propofol administration

The event-based control architecture for propofol administration is shown in Figure 2.5 and it has been proposed in [96]. The event-based approach, for anesthesia control, allows the way of operating of the anesthesiologist to be replicated. In fact, in clinical practice the drug infusion is changed by the anesthesiologist only when relevant events occur. Moreover, it reduces the control effort required to the actuator. Event-based control schemes are based on the presence of an event generator that triggers an event each time an integral function of the BIS exceeds a given threshold. Using an integral function that is re-set at each event results in a strong noise filtering action, without adding a significant phase lag [97]. More in detail, the event generator triggers an event when the following condition occurs:

$$\left| \int_{t_{last}}^{t} BIS(t) - BIS_f(t_{last})dt \right| > \Delta_i \quad OR \quad t_{last} - t > t_{max}, \qquad (2.8)$$

where $BIS_f(t_{last})$ is the last output of the event generator that has been generated at the time instant t_{last}, i.e., when the last event has been triggered. The tuning parameters of the event generator are Δ_i and t_{max}. The threshold Δ_i handles the trade-off between the filtering effect of the event generator and its ability to detect changes in the BIS due to an actual variations of DoH. The timeout parameter t_{max} sets the maximum delay between the generation of two consecutive events and, thus, represents a safety condition. The value $BIS_f(t)$ is transmitted
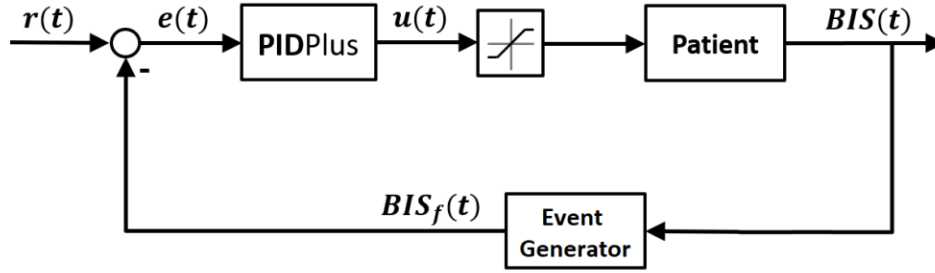
Figure 2.5: *Event-based SISO control architecture for propofol administration proposed in [96].*

	Induction phase	Maintenance phase
$\mathbf{K_p}$ $[mg/s]$	0.04	0.02
$\mathbf{T_i}$ $[s]$	199	321
$\mathbf{T_d}$ $[s]$	26	8
$\mathbf{\Delta_i}$	31	25
$\mathbf{t_{max}}$ $[s]$	20	20
$\mathbf{T_f}$ $[s]$	0.1	0.1

Table 2.6: *Optimal tuning parameters for the SISO event-based control scheme obtained in [96].*

to the controller when an event is triggered, and it is computed as:

$$BIS_f(t) = \frac{\int_{t_{last}}^{t} BIS(t)dt}{t - t_{last}}. \tag{2.9}$$

The feedback regulator is a PIDPlus controller [98], which is derived from the standard PID controller in automatic reset configuration adapted to handle the non-periodic sampling introduced by the event generator. The tuning parameters of the PIDPlus are the same of a standard PID controller, namely, the proportional gain K_p, the integral time constant T_i and the derivative time constant T_d. The PIDPlus tuning parameters K_p, T_i, T_d and Δ_i have been determined by solving the optimization problem (2.2) by means of PSO with a swarm size of 40 particles and by stopping the optimization when the relative change in the cost function value over the last 50 iterations is less than 0.001. The optimization problem has been solved separately for the induction phase and for the maintenance phase. The parameter t_{max} has been fixed equal to 20 s in order to guarantee an adequate safety of the patient and T_f has been tuned in an empirical way by taking into account the time constants of the system. The tuning parameters for both the induction and maintenance phases are shown in Table 2.6.

Event-based control for propofol and remifentanil coadministration

The event-based SISO control architecture has been extended to the MISO case of propofol and remifentanil coadministration in [99] and it is shown in Figure 2.6. The same control architecture of Section 2.2.2 has been considered while the same event generator and PIDPlus controller of Section 2.2.2 have been used. The PIDPlus tuning parameters K_p, T_i, T_d and Δ_i have been determined by solving the optimization problem (2.2) by means of PSO with a swarm size of 40 particles and by stopping the optimization when the relative change in the
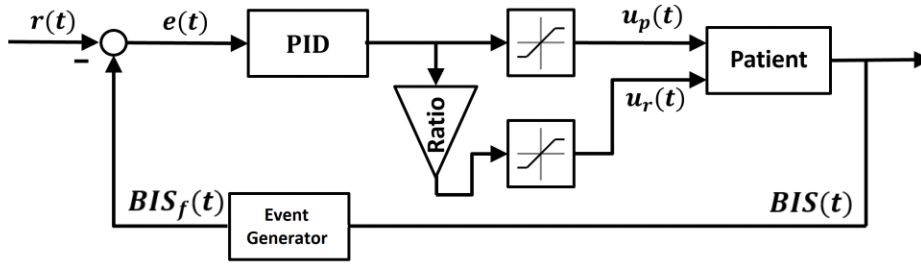
Figure 2.6: *Event-based MISO control architecture for propofol and remifentanil coadministration proposed in [99].*

	Induction phase	**Maintenance phase**
$\mathbf{K_p}\ [mg/s]$	$0.0139(ratio)^{-0.44} - 0.0015$	$0.0136(ratio)^{-0.43} - 0.0018$
$\mathbf{T_i}\ [s]$	197	288
$\mathbf{T_d}\ [s]$	29	6
$\mathbf{\Delta_i}$	9	21
$\mathbf{t_{max}}\ [s]$	20	20

Table 2.7: *Tuning rules for the MISO event-based control scheme obtained in [99].*

cost function value over the last 50 iterations is less than 0.001. The optimization problem has been solved separately for the induction phase and for the maintenance phase. The parameter t_{max} has been fixed equal to 20 s and T_f has been tuned in an empirical way by taking into account the time constants of the system. The tuning parameters for both the induction and maintenance phases are shown in Table 2.7. It is worth noting that, as in Section 2.2.2, the optimal K_p varies with the propofol/remifentanil ratio that can be freely selected in the range 0.5-15.

2.2.3 Experimental setup

Thanks to the collaboration with the Anesthesia and Intensive Care Unit 2 of Spedali Civili di Brescia Hospital, and after obtaining approval by the Ethics Committee of Brescia (number of the study: NP12861), a clinical experimentation campaign has started. The aim is to test the control solutions developed on real patients in the operating room. To this end, a control system has been developed and implemented. Its schematic representation is shown in Figure 2.7. The control algorithm is implemented as a part of a full control software that runs on a standard personal computer (PC). The control software also manages the communication with data acquisition and actuation devices. The first consists in a Dräger Infinity Delta monitor (Drägerwerk, Lübeck, DE) while the latter consists of two Graseby 3500 syringe pumps. These devices are connected to the PC through three USB-RS232 converter cables. These particular models and brands of medical devices have been chosen because they are already present in the operating room selected to perform the clinical experimentation. that is the plastic surgery operating room at Spedali Civili di Brescia Hospital. A suitable graphical user interface (GUI) has also been developed. It allows the anesthesiologist to easily use and supervise the system. A screenshot of the GUI is shown in Figure 2.8. On the left side of the GUI there is a box dedicated to system initialization where it is required to insert

the patient's demographic data and the COM ports where the medical devices are connected. Then there is a box to select the BIS target value, a box to insert notes and a box where the status of the connected medical devices is shown by means of red and green indicators. In the central part of the GUI there is a box where it is possible to interact with the control system algorithm. In particular, on the top part there are the buttons to start and stop the control algorithm and to temporarily suspend it. The blue button "Switch Mode" can be used to switch the control system mode between induction and maintenance. The mode selected is indicated with a green light. The two "Change" buttons can be used to safely replace an empty drug syringe from the syringe pumps. The orange "Bolus" buttons can be used by the anesthesiologist to manually perform boluses. The bolus dose can be freely chosen by the anesthesiologist by holding the button pressed for the desired amount of time. The dose that is currently administered is shown in real time in the displays placed to the right of the "Bolus" buttons. To guarantee a precise drug dosing and thus ensuring safety, boluses administration is immediately discontinued when the buttons are released. The yellow button in the "Manual Control" box can be used by the anesthesiologist to switch the system from automatic control to manual control and vice-versa. When manual control is activated a blinking yellow light indicates this situation to the user. The propofol and remifentanil infusion rates are decided by the anesthesiologist by means of the two text boxes placed in the "Manual Control" box. Manual control is also automatically activated when the control system enters in safety mode. The latter is activated when the BIS signal is not available or it is not reliable. In these situations, the control system is in open loop. It can happen, for example, when there is an excessive amount of electromagnetic noise due to the use of the electrocautery device or when the BIS sensor is accidentally detached. When the BIS signal is missing or its signal quality index (SQI) is below 40 for more than 5 consecutive seconds, the control system automatically activates the safety mode that is signaled to the anesthesiologist through a specific alarm displayed on the GUI. When the BIS returns available and the SQI is above 40 for 5 consecutive seconds, the system automatically ends the safety mode and closed-loop control is resumed. On the right side of the GUI there are plots and indicators that allow the anesthesiologist to easily supervise the system during its functioning. The control software also records on a file patient's demographic data, controller logs, pumps infusion rates and the patient's physiological data read from the monitor. These data are then used to evaluate the performance of the control system.

2.3   Thesis contribution

The aim of this thesis is to contribute in the development of closed-loop systems for anesthesia that can go beyond the scope of research and be used in routine clinical practice. To pursue this objective, solutions to overcome the obstacles that hinders their diffusion, discussed in Section 2.1, have been proposed. Particular attention has been given to applicability in the real clinical scenario. To this end, it is of paramount importance to ensure that the controllers have a behavior that is intuitive and consistent with that of manual control. Indeed, these systems must be operated by anesthesiologists that acts as supervisors and need to fully understand the behavior of the controllers in order to trust them. In this context, to provide control solutions that mimic the anesthesiologist behavior event-based control strategies have been applied for the first time in this field. As regards the anesthesiologist-in-the-loop issue, the implementation of collaborative control strategies that combines the actions of the
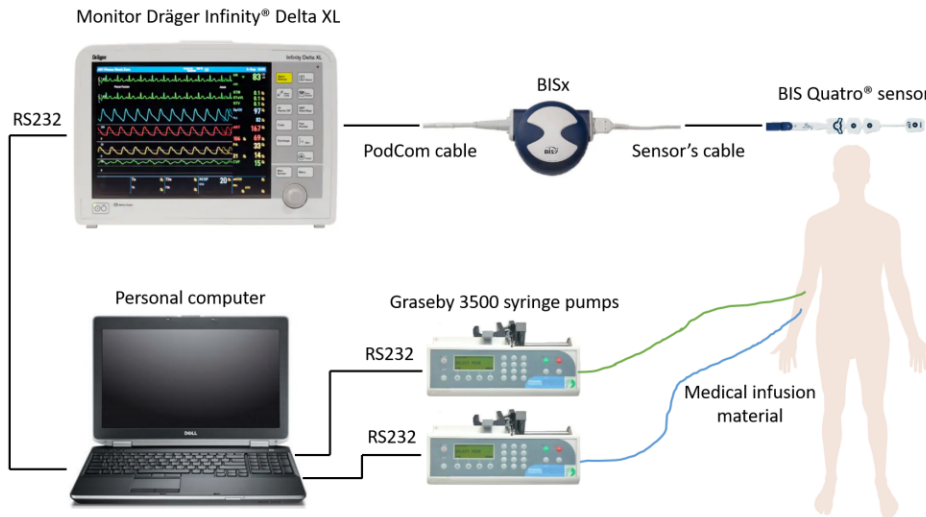
Figure 2.7: *Schematic representation of the control system used in the operating room.*
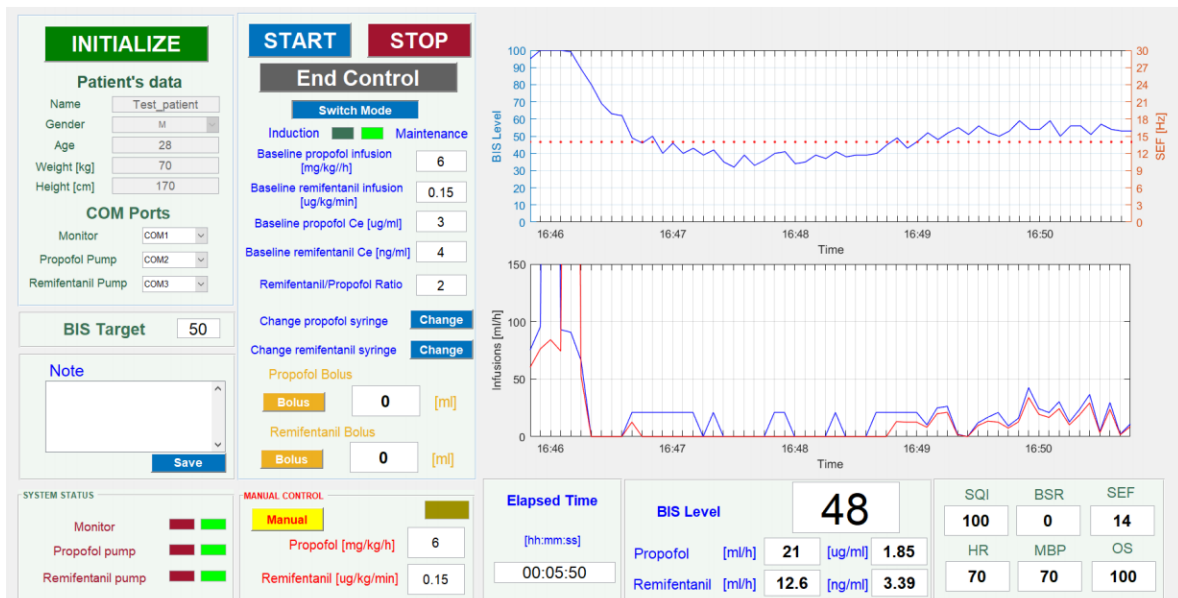
Figure 2.8: *Screenshot of the control system GUI during run-time operation.*

controller with manual interventions performed by the anesthesiologist has been considered. This allows the behavior of the control system to be better tailored to specific clinical needs by exploiting anesthesiologist's knowledge and expertise. Problems arising from the practical implementation of the control device have also been tackled. Steps towards the development of MIMO control schemes have been made thanks to the recent introduction of open-source multi-variable simulation tools [49]. Contributions to the implementation of personalized control strategies have been made to account for the need of personalized medicine strategies. Particular attention has also been given to diversify the control strategies available to the anesthesiologist as some of them may be more suitable for some patients or types of surgery than others. Therefore, an automatic system for the control of anesthesia that can be effectively used in clinical practice should have several operating modes to choose from.

In detail, the clinical performance of the PID-based MISO control scheme described in Section 2.2.2 has been experimentally assessed [100, 101]. Then, a modified version of the control scheme has been proposed. It has been obtained by considering specific requirements related to the clinical practice that are relevant for the anesthesiologist [102]. An experiment has also been performed to evaluate the performance of the modified control system in terms of its ability to deal with issues that may arise during its practical use in a clinical setting and to the anesthesiologist in the control loop issue [103].
The clinical performance of the event-based MISO control scheme described in Section 2.2.2 has been experimentally assessed [104]. This is the first time that an event-based control scheme has been applied to closed-loop anesthesia.
A novel MPC methodology for anesthesia control have also been proposed. It integrates a model of the patient in the control architecture, thus obtaining an individualized controller. Moreover, the developed control structure is characterized by low complexity and low computational effort, so that it can be easily deployed to standard hardware and software platforms. First, the case for propofol only administration have been considered [105], the effect of measurement noise on control performance has been analyzed [106] and its clinical performance has been experimentally assessed [107]. The control system has also been extended to the case of propofol and remifentanil coadministration [108]. The control system for propofol only administration has then been extended with an event-based algorithm with sensor deadband to reduce the residual noise in the control action [109].
The open-source simulator proposed in [49] has been used to validate the performance of the PID-based and event-based MISO control schemes described in Sections 2.2.2 and 2.2.2 when the opioid-hypnotic balance is dynamically changed during anesthesia [110].
The theoretical development of new personalized control solutions based on the physical characteristics of each patient has also been performed. In this context, a novel tuning methodology that optimizes the PID tuning parameters according to patient's demographic data has been developed. The methodology focuses on the maintenance phase of anesthesia. It has been tested in simulation for the case of propofol only administration [111] and for propofol and remifentanil coadministration [112]. Also in this context, an optimized feedforward control strategy for anesthesia induction has been developed [113]. It consists in providing an optimized induction bolus of propofol. It aims to minimize the induction time while avoiding BIS undershoots. The optimization is performed for each patient by taking into account demographic data, so that the resulting bolus is personalized. A feedback PID controller is also included in the control scheme. It corrects the bolus based on the measured BIS to compensate for the unavoidable uncertainty in the response of each patient to drug admin-

istration. To increase the robustness of the proposed solution a reference (command) input design strategy has been devised [114]. It explicitly considers the dynamics of the feedback PID controller in the calculation of the feedforward propofol bolus. Moreover, an optimized feedforward/feedback control strategy has been proposed [115]. It considers uncertainty in the computation of the feedforward propofol bolus. The first phase of anesthesia induction is performed in open loop. The feedback loop is then closed when the peak effect of the feedforward bolus is reached.

Chapter 3

PID-based MISO control: experimental results

In this chapter the experimental results obtained with the PID-based MISO control scheme described in Section 2.2.2 are presented. The control scheme is implemented in the control software and its effectiveness is assessed on 10 patients. The results obtained are also compared to those of manually controlled anesthesia to verify the applicability of the proposed control solution in the clinical practice [100, 101]. Then, a modified version of the original control scheme is proposed to take into account specific requirements related to the clinical practice. The effectiveness of this modified version is assessed on other 10 patients and the results are compared with those of the original version [102]. Given the satisfactory results obtained, the modified version is then tested on a larger population of 42 patients in order to assess its clinical performance. Here, clinically relevant performance indexes are considered and also the quality of the post-operative phase is assessed. Finally, the applicability of the modified control scheme in the clinical practice is further assessed on 9 patients. In particular, the anesthesiologist-in-the-loop issue is considered by allowing the anesthesiologist to perform manual drug boluses. Moreover, the robustness of the control system with respect to the use of different actuators is considered [103].

3.1 PID-based MISO control scheme

In this section the experimental results obtained by applying the control solution proposed in Section 2.2.2 to a population of 10 patients undergoing general anesthesia for plastic surgery are presented. The aim is to demonstrate the practical effectiveness of the proposed MISO control structure for the coadministration of propofol and remifentanil, and to demonstrate the viability of the optimization-based tuning approach based on classical PK/PD models available in the literature that has been presented in Section 2.2.1. The results are also compared with those obtained with manually controlled drug administration. This comparison should not be understood as a way to prove that closed-loop is, in any sense, better than manually controlled administration, but it provides a valid reference to better understand and evaluate the performance of the proposed automatic solution.

3.1.1 Material and methods

The experimental setup considered is that described in Section 2.2.3. The PID-based MISO control structure considered is that described in Section 2.2.2. To implement the control strategy on the control algorithm employed in the experimental setup the PID controller has been discretized with a sampling period of 1 s, according to the maximum update frequency provided by the Dräger Infinity Delta monitor. The control signal has been down-sampled by sending a new infusion rate to the syringe pumps every 5 s since the Graseby 3500 syringe pumps are not able to track infusion rates that are updated at higher frequencies. This is due to the internal controller of the pump, that has to elaborate the received command to actuate the syringe plunger motor to achieve the desired infusion rate. It has been decided to down-sample only the control signal and not the whole PID control algorithm to exploit the maximum update frequency provided by the BIS monitor and thus allowing the calculation of the integral and derivative action in a more precise way. It is worth noting that both 1 s and 5 s are sampling periods fully compatible with the patient dynamics, which has time constants in the order of minutes. An anti-windup strategy has been implemented by using the conditional integration technique and the derivative action has been applied to the feedback signal only, and not on the control error in order to avoid the derivative-kick phenomenon. In addition to the use of a low-pass filter on the derivative action, the measurement noise has been further filtered by implementing a moving average filter in order to smooth high noise peaks that can be amplified by the proportional and by the derivative actions. Furthermore, the filter removes the step transitions in the measured variable due to the quantization of the BIS, which is provided in the form of integer numbers. The moving average filter is in the form:

$$BIS_f(k) = \frac{1}{N_s} \sum_{i=0}^{N_s-1} BIS(k-i), \qquad (3.1)$$

where BIS_f is the filtered BIS signal and N_s is the number of samples used in the moving average. The latter has been set equal to 8 since it has been decided not to tolerate that a single step variation on the BIS signal due to measurement noise affects the control action for more than 12.5% of its amplitude, thus avoiding the risk of unjustified sudden increases of the infusion rates. The effect of the filter on the BIS signal is shown in Figure 3.1. The control architecture obtained with the addition of the filter is shown in Figure 3.2.

The optimization-based tuning procedure described in Section 2.2.2 has been repeated for this new configuration of the control scheme to consider the sampling period of 5 s on the control actions and the presence of the moving average filter. In this way, the resulting tuning takes automatically into account the phase lag that the filter introduces. The tuning rules obtained are shown in Table 3.1. A value of the remifentanil-propofol ratio equal to 2 has been considered for this experimentation. Thus, the PID parameters are calculated for this value of ratio and they are shown in Table 3.2. They will be used for all the patients enrolled. This specific value for the ratio has been chosen in accordance to the infusion scheme proposed in [94]. It aims to obtain a balanced effect-site concentration of propofol and remifentanil to guarantee the 50% probability of no response to surgical stimuli and the fastest return to consciousness after termination of the infusions. In particular, the aforementioned infusion scheme proposes a ratio of 1.86 for the first 40 min followed by a ratio of 1.92 until 150 min and a ratio of 2.3 thereafter. In order to accommodate for different durations of the infusion, the mean of these three values is considered, which is equal to 2. This choice has

been further supported by the fact that, in the clinical practice, advisable drug infusions are 6 mg/kg/h for propofol and 0.2 μg/kg/min for remifentanil, which leads to a ratio equal to 2 when these infusion are scaled by the weight of the patient and converted in mg/s and μg/s, respectively. Since two different sets of parameters are obtained, a gain scheduling approach is implemented. Initially, the PID controller regulates the induction with the set of parameters optimized for this task. Then, when the BIS settles steadily under 60, the anesthesiologist assesses the patient through observation of the clinical signs, and if the level of anesthesia is deemed as adequate, switches the controller to maintenance mode and the set of parameters optimized to compensate for disturbances is used until the end of the clinical procedure. In order to properly handle the transition between the two sets of parameters a bumpless switching mechanism has been implemented. In particular, when the switching happens, the value of the integral term is recalculated in such a way that the overall control action with the new set of parameters is equal to the overall control action obtained with the previous set of parameters at the switching time. The switching between the two sets of parameters is triggered by the anesthesiologist by pressing a specific button placed on the control system GUI shown in Figure 2.8. If the system enters in safety mode (see Section 2.7) the integral action of the PID controller is reset to zero.

In the experimentation, 10 adult patients ($\geq$18 years) without a history of neurological diseases or use of psychoactive medications scheduled for elective plastic surgery have been included. All patients gave their written informed consent for participation in the study. When the patient arrives in the preanesthetic care unit the anesthesiologist administers to anxious patient 0.5 μg/kg of fentanyl and 1-2 mg of midazolam as premedication to improve patient comfort. A cannula is also inserted into a vein on the dorsum of the hand, and the sensors to monitor the patient during surgery are applied. Anesthesia is induced automatically by the closed-loop control system. When the patient loses consciousness the anesthesiologist inserts the laryngeal mask or the endotracheal tube and the patient is connected to the controlled mechanical ventilation machine. Bolus of curare are administered in this phase to facilitate intubation at discretion of the anesthesiologist, usually 0.8 mg/kg of rocuronium. At the end of induction, when the patient achieves a stable level of BIS in the required range from 40 to 60 the anesthesiologist checks for clinical signs of adequate anesthesia to switch the system into maintenance mode by using the specific button on the control system GUI. Then, the anesthesiologist acts as a supervisor throughout the surgical procedure to ensure patient safety by monitoring the infusions rates, the presence of patient movements, the hemodynamic of the patient, the BIS level, blood loss and other clinical indicators. The anesthesiologist can decide to stop the closed-loop infusions and switch to manual control at any time in case of emergency or inadequate anesthesia level of the patient. Moreover, additional boluses of propofol and remifentanil can be administered in case of necessity. In addition to the BIS, the values of SQI, heart rate, burst suppression ratio (BSR), peripheral oxygen saturation (SpO$_2$), systolic, diastolic and mean blood pressures (BP$_s$, BP$_d$, BP$_m$) are recorded during the whole procedure. Muscle relaxant, vasopressor drugs, antihypertensive therapy, antiemetic drugs and fluids are administered at discretion of the anesthesiologist throughout the surgery. The patients are kept normothermic using forced-air blanket warmer. The automatic controller is stopped at completion of surgical procedures, i.e., after the surgeon finishes the skin sutures. Patients remain in the operating room until they regain consciousness, the ventilation device is removed and they can correctly state their date of birth. The patients are then taken to a recovery room for a few minutes where they are monitored and then they are visited on the first and on the second post-operative day.
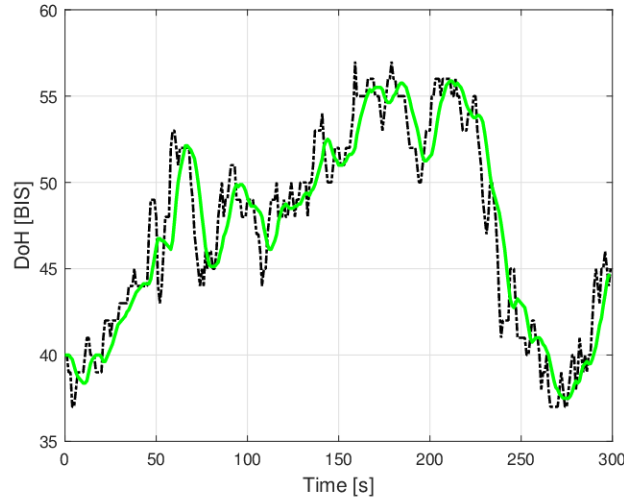
Figure 3.1: *BIS signal provided by the monitor (black dash-dot line) and BIS signal provided as output of the moving average filter (green solid line).*
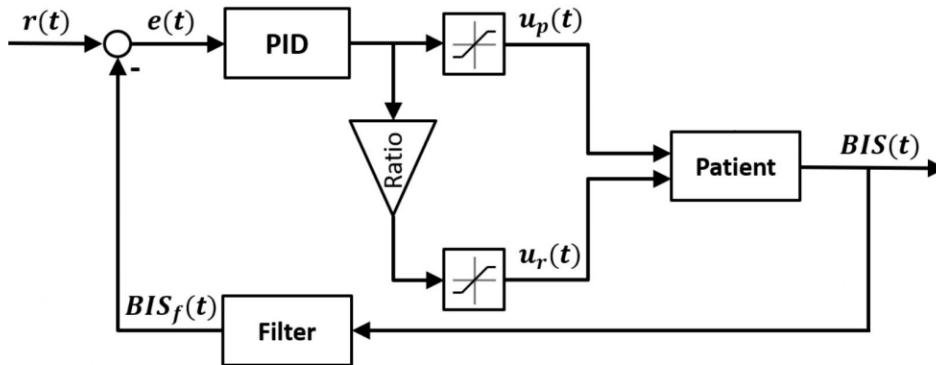
Figure 3.2: *Control architecture for propofol-remifentanil coadministration with the additional moving-average filter.*

	Induction phase	**Maintenance phase**
$\mathbf{K_p}$ $[mg/s]$	$0.015(ratio)^{-0.43} - 0.0019$	$0.045(ratio)^{-0.36} - 0.011$
$\mathbf{T_i}$ $[s]$	280	171
$\mathbf{T_d}$ $[s]$	33	19
N	5	5

Table 3.1: *Tuning rules of PID parameters for propofol and remifentanil coadministration with the discretized PID controller and the additional moving-average filter.*

	Induction phase	Maintenance phase
$\mathbf{K_p}$ $[mg/s]$	0.0093	0.025
$\mathbf{T_i}$ $[s]$	280	171
$\mathbf{T_d}$ $[s]$	33	19
N	5	5

Table 3.2: *PID parameters for the induction and maintenance phases with the opioid-hypnotic ratio of 2.*

3.1.2   Experimental results

In this section the results obtained in closed-loop are presented and they are compared with those obtained with manual regulation of anesthesia. It is worth stressing that this comparison has been made to better understand the performance of the closed-loop controller proposed and, in particular, to investigate its clinical soundness with respect to the manual administration. It is not within the objectives of this experiment to draw a conclusive evaluation about the improvement of performance achievable by automatic control with respect to manual control.

The demographic data of the 10 patients enrolled with closed-loop anesthesia regulation are shown in Table 3.3. They are 5 males and 5 females, and they cover a large range of heights, from 160 cm to 190 cm, weights, from 58 kg to 100 kg, and ages, from 39 years to 88 years. Furthermore, they were undergoing diverse surgical procedures as shown in Table 3.4 where it is possible to notice that the procedures differ considerably in duration, involved region of the body and level of painful stimulation. The parameter records are shown for each patient from Figure 3.3a to Figure 3.5b. The automatic control of anesthesia provides satisfactory performance for all the enrolled patients in both the induction and maintenance phases of anesthesia. In all cases the closed-loop system was able to induce and maintain anesthesia autonomously without the need for any intervention by the anesthesiologist. During the induction phase the BIS level attains the set-point reference without excessive undershoot and with an acceptable settling time during the induction phase. The system also provides adequate analgesic coverage as the BIS remained stable for all patients during the insertion of the mechanical ventilation device with the exception of patient 9 where the anesthesiologist experienced a difficult insertion of the laryngeal mask with consequent raising of the BIS level during this operation. During the maintenance phase, the system successfully keeps the BIS in the optimal range from 40 to 60 for most of the time. Moreover, the system provides acceptable disturbance rejection, guaranteeing bounded undershoot and overshoot. For example, in Figure 3.4d, at around minute 55, the response of the system to a sudden increase of the BIS value is clearly visible. The adequacy of DoH is also confirmed by the reduced onset of the BS phenomenon in almost all patients. Indeed, the BSR assumes values significantly different from 0 for some time intervals only in patients 2, 3 and 10. In patient 2 the phenomenon may be due to the patient's advanced age while in patients 3 and 10 it can be associated to the BIS undershooting during the induction phase. However, even in these patients the phenomenon is of limited entity and for short periods of time. The duration of the emergence phase is also in accordance with the clinical practice, where awaking time is approximately 10 min. Hemodynamic parameters are stable throughout the anesthesia for all the patients, indeed HR is always stable and in the range between 40 and 90 bpm, SpO_2 is always greater than 95% and BP values are in an acceptable range and remain stable during the whole surgical

procedure. For patient 4 the acquisition of BP was prevented by a technical issue, however the anesthesiologist did not report the onset of hypotensive or hypertensive phenomena. The drugs infusion rates are also satisfactory from a clinical point of view. They do not achieve excessively high or low values, which may involve the risk of overdosing or underdosing the patient. As expected from experimental data, infusion rates are affected by a residual noise, but such noise does not significantly influence the performance of the system. It is worth noting that the anesthesiologist did not administer additional boluses of propofol or remifentanil in any of the 10 cases. In order to quantify the performance of the closed-loop system, the performance indexes presented in Section 1.3.3 have been calculated for the induction phase and for the maintenance phase. To this end, performance indices for the induction phase are calculated using the first 10 min of acquisition for each patient. The rationale behind this choice is that the surgical procedures started at least 10 min after the beginning of the drugs infusion. Hence, the initial minutes where there is no surgical stimulation are not included in the maintenance phase. Moreover, by considering the duration of action of propofol, the clinical effects that are observed in the first 10 min can be attributed to the drug infused during the induction phase. The performance indexes for the induction phase are shown in Table 3.5 and the performance indexes for the maintenance phase are shown in Table 3.6. From the values of the performance indexes for induction it can be observed that the system is able to induce anesthesia in a reasonable time, on average in 3.8 min. In patients 3, 4, 7 and 10 the induction time is slightly longer than that indicated in the specification, but it remains in any case less than 6 min, thus remaining acceptable for the clinical practice. From the BIS-NADIR, it appears that the BIS never reaches excessively low values during induction. For the maintenance phase, the average performance indices show that the system is able to keep an adequate level of hypnosis, with the BIS remaining in the optimal range for the 77.81% of the time. The system is also able to effectively reject surgical disturbances without inducing excessive undershoot: the BIS rises over 60 only during the 3.08% of the maintenance time, and falls under 40 for the 19.11% of the maintenance time. The average awakening time of 7.88 min is fully compatible with the clinical practice. The long awakening time of patient 9 is due to the rejection of the surgical disturbance due to skin suturing that occurred during the last minutes of the maintenance phase. That causes the administration of a large amount of drugs just before the beginning of the emergence phase, see Figure 3.5a. The lowest percentages of BIS in the ideal range over the 10 patients where recorded in patients 6, 7 and 9. This is due to the fact that these individuals show an oscillatory behavior of the BIS during the maintenance phase, see Figures 3.4b, 3.4c and 3.5a. However, none of these patients show clinical signs of inadequate anesthesia or hemodynamic instability. Note that oscillations have also been noticed in other experiments of closed-loop anesthesia [59, 60, 64]. There are several possible explanations for these oscillations. One reason could be an inadequate BIS target [60]. In fact, in some patients and for certain surgical procedures, the set-point of the closed-loop system might require to be fixed at lower values in order to provide deeper anesthesia, thus reducing reactions of the BIS level to the surgical procedures. Another reason could be an inadequate analgesic state that causes oscillation as a result of external stimuli [59]. The latter hypothesis seems to be particularly appropriate for what is observed in this study since patients 7 and 9 underwent breast plastic surgery which involves a high level of painful stimulation. However this last observation must be confirmed by further studies with this closed-loop system. In this study an opioid-hypnotic ratio of 2 was kept for all the patients irrespectively of the surgical procedure. Future clinical experiments might involve addressing the oscillation problem by increasing the ratio in the most painful surgical

Patient	Age	Height [cm]	Weight [kg]	Gender
1	41	165	58	F
2	88	174	84	F
3	60	174	78	M
4	39	170	85	M
5	52	178	94	M
6	75	174	78	M
7	54	165	60	F
8	52	190	100	M
9	53	160	79	F
10	51	167	88	F

Table 3.3: *Demographic data of the patients enrolled with the PID-based MISO controller.*

procedures.

The performance of the closed-loop control of anesthesia is compared with those of manually controlled administration with the aim to verify the feasibility of the proposed closed-loop system for the coadministration of propofol and remifentanil from a clinical perspective. To this end, the data of 33 patients who received manually controlled anesthesia are considered. The data collection have been approved by the Ethics Committee of Brescia (number of the study: NP1843). In this group, anesthesia is induced by administering a bolus of propofol (2-3 mg/kg) and a bolus of fentanyl (1-2 μg/kg) both injected in about 1 min. During the maintenance phase, continuous infusions of propofol and remifentanil are then administered. The anesthesiologist manually regulates the infusion rates to maintain the BIS in the range between 40 and 60. Additional drug boluses can be administered in this phase in case of necessity, and they consists of about 20 mg of propofol and 50 μg of remifentanil. Population demographic data are shown in Table 3.7 where it is possible to see that there are no significant differences in terms of age, gender, height and weight between the two groups. Both studies where performed by the same anesthesiologist, in the same operating room and on patients undergoing general anesthesia for plastic surgery. The performance indexes presented in Section 1.3.3 have been calculated for both groups. For the induction phase the results are shown in Table 3.8. The induction performed with the manual administration is faster due to the use of boluses, but this comes at the cost of a lower value of BIS-NADIR. However, these differences in the performance do not imply significant differences from a clinical point of view. For the maintenance phase the results are shown in Table 3.9. The durations of the two groups are comparable. The BIS is maintained inside the optimal range from 40 to 60, on average, for the 43% of the time in the manual group and for the 78% of the time for the closed-loop group. During the remaining time the BIS level tends to remain, on average, under 40 rather than over 60 in both group preventing the risk of awareness. The BIS-NADIR value is again lower in the manual group, and the time of awakening is, on average, slightly shorter for the closed-loop group. From the MDPE it is possible to appreciate that both groups show a slight negative bias and that such bias is significantly lower in the closed-loop group. This result is confirmed by the MDAPE analysis. In fact, the closed-loop group shows an average MDAPE index that is the half of the average MDAPE calculated for the manual group. This means that the automatic system provides a tighter control by keeping the BIS closer to the set-point value. Finally, the WOBBLE analysis shows that the influence on performance of the intra-patient variability is lower in the closed-loop group.

Patient	Type of surgery
1	Left leg melanoma surgery excision and sentinel lymph node biopsy
2	Retroauricular melanoma surgery excision and hypodermic escharotomy
3	Right thigh lipoma surgery excision
4	Right leg escharotomy and microsurgical flap
5	Dorsal region melanoma surgery excision and sentinel lymph node biopsy
6	Thoracic region melanoma surgery excision and sentinel lymph node biopsy
7	Breast implant replacement and contralateral mastopexy
8	Interscapular region melanoma surgery excision and sentinel lymph node biopsy
9	Tissue expander removal, breast implant insertion and contralateral mastopexy
10	Left thigh lipoma surgery excision

Table 3.4: *Types of surgery undergone by the patients enrolled with the PID-based MISO controller.*

Patient	TT $[min]$	BIS-NADIR
1	2.57	38
2	3.50	35
3	5.43	28
4	5.05	34
5	2.80	36
6	3.68	29
7	4.35	29
8	3.18	39
9	3.23	31
10	4.60	31
Average	3.84	33

Table 3.5: *Performance indexes for the induction phase obtained with the PID-based MISO controller.*

(a) *Patient 1*

(b) *Patient 2*

(c) *Patient 3*
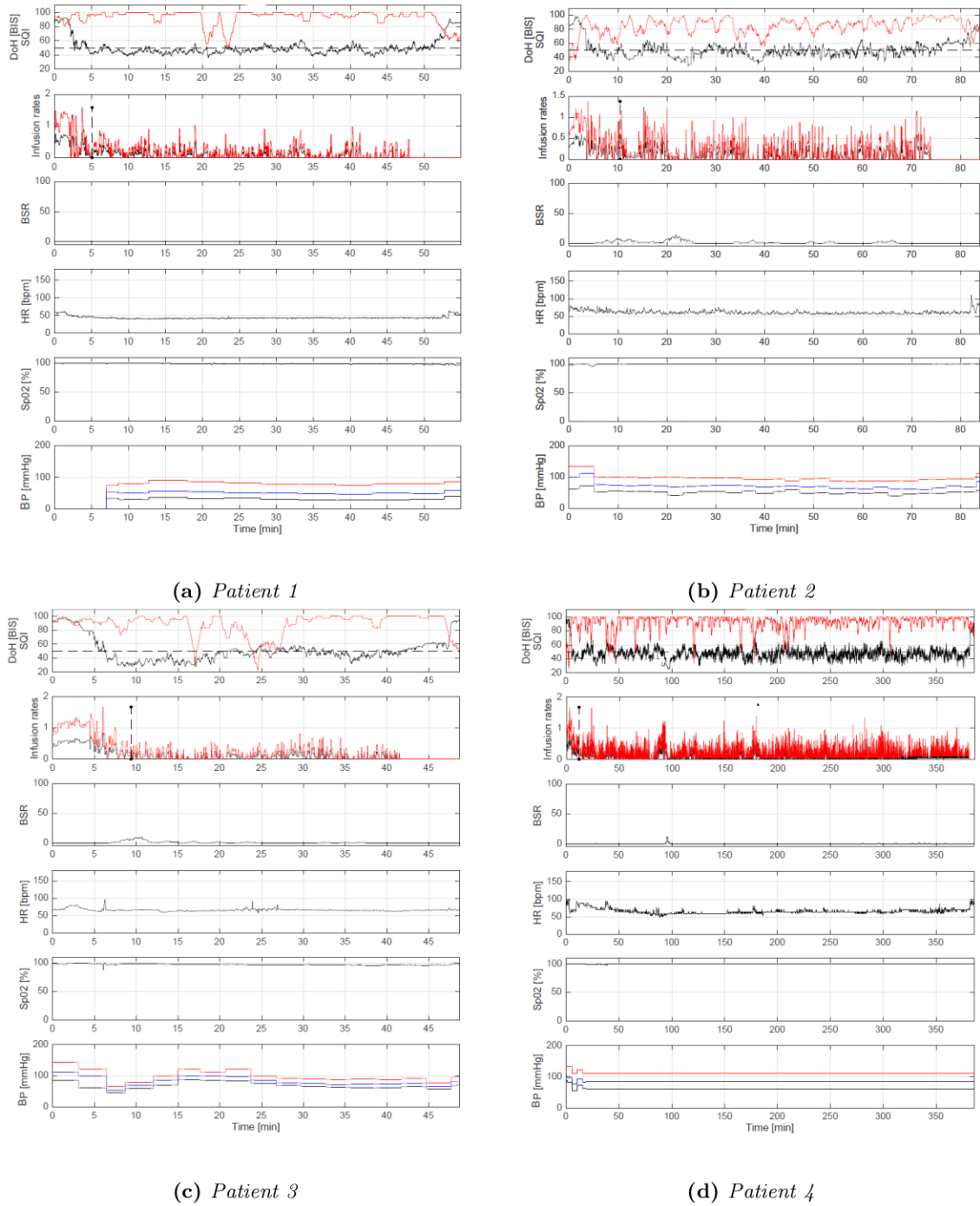
(d) *Patient 4*

Figure 3.3: *Recorded clinical data of the patients enrolled with the PID-based MISO controller. First plot from the top: BIS level of the patient (black solid line), SQI (red solid line) and the BIS set-point (black dashed line). Second plot from the top: propofol infusion rate expressed in mg/kg/min (black solid line) and remifentanil infusion rate expressed in μg/kg/min (red solid line). Third plot from the top: BSR. Fourth plot from the top: HR. Fifth plot from the top: SpO_2. Sixth plot from the top: BP_s (red solid line), BP_d (black solid line) and BP_m (blue solid line).*

(a) *Patient 5*

(b) *Patient 6*

(c) *Patient 7*
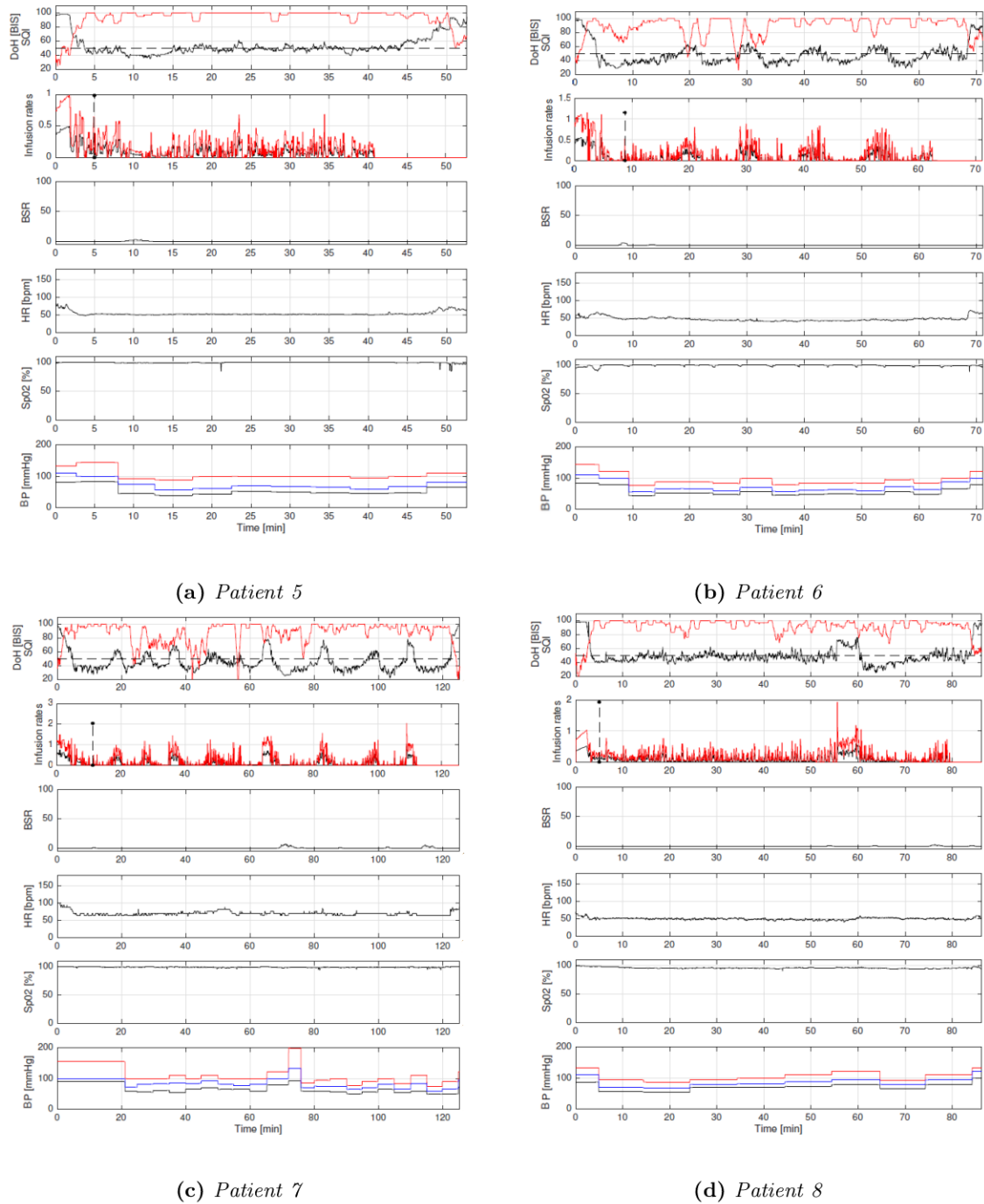
(d) *Patient 8*

Figure 3.4: *Recorded clinical data of the patients enrolled with the PID-based MISO controller. First plot from the top: BIS level of the patient (black solid line), SQI (red solid line) and the BIS set-point (black dashed line). Second plot from the top: propofol infusion rate expressed in mg/kg/min (black solid line) and remifentanil infusion rate expressed in µg/kg/min (red solid line). Third plot from the top: BSR. Fourth plot from the top: HR. Fifth plot from the top: SpO_2. Sixth plot from the top: BP_s (red solid line), BP_d (black solid line) and BP_m (blue solid line).*

(a) *Patient 9*   **(b)** *Patient 10*
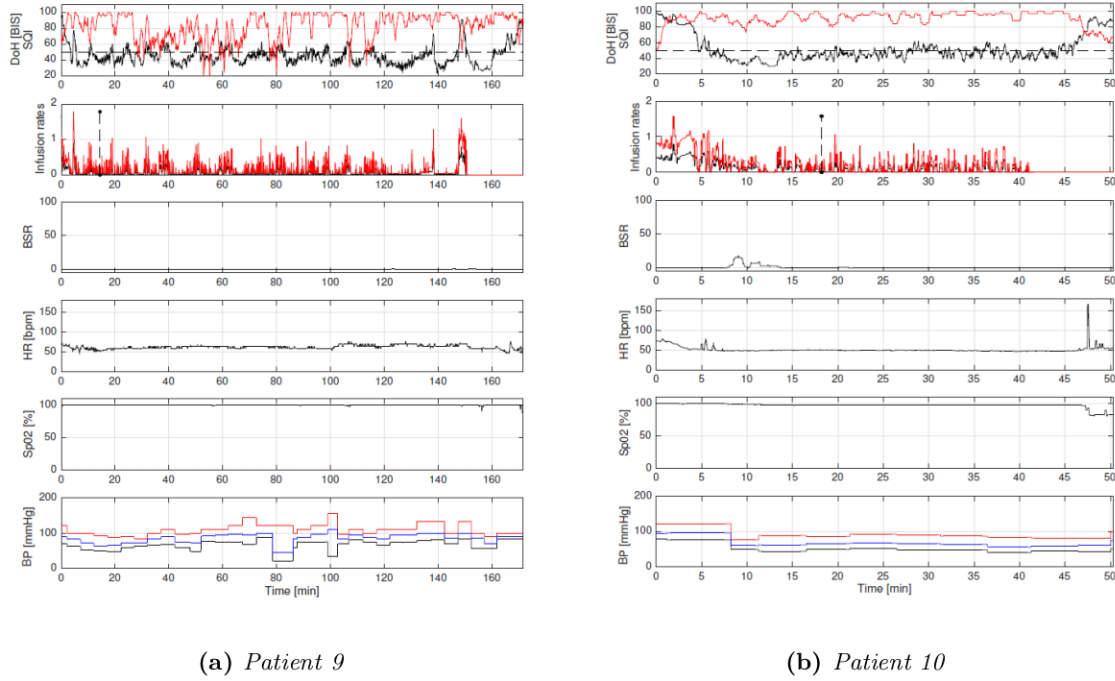
Figure 3.5: *Recorded clinical data of the patients enrolled with the PID-based MISO controller. First plot from the top: BIS level of the patient (black solid line), SQI (red solid line) and the BIS set-point (black dashed line). Second plot from the top: propofol infusion rate expressed in mg/kg/min (black solid line) and remifentanil infusion rate expressed in μg/kg/min (red solid line). Third plot from the top: BSR. Fourth plot from the top: HR. Fifth plot from the top: SpO_2. Sixth plot from the top: BP_s (red solid line), BP_d (black solid line) and BP_m (blue solid line).*

Patient	Duration	BIS [40-60]		BIS>60		BIS<40		BIS-NADIR	T awakening
	[min]	[min]	[%]	[min]	[%]	[min]	[%]		[min]
1	37.93	36.52	96.27	0.12	0.31	1.30	3.43	36	5.10
2	63.82	53.32	83.55	1.60	2.51	8.90	13.95	27	8.88
3	31.50	22.78	72.33	0.00	0.00	8.72	27.67	27	6.10
4	369.87	321.22	86.85	8.87	2.40	39.78	10.76	25	2.48
5	30.75	29.20	94.96	0.03	0.11	1.52	4.93	35	8.35
6	52.50	35.30	67.24	1.62	3.08	15.58	29.68	29	6.40
7	102.07	51.03	50.00	10.93	10.71	40.10	39.29	22	10.88
8	69.53	56.85	81.76	5.20	7.48	7.48	10.76	25	5.02
9	140.90	89.97	63.85	5.67	4.02	45.27	32.13	23	19.07
10	31.02	25.20	81.25	0.07	0.21	5.75	18.54	30	6.52
Average	-	-	77.81	-	3.08	-	19.11	28	7.88

Table 3.6: *Performance indexes for the maintenance phase obtained with the PID-based MISO controller.*

	Manual (n=33)	Closed-loop (n=10)
Age	58 (43-90)	57 (39-88)
Gender (M/F)	12/21	5/5
Height [cm]	164 (148-175)	172 (160-190)
Weight [kg]	67 (40-115)	80 (58-100)

Table 3.7: *Demographic data of the patients enrolled with manually controlled anesthesia and with the PID-based MISO controller. Data are presented as mean (range).*

	Manual (n=33)	Closed-loop (n=10)
TT [min]	2.9 (0.8-5.4)	3.8 (2.6-5.4)
BIS-NADIR	27 (15-45)	33 (28-39)

Table 3.8: *Induction phase performance comparison between manually controlled anesthesia and closed-loop anesthesia performed with the PID-based MISO controller. Data are presented as mean (range).*

	Manual (n=33)	Closed-loop (n=10)
Duration [min]	77 (20-130)	62 (30-370)
BIS [40-60] [%]	43 (1-81)	78 (50-96)
BIS>60 [%]	5 (0-35)	3 (0-11)
BIS<40 [%]	52 (0-99)	19 (3-40)
BIS-NADIR	22 (13-30)	28 (22-36)
MDPE [%]	-19.5 (-52 - 18)	-7.8 (-18 - -2)
MDAPE [%]	27.5 (14-52)	14 (8-22)
WOBBLE [%]	49.2 (16-104)	25.0 (14-42)
T awakening [min]	10 (2-27)	8 (2-19)

Table 3.9: *Maintenance phase performance comparison between manually controlled anesthesia and closed-loop anesthesia performed with the PID-based MISO controller. Data are presented as mean (range).*

3.2 Modified PID-based MISO control scheme

3.2.1 Introduction

In this section, a modified version of the control scheme proposed in Section 3.1 is presented. It has been designed to take into account specific requirements related to the clinical practice that have been suggested by the anesthesiologist who performed the clinical experiment described in Section 3.1. However, it is worth noting that clinical requirements might be slightly different depending on the anesthesiologist.

In particular, in addition to the PID based continuous regulation of the infusions, the control system automatically administers propofol and remifentanil boluses at the beginning of the induction phase. This addition to the original control system has been implemented to bridge the gap between the automatic regulation and the clinical practice by delivering a faster loss of consciousness. In this way, the risk for patients to experience discomfort and anxiety due to pain on propofol injection is reduced and better conditions for manually assisted ventilation are created. Indeed, even if in Section 3.1 the PID controller alone was sufficient to adequately induce anesthesia and no problems were experienced during the insertion of laryngeal mask or endotracheal tube, the anesthesiologist might prefer the use of a bolus to fully ensure a rapid induction phase. This phase is critical, indeed anesthesia must be induced in a short time in order to rapidly secure the patient's airway. Concurrently, overdosing must be avoided as it can provoke side-effects such as severe arterial hypotension. Taking these issues into account, control solutions specifically designed for the induction phase have been proposed in the literature. To formally guarantee overdosing prevention, an explicit reference governor control scheme has been proposed in [116]. In [62] a fixed volume of propofol is administered as bolus at the beginning of anesthesia to reduce the induction time. In [67] an induction sequence of an initial bolus of propofol followed by a continuous infusion is employed. The propofol dosage is calculated based on the patient's weight. Being a feedforward approach, it guarantees that the desired amount of drug is administered but it has the disadvantage of not taking into account the actual value of DoH. In [63] the derivative action of a PID controller is exploited to produce a bolus of propofol at the beginning of anesthesia induction. This is a feedback approach that takes into account the actual value of DoH but, in case of loss of the feedback signal, it does not guarantee that the desired amount of drug is administered to the patient. In this section, both boluses of propofol and remifentanil are automatically administered by the control system while control solutions proposed so far consider only propofol. Moreover, here, a combined feedforward/feedback approach is proposed. The first phase of induction is performed by administering the drug boluses in feedforward. However, the dose of drugs administered with the boluses is not sufficient to reach the target level of DoH. Hence, the induction phase is completed in feedback by the PID controller. This allows the advantages of both feedforward and feedback approaches to be combined.

Another improvement of the original algorithm is the administration of a nonzero baseline infusion during the maintenance phase when the predicted effect-site concentration drops below a safety threshold. These baseline infusions are inherited form the clinical practice where drug infusions are never set to zero during the maintenance phase. Conversely, this might occur when a PID controller is used and the BIS value is below the set-point value. The baseline infusions also help to avoid the oscillations in the feedback variable observed in three patients of Section 3.1. This situation occurs because, during phases of low surgical stimulation, the BIS remains below the target value for long time intervals. Consequently,

the infusions are zero and the drugs are metabolized. This should be avoided as, when the surgical stimulation is resumed, the drug dosage is not sufficient to compensate for it. This causes a quick surge of the BIS that is compensated by the controller resulting in a subsequent reduction of the BIS and to the possible repetition of the phenomenon. Although no negative clinical consequences were observed, it appeared that the performance could have been improved. By introducing the baseline infusions, the system always guarantees that a minimum amount of drug is administered to the patient, thus preventing an excessive increase of the BIS. To account for the different metabolization times, the baseline infusions for propofol and remifentanil are handled separately. The introduction of baseline infusions and of safety constraints on the effect-site concentrations have been already proposed and discussed in the literature. In [117, 118] safety constraints on the minimum and maximum values of propofol effect-site concentration have been considered by imposing a saturation of the control action when the bounds are reached. In [83] safety bounds on the effect-site concentrations of both propofol and remifentanil are considered. In [119] a baseline infusion of remifentanil is administered in order to guarantee a desired effect-site concentration. These methodologies impose fixed bounds on the estimated effect-site concentrations of the drugs. However, due to model uncertainties and to the high variability of the response to drug administration, the imposed bounds could be inappropriate for some patients. In this case, the anesthesiologist must intervene manually to adjust those bounds. Thus, the advantage of closed-loop systems in reducing the anesthesiologist workload is partially lost. In the approach proposed in this work, the baseline infusions are activated only when the BIS is above the safety threshold of 40. By doing so, the baseline infusions are administered on the basis of the effect-site concentration estimated by the model and by the actual level of DoH of the patient. Thus, the risk of overdosing is reduced and the manual intervention of the anesthesiologist is not required. The effectiveness of the changes described above has been experimentally assessed on a population of 10 patients undergoing general anesthesia for elective plastic surgery and the obtained experimental results are presented in this section.

3.2.2   Material and methods

The experimental setup and the PID-based MISO control structure considered is that described in Section 3.1.1. However, here two major modifications to the original control system are made to better match the clinical needs.
A schematic representation of the modified control system is shown in Figure 3.6. The PID controller structure and its tuning have not been changed with respect to Section 3.1.1. The two changes affect the induction phase and the maintenance phase, respectively. As regards the induction phase, the automatic induction sequence has been redesigned to administer a 1 mg/kg bolus of propofol $bolus_p(t)$ and a 1 μg/kg bolus of remifentanil $bolus_r(t)$. The boluses are given as feedforward control actions in open loop (that is, the PID controller is disconnected). The patient's weight is provided to the system and the bolus volumes of propofol and remifentanil are calculated accordingly. When the control system is started, the bolus of propofol is administered by setting the propofol infusion pump at its maximum infusion rate for the time required to administer the target volume. After a pause of 5 s the bolus of remifentanil is administered by following the same procedure with the remifentanil infusion pump. Immediately after the end of the remifentanil bolus the loop is closed and the PID controller is applied with the integral action that is reset to zero. The dosage of the bolus of propofol has been chosen according to Roberts manual infusion scheme [120],
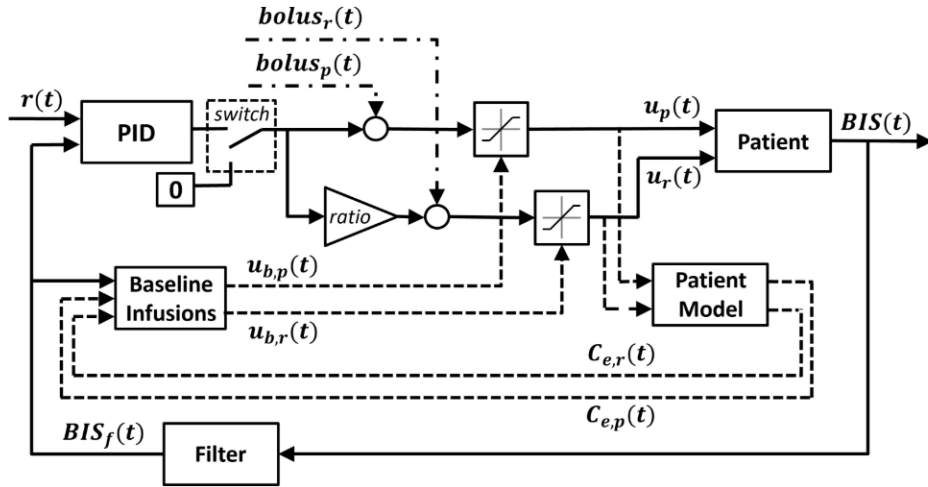
Figure 3.6: *Block diagram of the modified PID-based MISO control architecture.*

while for remifentanil it has been chosen according to the dosing guidelines reported on the remifentanil data sheet. Boluses are administered sequentially and not simultaneously as this last modality would result in a high flow rate that could damage the vein as the two drugs share the same venous access. Moreover, the propofol bolus is given before the bolus of remifentanil to ensure that propofol-induced loss of consciousness occurs before the onset of the respiratory depressive side effect of remifentanil, as this could cause discomfort to the patient.

As regards the maintenance phase, the baseline infusion of propofol $u_{b,p}(t)$ is administered when the predicted effect-site concentration $C_{e,p}(t)$ falls below a safety threshold and the low-pass filtered BIS value $BIS_f(t)$ is above 40. The same applies for remifentanil with $u_{b,r}(t)$ and $C_{e,r}(t)$. The predicted effect-site concentrations of propofol and remifentanil are calculated by using the nominal PK/PD model of Schnider [25, 26] and Minto [27], respectively, which have been implemented in the *Patient Model* block shown in Figure 3.6. In this study $u_{b,p}(t)$ and $u_{b,r}(t)$ have been set equal to 6 mg/kg/h and 0.15 μg/kg/min, respectively, while $C_{e,p}(t)$ and $C_{e,r}(t)$ have been set equal to 3 μg/ml and 4 ng/ml, respectively. These values has been chosen by considering standard dosages that are usually recommended in the clinical practice of TIVA. In particular, $u_{b,p}(t)$ and $C_{e,p}(t)$ have been chosen according to Roberts manual infusion scheme [120], while $u_{b,r}(t)$ and $C_{e,r}(t)$ has been chosen according to the guidelines reported in [121].

3.2.3 Experimental results

In this trial 10 patients scheduled for elective plastic surgery have been enrolled. Their demographic data are shown in Table 3.10 while the types of surgery and the number of patients is shown in Table 3.11. The duration of surgery, the region of the body involved, and the amount of painful stimulation vary significantly. The same clinical protocol described in Section 3.1.1 has been used. The recorded BIS, HR, BP$_m$, drugs infusion rates are shown, for each patient, in Figures 3.7-3.9. From the individual values of time courses it is possible to observe that the variables remain within clinically acceptable limits through the entire procedure and for all patients. Propofol and remifentanil infusion rates always assumed sensible

values, common for the clinical practice. The closed-loop system autonomously induced and maintained anesthesia for all the patients enrolled, without the need for the anesthesiologist to intervene.

The results achieved during the induction phase are shown in Table 3.12. A fast induction was achieved in all patients. In particular, anesthesia was induced, on average, in 2.12 min. The longest induction time of 4.68 min was observed in patient 9 and was caused by the temporary loss of the BIS signal during the induction phase. This was in turn caused by the artifacts introduced by anesthesiologist's movements during intubation. These results meet the target induction time, which, in this clinical context, i.e., elective plastic surgery, was of 3 min with the possibility to tolerate an induction time up to 5 min and no problems were reported by the anesthesiologist. For all the patients enrolled, the insertion of the endotracheal tube or the laryngeal mask was performed without difficulties or clinically relevant reactions, thus indicating an appropriate anesthetic coverage. The fast induction was achieved without causing an excessive BIS undershoot as it is possible to notice by observing the lowest BIS. In particular, the lowest average value of BIS after induction is 44. Two patients out of ten show an undershoot of the BIS below the recommended value of 40, namely patient 5 and patient 10. They have a lowest BIS of 37 and 36 respectively. However, as it is shown in Figure 3.8a and Figure 3.9d, the undershoot is short-lasting and there are no signs of hypotension or bradycardia. Moreover, none of the patients shows the onset of BS which is a phenomenon that is correlated with an excessive level of DoH. The propofol and remifentanil induction dosages are compatible with the clinical practice. In particular, on average, anesthesia is induced with 1.65 mg/kg of propofol and 2.09 μg/kg of remifentanil.

The results achieved during the maintenance phase are shown in Table 3.13. It appears that the BIS was maintained inside the recommended range for most of the maintenance time. In particular, on average, the BIS was kept inside the recommended range for the 83.17% of the maintenance time, with a minimum of 73.25% for patient 1. The system was also able to effectively reject surgical disturbances without causing excessive undershoot of the BIS. Indeed, the BIS has fallen under the recommended range, on average, for the 12.97% of maintenance time, and it has risen over 60, on average, for the 3.86% of maintenance time. These indexes show that, when the BIS is not in the recommended range, it is, for the most part, below 40 and not over 60. This is a sensible behavior because it prevents the risk of intra-operative awareness. The minimum value of BIS $40 - 60$ in this study is 73.25% and it has been obtained for patient 1, who also has the highest $BIS < 40$ value of 25.21%. Hence, this patient can be considered as the one with the higher risk of overdosing. However, by checking the propofol and remifentanil maintenance dosages, it is possible to note that they are below the average of the considered population and they are also below the recommended values used in the clinical practice of 6 mg/kg/h of propofol and 0.15 μg/kg/min of remifentanil. Moreover, the patient does not show the onset of BS. In addition, the patient does not exhibit clinical signs of hypotension or bradycardia, see Figure 3.7a. The sharp rise in the value of HR and BP recorded around minute 30 is due to the administration of an ephedrine bolus that was requested to the anesthesiologist by the surgeons in order to facilitate the hemostasis procedure. On the other hand, the patient with the highest risk of underdosing is patient 9, who has the highest $BIS > 60$ value of 7.04%. However, this patient has also the highest values of propofol and remifentanil maintenance dosages, which are above the recommended values. Moreover, hemodynamics remains stable throughout the whole surgical procedure, with no episodes of hypertension and tachycardia and no patient's movements have been reported by the anesthesiologist. The average propofol and remifentanil infusion rates are compatible

with the clinical practice. In particular, on average, anesthesia was maintained with 6.90 mg/kh/h of propofol and 0.19 μg/kg/min of remifentanil. Finally, the average T awakening of 8.11 min is fully compatible with the clinical practice.

To better evaluate the effectiveness of the additional functionalities implemented in the modified control system, a performance comparison with the previous version of the control system proposed in Section 3.1.2 is performed. For the sake of clarity, in the rest of this section the control system proposed in Section 3.1.1 will be indicated as **(a)** and the new control system proposed in this section will be indicated as **(b)**. Continuous data are analysed using a Mann-Whitney U test and categorical data are analyzed using a Fisher's Exact test [122]. Significance level is set at 5%. Data are presented with median and interquartile range (IQR). In both groups ten patients have been enrolled. Patients demographic data for both groups are compared in Table 3.14. There are no statistically significant differences between the two groups. To highlight the effect of propofol and remifentanil induction boluses, the induction performance indexes of the two control systems are compared in Table 3.15. Note that **(b)** provides a statistically significant ($P < 0.05$) reduction of the induction time and of the remifentanil induction dose, while there are no statistically significant differences ($P > 0.05$) between **(a)** and **(b)** regarding the lowest BIS and the propofol induction dose. The boxplots of the induction performance indexes are shown in Figure 3.10 where the differences between the two groups in the induction time and in the remifentanil induction dose are clearly visible. The outlier is due to patient 9. Regarding the propofol induction dose, the boxplots show that the results of the two groups are very similar. As regards the lowest BIS, although there are no statistically significant differences, **(b)** shows a reduced BIS undershoot with a smaller dispersion of values. The performance indexes of the two control systems in the maintenance phase are compared in Table 3.16 and the corresponding boxplots are shown in Figure 3.11. There are no statistically significant differences between the two groups ($P > 0.05$) for any of the considered performance indexes. However, interesting information can be obtained by observing the boxplots of Figure 3.11. The values of BIS 40-60 and BIS<40 in **(b)** show a lower dispersion with respect to those in **(a)**. On the contrary, the values of average propofol and remifentanil infusion rates show a higher dispersion in **(b)** than in **(a)**. All the other performance indexes do not show relevant differences between the two groups.

Despite the low number of patients enrolled with both control systems, interesting information can be obtained by the performance comparison in order to assess the effects of the changes made to the original control scheme. The introduction of a bolus in the induction phase has provided a reduction of the induction time. This reduces the risk for patients to experience discomfort and anxiety due to pain for the propofol injection and provides better conditions for manually assisted ventilation. The shorter induction time obtained with **(b)** has been obtained without increasing the propofol dose and reducing the administered remifentanil dose. This reduces the risk of opioid-induced side effects such as bradycardia and hypotension. Although not statistically significant, a reduced BIS undershoot with a lower variability is observed in **(b)**. This can suggest a more reliable induction of anesthesia with a reduced risk of undershoot with respect to **(a)**. In the maintenance phase there are no statistically significant differences between the two groups for the performance indexes considered. However, in **(b)**, with respect to **(a)**, there is an increase in the median value of BIS 40-60 and a reduction in the median value of BIS<40. There is also a reduction in the variability for both indexes as indicated by the IQR. This denotes a more reliable control performance. In **(b)** it is also possible to observe a greater variability of propofol and remifentanil average infusion rates. This is due to the presence of baseline infusions that are calculated based on

Patient	Age	Height [cm]	Weight [kg]	Gender
1	80	170	75	M
2	43	174	114	F
3	69	162	75	F
4	58	167	63	F
5	28	160	50	F
6	60	188	120	M
7	44	170	90	M
8	37	163	55	F
9	54	164	59	F
10	68	156	70	F

Table 3.10: *Demographic data of the patients enrolled with the modified PID-based MISO controller.*

Type of surgery	Patients involved	Patients Id
Skin cancer exeresis	4	1, 4. 7, 8
Mastoplasty	4	3, 5, 9, 10
Mastectomy	1	2
Escharotomy and microsurgical flap	1	6

Table 3.11: *Types of surgery undergone by the patients enrolled with the modified PID-based MISO controller, number of patients involved and patients identifiers.*

patient's demographic data so that the modified controller provides a patient-individualized drug administration. Both controllers **(a)** and **(b)** provided results that are fully compatible with the clinical practice for all the patients enrolled. It is worth nothing that, despite the experimentation has been carried out in the context of plastic surgery, the types of surgical procedures differs significantly in duration and level of surgical stimulation, as shown in Table 3.11. Indeed, surgical interventions such as melanoma excision and sentinel lymph node biopsy have a short duration and a relatively low level of painful stimulation. Escharotomy has a short duration but a high level of painful stimulation. Finally, mastectomy and mastoplasty are surgical interventions that last for several hours and alternate phases of strong and moderate surgical stimulation. The fact that the controller has provided a performance that is fully compatible with the clinical practice for all the types of intervention gives reason to believe that it can be also applied to different types of surgery. However, a definitive answer can only be obtained through experimentation in other operating scenarios.

3.3   Clinical evaluation

Following the good clinical results obtained in the experiment described in Section 3.2, the modified PID-based control scheme for propofol and remifentanil coadministration has been tested on a wider population. In particular, 42 patients undergoing general anesthesia for elective plastic surgery have been enrolled. The evaluation of DoH, hemodynamic stability, drug consumption, response to painful stimulation and quality of post-operative phase have been performed.

The same controller described in Section 3.2.2 has been used and the same clinical protocol described in Section 3.1.1 has been considered. Here, also hemodynamic variables and the

(a) *Patient 1*   **(b)** *Patient 2*

(c) *Patient 3*   **(d)** *Patient 4*
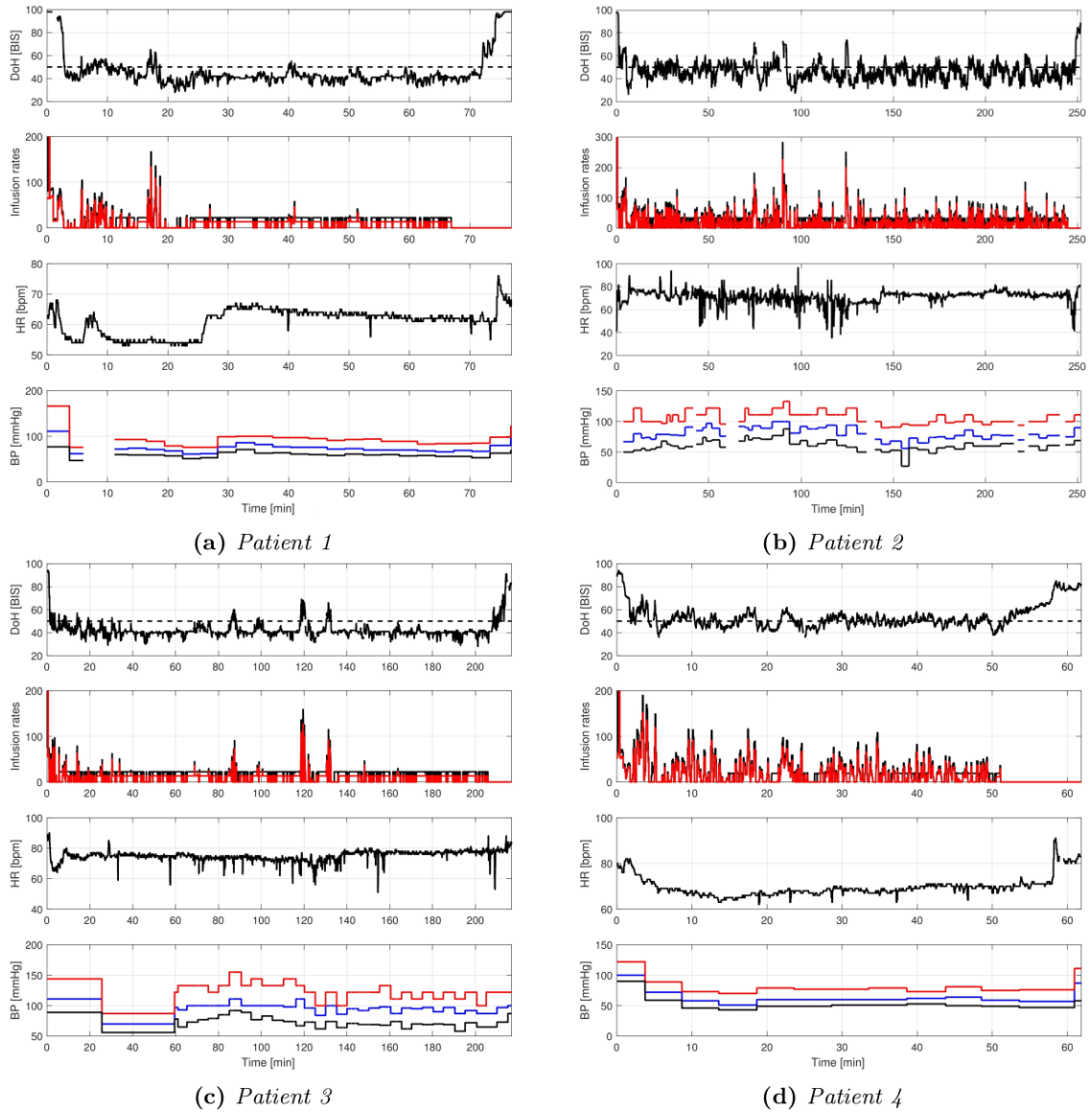
Figure 3.7: *Recorded clinical data of the patients enrolled with the modified PID-based MISO controller. From top to bottom: BIS (solid line) and BIS set-point (dashed line); propofol (black) and remifentanil (red) infusion rates in ml/h; HR; BP_s (red), BP_d (black) and BP_m (blue). In patient 1, after the induction phase, the BIS remains steadily around the value of 40 while the controller is infusing almost only the baseline drugs infusions with the exception of a rise around minute 20 that is rapidly compensated by the controller. In patient 2, after the induction phase the BIS shows limited oscillations inside the interval from 40 to 60 with the exception of three rises around minutes 75, 20 and 125 that are rapidly compensated by the controller. The sharp rise in the value of HR and BP around minute 30 is due to the administration of ephedrine. In patient 3, after the induction phase the BIS remains steadily around the value of 40 while the controller is infusing almost only the baseline drugs infusions with the exception of three rises around minutes 90, 120 and 130 that are rapidly compensated by the controller. In patient 4, after the induction phase the BIS remains steadily inside the recommended range from 40 to 60. Missing data were due to temporary issues with sensors reading. The lack of update of the BP for Patient 3 during the first 60 min is due to a data recording issue.*

(a) *Patient 5*   (b) *Patient 6*
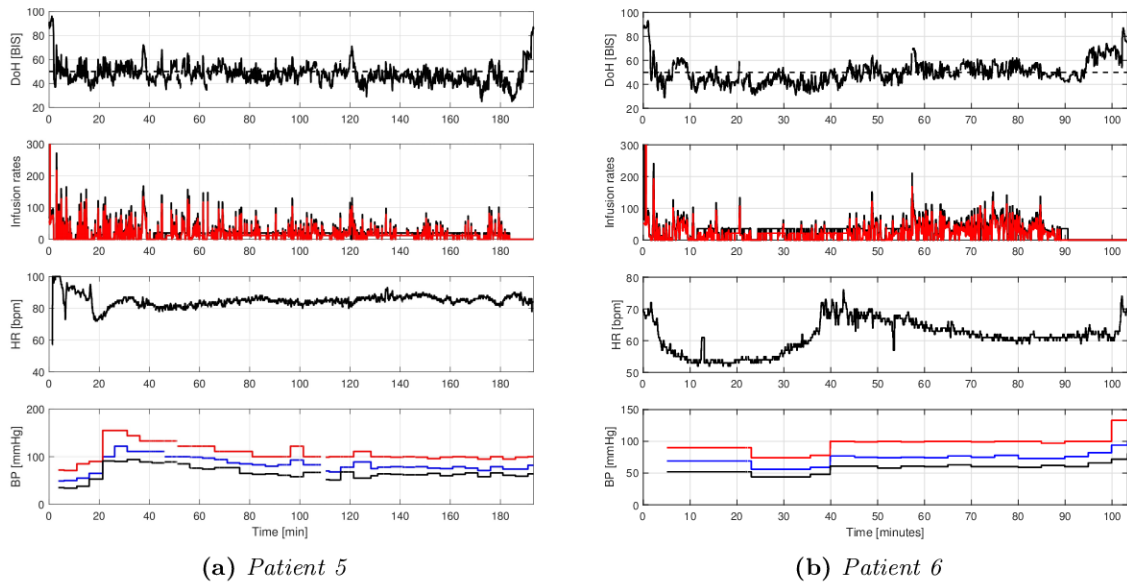
Figure 3.8: *Recorded clinical data of the patients enrolled with the modified PID-based MISO controller. From top to bottom: BIS (solid line) and BIS set-point (dashed line); propofol (black) and remifentanil (red) infusion rates in ml/h; HR; BP_s (red), BP_d (black) and BP_m (blue) blood pressure. In patient 5, the BIS shows limited oscillations inside the interval from 40 to 60 with the exception of two rises around minutes 40 and 120 that are rapidly compensated by the controller. The sharp rise in the value of HR and BP around minute 20 is due to the administration of ephedrine. In patient 6, it is possible to notice a phase of low surgical stimulation followed by a phase of strong surgical stimulation which begins around minute 40. During the first phase the BIS remains steadily around the value of 40 while the controller is infusing almost only the baseline drugs infusions. During the second phase the infusions are increased by the controller. The effect of surgical stimulation is also visible on the hemodynamic variable that increase around minute 40. However, the values remains within clinical acceptable limits and the patient does not show tachycardia or hypertension. Missing data were due to temporary issues with sensors reading*

Patient	Induction time [min]	Lowest BIS	Propofol dose [mg/kg]	Remifentanil dose [µg/kg]
1	2.73	40	1.59	2.21
2	1.65	49	1.09	1.38
3	1.18	45	1.23	1.25
4	1.7	47	1.55	1.68
5	1.87	37	2.07	2.83
6	1.55	43	1.25	1.57
7	2.05	42	1.31	1.71
8	2.7	51	2.17	2.48
9	4.68	51	2.77	4.45
10	1.07	36	1.50	1.36
Average	2.12	44	1.65	2.09

Table 3.12: *Performance indexes for the induction phase obtained with the modified PID-based MISO controller.*

(a) *Patient 7*   **(b)** *Patient 8*

(c) *Patient 9*   **(d)** *Patient 10*
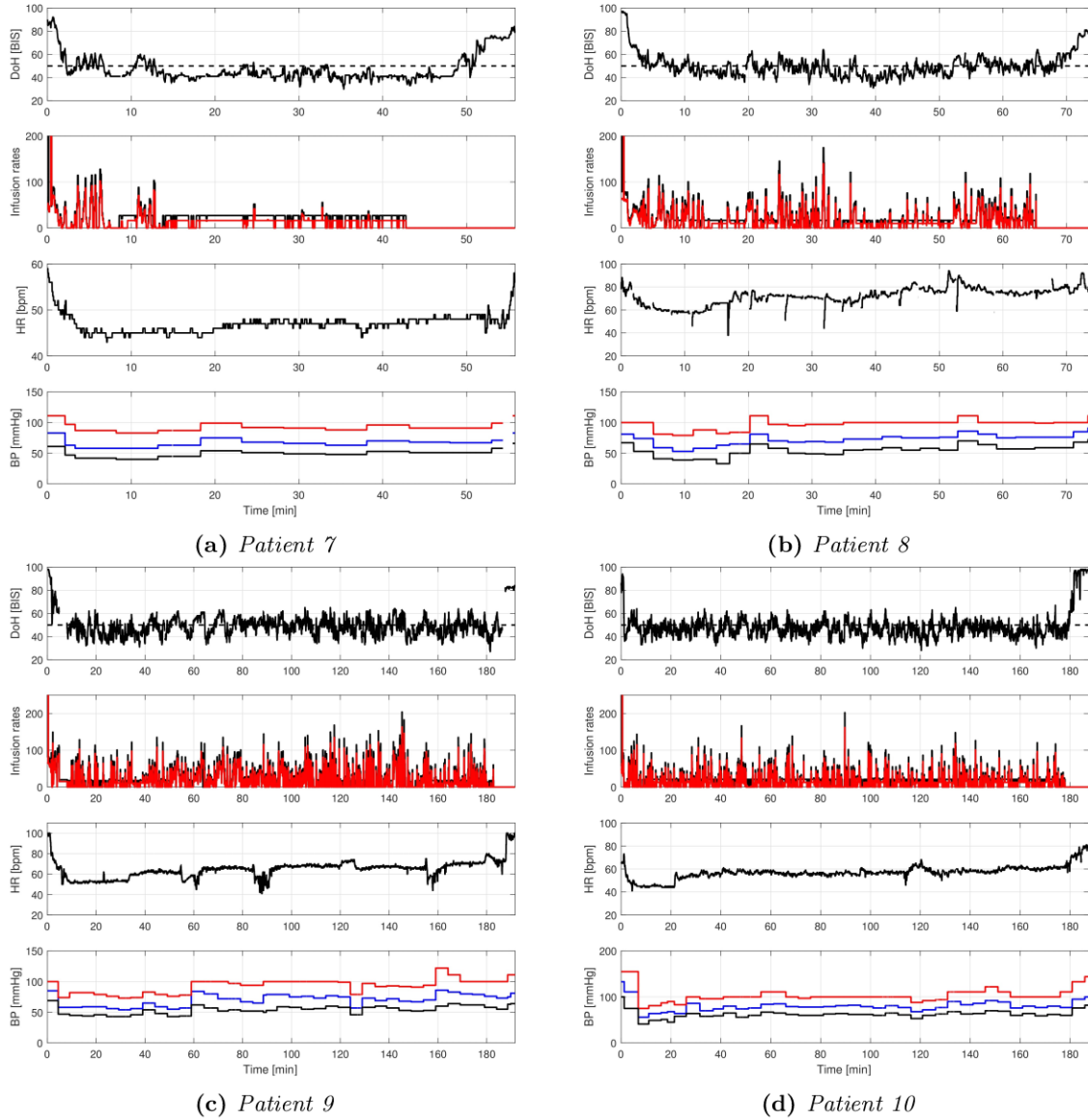
Figure 3.9: *Recorded clinical data of the patients enrolled with the modified PID-based MISO controller. From top to bottom: BIS (solid line) and BIS set-point (dashed line); propofol (black) and remifentanil (red) infusion rates in ml/h; HR; BP_s (red), BP_d (black) and BP_m (blue). In patient 7, after the induction phase the BIS remains steadily around the value of 40 while the controller is infusing almost only the baseline drugs infusions. In patients 8,9 and 10, after the induction phase the BIS shows limited oscillations inside the interval from 40 to 60. In all the patients the hemodynamic variables remain stable throughout the surgical procedure. Missing data are due to temporary issues with sensors reading.*

Patient	Duration	BIS 40 − 60	BIS < 40	BIS > 60	Propofol	Remifentanil	T awakening
	[min]	[%]	[%]	[%]	[mg/kg/h]	[μg/kg/min]	[min]
1	64.18	73.25	25.21	1.54	4.55	0.12	7.57
2	243.17	73.97	20.40	5.63	5.38	0.12	10.13
3	204.67	75.15	22.00	2.85	4.78	0.12	8.4
4	49.40	93.83	1.55	4.62	8.16	0.23	7.12
5	181.77	86.59	8.00	5.41	9.82	0.30	8.48
6	89.03	84.14	11.77	4.09	5.48	0.16	11.25
7	40.70	87.06	11.43	1.51	5.28	0.14	12.30
8	62.50	89.73	7.15	3.12	9.29	0.26	6.73
9	178.15	81.77	11.19	7.04	9.17	0.27	5.08
10	176.93	86.25	10.97	2.78	7.04	0.17	4.00
Average	129.05	83.17	12.97	3.86	6.90	0.19	8.11

Table 3.13: *Performance indexes for the maintenance phase obtained with the modified PID-based MISO controller.*

	(a)	(b)	P value
Age [years]	52.5 (9)	56.0 (25)	1.00
Height [cm]	172.0 (9)	165.5 (8)	0.17
Weight [kg]	81.5 (10)	72.5 (31)	0.34
Gender [M/F]	5/5	3/7	0.65

Table 3.14: *Demographic data comparison between the patients enrolled with the standard (a) and with the modified (b) PID-based MISO controller. Data are presented as median (IQR), gender is expressed as male/female ratio. There are no statistically significant difference between the two groups (P > 0.05).*

	(a)	(b)	P value
Induction time [min]	3.80 (1.28)	1.78 (0.96)	0.0028*
Lowest BIS	42 (9)	44 (8)	0.3066
Propofol dose [mg/kg]	1.64 (0.81)	1.53 (0.69)	0.7337
Remifentanil dose [μg/kg]	3.14 (1.63)	1.69 (0.98)	0.0140*

Table 3.15: *Comparison of the performance indexes for the induction phase obtained with the standard (a) and with the modified (b) PID-based MISO controller. Data are presented as median (IQR). Statistically significant differences between groups are marked with an asterisk (P < 0.05).*

	(a)	(b)	P value
BIS 40-60	79.79 (22.54)	85.20 (10.13)	0.3075
BIS<40	17.47 (23.15)	11.31 (9.50)	0.3447
BIS>60	2.97 (3.29)	3.60 (2.42)	0.5708
Propofol [mg/kg/h]	5.85 (1.14)	6.26 (3.61)	0.4274
Remifentanil [μg/kg/min]	0.20 (0.04)	0.17 (0.13)	0.7337
MDPE [%]	-9 (6.5)	-7 (10)	0.6189
MDAPE [%]	11 (6.5)	10 (5)	0.7198
WOBBLE [%]	9.2 (3.5)	7.2 (4.5)	0.5403
T awakening [min]	6.46 (4.10)	7.51 (2.92)	0.8501

Table 3.16: *Comparison of the performance indexes for the maintenance phase obtained with the standard (a) and with the modified (b) PID-based MISO controller. Data are presented as median (IQR). There are no statistically significant difference between the two groups (P > 0.05).*
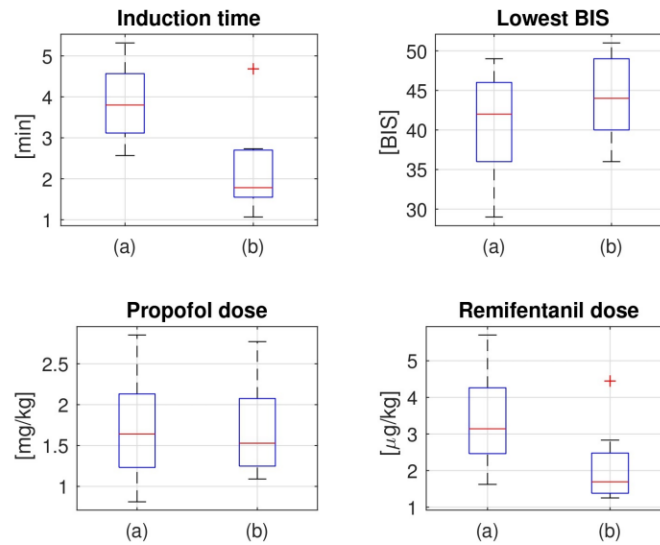
Figure 3.10: *Boxplots of induction performance indexes obtained with the standard **(a)** and with the modified **(b)** PID-based MISO controller. The red horizontal line indicates the median. The bottom and the top edges of the blue box indicate the 25th and the 75th percentiles, respectively. The whiskers indicate the maximum and minimum considered values. Outliers are plotted individually with a red cross.*
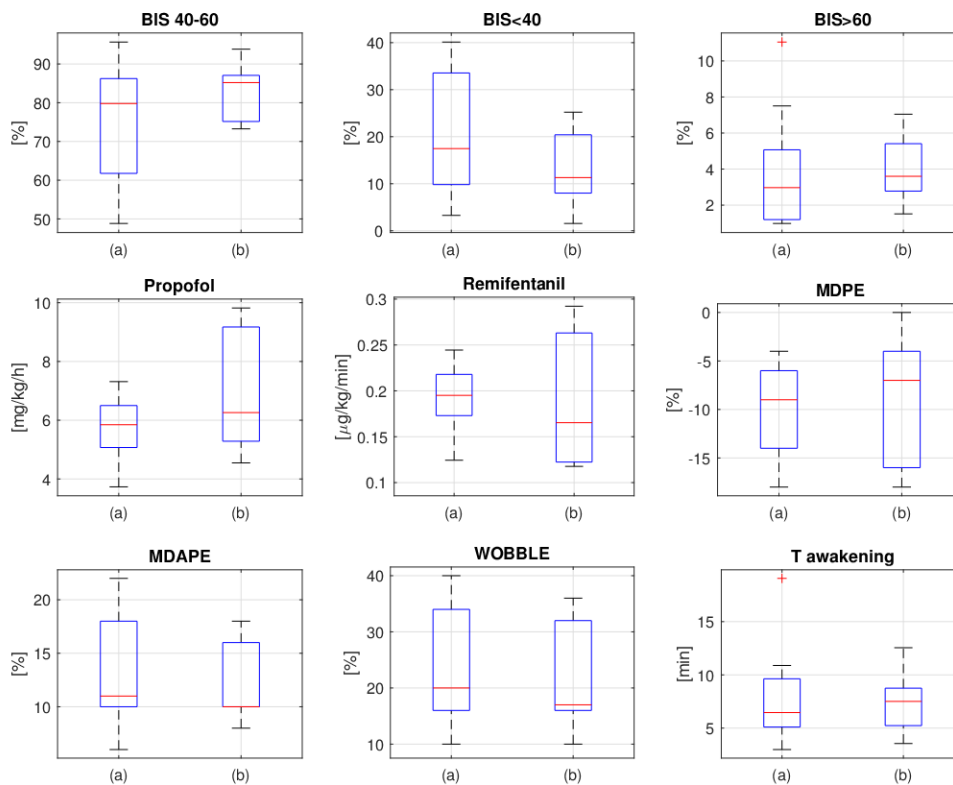
Figure 3.11: *Boxplots of maintenance performance indexes obtained with **(a)** and with **(b)**. The red horizontal line indicates the median. The bottom and the top edges of the blue box indicate the 25th and the 75th percentiles, respectively. The whiskers indicate the maximum and minimum considered values. Outliers are marked individually with a red cross.*

SS	Description
0	Awake
1	Asleep, awakened with verbal stimulus
2	Asleep, awakened with tactile stimulus
3	Asleep, awakened with tactile stimulus
3	Asleep, difficult to awake

Table 3.17: *Sedetion score used to assess post-operative sedation.*

PONV	Description
0	No nausea
1	Nausea
2	Unproductive retching
3	Vomiting

Table 3.18: *Scale used to assess PONV.*

quality of the post-operative phase have been assessed. The latter is assessed by the anesthesiologist during routine post-operative follow up. In particular, hemodynamic stability, post-operative sedation, PONV and post-operative pain are assessed at recovery room arrival and discharge, 8 hours post-surgery and 24 hours post-surgery. Hemodynamic stability has been assessed by measuring HR and BP_m. Post-operative sedation has been assessed with the sedation score (SS) shown in Table 3.17. PONV has been assessed with the scale from 0 to 3 shown in Table 3.18. Post-operative pain has been assessed with numeric rating scale (NRS) from 0 (no pain) to 10 (unbearable pain).

The enrolled patients cover a wide range of physical characteristics as shown in Table 3.19. They were all patients scheduled for elective plastic surgery, in particular the types of surgery and the number of patients who undergone them is shown in Table 3.20. These types of surgery differ considerably in duration, involved region of the body and level of painful stimulation.

The time courses of BIS, HR, BP_m, propofol infusion rates are shown in Figure 3.12. In particular, as it is typically done in the literature, in these figures the time course of each variable for each patient of the population is shown along with median values, 10th and 90th percentiles. The time course of remifentanil infusion rate is not shown since it is simply a scaled version of that for propofol infusion rate. In particular, in Figure 3.12a the time course of BIS is shown. From the individual values it is possible to observe that the BIS always remains within clinically acceptable limits for all patients. There was only a more pronounced undershoot event for one patient around minute 200. It is also possible to observe that the median BIS values remain within the recommended range from 40 to 60, slightly below the target value of 50. The 10th and 90th percentiles are slightly below the values of 40 and 60 respectively. The time courses of the hemodynamic variables HR and BP_m are shown in Figures 3.12b and 3.12c, respectively, where it is possible to observe that they always remains within clinically acceptable limits for all patients. Propofol infusion rates are shown in Figure 3.12d where it is possible to observe that they always assume values that are sensible for the clinical practice.

(a) *BIS*

(b) *HR*

(c) BP_m

(d) *Propofol infusion rate*
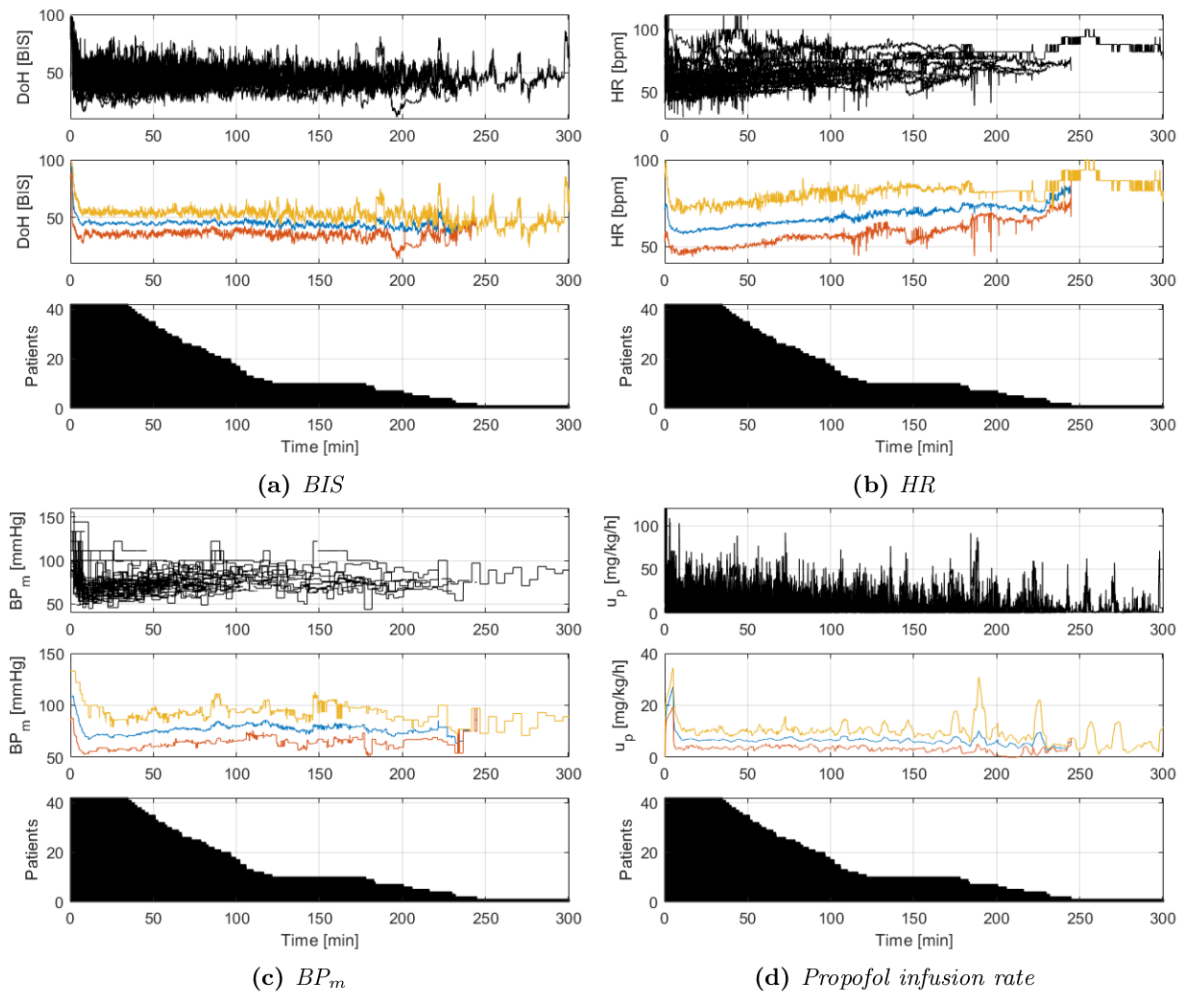
Figure 3.12: *Time courses of clinical variables from induction to end of surgery of the 42 patients enrolled with the modified PID-based MISO controller. The top plot shows the values for all patients. The middle plot shows the median values (blue solid line), 10th percentile (red solid line) and 90th percentile (yellow solid line). For propofol infusion rate data are averaged for graphical representation with a moving average filter of 5 min duration. The bottom plot shows the number of patients still undergoing surgery at each time instant.*

Age [years]	58 (28-90)
Height [cm]	167 (154-188)
Weight [kg]	74 (50-120)
Gender (M/F)	15/27

Table 3.19: *Demographic data of the patients enrolled with the modified PID-based MISO controller in the study on a wide population. Age, height and weight are expressed as mean (range). Gender is expressed as number of male patients/number of female patients.*

Type of surgery	Number of patients
Melanoma excision and sentinel lymph node biopsy	17
Mastoplasty	10
Mastectomy	8
Electrochemotherapy	3
Escharotomy and microsurgical flap	2
Scalp tumor excision	1
Blepharoplasty	1

Table 3.20: *Types of surgery and number of patients who undergone them in the study on a wide population performed with the modified PID-based MISO controller.*

3.3.1   Induction phase

For the induction phase the results obtained are shown in Table 3.21. The lowest HR and BP_m are the minimum values of these hemodynamic variables observed in the 180 s following the induction time. Patients requiring ephedrine bolus is the number of patients for whom the anesthesiologist has deemed it appropriate to administer vasopressors following induction. Patients with BS episode is the number of patients who have experienced an episode of BS in the 180 s following induction. A BS episode occurs when BSR>10% for at least 60 s [123]. BS is a condition that should be avoided as it is an indicator of excessively deep anesthesia and it has been associated with the onset of post-operative delirium [124]. By observing the values shown in Table 3.21, it is possible to notice that the control system delivered satisfactory results. Anesthesia has been rapidly induced in all patients. No problems were reported by the anesthesiologists during the insertion of the invasive ventilation device, thus indicating an appropriate anesthetic coverage. The rapid induction has been achieved without causing excessively deep hypnotic states or drug induced side effects, such as hemodynamic instability, as suggested by the limited onset of BS episodes and the limited administration of ephedrine boluses. In particular, BS occurred in a 90 years old male patient and in a 69 years old female patient undergoing electrochemotherapy. The onset of BS in the first patient could be due to the presence of both the main risk factors for BS, i.e. advanced age and male gender [123], while for the second patient it could be due to age and medical history.

3.3.2   Maintenance phase

For the maintenance phase, the results obtained are shown in Table 3.22. Mean HR and BP_m are calculated on the maintenance duration. Patients requiring ephedrine bolus is the number of patients who required treatment for hypotension during the maintenance phase. Patients with BS episode is the number of patients who experienced at least one BS episode

Induction time [s]	137 (64-322)
Propofol dose [mg/kg]	1.8 (1.1-3.0)
Remifentanil dose [μg/kg]	2.3 (1.2-5.0)
Lowest BIS	43 (28-56)
Lowest HR [bpm]	54 (35-89)
Lowest BP$_m$ [mmHg]	72 (46-144)
Patients requiring ephedrine bolus	8
Patients with BS episode	2

Table 3.21: *Performance indexes for the induction phase obtained with the modified PID-based controller on a wide population. Data are presented as mean (range) with the exception of patients requiring ephedrine bolus and patients with BS episode which are expressed as numbers.*

during the maintenance phase. BS max and max duration are the maximum BSR value and the duration of the longest BS episode recorded during the maintenance phase. From Table 3.22, it is possible to notice that the control system delivered satisfactory results even during the maintenance phase. In particular, anesthesia was adequately maintained and manual interventions were never required. The BIS was maintained inside the recommended range for most of the maintenance time and a good hemodynamic stability was maintained as shown by the mean values of HR and BP$_m$ and by the reduced number of patients who required pharmacological treatment for hypotension. The mean propofol and remifentanil infusions are compatible with the doses commonly used in the clinical practice. As for the induction phase, the number of patients experiencing BS episodes is limited and, with the exception of one patient, it only occurred in elderly patients. The performance obtained by the system in maintaining the BIS inside the recommended range is highlighted in Figure 3.13a, where the histogram of all the BIS samples collected on the study population during the maintenance phase is shown. It has the BIS on the horizontal axis. On the vertical axis it has the normalized number of samples, which is obtained by dividing the number of samples in each bin of the histogram by the total number of samples collected. Omitting the unusual peak in the distribution at the value of 41, which could be due to the BIS calculation algorithm as pointed out in [125], the average BIS for each patient assume a normal distribution with its mean at 45. It is worth noting that, as observed in Figure 3.12a, the BIS values are slightly below the target value of 50. Moreover, in Figure 3.14a, the histogram of the percentage of BIS inside the recommended range from 40 to 60 during the maintenance phase is shown. On the vertical axis it has the normalized number of patients, which is obtained by dividing the number of elements in each bin of the histogram by the total number of patients enrolled. The system kept the BIS inside the recommended range for more than 70% of maintenance time in more than 70% of the patients enrolled. The results related to MDPE, MDAPE and WOBBLE are shown in Figures 3.14. The histograms have on the horizontal axis the values of MDPE, MDAPE and WOBBLE respectively. On the vertical axis they have the normalized number of patients which is obtained by dividing the number of elements in each bin of the histogram by the total number of patients enrolled. The negative MDPE values confirm that the system tends to keep the BIS below the target value of 50. In particular the mean value of -10 indicates that the system tends to keep the BIS around 45. From Figure 3.14b it is possible to observe that in the 95% of patients the bias remains bounded between -20% and 5% of the target. The mean MDAPE value indicates that the system achieves, on average, an inaccuracy of 12% with respect to the BIS target. From Figure 3.14c it is possible to observe

that, like for MDPE, in the 95% of patients the inaccuracy remains bounded between 5% and 20% of the target. The mean WOBBLE indicates that the impact of intra-patient variability on the performance error is, on average, of about 11% of the target value. From Figure 3.14d it is possible to observe that in the 85% of patients WOBBLE remains bounded between 6% and 14% of the target value. The good performance with respect to hemodynamic stability is also highlighted in Figures 3.13b and 3.13c, where it is possible to observe that the values of HR and BP_m are distributed over clinical acceptable values during the maintenance phase of anesthesia. The histograms have on the horizontal axis HR and BP_m respectively. On the vertical axis they have the normalized number of samples which is obtained by dividing the number of samples in each bin of the histograms by the total number of samples collected.

In order to evaluate the analgesic coverage, the response to incision has been evaluated. In particular, after anesthesia induction the sterile surgical field is prepared. Then, approximately 15 min elapse between anesthesia induction and incision. During this time interval patients do not receive any surgical stimulation. Hence, when the surgeon begins the incision it can be seen as the beginning of the nociceptive stimulation and the patient's response can be used to assess the anesthetic coverage. In order to do so, the beginning of incision is noted by the anesthesiologist using the GUI shown in Figure 2.8. Then BIS, HR and BP_m are assessed 2 min before incision, at the time of incision and 2, 5 and 10 min after incision. The results for all the patients of the study are shown in Figure 3.15. The hemodynamic variables remained stable even in presence of surgical stimulation, thus indicating an adequate analgesic coverage. The BIS shows a slight increase in the 2 min after incision that could be due to the arousal caused by the beginning of the surgical stimulation. However, it is worth noting that the BIS remains bounded inside the recommended range and then at 5 and 10 min after incision the BIS returns at the pre-incision values thanks to the control system regulation. Moreover, no somatic events were reported by the anesthesiologist during incision. These results suggest the effectiveness of the opioid-hypnotic balance methodology employed in this study.

In order to further characterize the performance of the control system the best and worst cases are analyzed. The full time course of the BIS for the patients that obtained the best and the worst performance are shown in Figure 3.17. These two patients obtained the best and worst performance respectively in terms of percentage of BIS inside the recommended range (22% and 94% respectively), MDPE (0% and -32% respectively), MDAPE (8% and 32% respectively) and WOBBLE (6% and 20% respectively). The worst performance has been obtained in a 70 years old female patient undergoing mastectomy, while the best performance has been obtained in a 58 years old female patient undergoing mastoplasty. By observing the BIS time course of the best patient it is possible to observe that, after anesthesia induction, the BIS enters inside the recommended range and stably remains inside it until the emergence phase. On the contrary, for the worst patient, the BIS settles below the recommended range for most of the duration of the surgery. The BIS shows two rises that could be due to arousal resulting from surgical stimulation. In particular the first one corresponds to tumor resection and the second one to breast implant insertion. It is worth noting that the controller has been able to rapidly compensate for both surgical disturbances without any intervention by the anesthesiologist. The first disturbance has been compensated without causing an excessive undershoot of the BIS, while for the second one an undershoot occurred. However, this situation was not harmful for patient's health as hemodynamics remained stable and the emergence phase was fast (extubation after 469 s) and of good quality (SS=1 was reported in the recovery room without any other side effect). The fact that BIS remained below the target range in the

Maintenance duration [s]	6348 (1890-17755)
40≤BIS≤60 [%]	76 (22-94)
BIS<40 [%]	19 (2-73)
MDPE [%]	-10 (-32 - 2)
MDAPE [%]	12 (8 - 32)
WOBBLE [%]	11 (6 - 20)
Mean HR [bpm]	63 (46-88)
Mean BP$_m$ [mmHg]	73 (55-104)
Propofol mean infusion [mg/kg/h]	6.64 (3.87-9.82)
Remifentanil mean infusion [μg/kg/min]	0.19 (0.02-0.32)
Patients requiring ephedrine bolus	14
Patients with BS episode	9
BS max [%]	27 (10-71)
BS max duration [s]	354 (64-842)

Table 3.22: *Performance indexes for the maintenance phase obtained with the modified PID-based controller on a wide population. Data are presented as mean (range) with the exception of patients requiring ephedrine bolus and patients with BS episode which are expressed as numbers.*

worst patient could be caused by the baseline infusions of propofol and remifentanil. Indeed, this offset is present even in other patients as highlighted by the mean value of MDPE, and by observing Figures 3.12a and 3.13a. For most patients this offset remains within the recommended BIS range, while for some patients (such as the worst one) this offset causes the BIS to drop below the recommended range. This effect may be due to the fact that, in this study, the baseline flow rates were decided in advance and left unchanged for each patient. So for some patients who have a lower need for drugs this may have led to the introduction of a more pronounced offset of the BIS. For example, Figure 3.16 shows the time course of BIS and of the infusion rates of a 59 years old male patient undergoing melanoma excision and sentinel lymph node biopsy. The BIS remained mostly around the value of 40 manly using only baseline infusions. On the other side, the introduction of these baseline infusions appear to have been effective in reducing the onset of oscillations. Indeed, in the experimentation presented in Section 3.1 3 out of 10 patients showed oscillations in the BIS while in this study none of the patients showed low frequency, periodic oscillations. Rises in the BIS value are still present in this study, but they are compensated by the controller without triggering oscillations.

In order to assess the performance in the emergence phase the time to extubation has been assessed. It ranges from 198 s to 839 s with a mean value of 511 s. These values are comparable with the one usually obtained in the clinical practice of TIVA. The number of patients of that are still intubated at each time instant during the emergence phase is shown in Figure 3.18.

3.3.3 Post-operative phases

As regards the post-operative phase, the main results are summarized in Table 3.23. The number of patients decreases when the time window increases since some have been discharged from the hospital prior to data collection. Hemodynamics remained stable in all patients as shown by the values of HR and BP$_m$. Only a reduced number of patients showed a SS greater than 0 and for none of them SS was greater than 1. PONV has only been observed in a

Figure 3.13: *Histogram of BIS, HR and BP_m collected during the maintenance phase on the 42 patients enrolled with the modified PID-based MISO controller. The black vertical dashed lines in the BIS samples histogram represent the recommended range boundaries.*

Figure 3.14: *Histograms of the percentage of BIS in the range from 40 to 60, MDPE, MDAPE and WOBBLE obtained on the 42 patients enrolled with the modified PID-based MISO controller during the maintenance phase.*

Figure 3.15: *Box plot of BIS, HR and BP_m collected during incision on the 42 patients enrolled with the modified PID-based MISO controller. On each box the central red line represents the median, bottom and top blue edges represent the 25th and 75th percentiles, respectively. The black whiskers represent the range. Outliers are marked individually with red crosses. The horizontal axis represents the time difference with respect to incision time. The statistics are calculated on the 60 s preceding the instant of time reported on the horizontal axis.*
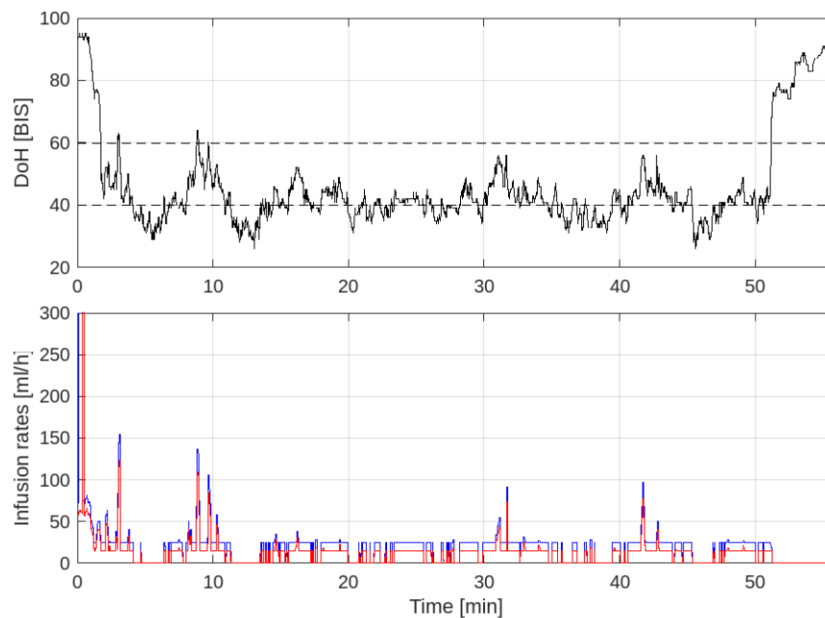
Figure 3.16: *Time course of the BIS (black solid line), propofol infusion rate (blue solid line) and remifentanil infusion rate (red solid line) of a 59 years old male patient undergoing melanoma excision and sentinel lymph node biopsy enrolled with the modified PID-based MISO controller in the study on a wide population. The BIS target range is shown with dashed lines.*
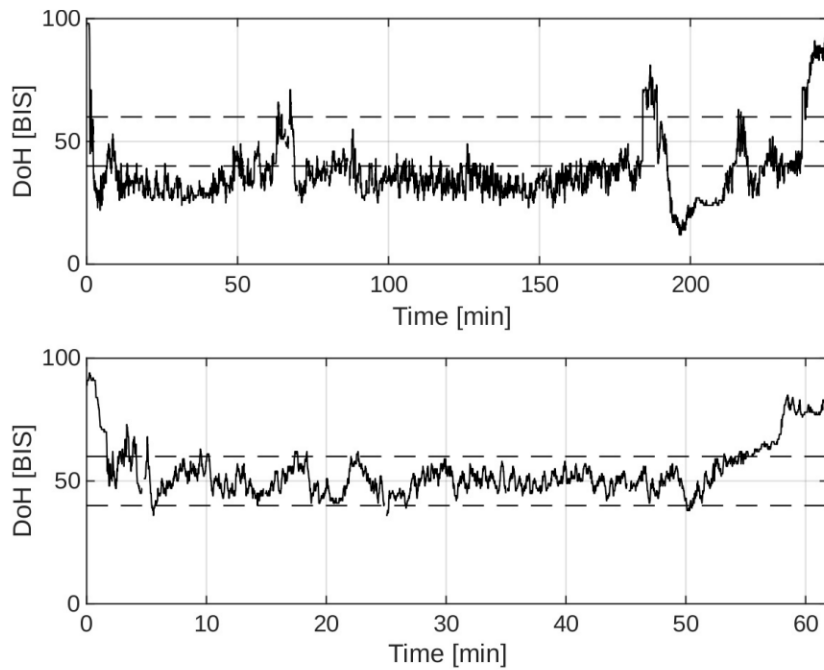
Figure 3.17: *Time course of the BIS for the patients that obtained the worst (top plot) and the best (bottom plot) performance among the 42 patients enrolled with the modified PID-based MISO controller. The BIS is shown with solid line and the BIS target range is shown with dashed lines.*
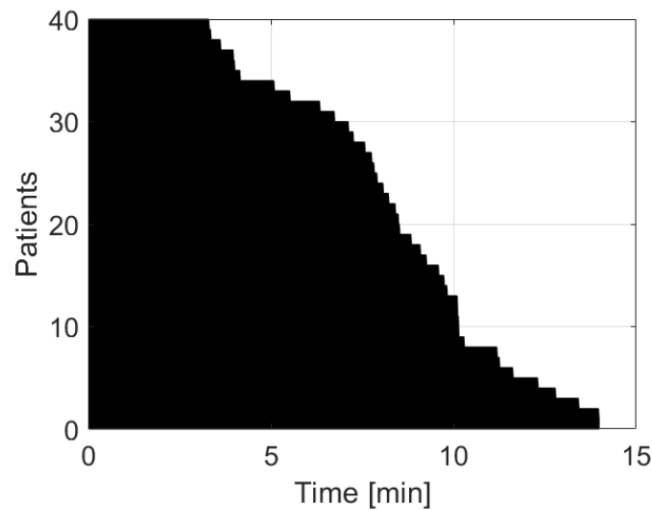
Figure 3.18: *Extubation times obtained with the modified PID-based MISO controller in the study on a wide population. The horizontal axis shows the elapsed time from the end of automatic control and the vertical axis the number of patients that is still intubated.*

	Ra	**Rd**	**8h**	**24h**
Total number of patients	42	42	41	31
HR	75 (52-118)	75 (50-110)	75 (56-110)	75 (60-100)
BP$_m$	81 (62-113)	84 (64-113)	90 (71-112)	83 (73-113)
Patients with SS>0	9	6	1	0
Patients with NRS>0	12	14	17	10
Patients with PONV>0	1	3	2	1

Table 3.23: *Post-operative evaluation summary of the 42 patients enrolled with the modified PID-based MISO controller. Ra, Rd, 8h and 24h stand for recovery admission, recovery discharge, 8 hours post-surgery and 24 hours post-surgery respectively. HR and BP$_m$ are expressed as mean (range), while all the other values are expressed as numbers.*

reduced number of patients. In particular only one patient was assessed with a PONV=1 at recovery room admission. The same patient kept PONV=1 during the stay in the recovery room, while other 2 patients showed PONV=2 and PONV=3. These patients were treated with the antiemetic drug metoclopramide. Two patients experienced PONV=1 at 8 hours post-surgery. The NRS assessment of post-operative pain is shown in Figure 3.19. Post-operative pain was treated with morphine. Overall, the post-operative evaluation shows that the results obtained with the control system are comparable with the one usually obtained in the clinical practice of TIVA.

3.4 Practical use of the modified PID-based MISO control scheme

In this section, the PID-based control scheme discussed in Sections 3.2 and 3.3 is considered. Here, its performance is further assessed when additional boluses are manually administered by the anesthesiologist and different brands of infusion pumps are used. In particular, two different models of infusion pumps have been tested, namely the Graseby 3500 and the Alaris GH.
Manual boluses of propofol and remifentanil can be triggered by pressing the two orange buttons in the lower left part of the GUI shown in Figure 2.8. The top button triggers a bolus of propofol, while the bottom button triggers a bolus of remifentanil. For safety reasons, boluses are administered as long as the anesthesiologist keeps the buttons pressed and they are automatically stopped when the buttons are released. The bolus dosage can be freely chosen by the anesthesiologist by keeping pressed the button for the desired amount of time. The dosage that is currently administered is shown in real time in the displays placed to the right of the bolus buttons. This feature reduces the risk of intra-operative awareness. The anesthesiologist can perform boluses to quickly restore an adequate anesthetic state when the patient shows clinical signs of light anesthesia. Moreover, boluses can be used as a preventive measure to anticipate phases of strong surgical stimulation. Boluses are administered by driving the infusion pumps at their maximum speed. When a bolus is triggered, the integral action of the PID controller is set to zero in order to obtain a more precise drug dosing and thus making the maneuver safe.
The performance of the proposed control system has been experimentally assessed on a group of nine patients. In order to evaluate the behavior of the system in presence of different actuator dynamics and of manual boluses the patients have been assigned to three different
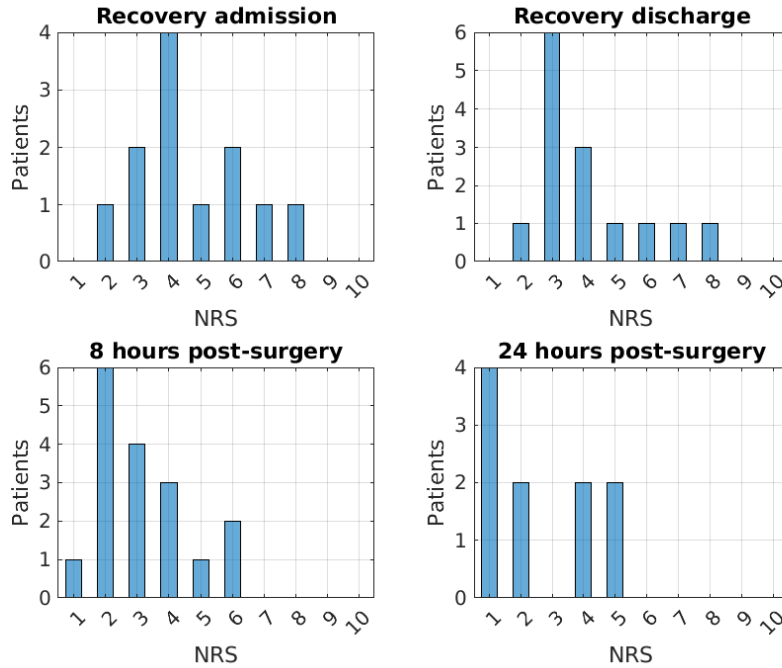
Figure 3.19: *Assessment of post-operative pain on the 42 patients enrolled with the modified PID-based MISO controller according to the NRS proposed from 1 to 10.*

groups that, for the sake of clarity, in the rest of the section will be referred to as **(a)**, **(b)** and **(c)**. Group **(a)** represents the nominal conditions for which the control system has been designed. In this group the Graseby 3500 pumps have been used as actuators for propofol and remifentanil and no manual boluses are performed by the anesthesiologist. In group **(b)** the same actuators of group **(a)** have been used but the anesthesiologist performed manual boluses. In group **(c)** the Alaris GH pumps have been used and no manual boluses have been performed by the anesthesiologist. The nine patients enrolled in this study were all scheduled for elective plastic surgery. Their demographic data and the group to which they were assigned are shown in Table 3.24. The same clinical protocol described in Section 3.1.1 has been applied for all patients with the exception for those enrolled in group **(b)** where the anesthesiologist performed manual boluses when it was deemed as necessary. The BIS and drugs infusion rates obtained for each patient are shown in Figure 3.20. Table 3.25 shows the results achieved during the induction phase. Table 3.26 shows the results achieved during the maintenance phase.

The results obtained for patient 1, patient 2 and patient 3 of group **(a)**, show that the control system provides a satisfactory performance during both the induction and maintenance phases. Indeed, hypnosis has been rapidly induced in all patients without causing BIS undershoot. During the maintenance phase the BIS has been kept inside the recommended range for more than 80% of maintenance duration. As it is possible to observe in Figures 3.20a and 3.20b, the BIS has been almost always kept inside the recommended range, with the exceptions of some rises slightly above the threshold value of 60 due to the presence of surgical stimulation. However, the controller has properly rejected these disturbances without causing excessive undershoots. The disturbance rejection can be clearly observed, for example,

around minute 200 for patient 1 and around minute 20 and 30 in patient 2. For patient 3 the rises of the BIS due to surgical stimulation have been more significant, as shown in Figure 3.20c. Indeed, the BIS has risen up to the value of 80, for example around minute 20 and minute 40, due to a particularly painful surgical procedure. Nevertheless, the control system has always properly rejected the disturbances without causing undershoot.

For patient 4, patient 5 and patient 6 of group **(b)** the anesthesiologist could perform boluses of drugs if deemed as appropriate. In patient 4 three boluses of propofol and one bolus of remifentanil have been administered around minute 100 as shown in Figure 3.20d. The boluses have been administered during a phase of strong surgical stimulation corresponding to the disarticulation of a toe. A bolus of 1 ml of propofol followed 5 min later by a bolus of 1.3 ml of propofol and 1 ml of remifentanil has been administered. After 3 min, another bolus of 1.3 ml of propofol has been given. In patient 5 two boluses of propofol of 1 ml each have been administered around minute 70 as shown in Figure 3.20e. The boluses have been administered during a delicate phase of the surgical procedure corresponding to cranial scalloping. The anesthesiologist performed the boluses to obtain a deep level of hypnosis during this phase, thus ensuring optimal conditions for the surgeons. In patient 6 seven boluses of propofol have been administered. In particular, four boluses of 1 ml each have been administered during anesthesia induction (in addition to that of the induction sequence) since difficulties have been encountered during intubation and the anesthesiologist wanted to ensure the full unconsciousness of the patient. The difficult intubation also determined the longest induction time recorded in the group of patients. Indeed, patient 6 has been the only patient with an induction time that exceeded 3 min. Another 1.3 ml bolus of propofol has been administered around minute 60 during mastectomy since the surgeons were causing a painful stimulation on the pectoralis nerve. A 2 ml bolus of propofol has been administered around minute 160 during breast prosthesis insertion and one last 1.3 ml bolus of propofol has been administered around minute 180 during skin suturing.

For patient 7, patient 8 and patient 9 of group **(c)** the Alaris GH syringe pump has been used as actuator for propofol and remifentanil administration and no boluses were performed by the anesthesiologist. As for the patients of group **(a)**, a satisfactory performance during both the induction and maintenance phases of anesthesia have been obtained. The induction phase has been rapid in all patients without causing BIS undershoot and during the maintenance phase the BIS has been kept inside the recommended range on average for about 80% of maintenance duration. As shown in Figure 3.20g and Figure 3.20h, for patient 7 and patient 8 the BIS has been almost always kept inside the recommended range. In Figure 3.20i it is possible to notice the presence of a disturbance around minute 60 that has been properly rejected by the controller.

To better compare performance between groups, the median and the IQR of the performance indexes for the induction and maintenance phases are shown in Table 3.27. The experimental results obtained show that the closed-loop system is capable to meet all the clinical requirements for all the patients enrolled.

During the induction phase, as shown in Table 3.25, anesthesia is rapidly induced in all patients. In particular, the induction time is shorter than 3 min for all patients with the exception of patient 6 for which anesthesia has been induced in 3.27 min. However, this last value is fully acceptable for the clinical practice. The short induction time is obtained without causing undershoots, as it is possible to notice by observing the lowest BIS value. In particular, the BIS always remains above the recommended threshold of 40 for all patients with the exception of patient 9 where a harmless undershoot to a BIS value of 37 is observed. The

Patient	Age	Height [cm]	Weight [kg]	Gender	Group	Type of surgery
1	46	168	51	F	a	Breast mastectomy and mastoplasty
2	54	167	74	F	a	Right breast mastoplasty
3	72	170	86	M	a	Burned tissues escharotomy and microsurgical flap
4	67	169	83	F	b	Melanoma excision and left foot toe disarticulation
5	72	165	74	F	b	Scalp tumor excision and cranial scalloping
6	58	165	88	F	b	Breast mastectomy and mastoplasty
7	62	160	75	F	c	Breast mastectomy and mastoplasty
8	71	170	67	F	c	Breast mastectomy and mastoplasty
9	59	160	57	F	c	Breast mastectomy and mastoplasty

Table 3.24: *Demographic data, group and surgical procedure of the patients enrolled with the modified PID-based MISO controller to assess the performance when additional boluses are manually administered by the anesthesiologist and different brands of infusion pumps are used.*

propofol and remifentanil induction dosages are fully compatible with the dosages used in the clinical practice. These results confirm the effectiveness of the proposed induction sequence. As shown in Table 3.26, the maintenance phase is also satisfactory. The BIS is always maintained within the recommended range for more than 70 % of the maintenance phase duration. Propofol and remifentanil infusion rates and the time-to-extubation are fully compatible with the clinical practice.

A similar performance is actually obtained for the different groups of patients. As shown in Table 3.27 the performance indexes are similar between all groups. The longer median induction time obtained in the group **(b)** is due to patient 6 who had difficulties during intubation. By comparing the results obtained by group **(a)** and group **(b)**, it appears that the control system can safely handle the presence of manual boluses performed by the anesthesiologist without performance deterioration. The possibility for the anesthesiologist to safely administer additional drug boluses is a critical feature because it gives the possibility to better manage the anesthetic state of the patient. Indeed, the anesthesiologist can decide to administer an additional amount of drug when it is deemed necessary for specific clinical requirements. For example, in patient 4 the anesthesiologist performed additional boluses to improve the anesthetic coverage during a particularly painful part of the surgical procedure. In patient 5 the boluses have been performed to guarantee optimal conditions for the surgeons in a delicate phase of surgery. In patient 6 additional boluses have been administered to manage a difficult intubation and to improve the anesthetic coverage during the most painful parts of surgery. It is worth stressing that these boluses should be intended as a feedforward action performed by the anesthesiologist that is based on clinical information that are not available to the controller. In all patents of group **(b)** the boluses have been administered to improve the actions of the control system and not to compensate for its shortcomings. Indeed, the controller has demonstrated its effectiveness in rejecting disturbances as shown, for example, in Figure 3.20c. Also for patient 4 the sharpest rises of the BIS that occurred around minute 120 has been managed autonomously by the controller.

By comparing the results obtained by group **(a)** and group **(c)**, it appears that the control system is able to compensate for the dynamics of the different actuators. Many brands and models of infusion pumps are commercially available and are commonly used in the clinical practice. Hence, for a closed-loop control system to be routinely used in the clinical practice, it is fundamental to be compatible with different actuators without any significant performance deterioration.

Patient	Induction time [min]	Lowest BIS	Propofol dose [mg/kg]	Remifentanil dose [μg/kg]
1	1.17	40	2.02	2.59
2	1.27	41	1.72	2.19
3	2.25	40	1.18	1.74
4	1.45	41	1.44	1.35
5	2.40	45	1.54	2.15
6	3.27	45	1.94	2.62
7	1.20	41	1.73	1.66
8	1.03	41	1.97	1.72
9	0.95	37	1.71	1.65

Table 3.25: *Performance indexes for the induction phase obtained with the modified PID-based MISO controller to assess the performance when additional boluses are manually administered by the anesthesiologist and different brands of infusion pumps are used.*

Patient	Duration [min]	BIS $40-60$ [%]	BIS < 40 [%]	BIS > 60 [%]	Propofol [mg/kg/h]	Remifentanil [μg/kg/min]	T awakening [min]
1	215.00	87	9	4	6.68	0.19	7.75
2	59.70	83	11	6	7.53	0.21	7.25
3	64.93	86	2	12	5.00	0.14	8.83
4	147.13	73	24	3	5.50	0.14	6.58
5	114.97	84	10	6	7.75	0.19	9.28
6	195.17	76	14	10	9.58	0.26	6.77
7	275.23	73	25	2	4.55	0.09	11.27
8	220.23	86	12	2	5.77	0.12	6.65
9	137.83	82	16	2	6.35	0.15	7.43

Table 3.26: *Performance indexes for the maintenance phase obtained with the modified PID-based MISO controller to assess the performance when additional boluses are manually administered by the anesthesiologist and different brands of infusion pumps are used.*

	(a)	(b)	(c)
Induction time [min]	1.27 (0.54)	2.40 (0.91)	1.03 (0.13)
Lowest BIS	40 (0.5)	45 (2)	41 (2)
Propofol dose [mg/kg]	1.72 (0.42)	1.54 (0.25)	1.73 (0.13)
Remifentanil dose [μg/kg]	2.19 (0.43)	2.15 (0.64)	1.66 (0.04)
BIS 40-60	86 (2)	76 (5.5)	82 (6.5)
BIS<40	9 (4.5)	14 (7)	16 (6.5)
BIS>60	6 (4)	6 (3.5)	2 (0)
Propofol [mg/kg/h]	6.68 (1.27)	7.75 (2.04)	5.77 (0.90)
Remifentanil [μg/kg/min]	0.19 (0.04)	0.19 (0.06)	0.12 (0.03)
MDPE [%]	-8 (6)	-8 (5)	-12 (2)
MDAPE [%]	12 (1)	12 (3)	14 (2)
WOBBLE [%]	8 (2)	8 (1)	8 (1)
T awakening [min]	7.75 (0.79)	6.77 (1.35)	7.43 (2.31)

Table 3.27: *Comparison of performance indexes obtained with the modified PID-based MISO controller in the nominal conditions (a), when additional boluses are manually administered by the anesthesiologist (b) and when a different brand of infusion pumps is used (b). Data are presented as median (IQR).*
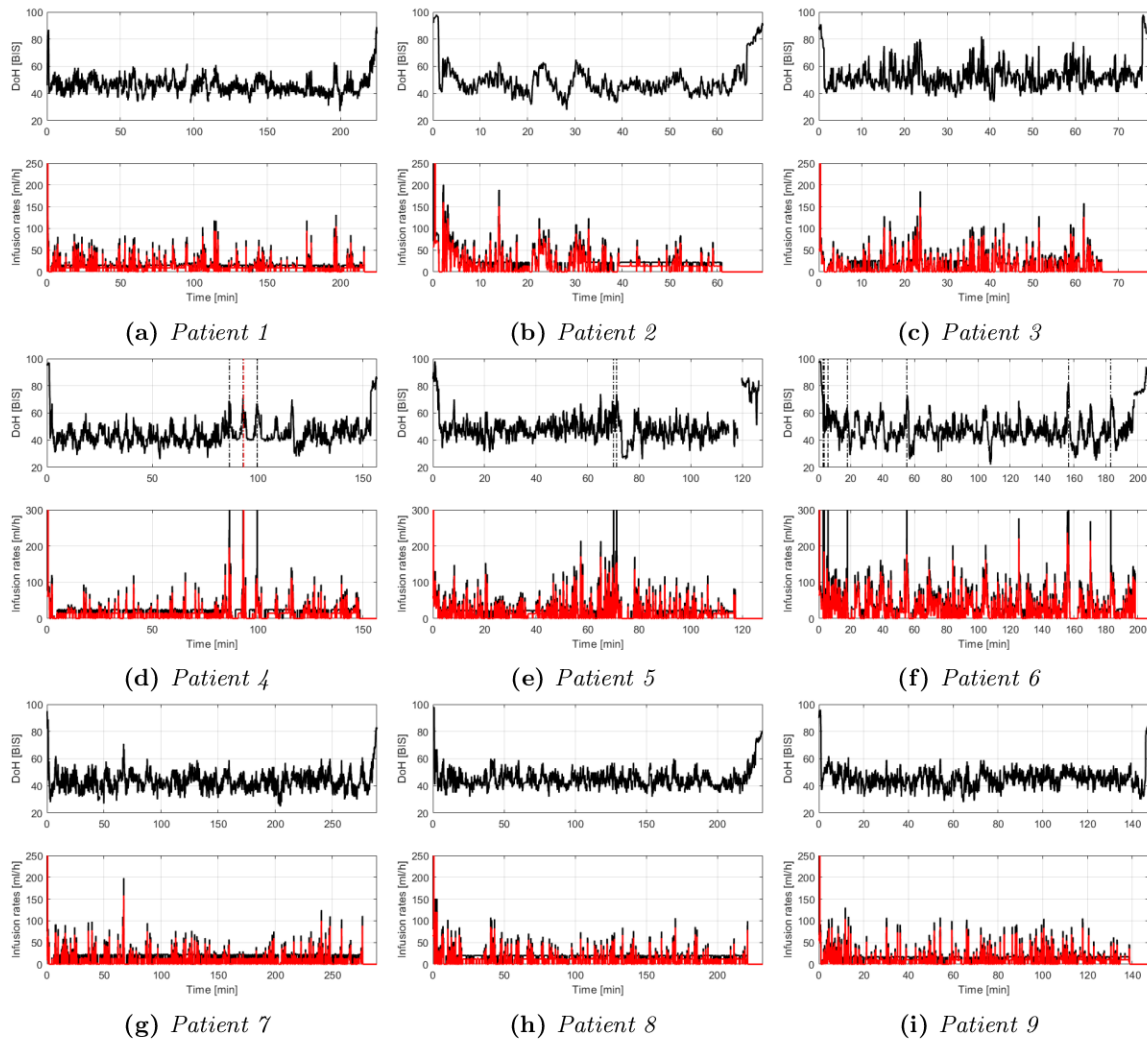
Figure 3.20: *BIS and infusion rates of propofol (black) and remifentanil (red) obtained with the modified PID-based MISO controller to assess the performance when additional boluses are manually administered by the anesthesiologist and different brands of infusion pumps are used. The vertical dash-dotted lines are the boluses of propofol (black) and remifentanil (red). The missing data are due to temporary issues with BIS sensor reading.*

3.5   Conclusions

In this chapter the PID-based MISO control scheme described in Section 2.2.2 have been tested in an in-vivo study on patients undergoing general anesthesia for elective plastic surgery. In a first study involving 10 patients the closed-loop system demonstrated its ability to satisfactorily handle both the induction and maintenance phases of anesthesia fulfilling all clinical specifications. Anesthesia has been automatically performed by the closed-loop system throughout the whole surgical procedure, without the need of any manual intervention by the anesthesiologists, neither in the induction nor in the maintenance phase. The obtained results are very promising as they show that the control system is able to induce and maintain a suitable DoH while providing a good hemodynamic stability. Furthermore, the comparison of the performance of the closed-loop system with that of manual control shows that the behavior of the automatic solution is sensible and consistent with the clinical practice. These findings suggest that the approach presented in [93] can be safely used in the operating room. In particular, the conclusion drawn on the robustness of the system through a Monte Carlo simulation have been confirmed by experimentally testing it on 10 individuals with significantly different physical characteristics. This demonstrates that the optimal PID parameter obtained through the optimization-based tuning approach performed on a representative data set of 13 patients can be employed in a general population.

Then a modified version of the PID-based MISO control scheme has been presented The changes to the original control scheme have been made to satisfy specific clinical requirements that are relevant for the anesthesiologists. The effectiveness of the modified control has been experimentally assessed on a population of 10 patients. The control system was able to induce and maintain adequate anesthesia without the need for manual intervention from the anesthesiologist for all patients enrolled, thus confirming the effectiveness of the overall design approach. The obtained results suggest that the proposed changes are a significant step toward the integration of the system into the clinical practice and provide measurable clinical advantages for the patients.

Encouraged by the positive results obtained, a higher number of patients (specifically, 42 patients) have been enrolled with the modified version of the controller. The patients enrolled had a wide range of physical characteristics and were scheduled for procedures that greatly varied in length, body location, and level of painful stimulation. Even on this wider population, the control system showed good clinical performance during both the induction and maintenance phases for all the patients enrolled, thus demonstrating its robustness. Moreover, the control system has demonstrated good clinical performance concerning DoH, hemodynamic stability, analgesic coverage, drug consumption, emergence and quality of postoperative recovery.

Finally, an experiment has been performed on 9 patients to evaluate the performance of the modified control system in terms of its ability to deal with issues that may arise during its practical use in a clinical setting. In particular, the aim was to assess the performance of the control system when manual drug boluses are performed by the anesthesiologist, and when different brands of syringe pumps are used. Results demonstrate that the control system is capable to handle these practical issues and it is therefore suitable to be used in the clinical practice. Moreover, the possibility for the anesthesiologist to intervene with manual boluses, if deemed as appropriate, represents a step toward the anesthesiologist-in-the-loop paradigm.

Chapter 4

Event-based PID MISO control: experimental results

The presence of noise in the controlled variable usually results in a noisy control action that, in many cases, implies a non-optimal use of control resources. This problem can be partially addressed by placing a noise filter in the feedback-loop. However, the filtering action needs to be a compromise between noise attenuation and process dynamics modification. Taking into account this problem, an event-based control system can be used as a flexible alternative to classic time-based schemes as it can reduce the noise impact on the control action variability providing efficient use of control resources. The application of an event-based paradigm enables the possibility to trigger the controller task on the basis of the controlled variable dynamics rather than a time progress, which is the main difference when compared to the classical time-based control system. The event-based control approach is an effective and efficient control technique that was already proposed for bio-processes and energy systems, where the optimal usage of control resources is critical. These properties are also interesting from the anaesthesia process control perspective since the BIS is affected by a significant amount of noise. Indeed, the experimental results presented in Chapter 3 with a standard PID controller show that the control action is affected by residual noise. Although this does not significantly affect the performance of the system, it causes an unnecessary stress on the actuators, as a change in the control action is driven by noise and not by an actual variation of DoH. Moreover, this behavior differs significantly from what the anesthesiologist is used to and this can limit the acceptance of such systems in clinical practice.

The event-based approach for DoH control with propofol by using PID-based controllers was proposed in [96, 97], and briefly summarized in Section 2.2.2. It was shown in simulation that the devised event-based controller delivers a noise-free control action, with a consequent reduction of the mechanical stress on the actuator and an infusion profile that only changes a finite number of times, thereby mimicking the behavior of the anesthesiologist. In the light of the good results obtained, the proposed approach was extended to the case of propofol and remifentanil coadministration [99] as briefly summarized in Section 2.2.2. Simulation results have shown that, also in this case, this control strategy provides a strong filtering effect without introducing a significant decrement in performance.

In this chapter the experimental results obtained with the event-based PID MISO control scheme proposed in [99] are presented. The control scheme is implemented in the control software and its effectiveness is assessed on 14 patients. The results are compared with those

obtained with the PID-based control scheme, which have been discussed in Section 3.2, to evaluate the improvements that the event-based control can provide over time-based control. The obtained results are also compared with those of manually controlled anesthesia to assess the consistency of the proposed control solution with the clinical practice [104].

4.1   Event-based PID MISO control scheme

The event-based MISO control scheme for propofol and remifentanil coadministration proposed in Section 2.2.2 is considered. Despite the satisfactory performance obtained in simulation [99], the control system is further modified to include the improvements proposed in Section 3.2 to ameliorate patient safety, which is, of course, always of primary concern [126, 127]. The resulting controller is validated via in-vivo clinical experimentation on 14 patients. The experiments have been conducted under conditions that are well representative of the routine clinical practice. In particular, different brands of actuators and different drug dilutions are used. Moreover, manual interventions are also performed by the anesthesiologist.

4.1.1   Material and methods

The experimental setup and the event-based MISO control structure considered are those described in Section 2.2.3 and in Section 2.2.2, respectively. To implement the control strategy on the control algorithm employed in the experimental setup the event generator has been discretized with a sampling period of 1 s, according to the maximum update frequency provided by the Dräger Infinity Delta monitor. An example of the strong filtering effect on the BIS signal provided by the event generator is shown in Figure 4.1. The PIDplus controller has a variable sampling period that depends on the frequency of the events generated by the event generator. The tuning parameters considered are those shown in Table 2.7. A bumpless switching mechanism has been implemented to ensure a smooth transition between the sets of parameters for the induction phase and for the maintenance phase. The switching from the induction phase to the maintenance phase is automatically triggered by the system when the BIS drops below 60 and remains there steadily for 30 consecutive seconds. The additional features proposed in Section 3.2, namely the induction boluses and the baseline infusions, have been integrated in the original event-based control scheme because they can provide tangible clinical benefits, as demonstrated in Section 3.2. The block diagram of the overall control system is shown in Figure 4.2. The BIS set-point $r(t)$ has been fixed to 50 and the *ratio* that determines the opioid-hypnotic balance has been set to 2. The tuning parameters employed are shown in Table 4.1.
The same clinical protocol employed for the time-based PID controller, described in Section 3.1.1, has been used. The only difference is that, here, the switch from induction tuning parameters to maintenance tuning parameters is automatically performed by the control system and it is not triggered by the anesthesiologist. This change in the clinical protocol has been done to standardize the condition that triggers the switching between the two tuning sets. The control system has been tested under conditions that are well representative of the clinical practice, different brands of syringe pumps and additional boluses performed by the anesthesiologist have been considered as explained in Section 3.4. Moreover, here, different propofol dilutions are also considered. In particular, 10 mg/ml and 20 mg/ml are employed. Conversely, a fixed dilution of remifentanil, equal to 50 μg/ml, has been considered. To take into account the different drugs dilutions, the G_p and G_r gains convert the controller outputs,
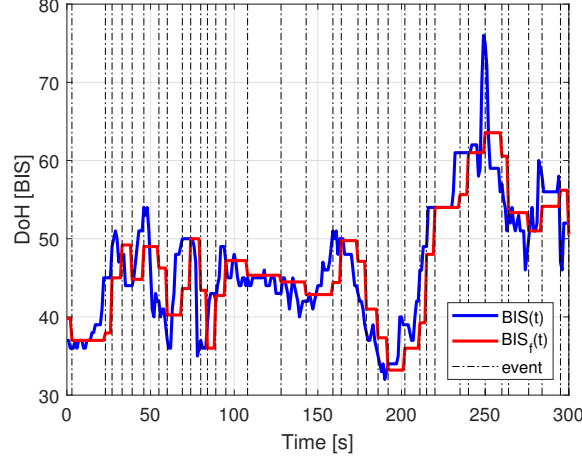
Figure 4.1: *Filtering effect of the event generator employed in the event-based PID MISO control scheme (Δ_i=20.57, t_{max}=20 s) on the BIS signal.*
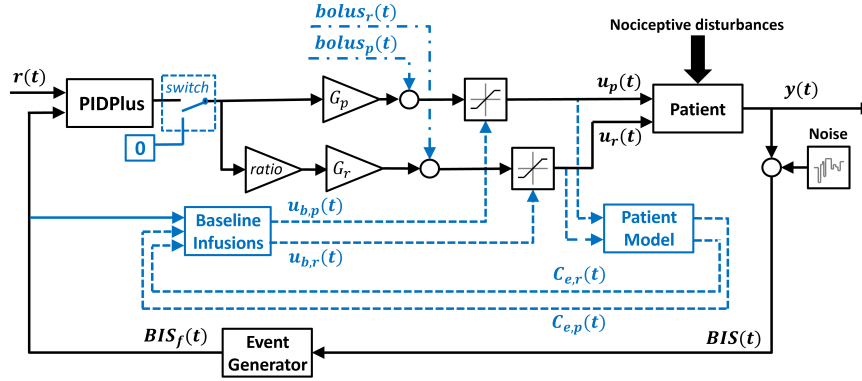
Figure 4.2: *Architecture of the proposed event-based PID controller for propofol and remifentanil coadministration. The modifications done with respect to the original control scheme proposed in [99] are highlighted in blue.*

which are expressed in mg/s for propofol and μg/s for remifentanil, to the driving signals for the syringe pumps, which are expressed in ml/h. They are defined as

$$G_p = \frac{3600}{C_p}; \quad G_r = \frac{3600}{C_r}, \tag{4.1}$$

where the value 3600 converts seconds in hours, and C_p and C_r are the dilutions of propofol and remifentanil expressed in mg/ml and μg/ml, respectively. The resulting algebraic models of the syringe pumps comprises the series of the gains G_p and G_r, and the saturation block. The dynamic behavior of the actuators is not considered since it does not affect the performance of the control system as experimentally evaluated in Section 3.4.

Note that, as done for the time-based PID controller proposed in Chapter 3, if the system enters in safety mode (see Section 2.7) or if manual boluses are triggered by the anesthesiologist, the integral action of the PIDPlus controller is reset to zero.

Parameter	Induction	Maintenance
K_p $[mg/s]$	0.0087	0.0083
T_i $[s]$	197.47	287.62
T_d $[s]$	29.18	6.25
Δ_i	9.45	20.57
t_{max} $[s]$	20	20

Table 4.1: *Tuning parameters of the event-based PID MISO controller for the induction and maintenance phases with the opioid-hypnotic ratio of 2.*

4.1.2 Experimental results

The performance of the proposed event-based control system has been experimentally assessed on fourteen patients that needed to undergo general anesthesia for elective plastic surgery. Patients data are shown in Table 4.2. The details of the surgical procedures are shown in Table 4.3. The individual records of the clinical variables of interest are shown in Figures 4.3, 4.4 and 4.5. The event-based controller successfully induced and maintained anesthesia for each enrolled patient. The variables always remained within clinically acceptable ranges throughout the surgical procedures. The drug infusion rates were always consistent with clinical practice. The relationship between the feedback variable (BIS) and the control variables (infusion rates) shows the strong filtering capability provided by the event-based controller. Indeed, the amount of residual noise in the control variables is limited. This aspect is particularly evident in Figure 4.3b, relative to patient 2, where the BIS signal was affected by a significant amount of noise and artifacts. Indeed, the patient was subjected to eyelid reconstructive surgery, then the surgeons worked near the forehead of the patient were the BIS sensor was placed, thus introducing a considerable amount of artifacts.

The results related to the induction phase are summarized in Table 4.4. The induction time was of 2.39 min on average. This result is consistent with the target value for elective plastic surgery in a clinical context, which ranges from 3 to 5 min. This specification was satisfied for all the patients with the exception of patient 12, for which an induction time of 5.97 min was obtained. As shown in Figure 4.4c, the BIS dropped quickly but then settled around the value of 60. This fact did not cause any problems from a clinical point of view. The evaluation of analgesia has been performed by observing the stability of the hemodynamic variables. Indeed, insufficient analgesia would result in a sudden rise of BP and HR in response to noxious stimuli. Conversely, a remifentanil overdose would result in hypotension and bradycardia. For all the enrolled patients, the hemodynamic variables remained within clinically recommended ranges. No problems were reported by the anesthesiologist during the positioning of the laryngeal mask or the endotracheal tube and no clinically relevant reactions were recorded, thus suggesting an appropriate analgesic coverage. As regards the BIS undershoot, the average lowest BIS value was 43, which is above the recommended value of 40. Patients 1, 2, 3, 7 and 10 showed a lowest BIS below this threshold. However, as it is shown in Figures 4.3a, 4.3b, 4.3c, 4.3f and 4.5b, the undershoot did not last for a long time and it did not cause hypotension or bradycardia. Moreover, BS did not appear in any of the patients. Both propofol and remifentanil induction doses were in accordance with clinical guidelines. In particular, anesthesia was induced, on average, with 2.02 mg/kg of propofol and 2.54 μg/kg of remifentanil.

The results achieved during the maintenance phase are shown in Table 4.5. The BIS was kept inside the range from 40 to 60, on average for the 80.32% of the maintenance duration, with a

minimum of 61.99% for patient 2 and a maximum of 92.89% for patient 10. It was below the value of 40 and above the value of 60 for 18.13% and 1.55% of maintenance time, respectively. This result suggests a reduced risk of intra-operative awareness. The average drugs infusion rates were in accordance with clinical guidelines. In particular, 5.30 mg/kg/h of propofol and 0.14 μg/kg/min of remifentanil were administered. The average time-to-extubation of 8.83 min was coherent with that usually obtained in TIVA. The hemodynamic variables remained within clinically recommended ranges for all the patients thus indicating adequate analgesia. A sudden rise in the values of the hemodynamics variables was recorded in patient 11, as shown in Figure 4.5c. However, this was due to the injection of an etilefrine bolus and not to inadequate analgesia. The claim of a sufficient analgesic coverage is further confirmed by the administered remifentanil infusions, which were in line with those expected in the standard clinical practice.

The results obtained using the event-based controller are compared with those of Section 3.2, which were obtained using a standard time-based PID controller. The Mann-Whitney U test is used to analyze continuous data while the Fisher's Exact test is used to analyze categorical data [122]. The threshold for significance is 5%. In the tables, the data are shown with median and IQR. Patients demographic data comparison between the two groups is shown in Table 4.6 and no statistically relevant differences are present. Both groups comprises plastic surgery patients which were enrolled in the same operating room with the same clinical setting. The comparison of performance regarding induction is shown in Table 4.7. The event-based controller shows a statistically relevant ($P < 0.05$) slight increase in the propofol induction dose. There are no statistically relevant differences ($P > 0.05$) between the two groups regarding the induction time, the lowest BIS and the remifentanil induction dose. The comparison of performance regarding maintenance is shown in Table 4.8. The event-based controller provides a statistically relevant ($P < 0.05$) reduction in the values of TV and of $BIS > 60$. There are no other statistically relevant differences ($P > 0.05$) between the two groups in any of the other performance index.

The experimental results show that the proposed event-based control system performs well when applied in the routine clinical practice of TIVA in the context of elective plastic surgery. During the induction phase, the controller met the specification on the target induction time for all patients except one, namely patient 12. However, the longer induction time in this single case did not cause clinically relevant issues. Indeed, the controller quickly drove the BIS to the value of 60, causing loss of consciousness and providing an adequate anesthetic coverage. This is confirmed by the fact that the anesthesiologist performed the insertion of the laryngeal mask without difficulties and without causing a physiological response in the patient. Moreover, the anesthesiologist did not performed additional drug boluses in this phase even if they were acceptable in the clinical protocol. Induction was also performed without causing excessively deep hypnotic states. Indeed, the BIS remained above the recommended threshold of 40 in nine patients out of fourteen. In the remaining patients, the BIS undershoot was short-lasting, as visible in the time course of the clinical variables, and it did not cause side effects such as the onset of BS, bradycardia or hypotension, see Figures 4.3a, 4.3b, 4.3c, 4.3f, 4.5b. Drugs induction doses were fully compatible with those used in the clinical practice. For all patients, during the maintenance phase the BIS was mainly maintained inside the range from 40 to 60. Indeed, the minimum value achieved was of 61.99%, while the maximum value was of 92.89%. In the remaining percentage of time, the BIS was kept mainly below the value of 40. Consequently, the BIS rose above the value of 60 only for a marginal amount of time. This behavior is desirable, as long as overdosing is avoided, because it reduces the

probability of intra-operative awareness. In the population enrolled, no clinical signs of drug overdosing were observed. Hemodynamic variables remained within recommended clinical ranges and there were no episodes of bradycardia or hypotension. Average drugs infusion rates were fully comparable with those clinically recommended [121]. It is worth discussing the results obtained with patient 9, who has the highest average propofol and remifentanil infusion rates, well above the average infusion rates of the rest of the population. Despite this patient requiring a higher dosage, the BIS was maintained inside the range from 40 to 60 for the 90.23% of maintenance time, thus indicating a remarkable regulation of DoH, hardly obtainable with a manual control relying on recommended dosages. This shows the ability of the closed-loop system to administer the drugs according to the real needs of the patient. The system also showed its robustness with respect to the use of two different dilutions of propofol and, most of all, to two different brands of infusion pumps, which is not obvious, since infusion pumps might have different mechanical characteristics [46, 47]. Further, the system can seamlessly manage additional boluses performed by the anesthesiologist as performance was not affected by these perturbations (see the results of patients 4, 10 and 11). In fact, the system allows the anesthesiologist to act as a supervisor, and boluses were used as preventive measure when particularly painful phases of surgery were expected. From a control engineering perspective, these boluses should be interpreted as a feedforward action (performed by the anesthesiologist) that is based on future clinical information that is not yet available to the controller. They were administered to improve the actions of the control system and not to compensate for its shortcomings. Indeed, the controller has demonstrated its effectiveness in rejecting disturbances as shown, for example, in Figure 4.3d and 4.3f. Note that, in terms of percentage of BIS in the recommended range, the patient that achieved the better performance was patient 10, who also received an additional bolus of propofol around minute 25, see Figure 4.5b. The performance comparison between the proposed event-based controller and the time-based PID controller shows that there are no statistically significant differences for most of the performance indexes. Indeed, both the techniques obtained remarkable performance in terms of induction time, lowest BIS, BIS 40-60, MDPE, MDAPE and WOBBLE. The only exception in the induction phase is propofol dosing. Although the event-based controller provided a slightly higher propofol induction dose, the dosages provided by both controllers are both fully compatible with those commonly used in the clinical practice. For maintenance phase, the event-based controller provided a statistically significant reduction in the values of $BIS > 60$, TV Propofol and TV Remifentanil, thus improving the performance both in terms of patient experience and control action. The statistically significant reduction in the values of TV obtained with the event-based controller shows the effectiveness of the event-based strategy in reducing the control effort thereby delivering a control action that is updated far less frequently than that of the time-based controller. This is the consequence of a strong filtering effect that implies a smoother control action, which is more similar to that employed by the anesthesiologist in the standard clinical practice. To further highlight this aspect, the results obtained with the event-based controller and with the time-based controller are graphically compared in Figure 4.6. This provides two main advantages. The first one is that the behavior of the control system is more intuitive for the anesthesiologist that is supervising the control system because the infusion rate does not change at each sampling time due to the noise. The second advantage is that the reduced number and frequency of update commands sent to the pumps can help to overcome problems related with variable start-up and update delays observed in commercially available infusion pumps [46, 47]. This explains the differences in the propofol induction dosage and in the

Patient Id	Age	Height [cm]	Weight [kg]	Gender
1	26	160	56	F
2	71	178	78	M
3	53	173	57	F
4	37	165	61	F
5	75	166	77	M
6	73	180	90	M
7	46	164	58	F
8	63	185	98	M
9	75	175	63	M
10	74	172	100	M
11	62	160	54	F
12	50	178	98	M
13	60	160	72	F
14	34	165	73	F

Table 4.2: *Physical characteristics of the patient enrolled with the event-based PID MISO control scheme.*

Type of surgery	Patients involved	Patients Id
Skin cancer exeresis	7	1, 5, 6, 8, 9, 10, 12
Mastectomy	4	3, 4, 7, 14
Mastoplasty	2	11, 13
Eyelid reconstructive surgery	1	2

Table 4.3: *Types of surgery undergone by the patients enrolled with the event-based PID MISO controller, number of patients involved and patients identifiers.*

$BIS > 60$. Indeed, the event-based controller provides a more consistent infusion of drugs with a consequent reduced risk of under-dosing, as suggested also by the increased average values of $BIS < 40$ and MDPE compared to the time-based controller. Importantly, this effect is obtained without increasing the average infusion rates of propofol and remifentanil.

4.2   Comparison with manual control

To further validate the applicability to the clinical practice of the event-based MISO control solution proposed, the results obtained on the 14 patients enrolled in Section 4.1 have been compared with those of manually controlled anesthesia. It is important to underline that this comparative study is not intended to prove the superiority of automatic control over manual control. On the contrary, it is aimed at evaluating the consistency of the results obtained with the event-based controller with those commonly obtained in routine clinical practice. To this end, 14 patients have been enrolled with the clinical protocol for manual control described in Section 3.1.2. Patients data are shown in Table 4.9. The details of the surgical procedures are shown in Table 4.3. For the sake of clarity, in the rest of this section the closed-loop control group will be indicated as **(c)** and the manual control group will be indicated as **(m)**. Both groups comprises elective plastic surgery patients which were enrolled in the same operating room with the same clinical setting. The Mann-Whitney U test is used to analyze continuous data while the Fisher's Exact test is used to analyze categorical data.

Patient Id	Induction time [min]	Lowest BIS	Propofol dose [mg/kg]	Remifentanil dose [μg/kg]
1	1.17	28	2.20	2.16
2	1.28	26	1.84	1.60
3	0.93	33	1.65	1.79
4	1.38	48	1.89	2.52
5	1.68	45	1.53	1.89
6	3.98	44	1.72	2.50
7	2.51	31	2.10	1.90
8	1.10	47	1.37	2.55
9	3.08	50	2.92	4.18
10	5.05	38	2.17	2.60
11	1.10	40	2.42	4.14
12	5.97	45	2.44	3.43
13	2.58	45	2.04	2.40
14	2.58	42	1.92	1.95
Average	2.39	43	2.02	2.54

Table 4.4: *Induction performance indexes obtained for each patient enrolled with the event-based PID MISO controller.*

Patient Id	Duration [min]	BIS $40-60$ [%]	BIS < 40 [%]	BIS > 60 [%]	Propofol [mg/kg/h]	Remifentanil [μg/kg/min]	T awakening [min]
1	51.55	74.89	25.11	0.00	4.64	0.12	5.33
2	138.02	61.99	37.18	0.83	3.53	0.09	12.00
3	198.93	78.26	21.30	0.44	5.12	0.13	7.52
4	181.63	82.01	16.91	1.08	5.02	0.13	6.80
5	145.45	63.46	32.42	4.12	4.34	0.11	8.12
6	65.73	87.30	11.98	0.72	5.22	0.12	12.12
7	208.48	83.10	16.65	0.25	5.00	0.13	7.38
8	72.95	74.90	23.48	1.62	4.30	0.11	9.93
9	38.67	90.23	3.90	5.87	8.67	0.26	12.48
10	90.35	92.89	6.81	0.37	5.48	0.13	8.63
11	114.07	79.79	20.11	0.10	5.10	0.13	6.13
12	94.52	84.31	14.43	1.26	5.59	0.16	6.00
13	87.25	82.99	12.77	4.24	6.39	0.17	12.63
14	207.32	88.46	10.79	0.75	5.81	0.16	8.50
Average	121.07	80.32	18.13	1.55	5.30	0.14	8.83

Table 4.5: *Maintenance performance indexes obtained for each patient enrolled with the event-based PID MISO controller.*

	Event-based	Time-based	P value
Age [years]	61.0 (27)	56.0 (25)	0.58
Height [cm]	169.0 (14)	165.5 (8)	0.39
Weight [kg]	72.5 (32)	72.5 (31)	0.98
Gender [M/F]	7/7	3/7	0.42

Table 4.6: *Demographic data comparison between the patients enrolled with the time-based and with the event-based PID MISO controller. Age, height and weight are expressed as median (IQR), gender is expressed as male/female. There are no statistically relevant differences between the two groups ($P > 0.05$).*
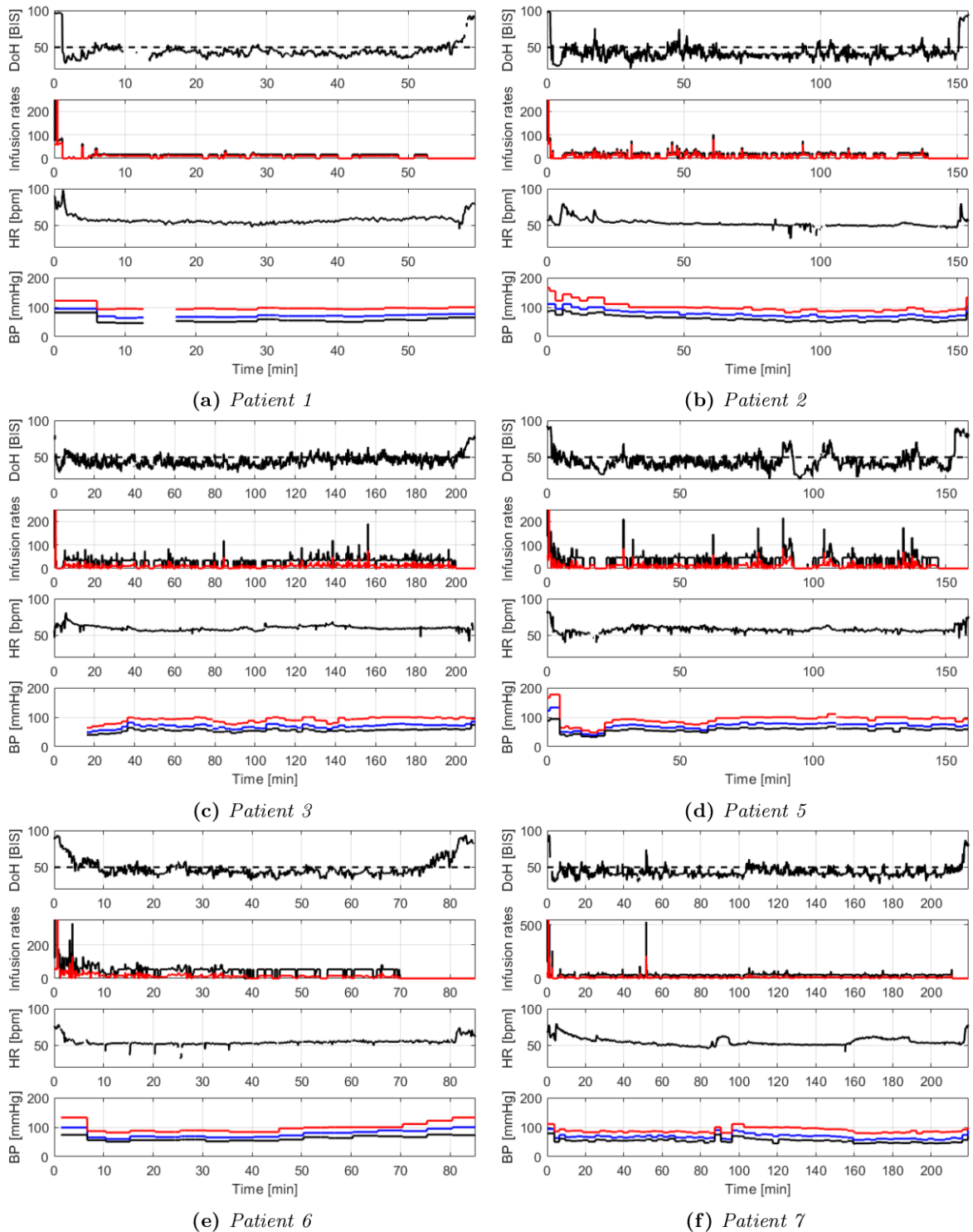
Figure 4.3: *Recorded clinical data of the patients enrolled with the event-based PID MISO controller. From top to bottom: BIS (solid line) and BIS set-point (dashed line); propofol (black) and remifentanil (red) infusion rates in ml/h; HR; BP_s (red), BP_d (black) and BP_m (blue). Missing data were due to temporary issues with sensors reading. Infusion pumps: Alaris GH. Propofol dilution: 20 mg/ml for patients 1, 2 and 10 mg/ml for patients 3, 5, 6, 7.*

(a) *Patient 8*

(b) *Patient 9*

(c) *Patient 12*

(d) *Patient 13*
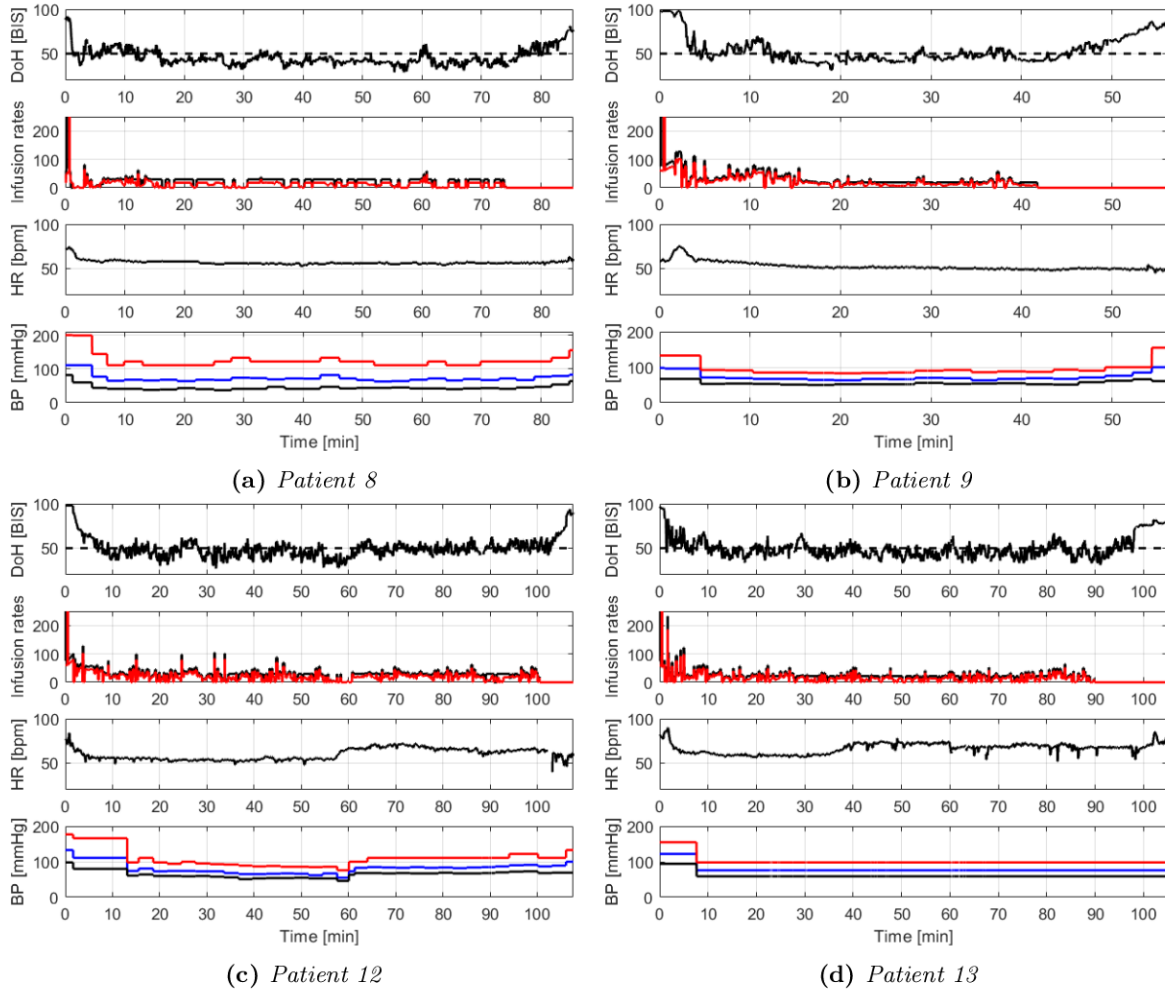
Figure 4.4: *Recorded clinical data of the patients enrolled with the event-based PID MISO controller. From top to bottom: BIS (solid line) and BIS set-point (dashed line); propofol (black) and remifentanil (red) infusion rates in ml/h; HR; BP_s (red), BP_d (black) and BP_m (blue). Missing data were due to temporary issues with sensors reading. Infusion pumps: Graseby 3500. Propofol dilution: 20 mg/ml. BP were not recorded properly for Patient 13 due to an issue with data recording.*

	Event-based	Time-based	P value
Induction time [min]	1.65 (1.92)	1.78 (0.96)	0.08
Lowest BIS	43 (12)	44 (8)	0.28
Propofol dose [mg/kg]	1.98 (0.44)	1.53 (0.69)	0.04*
Remifentanil dose [μg/kg]	2.45 (0.68)	1.69 (0.98)	0.08

Table 4.7: *Comparison of the performance indexes for the induction phase obtained with the time-based and with the event-based PID MISO controller. Data are presented as median (IQR). Statistically significant differences between groups are marked with an asterisk ($P < 0.05$).*
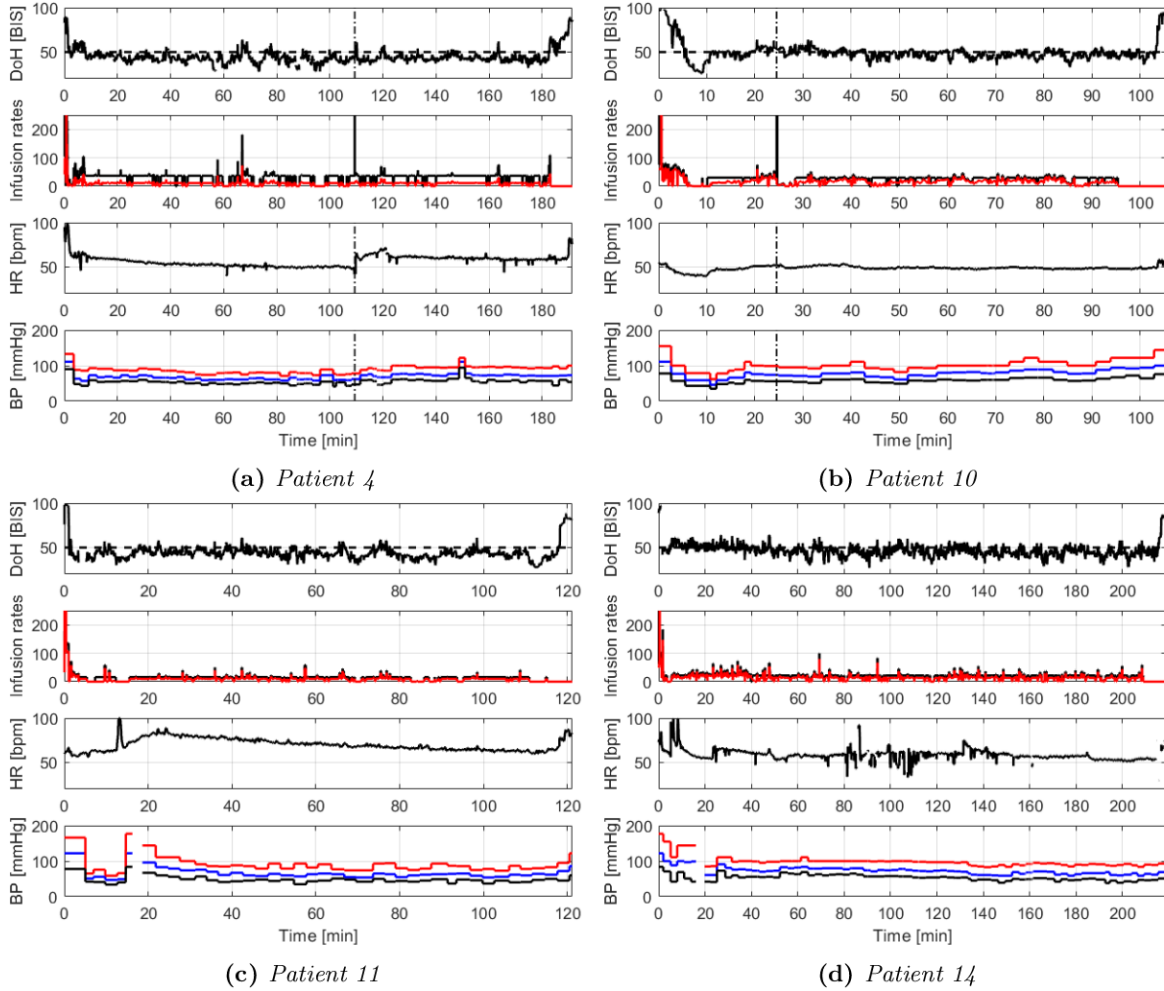
Figure 4.5: *Recorded clinical data of the patients enrolled with the event-based PID MISO controller. From top to bottom: BIS (solid line) and BIS set-point (dashed line); propofol (black) and remifentanil (red) infusion rates in ml/h; HR; BP_s (red), BP_d (black) and BP_m (blue). The vertical black dash-dotted lines are the boluses of propofol. Missing data were due to temporary issues with sensors reading. Infusion pumps: Alaris GH for patient 4 and Graseby 3500 for patients 10, 11, 14. Propofol dilution: 10 mg/ml for patient 4 and 20 mg/ml for patients 10, 11, 14. In patient 4, around minute 110, the anesthesiologist performed a preventive 0.2 mg/kg bolus of propofol. In patient 10, around minute 25, the anesthesiologist performed a preventive 0.4 mg/kg bolus of propofol. In both patients the bolus was performed to increase the hypnotic dosage before the beginning of a phase of strong surgical stimulation. In patient 11, the sudden rise in the values of the hemodynamics variables around minute 30 was caused by a bolus of etilefrine. In patient 14, the HR shows a large noise due to the electromagnetic interference produced by the electrocautery device.*

	Event-based	Time-based	P value
BIS 40-60	82.50 (12.40)	85.20 (10.13)	0.6186
BIS<40	16.78 (11.50)	11.31 (9.50)	0.1684
BIS>60	0.79 (1.25)	3.60 (2.42)	0.0054*
Propofol [mg/kg/h]	5.11 (0.95)	6.26 (3.61)	0.0609
Remifentanil [μg/kg/min]	0.13 (0.04)	0.17 (0.13)	0.0809
TV Propofol [mg/s^2]	0.0052 (0.0036)	0.018 (0.0046)	<0.0001*
TV Remifentanil [μg/s^2]	0.012 (0.0071)	0.035 (0.013)	0.0002*
MDPE [%]	-13 (10)	-7 (10)	0.3149
MDAPE [%]	14 (6)	10 (5)	0.3840
WOBBLE [%]	6 (2)	7.2 (4.5)	0.6274
T awakening [min]	7.36 (5.63)	7.51 (2.92)	0.5387

Table 4.8: *Comparison of the performance indexes for the maintenance phase obtained with the time-based and with the event-based PID MISO controller. Data are presented as median (IQR). Statistically significant differences between groups are marked with an asterisk ($P < 0.05$).*

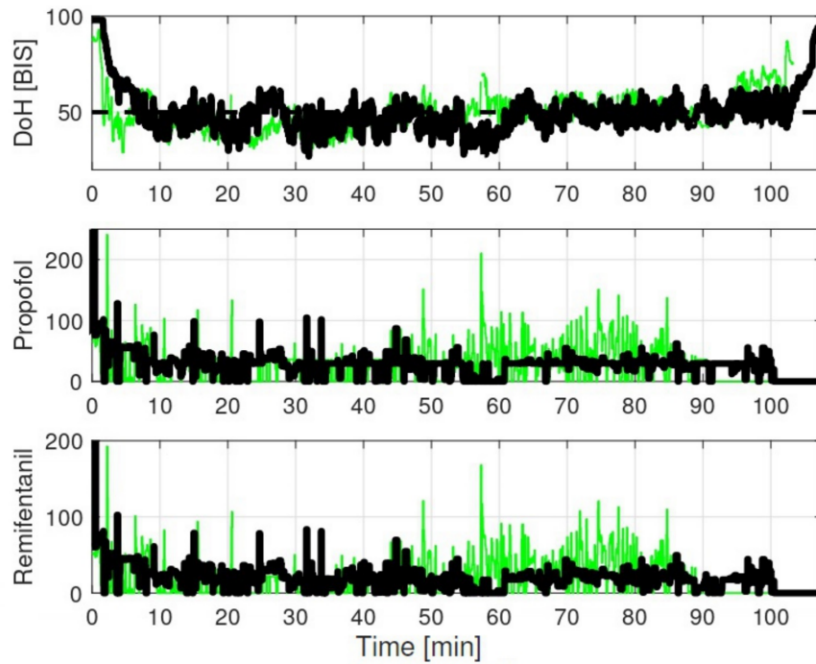**Figure 4.6:** *Graphical comparison between the results obtained with the time-based (green - Patient 6 of Section 3.2) and with the event-based PID MISO controller (black - Patient 12). Propofol and remifentanil infusion rates are expressed in ml/h.*

The threshold for significance is 5%. In the tables the data are shown with median and IQR. Patients demographic data comparison between the two groups is shown in Table 4.6 and there are no statistically significant differences between groups.

The comparison of performance regarding induction is shown in Table 4.12. The boxplots of the *Induction time*, the *Lowest BIS* and the *Intubation time* are shown in Figure 4.7. The boxplot for the *Median HR* and the *Median BP$_m$* are shown in Figure 4.8. These latter are the median values of the two hemodynamic variables calculated in the 5 min that follow the induction time. As it is possible to observe, there are no statistically significant differences in the performance indexes for the induction phase with the exception of the *Median HR*. In particular, a lower median value of HR is observed in **(c)** with respect to **(m)**. Although it is not statistically significant, in **(c)** also a lower value of *Median BP$_m$* is observed, as shown in Figure 4.8. These results can be explained by considering the differences in the clinical protocol used for the two groups. In particular, in **(m)** anesthesia is induced with a bolus of propofol and a bolus of fentanyl. In **(c)** anesthesia is automatically induced by the event-based MISO controller by using propofol and remifentanil. As it is known in the literature [128], patients treated with remifentanil show lower values of BP$_m$ and HR with respect to patients treated with fentanyl. However, these differences are not relevant from a clinical point of view as, for both groups, the values of BP$_m$ and HR are fully compatible with those recommended by clinical guidelines. This aspect is further confirmed by the fact that there are no statistically significant differences in the number of vasopressors administered in both groups. The absence of statistically significant differences in the *Induction time* and *Intubation time* indicates that the event-based controller is able to well replicate the anesthesia induction performed by manual administration of drugs without introducing delays in the loss of consciousness or in the timing of intubation. Although there are no statistically significant differences, the boxplot related to the *Lowest BIS* in Figure 4.8 shows that **(c)** provides a reduced range of values with respect to **(m)**. This can suggest that the event-based MISO controller can reduce the variability of the effect achieved on the BIS, thus reducing the risk of inducing excessively deep anesthesia. However, the number of enrolled patients is too limited to draw definitive conclusions.

The comparison of performance regarding the maintenance phase is shown in Table 4.13 and in Figure 4.9. In this context the median HR and median BP$_m$ are the median values of these two hemodynamic variables calculated throughout the maintenance phase. There are statistically significant differences in the BIS 40-60, BIS<40, MDAPE and the number of ephedrine boluses. The event-based controller achieves higher values of BIS 40-60 (with a consequent reduction of BIS<40) and a lower value of MDAPE with respect to manual control. This suggest that the closed-loop system provides values of BIS that are inside the recommended range for most of the maintenance phase. It is worth noting that this result is achieved with the same average propofol and remifentanil infusion rates. This suggest that the closed-loop controller can regulate the drugs infusion rates according to the actual need of the patient. This is obtained without affecting the hemodynamic stability as suggested by the fact that there are no differences in the values of *Median HR* and *Median BP$_m$* between the two groups. With closed-loop control less patients required vasopressors administration, however, this is not particularly relevant since, often, these drugs are requested by the surgeons to facilitate hemostasis. Hence, they are not administered by the anesthesiologist to compensate for inadequate hemodynamics. It is worth noting that, conversely to what happens for MDAPE, there are no statistically significant differences for MDPE between the two groups. With both control strategies negative values of MDPE are obtained. This indicates that the event-based

Patient Id	Age	Height [cm]	Weight [kg]	Gender
1	66	154	79	F
2	81	165	65	M
3	48	174	74	M
4	46	164	62	F
5	66	153	50	F
6	62	160	56	F
7	63	175	86	M
8	67	165	57	F
9	50	165	83	F
10	40	156	62	F
11	55	178	82	M
12	55	164	64	F
13	68	160	60	F
14	71	170	57	F

Table 4.9: *Demographic data of the patient enrolled with manually controlled anesthesia.*

Surgery	Patients involved	Patients Id
Skin cancer exeresis	7	3, 4, 6, 7, 12, 13, 14
Mastectomy	5	1, 2, 5, 9, 10
Mastoplasty	1	8
Elettrochemotherapy	1	11

Table 4.10: *Types of surgery undergone by the patients enrolled with manually controlled anesthesia, number of patients involved and patients identifiers.*

controller tends to keep the BIS in the lower part of the recommended range (hence, below 50). This behavior is consistent with the clinical practice and mimics the anesthesiologist way of manage the BIS, but with a reduced bias and variability. This aspect has been already pointed out for the time-based PID controller in Section 3.3.

As regards the awakening time and the extubation time, there are no statistically significant differences between the two groups. However, the boxplots for these two indicators shown in Figure 4.9 indicate that closed-loop control provides a reduced range of values. This suggests that the time required for the patient to regain consciousness might be more predictable when closed-loop control is employed. This aspect can be beneficial for the anesthesiologist in the clinical practice. However, the number of enrolled patients is too limited to draw definitive conclusions.

	(c)	(m)	P value
Age [years]	61.0 (27)	64.5 (18)	0.63
Height [cm]	169.0 (14)	165.0 (14)	0.70
Weight [kg]	72.5 (32)	64.5 (20)	0.24
Gender [M/F]	7/7	4/10	0.44

Table 4.11: *Demographic data comparison between the patients enrolled with the event-based PID MISO controller **(c)** and with manually controlled anesthesia **(m)**. Data are presented as median (IQR), gender is expressed as male/female ratio. There are no statistically significant difference between the two groups (P > 0.05).*

	(c)	**(m)**	**P value**
Induction time [min]	1.65 (1.92)	1.89 (1.75)	0.85
Lowest BIS	43 (12)	37 (14)	0.17
Intubation time [min]	4.82 (1.15)	3.83 (1.93)	0.19
Median HR [bpm]	60.5 (9)	70.5 (14)	0.008*
Median BP$_{\mathbf{m}}$ [mmHg]	67.0 (20)	76.0 (20)	0.09
Ephedrine bolus [Y/N]	4/10	2/12	0.64
BS episode [Y/N]	0/14	4/10	0.09

Table 4.12: *Comparison of the performance indexes for the induction phase obtained with the event-based PID MISO controller **(c)** and with manually controlled anesthesia **(m)**. Data are presented as median (IQR). There are no statistically significant differences between the two groups (P > 0.05).*
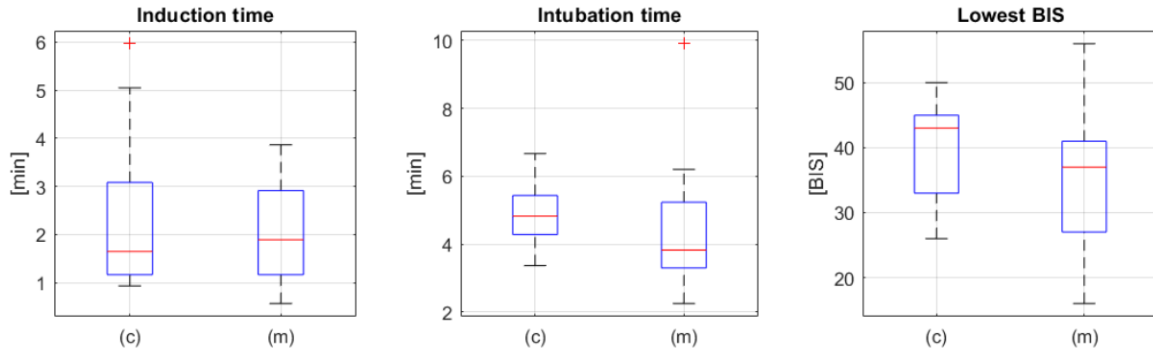
Figure 4.7: *Boxplots of induction performance indexes obtained with the event-based PID MISO controller **(c)** and with manually controlled anesthesia **(m)**. The red horizontal line indicates the median. The bottom and the top edges of the blue box indicate the 25th and the 75th percentiles, respectively. The whiskers indicate the maximum and minimum considered values. Outliers are plotted individually with a red cross.*
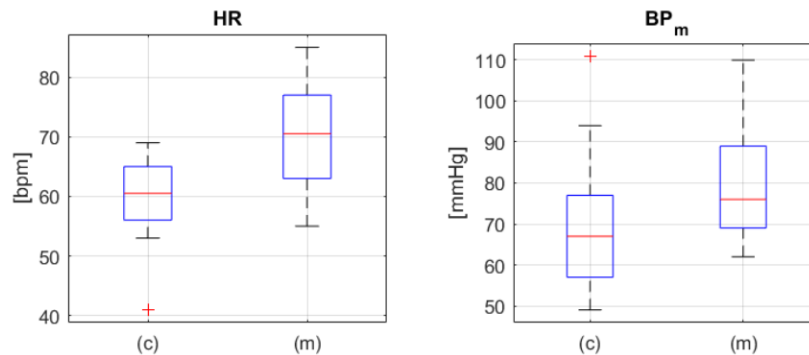
Figure 4.8: *Boxplots of hemodynamic variables during induction obtained with the event-based PID MISO controller **(c)** and with manually controlled anesthesia **(m)**. The red horizontal line indicates the median. The bottom and the top edges of the blue box indicate the 25th and the 75th percentiles, respectively. The whiskers indicate the maximum and minimum considered values. Outliers are plotted individually with a red cross.*
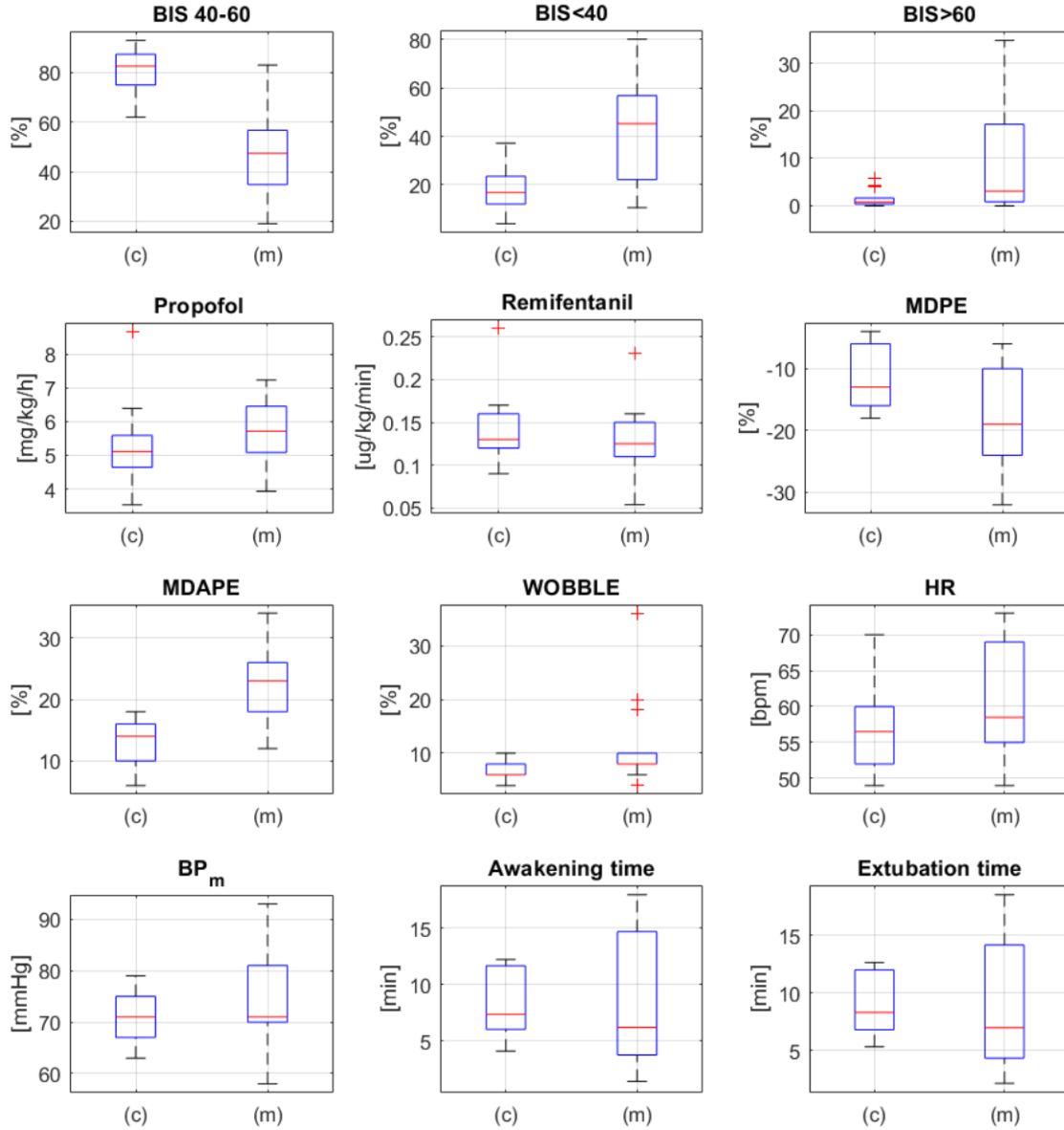
Figure 4.9: *Boxplots of maintenance performance indexes obtained with the event-based PID MISO controller* **(c)** *and with manually controlled anesthesia* **(m)**. *The red horizontal line indicates the median. The bottom and the top edges of the blue box indicate the 25th and the 75th percentiles, respectively. The whiskers indicate the maximum and minimum considered values. Outliers are plotted individually with a red cross.*

	(c)	(m)	P value
BIS 40-60	82.50 (12.40)	47.36 (21.83)	0.0001*
BIS<40	16.78 (11.50)	45.25 (34.73)	0.0019*
BIS>60	0.79 (1.25)	3.07 (16.29)	0.0536
Propofol [mg/kg/h]	5.11 (0.95)	5.72 (1.37)	0.2063
Remifentanil [μg/kg/min]	0.13 (0.04)	0.13 (0.04)	0.5302
MDPE [%]	-13 (10)	-19 (14)	0.0616
MDAPE [%]	14 (6)	23 (8)	0.0003*
WOBBLE [%]	6 (2)	8 (2)	0.0797
Median HR [bpm]	56.5 (8)	58.5 (14)	0.2789
Median BP$_m$ [mmHg]	71.0 (8)	71.0 (11)	0.3100
Ephedrine bolus [Y/N]	1/13	8/6	0.0128*
BS episode [Y/N]	1/13	5/9	0.1647
T awakening [min]	7.36 (5.63)	6.20 (10.93)	0.6033
Extubation time [min]	8.31 (5.20)	6.98 (9.79)	0.6448

Table 4.13: *Comparison of the performance indexes for the induction phase obtained with the event-based PID MISO controller **(c)** and with manually controlled anesthesia **(m)**. Data are presented as median (IQR). Statistically significant differences between groups are marked with an asterisk (P < 0.05).*

4.3   Conclusions

In this chapter the experimental results obtained with the event-based PID MISO control system proposed in [99] have been presented. The proposed solution has been developed with the aim to obtain a drug infusion profile that mimics the behavior of the anesthesiologist and that is not affected by the noise of the BIS signal. This is the first time that an event-based control strategy is tested in a clinical experimentation. The experiments were conducted on a group of 14 patients scheduled for elective plastic surgery. The experimental conditions were representative of the typical ones that can be found in the routine clinical practice. Indeed, clinical perturbations due to different brands of infusion pumps, different propofol dilutions and manual interventions by the anesthesiologist were present. The results obtained show that the performance of the event-based control system is always consistent with the clinical practice. In particular, an adequate DoH was induced and maintained while providing a good hemodynamics stability. The results also show that the design objective of providing noise-free infusion profiles that mimic those used by the anesthesiologist is achieved. The behavior of the resulting control system is more intuitive, thus making it easier for the anesthesiologist to supervise. Moreover, the event-based control action reduces the control effort on the infusion pumps. These aspects represent a step forward for the use of closed-loop control systems in routine practice.

To better verify and validate this aspect, the results obtained with the event-based PID MISO control system are compared with those obtained with manually controlled anesthesia. Comparison with the manual practice suggests that the system can be well integrated into clinical practice. In particular, in the induction phase there were no clinically relevant differences between the two control strategies. This implies that the automatic control can be safely used instead of the manual infusion of boluses without problems for patient's safety and without impacting what is the normal clinical practice. By evaluating some indicators of the maintenance phase, it would even seem that the system could improve the clinical performance

with respect to manual control. However, these observations need to be further verified with better structured clinical trials on a larger number of patients and also in surgical fields other than plastic surgery.

Chapter 5

Model predictive control of anesthesia

The use of MPC techniques to perform closed-loop anesthesia has been widely investigated, as described in Section 2.1. This interest is mainly motivated by the possibility to exploit the PK/PD models in the control system to predict the clinical response to drugs administration. They also allow for the anesthesia process constraints to be directly embedded into the cost function that is used to determine the control action. From the clinical point of view, they are also interesting since they fall in the framework of personalized medicine. Indeed, they exploit a parameterized patient model based on individual physical characteristics like gender, weight, height and age to improve the prediction capability.

Most of the approaches proposed in the literature use a state estimator, such as Kalman filter [129, 130]. However, this might yield to a long settling time. In [131, 132] a piece-wise linearization of the Hill function is proposed to eliminate the nonlinear component from the control loop. The control scheme, then, uses a hybrid multi-parametric-MPC (mp-MPC) approach. The computation of the control signal requires the use of computationally costly solvers, like multi-parametric Mixed Integer Quadratic Programming (mp-MIQP) or multi-parametric Quadratic Programming (mp-QP) for a simplified control approach. Another approach based on a mp-MPC has been proposed in [133, 134], where the controller is coupled with an external estimator exploiting two methods, a Kalman filter and an online/offline moving horizon, used to address the inter- and intra-patient variability. Additionally, the inverse of the static nonlinearity is used to linearize the system. This compensation of the PK/PD model nonlinear element and the application of a linear MPC is also proposed in [41]. In particular, the Extended Prediction Self-Adaptive Control (EPSAC) algorithm is used. The proposed controller exploits the clipping technique by limiting the control horizon up to one sampling instant, with the result of a sub-optimal tuning that yields a sub-optimal performance. Moreover, due to the clipping technique, the predictive controller does not take into account constraints when computing the optimal control signal for the process. They are applied *a posteriori* when the computed signal violates the saturation limits. The control system proposed in [67] also uses the inverse of the nonlinear part of the PD model to linearize the process. Different approaches for propofol dynamics, taking into account a time delay, are considered. The main issue analyzed concerns the mismatch in time delays between the model used and the patient. The results obtained from clinical trials show that an MPC-based system can be effective in DoH control in general anaesthesia. Anyway, it appears that there

is still the need to provide simple and efficient MPC strategies that can be easily applied in practice and whose robustness is clearly demonstrated.

In this chapter, a novel control architecture is proposed. The PID-based approach described in Section 2.2.2 is extended substituting the PID controller with a Generalized Predictive Control (GPC) algorithm to handle all the constraints. The GPC controller is widely used in many industrial process control applications due to its efficacy and adaptability [135, 136], but, with respect to the previously mentioned MPC techniques, here the PK/PD model is applied straightforwardly and it is integrated within the control scheme. In this way, the complex design of the state estimators is avoided. Consequently, an easily implementable and efficient solution that achieves a suitable trade-off between the model complexity and the accuracy of the real patient response approximation is provided. Moreover, the control system design is based on patient demographic data, that are used to define the model. Indeed, the linear PK/PD model is obtained separately for each patient, while the Hill function is compensated by inverting the average model, since it cannot be estimated for each individual. The linear model is used as a predictor, while a low-pass filter is employed for the attenuation of the differences between the model and the real patient responses. This filter provides an extra degree of freedom in the control system and it is designed for performance adjustment. Additionally, a reference filter leads to the achievement of the desired performance in the induction phase. Thus, a two-degree-of-freedom controller is obtained [137, 138]. Due to this configuration, the controller and the filter need a simultaneous co-design, which is performed using the optimization-based methodology. Then, the robustness of the system is verified through an extensive inter- and intra-patient variability analysis with the Monte Carlo method described in Section 2.2.1.

The design of the SISO control scheme for propofol administration is first described and the results obtained in simulation are presented [105]. Its behavior with respect to BIS noise is then investigated [106] and the experimental results obtained in an in-vivo study are presented [107]. The proposed architecture is then extended for the MISO case of propofol and remifentanil coadministration and simulation results are presented [108]. Finally, the SISO control scheme is extended by implementing an event-based technique and simulation results are presented [109].

5.1   Linear SISO MPC for anesthesia process with external predictor

In this section, a new SISO MPC control system for anesthesia regulation is presented. The BIS is used as feedback variable and it is controlled through propofol administration. The proposed control scheme is based on an external predictor that, by exploiting the PK/PD model of propofol, compensates for the process nonlinearity and increases the system robustness by means of an additional filter. The performance of the developed control scheme is evaluated through an extensive simulation study, which considers inter-patient and intra-patient variability by applying a Monte Carlo technique. The obtained results show that the proposed methodology is effective in both the induction and maintenance phases.

5.1.1 Control system architecture

The proposed control structure is shown in Figure 5.1. It embeds the PK/PD model and compensates for the effect of its nonlinear part by inverting the Hill function. The computation of GPC internal matrices is performed by taking into account the nominal linear part of the Schnider model, that depends on patient physical characteristics. In this way the demographic data of the patient, which are easily measurable, are embedded into the used model. In Figure 5.1, the true patient model is represented with its linear part P and with its nonlinear part H. However, in practice, exact values for these two components are unknown and need to be calculated with an inaccurate PK/PD model. For this reason, in the control structure these elements are referred to as $\tilde{P}$ and $\tilde{H}$ for the linear and the nonlinear part, respectively, in order to distinguish them clearly from the real ones. As already mentioned, $\tilde{P}$ can be obtained for each patient based on their demographic data. Conversely, since $\tilde{H}$ can not be obtained for each patient, its value is computed by taking into account the average values of Vanluchene shown in Table 1.3. The E_0 parameter can be measured before the induction phase and the actual value can be used for each patient. The $\tilde{P}$ block input signal $u(t)$ represents the propofol infusion rate and its output is the estimated effect site concentration $C_e(t)$ of the patient. To compensate for the nonlinear behavior, the inverse of average Hill function $\tilde{H}^{-1}$ is introduced and defined as:

$$\tilde{H}^{-1} = C_{e_{50}} \sqrt[\gamma]{\frac{\bar{E} - E_0}{E_0 - \bar{E} - E_{max}}},$$

where $\bar{E}$ is the current BIS signal value. In the nominal case, when there are no modelling errors and uncertainties between the model and the patient, (namely, $\tilde{P} = P$ and $\tilde{H} = H$), the architecture can be converted to a linear control system of the linear component of PK/PD model. In the resulting control scheme, $w(t)$ is the filtered value of $\hat{r}(t)$, which is the reference value of the effect site concentration that reflects the desired BIS reference $r(t)$. The $\hat{r}(t)$ value is computed using $\tilde{H}^{-1}$ that relates the BIS and the estimated effect site concentration $C_e(t)$ of the patient. Therefore, in the nominal case, $\hat{C}_e(t) = \tilde{C}_e(t)$ and the resulting feedback signal is equal to $\tilde{C}_e(t)$. This only changes when the controlled process output is affected by the disturbances $d(t)$. In practice, model uncertainties are unavoidable, in particular those related to the static nonlinearity in the Wiener model. This is because it is virtually impossible to know the exact values of the parameters *a priori*. Additionally, the linear component of the PK/PD model has uncertainties owing to model inaccuracy and parameters variability. For this reason, the $\theta(t)$ signal will be used to compensate differences related to modelling uncertainties and for the disturbances induced by surgical stimuli. The contribution of $\theta(t)$ depends on the error between the estimated effect site concentration $C_e(t)$ and the effect site concentration $\hat{C}_e(t)$ calculated with the BIS signal via the average Hill function inversion. In this way, the $w(t)$ signal is used as the reference for the GPC controller, while the controlled variable is $\tilde{y}(t)$, containing information about patient model mismatch and disturbances (the feedback signal). The resulting contribution of the $\theta(t)$ signal is attenuated by the F_d filter, placed in the feedback loop, which reduces the effect of uncertainties and disturbances on the GPC controller and simultaneously guarantees a zero steady-state tracking error. The F_d filter will affect directly the response of the control signal to the disturbances and to the model uncertainties. Moreover, it will provide additional robustness since filtered disturbances are

introduced into the control loop. It has been selected F_d as a first-order low-pass filter:

$$F_d(s) = \frac{1}{T_d s + 1}, \tag{5.1}$$

Additionally, in order to build a two-degree-of-freedom scheme, the F_r filter is used to achieve the desired set-point response, where the controller focuses on the disturbance rejection task. The F_r transfer function is:

$$F_r(s) = \frac{1}{T_r s + 1}, \tag{5.2}$$

The resulting control system needs to be tuned with the typical two-degree-of-freedom methodology, where the controller and the F_d filter are first tuned by focusing on the disturbance rejection performance (maintenance phase). Then, F_r is adjusted to obtain the desired performance for the reference tracking task (induction phase). An additional aspect to be considered concerns the minimum and maximum admissible infusion rates. The minimum value is 0 mg/s. The upper limit of the infusion rate has been set at 6.67 mg/s for the induction phase and at 4.00 mg/s for the maintenance phase. This latter value represents the maximum infusion rate typically used during a bolus in the maintenance phase when anesthesia is manually administered. The choice of using two different upper limits for the two phases of anesthesia is therefore in accordance to the clinical practice.

As it is well known [135], GPC consists of applying a control sequence that minimizes a multistage cost function of the form:

$$J = \sum_{j=N_1}^{N} [\hat{y}(t+j|t) - w(t+j)]^2 + \sum_{j=1}^{N_u} \lambda[\Delta u(t+j-1)]^2, \tag{5.3}$$

where $\hat{y}(k+j|t)$ is an optimal system output prediction sequence performed with known data up to discrete time t, $\Delta u(t+j-1)$ is a future control increment sequence obtained from cost function minimization with $\Delta = (1-z^{-1})$, N_1 and N are, respectively, the minimum and maximum prediction horizons, N_u is the control horizon and λ weights the future control efforts (with respect to the tracking errors) along the horizon. The horizons and weighting factor are design parameters used as tuning variables. The reference trajectory along the prediction horizon is represented by $w(k+j)$ [135]. In 5.3, the j-step ahead prediction of system output with data up to time t, $\hat{y}(k+j|t)$, is computed using the following model representation [135]:

$$A(z^{-1})\tilde{y}(t) = B(z^{-1})u(t-1) + \frac{e(t)}{\Delta}, \tag{5.4}$$

where A and B are adequate polynomials in the backward shift operator z^{-1} and $e(t)$ is a zero mean white noise that is set equal to zero. The prediction equation in vectorial form can be expressed as:

$$\widehat{\mathbf{y}} = \mathbf{G}\mathbf{u} + \mathbf{f}, \tag{5.5}$$

where $\widehat{\mathbf{y}}$ are the future process outputs, $\mathbf{G}$ is the dynamics matrix, $\mathbf{u}$ are the control signal values (decision variable) and $\mathbf{f}$ are the values of the free response of the process.

The predictive controller can handle the constraints in the optimization procedure. It is an important feature from a practical point of view since all limitations are considered in the computed control signal. This can be beneficial for the achievable performance. The limita-

tions of the control signal are included into the optimization procedure. For this purpose, the saturation limits, $u_{min} \leq u(t) \leq u_{max}$ can be expressed as a function of inequalities on the control signal increments:

$$\mathrm{l}u_{min} \leq \mathbf{T}\Delta\mathbf{u} + u(t-1) \leq \mathrm{l}u_{max}.$$

where $\mathbf{T}$ is $N \times N$ lower triangular matrix of ones, $\mathbf{l}$ is a $1 \times N$ vector of ones. The slew-rate constraints are imposed directly on the control signal increments vector Δu. In this case, the constraints can be expressed through the inequality $\Delta u_{min} \leqslant u(t) - u(t-1) \leqslant \Delta u_{max}$. As in the previous case, this can be rewritten in vectorial form as:

$$\mathrm{l}\Delta u_{min} \leqslant \Delta\mathbf{u} \leqslant \mathrm{l}\Delta u_{max},$$

The slew-rate constraints are also adjusted depending on the anaesthesia phase. In particular, $-1 \leqslant \Delta\mathbf{u} \leqslant 1 \ mg/s$ is considered for the induction phase, and $-0.4 \leqslant \Delta\mathbf{u} \leqslant 0.4 \ mg/s$ is considered for the maintenance phase. In order to obtain the desired behavior of the manipulated variable, it is also necessary to introduce additional constraints for the maintenance phase. In particular, if the sum of Δu in the last 5 samples is greater than $0.5 \ mg/s$, then the maximum allowed decrement of the manipulated variable (for the next calculation) is set to $\Delta u_{min} = -0.1 \ mg/s$. This compensates for positive disturbances preventing the controller output to decrease too fast. Additionally, if the BIS value is lower than the reference, then the maximum allowed increment of the manipulated variable is set to $\Delta u_{max} = +0.1 \ mg/s$. In this way, when there is a negative disturbance, the manipulated variable is forced to stay at low levels until the BIS reaches the reference. These constraints can be expressed, in general, as $\mathbf{R}\Delta\mathbf{u} \leqslant \mathbf{c}$ where:

$$\mathbf{R} = \left[\begin{array}{c} \mathbf{I}_{N \times N} \\ -\mathbf{I}_{N \times N} \\ \mathbf{T} \\ -\mathbf{T} \end{array} \right] ; \mathbf{c} = \left[\begin{array}{c} \mathrm{l}\Delta u_{min} \\ -\mathrm{l}\Delta u_{max} \\ \mathrm{l}u_{max} - \mathrm{l}u(t-1) \\ -\mathrm{l}u_{min} + \mathrm{l}u(t-1) \end{array} \right].$$

where $\mathbf{I}_{N \times N}$ is the identity $N \times N$ matrix. Finally, the QP optimization problem can be stated as:

$$J(\mathbf{u}) = \frac{1}{2}\mathbf{u}^T\mathbf{H}\mathbf{u} + \mathbf{b}^T\mathbf{u} + \mathbf{f}_0,$$

subject to:

$$\mathbf{R}\Delta\mathbf{u} \leqslant \mathbf{c},$$

where $\mathbf{H} = 2(\mathbf{G}^T\mathbf{G} + \lambda\mathbf{I})$, $\mathbf{b}^T = 2(\mathbf{f} - \mathbf{w})^T\mathbf{G}$, $\mathbf{f}_0 = (\mathbf{f} - \mathbf{w})^T(\mathbf{f} - \mathbf{w})$ and $\mathbf{w}$ is the vector of reference signals [135].

In order to obtain the performance that satisfies the clinical requirements, all the tuning parameters need to be adjusted to handle the set-point following and disturbances rejection tasks. Usually, the effective disturbance rejection in GPC algorithm requires an aggressive tuning of the controller [139], that might result in an undesired undershoot in the reference tracking performance. This requires to handle the set-point following and disturbance rejection tasks separately. Therefore, tuning is divided into two phases. First, the GPC controller is tuned by considering also the F_d filter and introducing the disturbance modelled as a two steps (one positive and the other negative) signal [138]. At this stage, the following parameters are obtained: N, N_u, λ, and T_d, which are, respectively, the prediction horizon, the
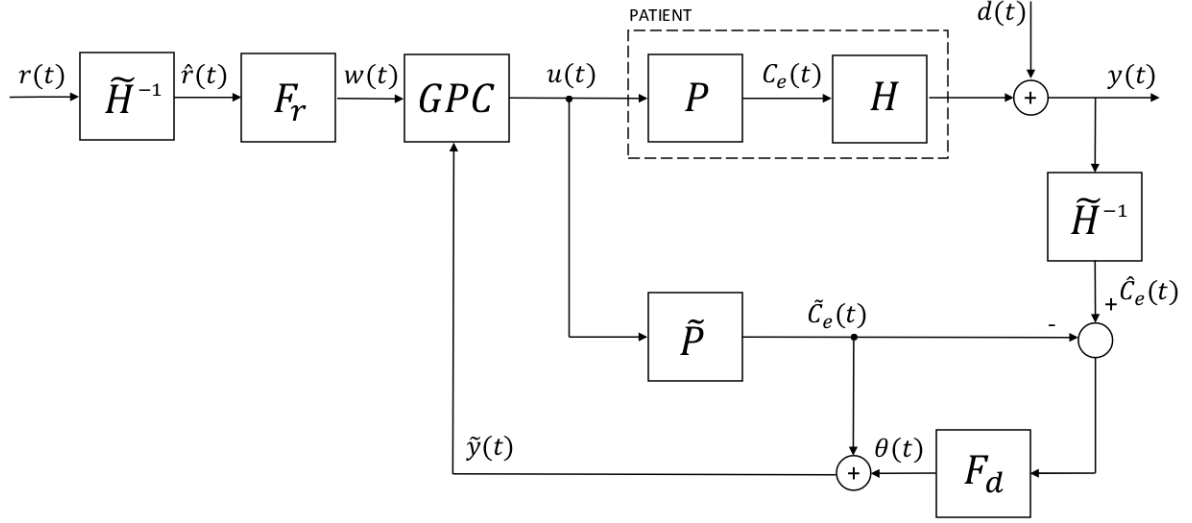
Figure 5.1: *Schematic representation of the SISO MPC control system with the external predictor.*

control horizon, the control signal weighing factor and the F_d filter time constant. Following the optimization-based approach presented in Section 2.2.1, the optimization problem (2.2) is solved by means of GA with a population size of 40 elements and by stopping the optimization when the relative change in the cost function value over the last 50 iterations is less than 0.001. The IAE is obtained by simulating the response to the double-step disturbance profile shown in Figure 1.6. Then, the F_r filter time constant T_r is determined by considering the already tuned GPC, but focusing only on the set-point response. Also in this case, the value of T_r is determined in order to minimize the worst-case IAE value in the set-point step response that is simulated by applying a set-point change from the initial BIS value to the desired hypnosis level of $BIS = 50$. The controller parameters obtained from the optimization procedure are: $N = 27$, $N_u = 7$, $\lambda = 1.6$, $T_d = 22.7$ s and $T_r = 22.4$ s.

5.1.2   Simulation results

The controller performance is analyzed in simulation both for the induction and maintenance phases. As regards the induction phase, a set-point change from the initial BIS value to the desired hypnosis level of $BIS = 50$ is performed. As regards the maintenance phase, the double-step disturbance profile shown in Figure 1.6 is applied. The controller performance is first analyzed on the tuning dataset shown in Table 2.1. As a first illustrative example, patient 13 is considered. Note that, since the Hill function parameters are not known and its average values are employed, there is a mismatch in the nonlinear element of the model that is used in the external predictor and the one that represents the virtual patient. Results are shown in Figure 5.2. It is noticeable that the performance achieved meets all the clinical requirements. In fact, the BIS level attains the set-point reference without undershoot and within the desired settling time. The numerical performance evaluation for the average patient is shown in Table 5.1. In this case, the TT is equal to the ST10 index, which means that the BIS signal does not exceed the 45 and 55 thresholds and BIS-NADIR indicates that there is no undershoot. Considering the disturbance rejection task, during the maintenance phase,

it is possible to see that the control action increases to compensate the first (positive) step in order to decrease the DoH of the patient and vice versa with the second (negative) step. The controller response for this task is much more aggressive compared to the set-point tracking one (see Figure 5.2), because a fast rejection of the disturbances is required. The indexes for each disturbance step are summarized in Table 5.2. The settling times TTn and TTp meet the clinical practice requirements, since the controller action yields a fast disturbance rejection without excessive undershoot and overshoot in the BIS level, as proved by BIS-NADIRp and BIS-NADIRn. The TTn value is higher than TTp because of the lower saturation limit of the pump. In fact, when a negative step disturbance occurs, the controller has to decrease the infusion in order to increase the DOH of the patient, but the lower infusion limit is zero. Therefore, the BIS level increases naturally, which implies a higher settling time.

Robustness is a critical issue for MPC approaches because model uncertainties can result in a significant performance deterioration or event instability. In order to validate the robustness to inter-patient variability, the same tests performed on the average patient 13 have been repeated for all the patients of the tuning dataset. Note that, also in these tests, the hypothesis of perfect knowledge of the linear part of the process model is applied ($\tilde{P} = P$) but the average Hill function is used in the controller instead of the actual patient's one ($\tilde{H} \neq H$). The process outputs and the control actions for the induction phase are shown in Figure 5.3a. It can be observed that the BIS signals are very similar: all the patients enter the BIS range from 40 to 60 in the required time interval and all settle at the established reference in comparable times. The transient responses are very similar.

The performance indexes for the analyzed cases are shown in Table 5.3, and they are referred to as "A". They are compared with the results obtained with the model-based PID control scheme presented in Section 2.2.2, which is referred to in Table 5.3 as scheme "B". From the comparison, it appears that the MPC system outperforms the PID-based control system, obtaining lower values of TT, TS10 and TS20, which implies a faster response. For example, the MPC-based scheme improves the average value of TT of about 21% with respect to the PID-based scheme. In addition, the average BIS-NADIR value is 48.22 with standard deviation of 3.38, which is comparable with the PID-based controller. Then, the proposed approach has been compared with previously developed MPC systems. In particular, the methods presented in [41] and [132] has been considered, since both use the same tuning dataset for performance evaluation. In [41] the reported results for the MPC control strategy (in this case the EPSAC algorithm is used) show an average TT of 1.8 min, which is 28% larger than the average TT obtained by the approach proposed in this paper. In addition, the ST10 index reported in [41] has a value of 2.05 min, in contrast to 1.66 min obtained by the control scheme proposed here, with an average BIS-NADIR index of 48.06. Finally, the average ST10 reported in [132] is around 4 min, which is higher than the one obtained with the proposed method. The control system robustness to inter-patient variability is also verified for the disturbance rejection test. In Figure 5.3b the response to the disturbances is shown for each patient, while the corresponding performance indexes are shown in Table 5.4. The obtained results meet all the clinical requirements. Comparing the obtained results with those reported in Section 2.2.2, it can be seen that both control systems have a similar performance for the positive disturbance step. However, the situation changes when the negative disturbance step occurs. In this case the proposed control scheme is significantly faster (about 25%) than the PID-based scheme, yet it obtains similar overshoot values.

To further validate the controller robustness to inter-patient variability the method described in Section 2.2.1 has been applied. The parameters of the Hill function have been generated

by considering the statistical properties given in [28]. As in the previous case, P is fixed equal to $\tilde{P}$ and $\tilde{H}$ is chosen as the average Hill function. The results of the induction phase are shown in Figure 5.4a, while those of the maintenance phase are shown in Figure 5.4b. The corresponding indexes are shown in Tables 5.5 and 5.6. Note that two patients have an undershoot that exceeds the lower limit of 40. The problem is not relevant, as the excessive undershoot is minimal, reaching a BIS of 38 and 39 respectively. The simulated results show that the control system is robust with respect to the inter-patient variability and the clinical specifications are always met.

In the previous tests a perfect knowledge of the linear part of the patient model has been assumed, because the objective was to test the robustness of the controller over a wide population. The robustness of the controller against the mismatches of the linear part of the model, that is, against intra-patient variability has also been tested. To simulate this variability, the method described in Section 2.2.1 has been applied with the statistical properties of the PK model given in [25], and for each of the perturbed models the response to disturbance has been simulated. In particular, for each patient of the tuning dataset, $\tilde{P}$ is calculated on the basis of the average parameters values and P is generated by using their statistical distributions. The responses of the average patient 13 for the induction phase are shown in Figure 5.5a and the corresponding performance indexes are summarized in Table 5.7. Despite the intra-patient variability, the set-point response is always satisfactory and the clinical specifications are always met. The results of this study, considering all the other patients, can be seen in Figure 5.5b. The results of the maintenance phase of the average patient 13 are shown in Figure 5.6 and the performance indexes are shown in Table 5.8, while the results of all the patients are shown in Figure 5.7. It appears that the specifications are also met in the presence of intra-patient variability.

The proposed method has also been evaluated with two different disturbance profiles, denoted as I and II, which have been previously used, respectively, in [43, 44] and [132, 134, 140]. They are shown in Figures 1.7 and 1.8. Analyzing the results obtained with the disturbance profile I, which are shown in Figure 5.8a, it is possible to observe that the controller provides a fast disturbance rejection as the BIS remains for a most of time at the desired level. Indeed, the BIS begins to reach the reference immediately after the step disturbance (A). The same happens for the last part (C) of the disturbance profile, resulting in a very small undershoot. The results with the disturbance profile II are shown in Figure 5.8b. In this case too the proposed control scheme obtains satisfactory results, handling properly all surgical stimuli. Note that the stage C in this disturbance profile provides a very challenging situation for the controller, since the absolute change in the disturbance is equal to 40. However, the proposed control system reacts very quickly and does not allow the BIS signal to exceed the set-point plus disturbance value. With these test scenarios it is confirmed that the proposed control system provides a reliable and robust solution for the DoH control in the anaesthesia process. All simulations have been performed in Matlab 2017a on a 64-bit PC platform (Intel i7 2.4 GHZ, 8 GB RAM) running Microsoft Windows 10. The formulated optimization problem has been solved online using classical QP from Matlab Optimization Toolbox. The average computational time required for the control signal calculation is 19 milliseconds.
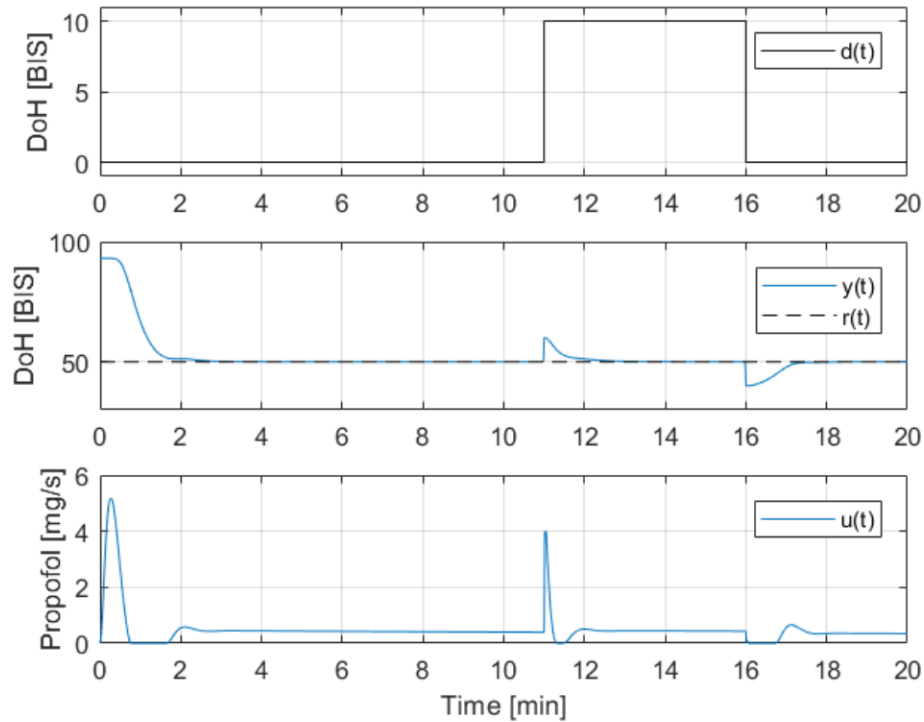
Figure 5.2: *Response obtained for the thirteenth patient of the tuning dataset using the SISO MPC control system.*

TT $[min]$	BIS-NADIR	ST20 $[min]$	ST10 $[min]$
1.37	50.00	1.18	1.37

Table 5.1: *Induction phase performance indexes obtained with the SISO MPC control system on the thirteenth patient of the tuning dataset.*

TTp $[min]$	BIS-NADIRp	TTn $[min]$	BIS-NADIRn
0.33	50.00	0.78	50.00

Table 5.2: *Maintenance phase performance indexes obtained with the SISO MPC control system on the thirteenth patient of the tuning dataset.*

(a) *Induction phase*   **(b)** *Maintenance phase*
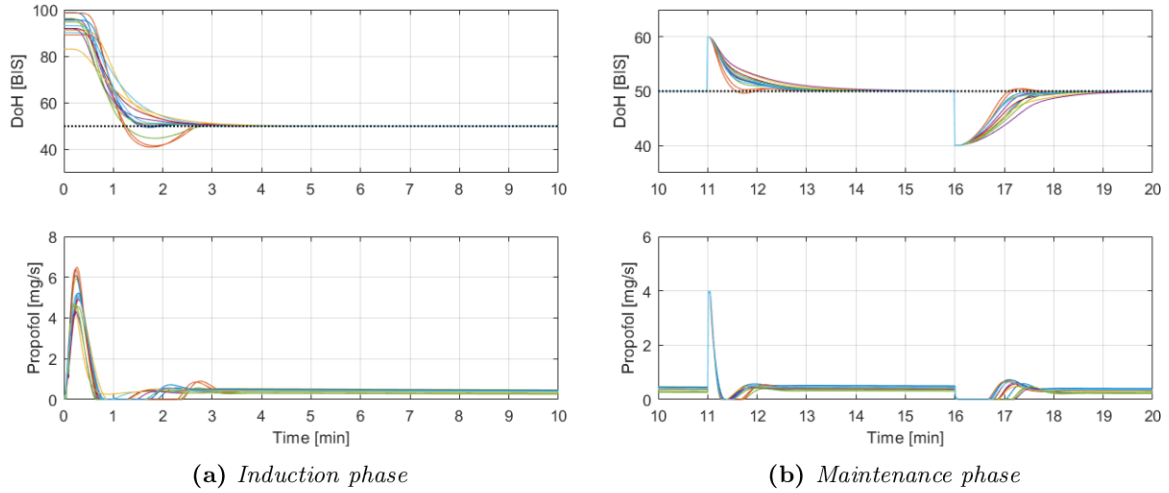
Figure 5.3: *Responses obtained for each patient of the tuning dataset with the SISO MPC control system.*

(a) *Induction phase*   **(b)** *Maintenance phase*

Figure 5.4: *Responses obtained with the SISO MPC control system on the population of 500 patients used to simulate inter-patient variability.*

Patient	Scheme	TT [min]	BIS-NADIR	ST20 [min]	ST10 [min]
1	A	1.27	49.89	1.08	1.27
	B	1.63	49.55	1.32	1.63
2	A	1.15	41.60	1.05	2.33
	B	1.38	48.29	1.25	1.38
3	A	1.75	50.00	1.40	1.75
	B	2.01	49.90	1.70	2.01
4	A	1.25	50.00	1.29	1.25
	B	1.60	49.72	1.07	1.60
5	A	1.07	44.86	0.95	1.95
	B	1.33	49.20	1.09	1.33
6	A	1.90	50.00	1.50	1.90
	B	2.21	49.91	1.80	2.21
7	A	1.68	50.00	1.27	1.68
	B	1.96	49.76	1.54	1.96
8	A	1.27	49.51	1.12	1.27
	B	1.60	49.88	1.37	1.60
9	A	1.12	41.01	1.05	2.28
	B	1.33	44.71	1.23	2.01
10	A	1.92	50.00	1.38	1.92
	B	2.30	49.89	1.68	2.30
11	A	1.35	50.00	1.03	1.35
	B	1.65	49.54	1.22	1.65
12	A	1.20	50.00	0.98	1.20
	B	1.48	49.44	1.14	1.48
13	A	1.37	50.00	1.18	1.37
	B	1.72	49.75	1.44	1.72
mean	A	1.41	48.22	1.16	1.66
	B	1.71	49.19	1.39	1.76
std.dev	A	0.30	3.38	0.17	0.40
	B	0.42	1.99	0.23	0.30
max.	A	1.92	50.00	1.50	2.33
	B	2.30	49.91	1.80	2.30
min.	A	1.07	41.01	0.95	1.20
	B	1.33	44.71	1.09	1.33

Table 5.3: *Performance indexes for the induction phase obtained for each patient of the tuning dataset, where A is the SISO MPC control system, and B is the PID-based control system from Section 2.2.2.*

Patient	Scheme	TTp [min]	BIS-NADIRp	TTn [min]	BIS-NADIRn
1	A	0.40	50.00	0.98	49.99
	B	0.42	50.02	1.26	50.03
2	A	0.28	50.00	0.75	50.46
	B	0.29	49.84	0.97	50.08
3	A	0.37	50.00	0.77	50.00
	B	0.39	50.02	1.00	50.05
4	A	0.37	50.00	0.85	50.00
	B	0.38	50.01	1.00	50.05
5	A	0.33	50.00	1.02	50.00
	B	0.36	50.00	1.37	50.03
6	A	0.38	50.00	0.77	49.99
	B	0.41	50.02	0.97	50.05
7	A	0.42	50.01	0.92	49.98
	B	0.45	50.02	1.15	50.03
8	A	0.33	50.00	0.78	50.00
	B	0.36	50.02	0.93	50.06
9	A	0.27	49.63	0.70	50.42
	B	0.28	50.02	0.86	50.08
10	A	0.50	50.02	0.98	49.93
	B	0.53	50.02	1.24	50.02
11	A	0.50	50.05	1.22	49.93
	B	0.53	50.01	1.53	50.00
12	A	0.40	50.01	1.08	49.99
	B	0.43	50.00	1.38	50.02
13	A	0.33	50.00	0.78	50.00
	B	0.36	50.02	0.97	50.06
mean	A	0.38	49.98	0.89	50.05
	B	0.40	50.00	1.12	50.04
std.dev	A	0.07	0.10	0.16	0.17
	B	0.08	0.05	0.21	0.02
max.	A	0.50	50.05	1.22	50.46
	B	0.53	50.02	1.52	50.08
min.	A	0.27	49.63	0.70	49.93
	B	0.28	49.84	0.86	50.00

Table 5.4: *Performance indexes for the maintenance phase for each patient of the tuning dataset, where A is the SISO MPC control system, and B is the PID-based control system from Section 2.2.2.*

	TT $[min]$	BIS NADIR	ST10 $[min]$	ST20 $[min]$
mean	1.46	49.16	1.18	1.51
std.dev	0.21	1.91	0.13	0.29
min.	0.98	37.64	0.88	1.08
max.	2.03	50.00	2.43	2.87

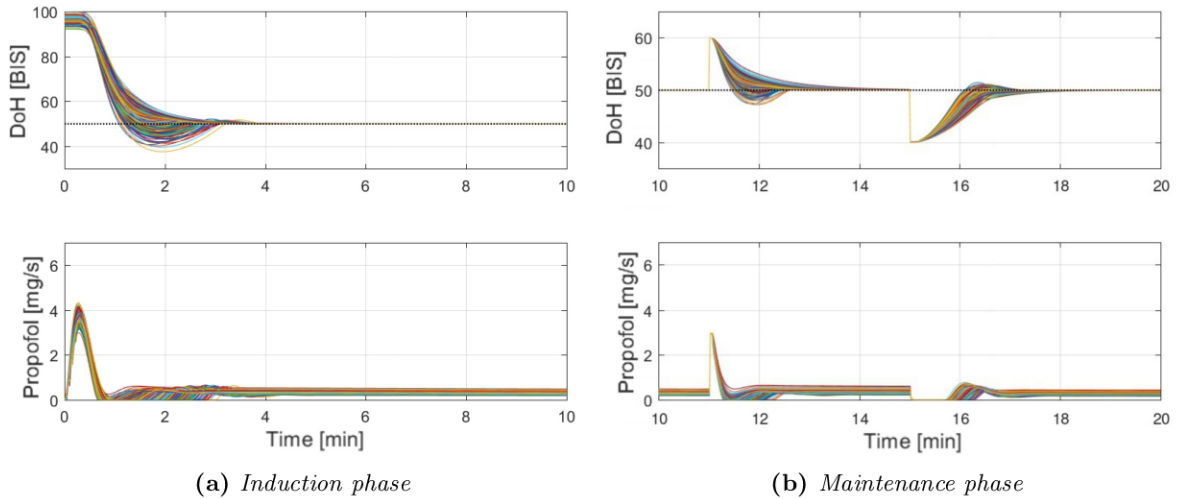**Table 5.5:** *Induction phase performance indexes obtained with the SISO MPC control system on the population of 500 patients used to simulate inter-patient variability.*

	TTp $[min]$	BIS-NADIRp	TTn $[min]$	BIS-NADIRn
mean	0.37	49.91	0.89	50.21
std.dev	0.05	0.34	0.08	0.26
min.	0.25	47.24	0.70	50.00
max.	0.60	50.00	1.13	51.45

Table 5.6: *Maintenance phase performance indexes obtained with the SISO MPC control system on the population of 500 patients used to simulate inter-patient variability.*

	TT $[min]$	BIS-NADIR	ST20 $[min]$	ST10 $[min]$
mean	1.40	49.57	1.17	1.39
std.dev	0.11	0.88	0.05	0.12
min.	1.17	44.10	1.02	1.15
max.	1.90	50.21	1.40	2.17

Table 5.7: *Induction phase performance indexes obtained with the SISO MPC control system on the 500 perturbed models generated starting from the nominal model of the thirteenth patient of the tuning dataset to simulate intra-patient variability.*

	TTp $[min]$	BIS-NADIRp	TTn $[min]$	BIS-NADIRn
mean	0.39	49.98	0.78	50.04
std.dev	0.02	0.07	0.04	0.05
min.	0.33	49.74	0.67	49.93
max.	0.45	50.20	0.90	50.31

Table 5.8: *Maintenance phase performance indexes obtained with the SISO MPC control system on the 500 perturbed models generated starting from the nominal model of the thirteenth patient of the tuning dataset to simulate intra-patient variability.*

Figure 5.5: *Responses obtained with the SISO MPC control system on the 500 perturbed models generated starting from the nominal model of the thirteenth patient of the tuning dataset to simulate intra-patient variability.*
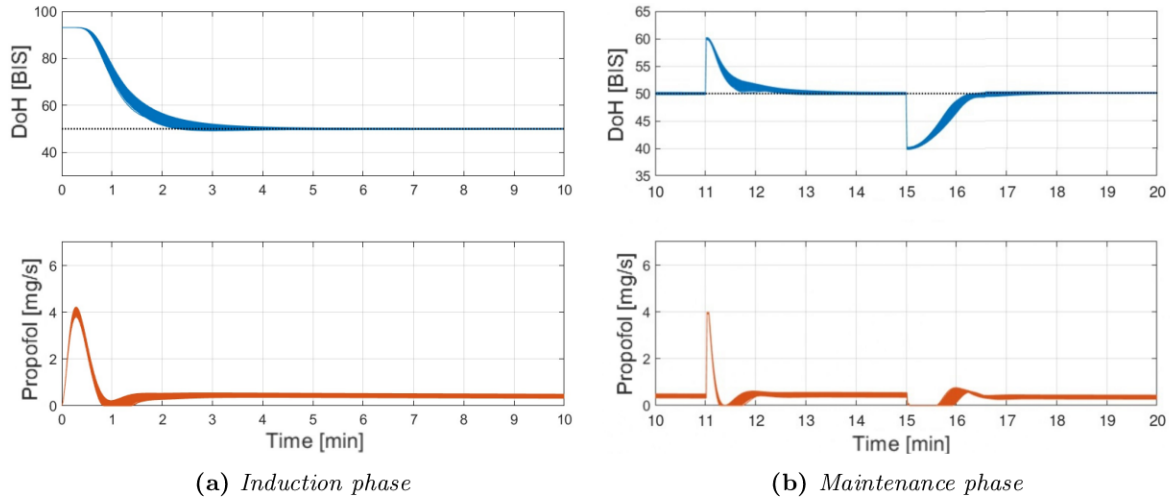
5.2 Handling measurement noise

From the results obtained in Section 5.1, it appears that the SISO MPC control system is able to provide a satisfactory performance, that is, to meet the clinical requirements. However, the BIS signal used as a feedback measure is affected by a strong noise that needs to be considered in the control algorithm [141, 142]. Despite this, the noise handling issue in the anaesthesia process is frequently treated as a secondary problem or even neglected during the control system design. However, it is well known that the process noise, if not properly handled, can lead to severe performance degradation or even to controller instability. Bearing in mind the previously mentioned aspects, this section is dedicated to analyze the performance of the SISO MPC control system for propofol anaesthesia affected by the process noise. The main goal of this study is to provide a quantitative measure that reflects the performance degradation due to the noise presence when compared to the noise-free case. The original structure is here extended with a suitably designed additional low-pass filter that attenuates the process noise. The system has been tested by using both white noise and real process noise that reflects not only the noise related with signal acquisition process, but also other unmeasurable interferences and disturbances. Furthermore, the use of different sampling periods for the feedback controller has been analyzed. The evaluation is made in simulation using widely accepted performance indexes.

5.2.1 Control system architecture

The considered control structure is shown in Figure 5.9. It is based on that shown in Figure 5.9. Here, the noise component $n(t)$ in the BIS feedback signal is also considered. Analyzing the real BIS signals obtained from clinical data provided by the Spedali Civili di Brescia Hospital it was obtained that its power spectral density (PSD) has the average value of 39.3392 [95]. An example of the BIS signal from the real clinical data is shown in Figure 1.9. From the signal processing point of view, this high measurement noise can be attenuated through a filter added *a posteriori*, which is designed to reduce the noise dominant frequencies

(a) *Patient 1*   **(b)** *Patient 2*   **(c)** *Patient 3*

(d) *Patient 4*   **(e)** *Patient 5*   **(f)** *Patient 6*

(g) *Patient 7*   **(h)** *Patient 8*   **(i)** *Patient 9*

(j) *Patient 10*   **(k)** *Patient 11*   **(l)** *Patient 12*

Figure 5.6: *Induction phase responses obtained with the SISO MPC control system on the 500 perturbed models generated starting from the nominal model of each patient of the tuning dataset to simulate intra-patient variability.*

(a) *Patient 1*   **(b)** *Patient 2*   **(c)** *Patient 3*

(d) *Patient 4*   **(e)** *Patient 5*   **(f)** *Patient 6*

(g) *Patient 7*   **(h)** *Patient 8*   **(i)** *Patient 9*

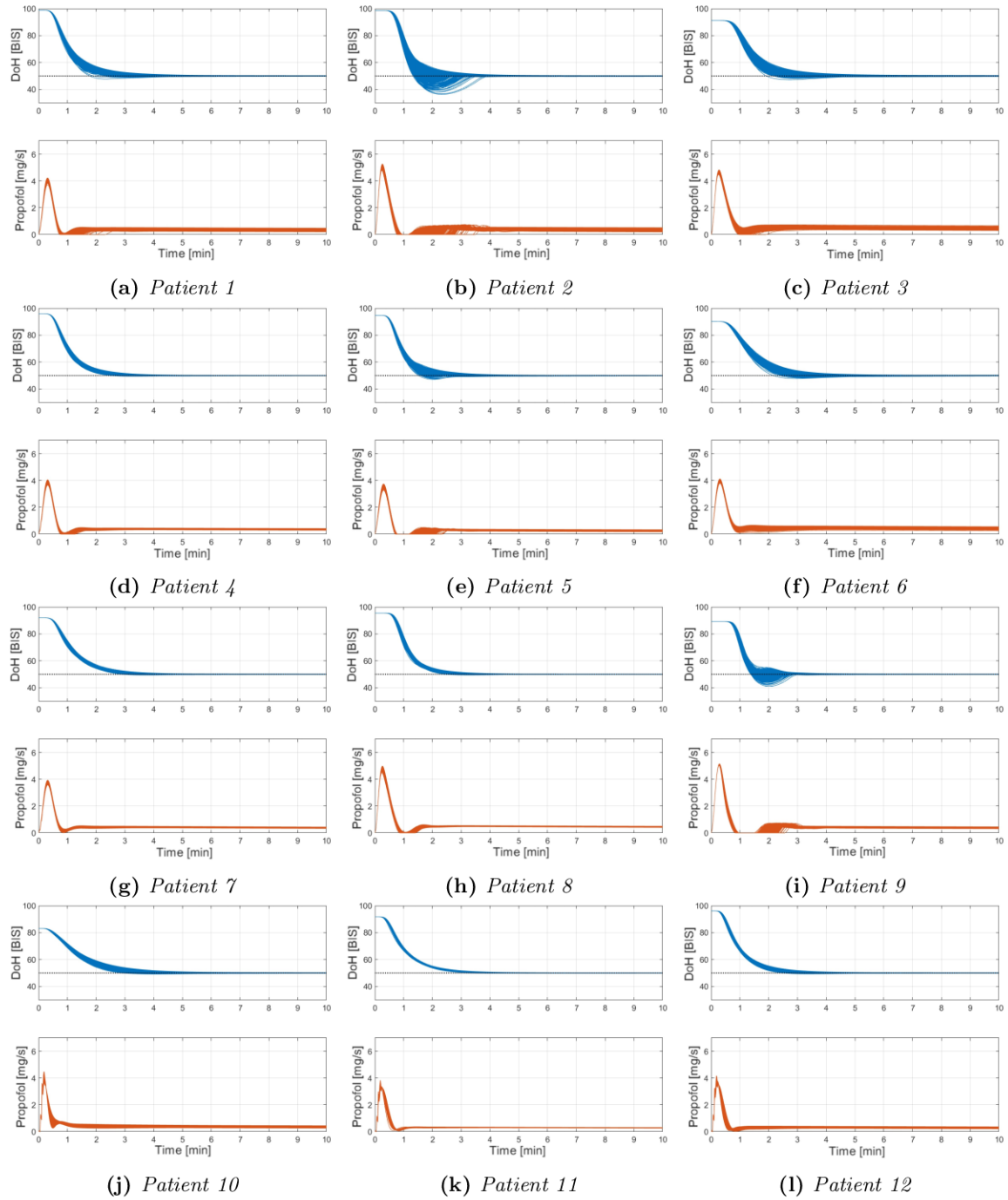**(j)** *Patient 10*   **(k)** *Patient 11*   **(l)** *Patient 12*

Figure 5.7: *Maintenance phase responses obtained with the SISO MPC control system on the 500 perturbed models generated starting from the nominal model of each patient of the tuning dataset to simulate intra-patient variability.*
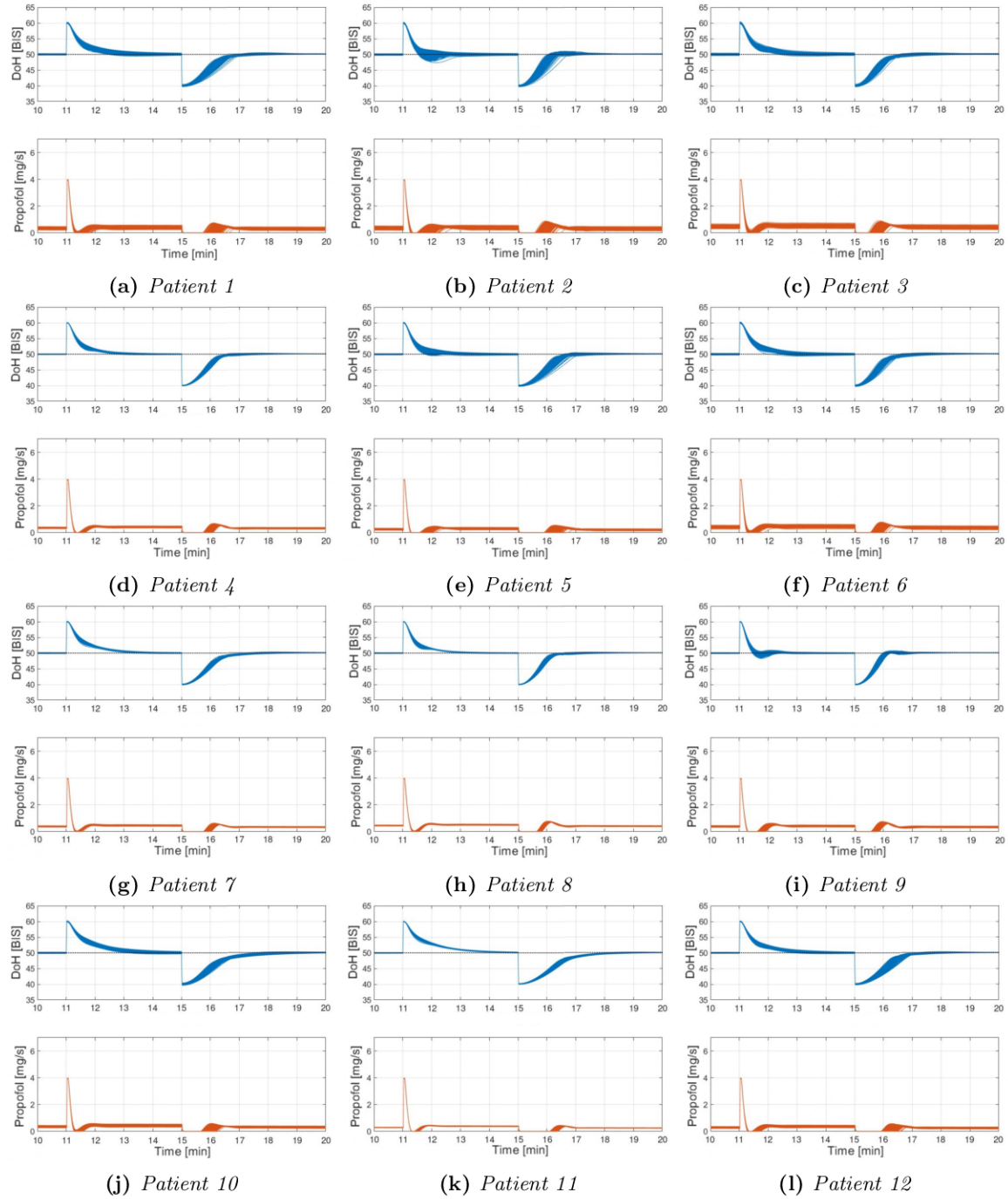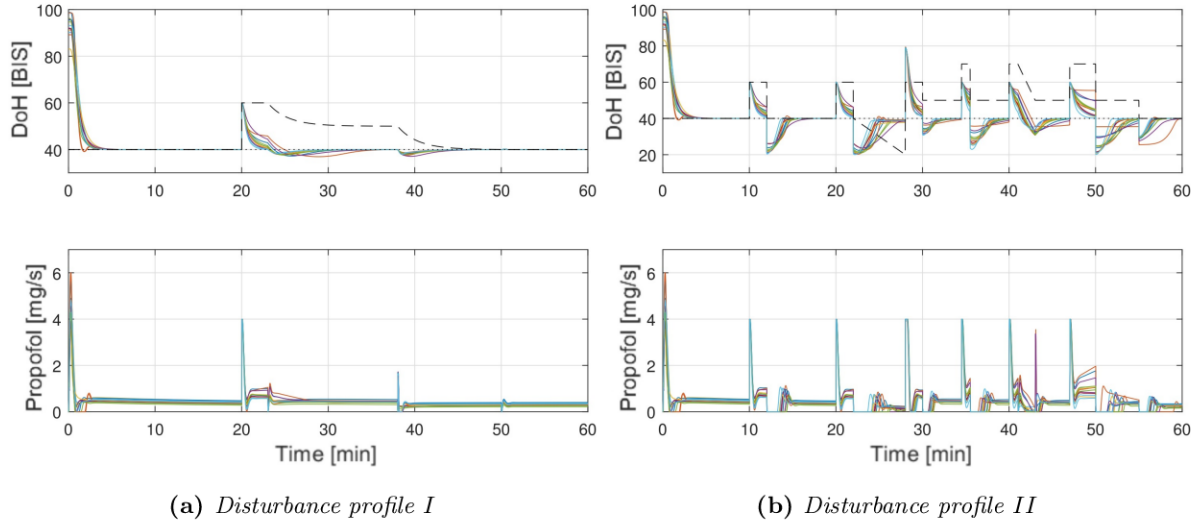
(a) *Disturbance profile I* **(b)** *Disturbance profile II*

Figure 5.8: *Responses to disturbance profiles obtained with the SISO MPC control system on the thirteen patients of the tuning dataset.*

and pass others in interesting bandwidth. To this end, the original scheme has been extended with the F_n filter that is a first-order low-pass filter:

$$F_n(s) = \frac{1}{T_n s + 1}, \tag{5.6}$$

where T_n represents its time constant. As it can be observed, F_n affects the control loop dynamics and the overall accuracy of the control system. For example, it might result in a sluggish response or there can be robustness issues due to the changes in the control loop dynamics. For this reason, T_n needs to be properly adjusted among other design variables in the control system tuning procedure. Hence, the proposed control system requires the tuning of the GPC controller parameters N, N_u and λ, as well as of the proposed filters parameters, T_r, T_d and T_n. In the analyzed system, the performance in the induction phase is mainly limited by the F_r filter time constant T_r and for comparison purposes the value $T_r = 22.4$ s proposed in Section 5.1 is used, that is fixed for all the tested configurations. In this way, it is assured that the resulting changes in the control system performance are directly linked to the effect of the noise. The remaining tuning parameters are obtained by using the optimization-based approach presented in Section 2.2.1. But here, the optimization problem (2.2) is rewritten as:

$$\min_\theta \text{IAE}, \tag{5.7}$$

where θ is the vector of PID tuning parameters. Hence, it is a minimization problem of the IAE for a specific patient and it is solved only for the average patient of the tuning dataset. The IAE is obtained by simulating the response to the double-step disturbance profile shown in Figure 1.6. Additionally, additive white Gaussian noise with the determined PSD and a noise amplitude of ± 2.5 is considered. The optimization is repeated for different sampling periods (namely 1, 2, 5 and 10 s) to test how this factor influences the control system performance in the presence of noise. In this way, the noise issue can be handled by the whole control system and not only by the specific filter. The optimization problem has been solved by means of
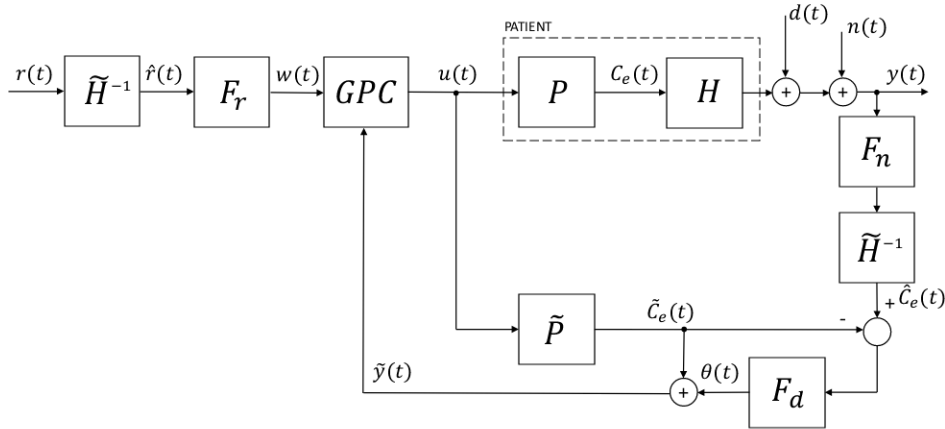
Figure 5.9: *Schematic representation of the SISO MPC control system with the additional filter F_n for noise attenuation.*

$\mathbf{T_m}$	$\mathbf{N}$	$\mathbf{N_u}$	$\boldsymbol{\lambda}$	$\mathbf{T_d}$	$\mathbf{T_r}$	$\mathbf{T_n}$
1_{nf}	27	7	1.60	22.7	22.4	–
1	24	2	14.43	47.33	22.4	24.64
2	15	19	10.27	54.36	22.4	16.63
5	15	18	100.80	32.59	22.4	57.66
10	13	5	94.66	63.37	22.4	86.99

Table 5.9: *Tuning parameters of the SISO MPC control system obtained for different sampling periods T_m.*

GA with a population size of 40 elements and by stopping the optimization when the relative change in the cost function value over the last 50 iterations is less than 0.001. As a result, the tuning parameters values that are summarized in Table 5.9 have been obtained. The determined set has been compared to the optimal tuning for analyzed control architecture for the noise-free configuration with a sampling period of 1 s (shown as 1_{nf}).

5.2.2 Simulation results

The obtained tuning parameters for different sampling periods have been evaluated on the tuning dataset shown in Table 2.1. However, it needs to be highlighted that during the tuning optimization procedure only the average patient has been used. Due to this, the performed simulations shows how the analyzed control scheme responds to the inter-patient variability simultaneously considering noise issues. The simulation scenario consists of a step change in the BIS reference from 100 to 50 at time 0, representing the induction phase. Once the induction phase target is achieved, the maintenance phase starts. In this phase the response of the system to disturbances represented as the double-step signal shown in Figure 1.6 is evaluated. During the simulation, additive white Gaussian noise is used to replicate the actual measurement noise. As an example, the result obtained for $T_m = 1$ s is shown in Figure 5.10a. It can be observed that, for this configuration, the control system provides a satisfactory performance for both the induction and maintenance phases, despite the presence of noise. Moreover, the control architecture adequately handles the inter-patient variability providing the necessary robustness to model uncertainties. Additionally, to show the influence of the sampling period, the same simulation is performed for $T_m = 5$ s and the obtained results

T_m	TT [min]	BIS-NADIR	ST20 [min]	ST10 [min]
1_{nf}	1.41	48.22	1.16	1.66
1	1.78	45.05	1.65	2.60
2	1.37	41.34	2.02	3.17
5	1.78	38.28	3.15	5.85
10	1.28	20.58	7.34	9.70

Table 5.10: *Average induction phase performance indexes obtained with the SISO MPC control system on the tuning dataset when white noise is considered.*

T_m	TTp [min]	BIS-NADIRp	TTn [min]	BIS-NADIRn
1_{nf}	0.38	49.98	0.89	50.05
1	0.72	47.19	1.30	52.34
2	0.88	47.07	1.14	51.98
5	1.22	45.01	1.29	56.85
10	0.95	43.68	1.36	53.44

Table 5.11: *Average maintenance phase performance indexes obtained with the SISO MPC control system on the tuning dataset when white noise is considered.*

are shown in Figure 5.10b. For this case, the control system needs slightly more time to reach the desired BIS zone for the induction phase. Regarding the maintenance phase, it can be observed that the disturbance compensation is similar to the previous case where $T_m = 1$ s was used. The performance evaluation for the induction phase, using the previously defined indexes, is summarized in Table 5.10, where the average values for all 13 patients are considered for all the tested sampling periods. For comparison purposes, the performance obtained for a noise-free case using the same control architecture with $T_m = 1$ s is also included and marked as 1_{nf}. The obtained values indicate that sampling periods between 1 and 5 s are acceptable from the performance point of view. Moreover, the performance evaluation for the maintenance phase is shown in Table 5.11. A performance degradation is also visible for this phase, obtaining the lowest performance for the configuration with $T_m = 10$. From the obtained results, it can be determined that the noise issue can be handled properly in the analyzed control scheme. However, the performance degradation is visible and grows when the sampling period increases. The response of the analyzed control system to real noise signal is shown in Figure 5.11, where the simulations considers also the step disturbances in the maintenance phase. As in the previous case, the obtained performance meets the requirements. It appears that the process noise can be properly handled by the control system if it is explicitly taken into account during the design stage. This property is especially important in the MPC-based control scheme, due to known sensibility to process noise that frequently results in a poor robustness of the controller. However, in the analyzed case, the increased robustness to the noisy BIS signal comes at the expense of the performance degradation.

5.3   Linear SISO MPC: experimental results

In this section the experimental results obtained with the proposed MPC control strategy are presented. This is a preliminary study that aims to verify the consistency of the results obtained in simulation. To this end, the SISO MPC control system for the administration of propofol only is first considered. The original control structure, which have been extensively discussed in Section 5.1, is adapted to implement it in the control algorithm. In particular, to

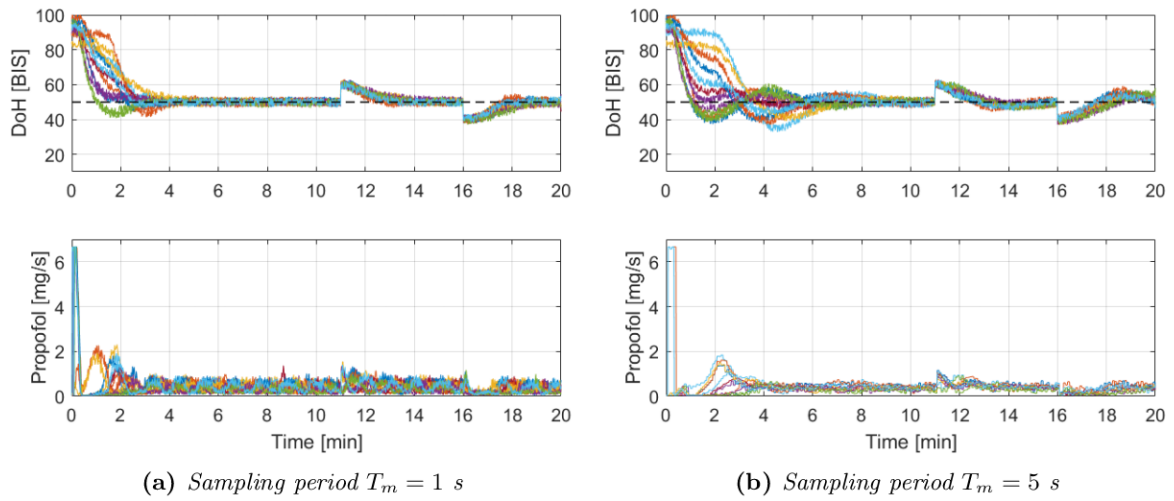**(a)** *Sampling period $T_m = 1$ s*   **(b)** *Sampling period $T_m = 5$ s*

Figure 5.10: *Responses obtained for each patient of the tuning dataset with the SISO MPC control system when white noise is considered.*
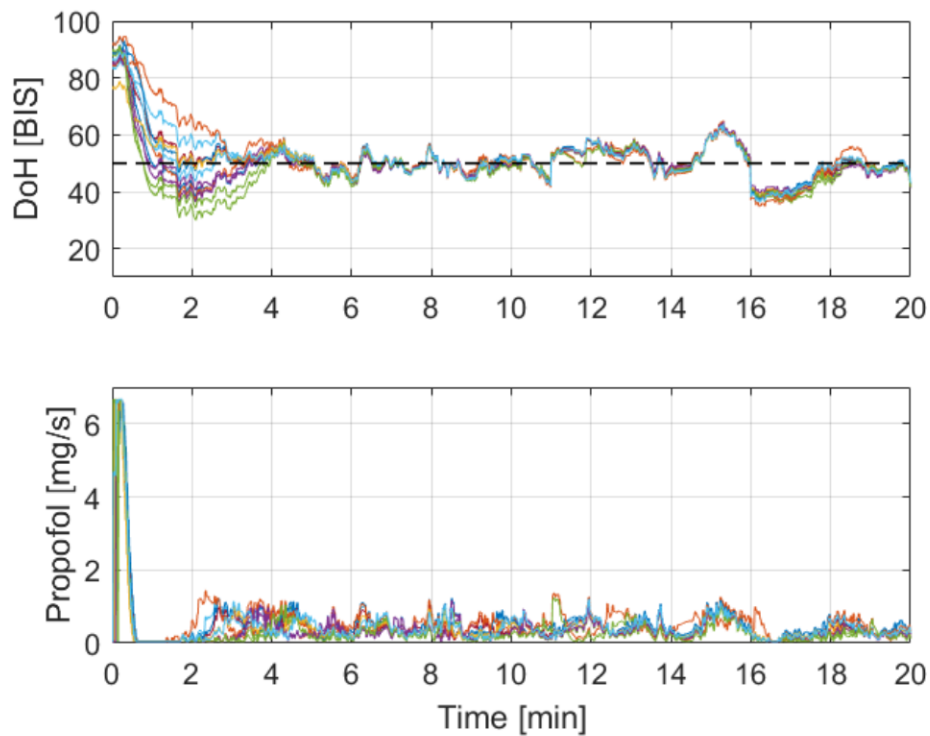

Figure 5.11: *Responses obtained for each patient of the tuning dataset with the SISO MPC control system when real noise and sampling time $T_m = 2$ s are considered.*

deal with the noise affecting the real BIS signal, the control structure with the additional filter presented in Section 5.2 have been considered. The control structure has been discretized with a sampling period of 1 s. Thus, the tuning parameters shown in Table 5.9 corresponding to the sampling period of 1 s have been here considered. As already done for the PID controller in Section 3.1.1, also here the control signal has been down-sampled by updating the infusion rate every 5 s. The value sent to the pump is calculated as the mean of the last 5 values of the control action. The Alaris GH syringe pumps have been used as actuators. The MPC controller is then implemented in the control software described in Section 2.2.3. The clinical protocol employed is the same described in Section 4.1.1 except for the fact that here the remifentanil infusion rate is manually regulated by the anesthesiologist by means of the specific text box placed in the "Manual Control" box on the GUI (see Section 2.2.3). The remifentanil infusion rate can be freely chosen by the anesthesiologist and it can be changed at any time during the experiment. Moreover, anesthesia is induced automatically by the SISO MPC controller as regards propofol infusion, while for the analgesic component a 1-2 μg/kg bolus of fentanyl is manually administered. It is worth noting that even though the controller parameters remain the same for both the induction and maintenance phases, the constraints posed in the optimization problem of the GPC controller change, as described in Section 5.1.1. For this reason it is still necessary to change the mode of the control system. The same automatic switching mechanism described in Section 4.1.1 is employed for this purpose.

Four patients undergoing general anesthesia for elective plastic surgery have been enrolled in the experiment, their demographic data and the type of surgical procedure are shown in Table 5.12. The individual records of the clinical variables of interest are shown in Figures 5.12. The values of the performance indexes related to the induction phase are shown in Table 5.13. The controller provided a fast induction of anesthesia. For all the patients, anesthesia was induced in less than 2 min, which is a time interval comparable with that obtained by using a bolus. This was paid at the cost of a slight undershoot of the BIS, as highlighted from the value of the *Lowest BIS*. However, it is worth stressing that this undershoot did not cause any clinically relevant consequence on the hemodynamic variables. Indeed, BP and HR remained within clinically recommended ranges. Moreover, the administered propofol dose in induction varies from 1.91 mg/kg to 2.52 mg/kg and they are fully compatible with those of the clinical practice. To better highlight the behavior of the controller in the induction phase, the values of BIS and infusion rates during the first 10 min are shown in Figure 5.13. It is worth noting that the controller automatically performs an induction bolus of propofol. The values of the performance indexes relative to the maintenance phase are shown in Table 5.14. The controller was able to keep the BIS inside the recommended range from a minimum of 58% to a maximum of 75% of the maintenance time. The *MDAPE* values indicate that the control inaccuracy remains below the threshold of 20% of the BIS target value. This means that the median absolute BIS value is inside the recommended range from 40 to 60. The *MDPE* values indicate that the obtained BIS has a negative bias with respect to its target value. This means that the controller tends to keep the BIS below 50. However, *MDPE* remains above the threshold of -20% of the BIS target value. This means that the median BIS value is above 40. By analyzing the values of $BIS < 40$, it appears that, when the BIS is not in the recommended range, it is, for the most part, below 40 and not over 60. This is a sensible behavior because it prevents the risk of intra-operative awareness. However, this is not obtained by overdosing the patients as indicated by the propofol maintenance dose that is, in each patient, below that normally used in the clinical practice of 6 mg/kg/h. It is worth

Patient	Age	Height [cm]	Weight [kg]	Gender	Type of surgery
1	44	170	70	F	Breast mastectomy and mastoplasty
2	63	165	90	F	Skin cancer exceresis
3	21	180	61	F	Burned tissue escharatomy and microsurgical flap
4	64	165	60	F	Lipoma removal

Table 5.12: *Demographic data and type of surgery undergone by the patients enrolled with the SISO MPC control system.*

stressing that the remifentanil maintenance dose is shown in Table 5.14 but it is not managed by the controller, indeed it is manually regulated by the anesthesiologist. As regards the emergence phase, the awakening time was short for all the patients enrolled and it was fully compatible with the clinical practice.

Anesthesia was automatically induced and maintained for all the patients without the need of anesthesiologist interventions. Only in patient 3 the anesthesiologist performed an additional bolus of propofol around minute 62 as a preventive measure for a particularly painful part of surgery on burned tissues. It is worth noting that the controller performance was not affected by this manual intervention. The hemodynamic variables remained stable for patient 1 and patient 3. In Patient 2 there was a rise of BP around minute 62 in response to painful stimulation. In patient 4 the sharp rise in the value of BP around minute 45 was caused by the administration of ephedrine to treat low BP.

In patient 1 an oscillatory behavior of the BIS is observed. However, oscillations remained bounded as indicated by the *WOBBLE*, which is 12% of the BIS target value, and they did not cause any significant consequences from a clinical point of view. In patient 2 the prolonged undershoot of the BIS that occurred after induction was due to the rejection of a rise in the BIS signal that occurred around minute 3 due to intubation. Then, around minute 62 another rise of the BIS signal due to painful stimulation was promptly rejected by the controller. In patient 3 the BIS remained stable with the exception of a sharp rise around minute 62 due to a particularly painful stimulation. In patient 4 the BIS remained stable throughout the whole surgical procedure although there were issues with the BIS sensor reading and the system automatically switched to manual control.

Overall, the SISO MPC controller showed a good performance and a behavior that is compatible with the clinical practice. Thus, it deserves further clinical investigations. This study shows only preliminary results with this type of control strategy that was aimed to test the applicability of the proposed strategy in the clinical practice. Future studies will focus on the MISO MPC controller that takes into account also the infusion of remifentanil. Indeed, in the design of the SISO MPC controller the infusion of remifentanil is not taken into account, while in the clinical practice it is always present. Hence, from the controller point of view, this is seen as a disturbance. Moreover, the oscillatory behavior of the BIS seen in patient 1 and the sharp rises in patient 2 and patient 3 can be due to a non optimal management of the remifentanil that is, indeed, manually regulated. Also the undershoot of the BIS seen in the induction phase can be due to the manual administration of fentanyl that is unknown to the controller.

(a) *Patient 1*

(b) *Patient 2*

(c) *Patient 3*

(d) *Patient 4*

Figure 5.12: *Recorded clinical data of the patients enrolled with the SISO MPC control system. From top to bottom: BIS (solid line) and BIS set-point (dashed line); propofol (black) and remifentanil (red) infusion rates in ml/h; HR; BP_s (red), BP_d (black) and BP_m (blue). The vertical dash-dotted black line indicates a manual bolus of propofol. Missing data were due to temporary issues with the sensors. The constant values in the propofol infusion rate are due to system automatically switching to manual control due to temporary issues with the BIS sensor reading. For Patient 4 the sharp rise in the values of BP around minute 45 is due to an ephedrine bolus.*

Patient Id	Induction time [min]	Lowest BIS	Propofol dose [mg/kg]
1	1.32	31	2.29
2	1.58	23	1.91
3	1.10	35	2.52
4	1.97	26	2.28

Table 5.13: *Performance indexes for the induction phase obtained with the SISO MPC control system.*

(a) *Patient 1*   **(b)** *Patient 2*

(c) *Patient 3*   **(d)** *Patient 4*

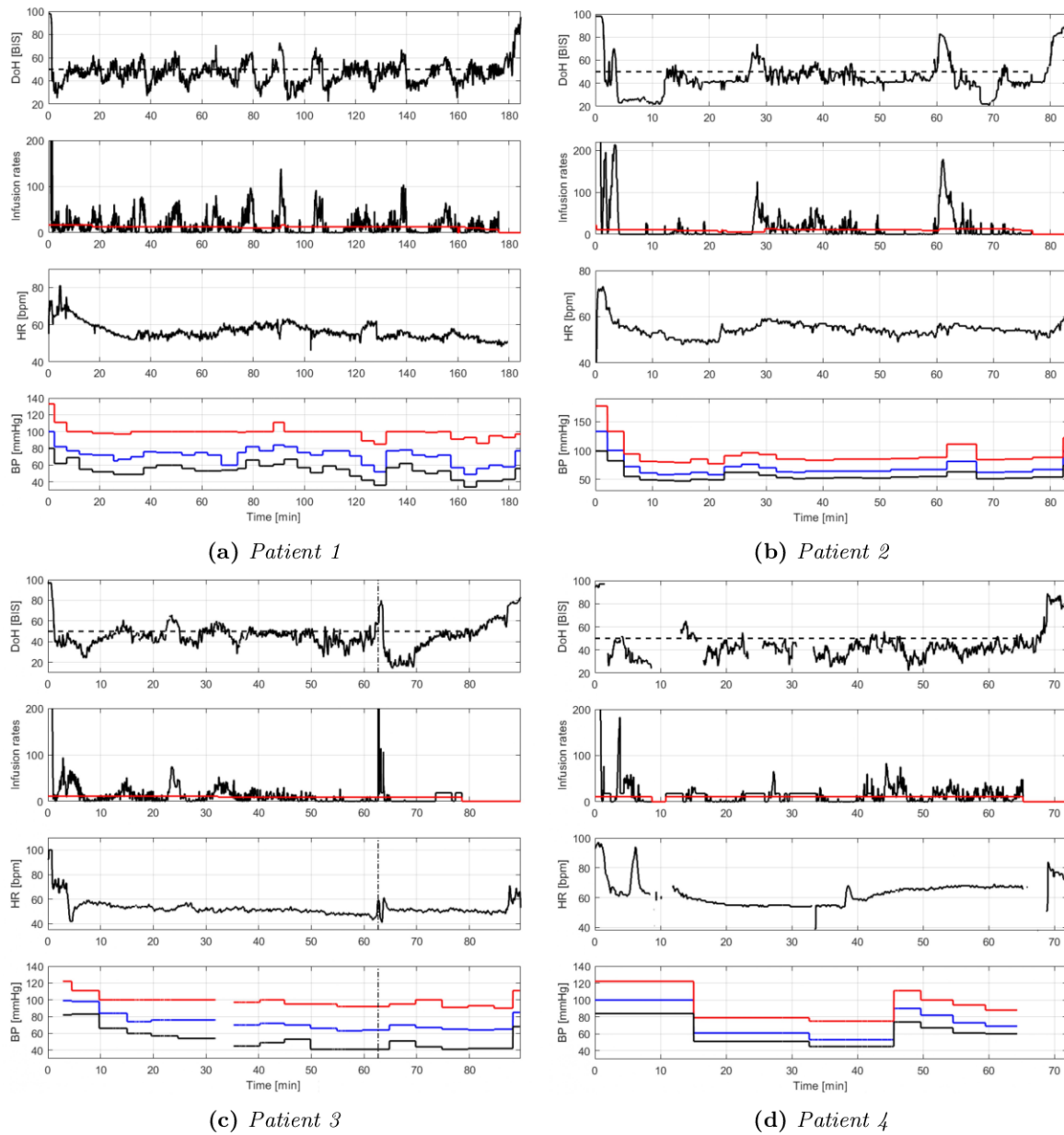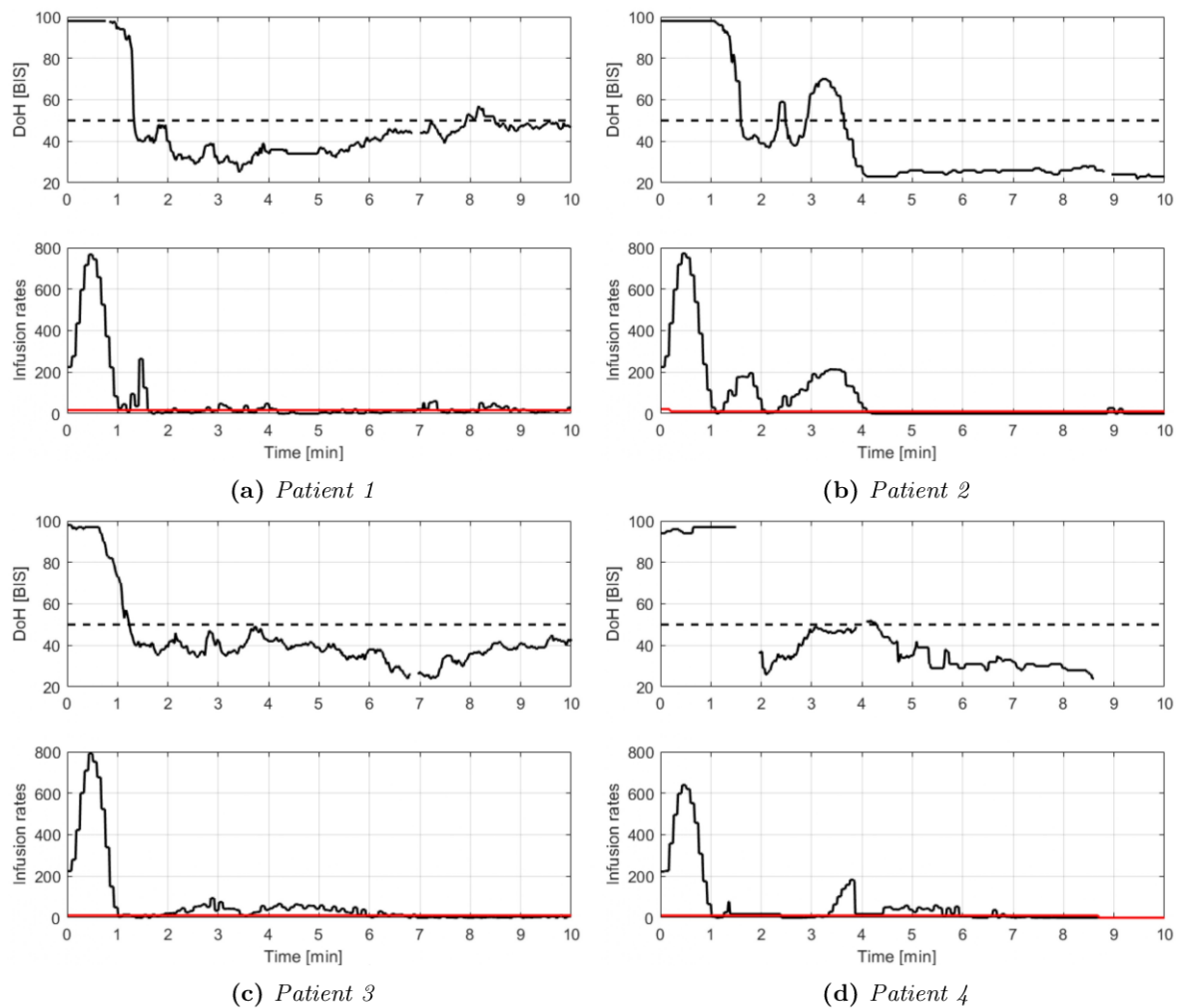**Figure 5.13:** *Induction phase responses of the patients enrolled with the SISO MPC control system. From top to bottom: BIS (solid line) and BIS set-point (dashed line); propofol (black) and remifentanil (red) infusion rates in ml/h. Missing data were due to temporary issues with BIS sensor reading forcing the system to automatically switch to manual control.*

Patient Id	BIS $40-60$ [%]	BIS < 40 [%]	MDPE [%]	MDAPE [%]	WOBBLE [%]	Propofol [mg/kg/h]	Remifentanil [μg/kg/min]	T awakening [min]
1	75.05	21.17	-8	14	12	4.25	0.15	7.07
2	70.26	23.38	-16	18	8	3.40	0.10	4.70
3	68.42	29.26	-12	14	10	4.44	0.13	8.98
4	57.78	41.30	-18	18	10	4.50	0.15	6.23

Table 5.14: *Performance indexes for the maintenance phase obtained with the SISO MPC control system.*

5.4   Model predictive control using MISO approach for drug coadministration

The availability of the interaction model between propofol and remifentanil has also stimulated the development of MPC systems for the MISO case [78, 119]. In this context, the predictive controller is built using a linearized interaction model for propofol and remifentanil, with the aim of keeping the desired level of the DoH [78]. The analgesic drug infusion rate is adapted to the propofol dose and the ratio is kept constant. Another example is shown in [119], where an habituating control technique for DoH control task is reformulated by taking into account the effect of remifentanil. In this control system, a reference signal is established for the infusion rate of remifentanil and this is modified by the controller according to the changes in propofol dosage. In this way, hypnosis is the main controlled variable and analgesia is adapted to the changes in the hypnosis feedback loop. Moreover, nonlinear MPC techniques have been analyzed in [143, 144], where conceptual developments are proposed for anaesthesia control. These works show that MPC controllers can address relevant issues that concern process constraints and prediction capability of synergistic effect of drugs interaction. However, on the one hand, their applicability is limited by the strong variability of the process, namely, inter- and intra-patient variability. On the other hand, due to nonlinear process characteristics, resulting control systems are complex and rarely robust enough to be exploited at the operating room. Additionally, there exists many types of medical interventions with different requirements during the anaesthesia procedure, which makes difficult to develop one control system that is suitable for all situations. Furthermore, a personalized controller design based on patient model can significantly improve the control performance. All aforementioned questions stimulate the development of new control systems based on MPC techniques. In this section, an MPC system for the MISO process is proposed. The nonlinear propofol-remifentanil interaction model on the BIS is exploited [145]. The method suitably generalizes the idea proposed in Section 5.1, where propofol is the only drug used. In particular, a GPC algorithm is used as feedback controller, that considers the effect of remifentanil over propofol. Therefore, it is able to handle the synergistic effect of both drugs in the computation of the control signal for the DoH. The dose of the two drugs is established by fixing a ratio between them [93]. The external predictor architecture is completed with the low-pass filter in the feedback loop. The tuning of the controller is performed by means of a GA addressing separate requirements for the induction and maintenance phases. Finally, the proposed control system is evaluated using a Monte Carlo technique for inter- and intra-patient variability using a wide distribution of patients population.

5.4.1   Control system architecture

The proposed control system is a generalization and extension to the MISO case of the architecture presented in Section 5.1. The main idea consists in the computation of the inverse of the nonlinear Hill function and in the use of a linear GPC algorithm. The MISO model described in Section 1.2.2 is used to consider the synergistic effect of the drug coadministration on the DoH represented by the BIS signal. The control scheme is shown in Figure 5.14. The main objective is that the measured DoH level, shown as $y(t)$, follows the reference signal $r(t)$. The patient model has been conveniently reorganized into three blocks P_{prop}, P_{remif} and H. In this configuration the first two elements represent the linear dynamics of propofol and remifentanil, respectively, and the H block represents the nonlinear Hill function. The main idea consists in using this model to construct an external predictor to estimate the patient state. The predictor blocks include the model of the linear dynamics $\tilde{P}_{prop}$ and $\tilde{P}_{remif}$ and the inverse of the nominal nonlinear function $\tilde{H}^{-1}$. The GPC block represents the feedback controller, K is the ratio between the co-administrated drugs and F_d is a low-pass filter. For the control system design, analysis and evaluation a fixed ratio of 2 between propofol and remifentanil doses is used as done in Section 2.2.2. In this control architecture, the GPC controls directly $\tilde{Y}_p$, namely, the propofol concentration required to achieve the desired BIS value. This value can also be obtained from the process (in this case it is denoted as $\hat{Y}_p$) by using the $\tilde{H}^{-1}$ block that requires, as inputs, the actual BIS value and the remifentanil concentration $\tilde{Y}_r$ estimated by the predictor. Due to the unavoidable process/model mismatches, the resulting difference signal between $\hat{Y}_p$ and $\tilde{Y}_p$ is filtered by F_d in order to compensate for this difference in the feedback loop. The introduced methodology requires a deeper analysis of the inverse nonlinear function block. The calculation of the inverse of the Hill function, which provides the value of $\hat{Y}_p$, requires the values of the BIS and of $\tilde{Y}_r$. The BIS value is provided by the DoH monitor, while $\tilde{Y}_r$ can be computed from the patient model. To apply this methodology, Equation 1.7 needs to be rewritten as $Y_p(t) = f(y(t), Y_r(t))$. To obtain this structure, it is necessary to rewrite (1.7) using a third-order polynomial form, resulting in following equation:

$$Y_p^3 + bY_p^2 + cY_p + d = 0, \tag{5.8}$$

where:

$$b = 3Y_r - \left(\frac{E_0 - BIS}{E_{max} - E_0 + BIS}\right)^{1/\gamma}$$

$$c = 3Y_r^2 - 2Y_r\left(\frac{E_0 - BIS}{E_{max} - E_0 + BIS}\right)^{1/\gamma} + \beta Y_r\left(\frac{E_0 - BIS}{E_{max} - E_0 + BIS}\right)^{1/\gamma}$$

$$d = Y_r^3 - Y_r^2\left(\frac{E_0 - BIS}{E_{max} - E_0 + BIS}\right)^{1/\gamma}.$$

Now, exploiting the current BIS signal measure and $\tilde{Y}_r(t)$ (which represents the estimated effect site concentration of remifentanil) it is possible to calculate $\hat{Y}_p(t)$, by solving Equation 5.8, to finally obtain the inverse of the Hill function. Once the inverse function is computed, its value from Equation 5.8 can be used to estimate the propofol concentration $\hat{Y}_p$. However, to integrate the effect of remifentanil over propofol, it is necessary to relate the desired propofol concentration (which is the reference signal for the GPC controller) to the remifentanil

concentration and to the BIS desired value $r(t)$. This is achieved by integrating the drugs co-administration effect into the $\tilde{Y}_p(t)$ value when computing the corresponding concentration for the BIS reference value. Thus, the calculation of the reference value (represented as $w(k)$ in the GPC structure for the propofol concentration needs to take into account the value of Y_r. In the analyzed scheme the remifentanil dose is related to the propofol infusion using a fixed gain K, as shown in simplified representation in Figure 5.15. Therefore, using basic properties of such a system, it is possible to obtain Y_r as an expression that depends on Y_p:

$$Y_p = G_p u_p; \qquad\qquad Y_r = G_r u_r = G_r K u_p.$$

From here, it is possible to obtain:

$$Y_r = G_p^{-1} G_r K Y_p, \tag{5.9}$$

and from this, it is possible to obtain a difference equation:

$$Y_r(k) = b_0 Y_p(k) + ... + b_{n_b} Y_p(k - n_b) - a_0 Y_r(k-1) - ... - a_{n_a} Y_r(k - 1 - n_a), \tag{5.10}$$

where the coefficients a, b and the degrees n_a, n_b of the nominator and denominator are obtained from the $G_p^{-1} G_r K$ term. At this point, Y_r in equation 5.8 can be substituted with Y_r from equation 5.10. In this way, an expression where the propofol concentration is linked only to the desired level of DoH (the BIS set-point value for the control system) is obtained. Thus, an optimal reference signal for the propofol infusion that takes into account the effect of remifentanil can be determined. This is possible thanks to the ratio block and to the exploitation of the propofol control signal values computed over the control horizon. The reference signal has slight variations at each sampling instant because the relation between Y_p and Y_r depends on the past values of Y_p and Y_r. To take into account this relationship, the reference $w(t)$ is computed at every sampling instant, using a receding horizon strategy. Thanks to the proposed architecture it possible to obtain MISO control system properties. However, the SISO model is considered for the GPC controller design. At this stage, the advantages of the proposed control scheme can be provided. Under nominal conditions, when there are no uncertainties and modelling errors among the patient and the derived model, (i.e. $\tilde{P}_{prop} = P_{prop}$, $\tilde{P}_{remif} = P_{remif}$ and $\tilde{H} = H$) the analyzed scheme can be transformed to a linear system, where the controller is focused on the linear element of the patient model. In such a scenario, $w(t)$ is obtained from $r(t)$ by applying H^{-1}, which includes the effect site concentration of remifentanil. In this way the BIS is linked to the $C_{e,p}(t)$ value, which is the estimated propofol effect-site concentration the patient. Then, $\hat{Y}_p(t) = \tilde{Y}_p(t)$ is obtained and the feedback signal corresponds to $\tilde{Y}_p(t)$. In this case, the controller reacts only when the reference changes or the process disturbances $d(t)$ influence the controlled variable. The algorithm flow chart for the proposed control scheme is shown in Figure 5.16. In the real case, there are model uncertainties, especially those related to the static nonlinearity, since it is impossible to know the exact values of the parameters *a priori*. Actually, the linear part of the PK/PD model is also affected by uncertainties, related to parameters variability and model inaccuracies. Taking into account these issues, the $i(t)$ signal is used both to compensate modelling uncertainties and to react to the disturbances induced by surgical stimuli. The $i(t)$ value is related to the error between $\tilde{Y}_p(t)$ (estimated propofol effect-site concentration using linear part of the model, $\tilde{P}_{prop}$) and $\hat{Y}_p(t)$ (propofol effect-site concentration obtained via average Hill function inversion based on the real BIS measure). Thus, the GPC controller uses

$\breve{Y}_p(t)$ as a feedback signal, which contains information regarding patient model mismatches and influence of disturbances. In the same way, the proposed control system handles the patient's state changes along time, which result in model inaccuracies. These could be related to a sudden change in patient's hemodynamics (which affects drugs clearances) that can be due to a severe blood loss or to the administration of vasoactive medications. As a consequence, the variation of the model parameters are considered as unmeasurable disturbances that needs to be compensated by the controller among other modelling errors. Moreover, the $i(t)$ signal passes through the low-pass filter F_d. The main purpose of F_d is to attenuate the result of disturbances and uncertainties on the GPC feedback controller and, at the same time, to guarantee a null steady-state reference tracking error in the feedback loop. The F_d filter is represented as a first order transfer function of the following form:

$$F_d(s) = \frac{1}{T_d s + 1}, \tag{5.11}$$

where T_d is a time constant that needs to be adjusted. Therefore, to obtain a satisfactory performance of the control system, it is required to tune the GPC controller parameters as well as T_d. It is worth stressing again that $\tilde{P}_{prop}$, $\tilde{P}_{remif}$ are computed using demographic parameters that result in an individualized controller. On the contrary, $\tilde{H}$ and $\tilde{H}^{-1}$ are obtained using average values for the population that are shown in Table 1.4. The parameter E_0 can be measured for each patient before the induction phase.

The same GPC architecture presented in Section 5.1 is used. Note that the constraints on the propofol infusion are considered in the optimization procedure, while the constraints for remifentanil are applied in accordance with the values obtained for propofol by taking into account the ratio gain K. The controller parameters N, N_u, and λ related to the GPC algorithm and T_d for the low-pass filter F_d, need to be tuned in order to provide the desired performance and to assure the required robustness. The parameters have been tuned separately for the induction and maintenance phases in a two steps approach. In the first step of the tuning procedure, the controller is tuned to provide an optimal set-point tracking response. During the second step, an additional tuning process is performed by keeping the values N and N_u obtained in the previous step and looking for λ and T_d values being optimized for disturbance rejection task. Thus, there are two sets of parameters; one is applied in the induction phase and the other one in the maintenance phase. In order to apply a bumpless switching for T_d, it is necessary to implement two different low-pass filters in the scheme, see Figure 5.17. When the filter of the induction phase is operating, the other one, for the maintenance phase, is in tracking mode assuring that its output is changed to be the same as $i(t)$ at the switching time instant. The tuning has been performed by using the optimization-based approach 2.2.1. The optimization problem is solved with GA with a population of 40 elements and by stopping the optimization when the relative change in the cost function value over the last 50 iterations is less than 0.001. The resulting parameters for the induction phase are $N = 36$, $N_u = 34$, $\lambda = 10$ and $T_d = 96$ s. For the maintenance phase, the λ and the T_d values are changed respectively to 3 and 23 s.

5.4.2 Simulation results

In this section, the results obtained in simulation with the proposed control architecture are presented. Both the induction and maintenance phases of anesthesia have been simulated, in order to verify the fulfilment of the clinical specifications and to assess the performance.
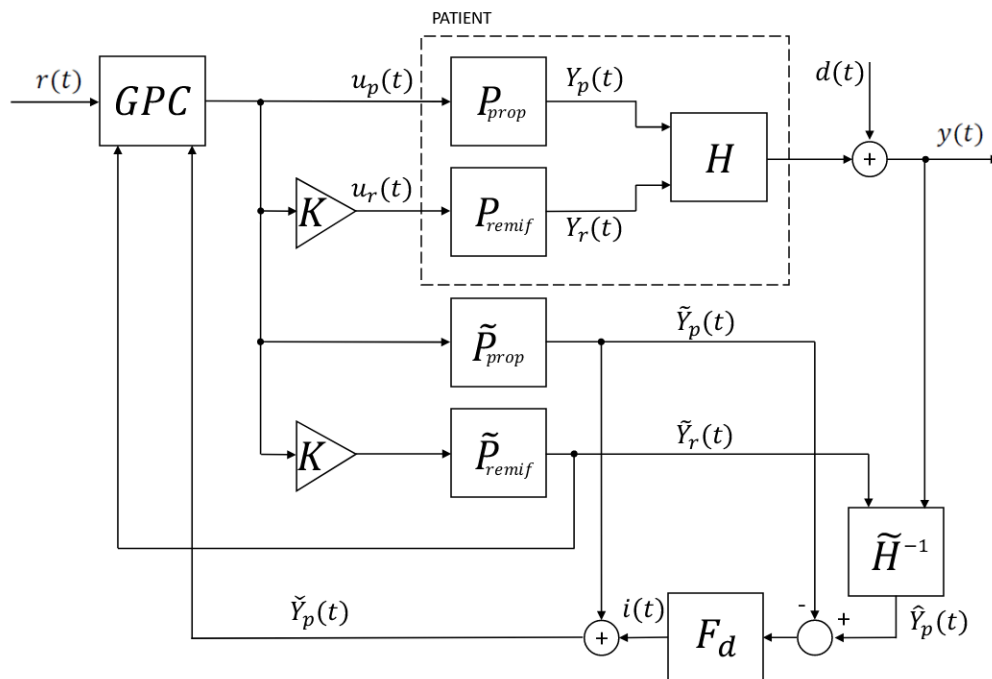
Figure 5.14: *Schematic representation of the MISO MPC control system for propofol-remifentanil coadministration.*
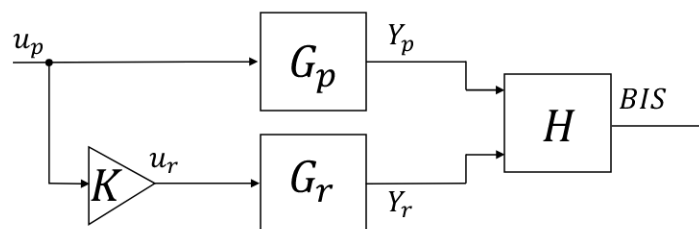

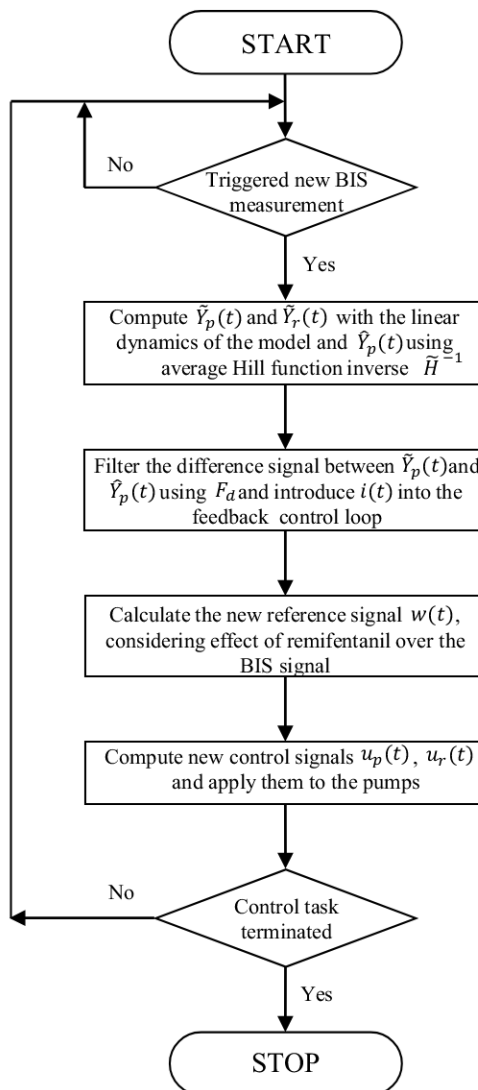**Figure 5.15:** *Simplified scheme of the external predictor employed in the MISO MPC control system.*

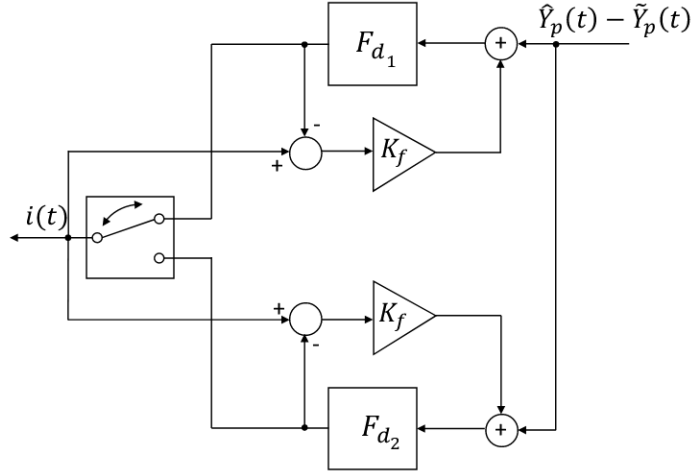**Figure 5.16:** *Algorithm flow chart of the MISO MPC control system.*

Figure 5.17: *Implementation details of the F_d block employed in the MISO MPC control system.*

The induction phase has been simulated providing to the controller a step reference signal, $r(t)$, that goes from the initial BIS value, E_0, to the target BIS value of 50. The maintenance phase is a disturbance rejection task where the BIS level of the patient is perturbed by the effect of the surgical stimulation. This has been simulated as an additive disturbance, $d(t)$, acting on patient's BIS. In particular, the double step disturbance signal shown in Figure 1.6 has been applied.

Simulation results obtained on the tuning dataset of Table 2.2 are presented. In this test, is assumed that the linear term of the considered process model is perfectly known ($\tilde{P}_{prop} = P_{prop}$ and $\tilde{P}_{remif} = P_{remif}$). However, the nonlinear element represented by the average Hill function is used instead of the actual patient's one ($\tilde{H} \neq H$). Figure 5.18 shows the control system performance for the induction and maintenance phases. The performance indexes related to the induction phase are shown in Table 5.15, while those of the maintenance phase are shown in Table 5.16. From the obtained results, it is possible to notice that the proposed control system provides a fast induction of anesthesia. Indeed, the mean TT over the whole dataset is 1.75 min, with a maximum value of 2.10 min obtained for patient 11. These values are fully compatible with the clinical specifications. The short TT has been achieved without causing an excessive undershoot of the BIS. In particular, BIS values below 50 have occurred in only two out of thirteen patients. Nevertheless, the BIS-NADIR has always remained above the recommended value of 40, and the undershoot has been short-lasting, as it appears from the values of ST10 and ST20. Indeed, ST20 is always shorter than TT. This indicates that the BIS quickly settles inside the recommended range from 40 to 60. As regards the ST10, it is equal to TT for all the patients, except in the two patients for which an undershoot occurs. In any case, the maximum value is 2.42 min, hence the BIS always settles in the range from 45 to 55 in less than 3 min. As regards the maintenance phase, the control system quickly compensates for the positive step disturbance as indicated by the TTp, without causing undershoot as the BIS-NADIRp never drops below 48. The TTn is longer than the TTp because the compensation of the negative step disturbance is mainly dominated by the patient natural dynamics. Indeed, when the negative step disturbance occurs, the controller reacts

by decreasing the drugs flows until they saturate to zero. Anyway, the controller behavior is sensible and the negative disturbance is compensated without causing a BIS overshoot, as it appears from the BIS-NADIRn index.

The robustness of the proposed control system has been assessed in the case of intra-patient variability with the method described in Section 2.2.1 based on the statistical properties of the PK models given in [27] and [25]. It is worth stressing that, for each of the thirteen patients of the tuning dataset, $\tilde{P}_{prop}$ and $\tilde{P}_{remif}$ are calculated with the average parameters values, while a set of 500 perturbed P_{prop} and P_{remif} models is generated. For each of these perturbed models, the induction and maintenance phases have been simulated. As regards the induction phase, the results for the average patient are shown in Figure 5.19a and the corresponding performance indexes are given in Table 5.17. The defined clinical requirements are always fulfilled. The same behavior has been obtained for all the other patients of the dataset and the corresponding results are shown in Figure 5.20. As regards the maintenance phase, the results for the average patient are shown in Figure 5.19b and the corresponding performance indexes are given in Table 5.18. Even in this scenario, the clinical requirements are always met. Moreover, the same behavior has been obtained for all the other patients of the tuning dataset and the results obtained are shown in Figure 5.21.

To further assess the controller robustness to inter-patient variability the method described in Section 2.2.1 has been applied. The parameters of the Hill function have been generated by considering the statistical properties given in [28, 29, 30]. In this context, it is assumed that the linear term of the considered process model is known ($\tilde{P}_{prop} = P_{prop}$ and $\tilde{P}_{remif} = P_{remif}$). On the contrary, the nonlinear element is represented by the average Hill function, that is implemented in the control scheme ($\tilde{H} \neq H$). The responses of the induction phase are shown in Figure 5.22a and the obtained performance indexes are given in Table 5.19. The controller quickly induces anesthesia in all patients. Indeed, the mean TT is 1.13 min and its maximum value is 2.23 min. Thus, the clinical requirements are fully satisfied. As regards the BIS-NADIR, the mean value of 44.23 implies that the control system does not cause an excessive undershoot of the BIS. In some patients the BIS falls below the recommended threshold of 40, as it is possible to notice by observing the minimum value of the BIS-NADIR, which is 31.46. However, the undershoot values obtained are acceptable as BIS values up to 30 are commonly reached in clinical practice and are not harmful to the patient health. The ST20 and ST10 values are, also in this case, fully compatible with the clinical practice. With respect to the test on the dataset of thirteen patients, it is possible to observe an increase in their maximum values that is due to the more pronounced undershoot observed in some patients of the population. However, these values remain well below the recommended value of 5 min given in the clinical requirements. Figure 5.22b shows the responses obtained in the maintenance phase and the performance indexes corresponding to this scenario are given in Table 5.20. The results on the whole population confirmed those obtained on the tuning dataset. Indeed, the control system is able to reject the disturbances quickly without causing undershoot or overshoot of the BIS.

5.4.3 Extension to the case of constant remifentanil infusion

It should be highlighted that the proposed control system based on the constant ratio between the two drugs is one of approaches that could be exploited in the clinical practice. However, it is also interesting to develop a control system that allows the anesthesiologist to use a mix between manual and automatic control to perform drugs coadministration. To this
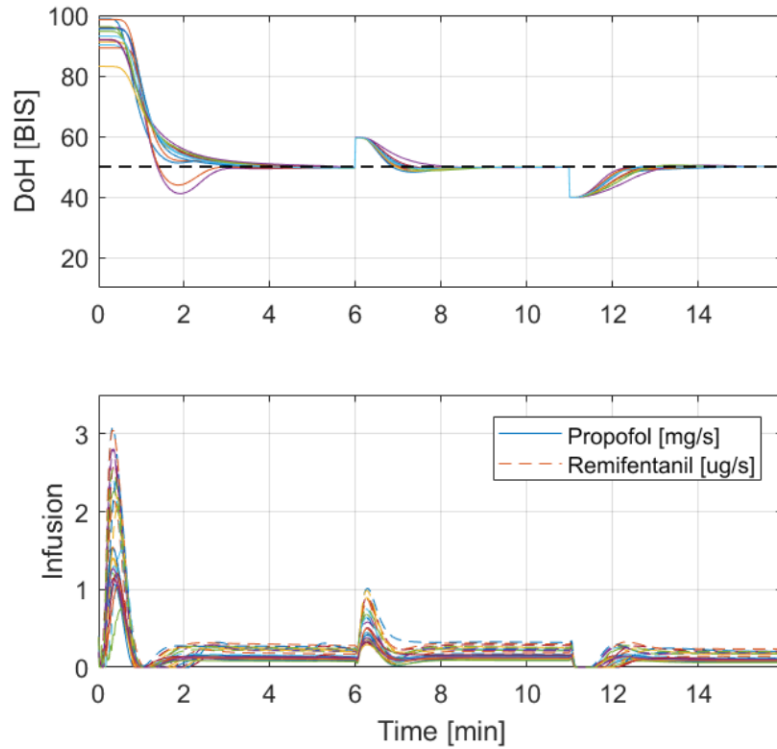
Figure 5.18: *Responses obtained for each patient of the tuning dataset with the MISO MPC control system.*

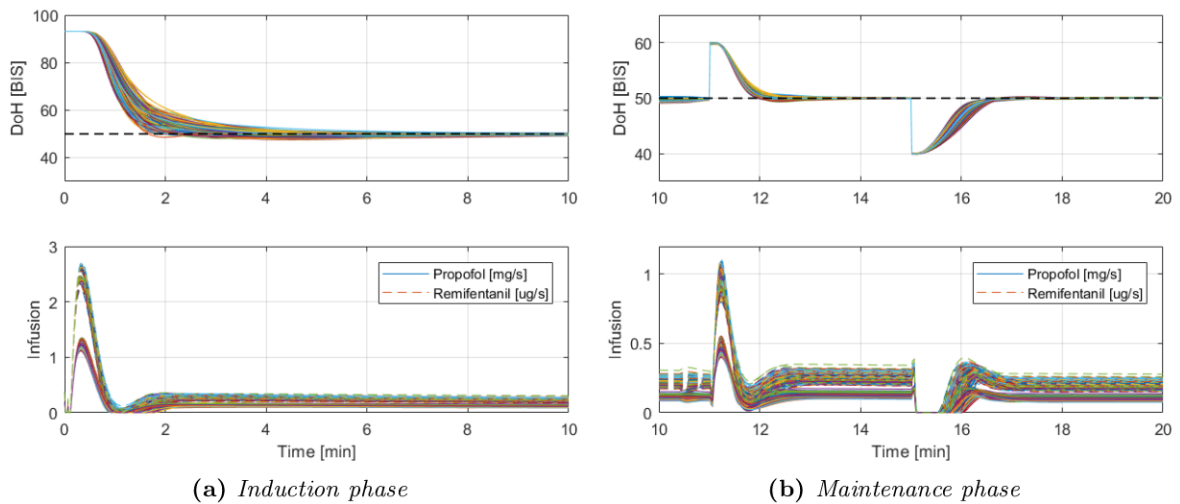(a) *Induction phase*   (b) *Maintenance phase*

Figure 5.19: *Responses obtained with the MISO MPC control system on the 500 perturbed models generated starting from the nominal model of the thirteenth patient of the tuning dataset to simulate intra-patient variability.*

Patient	TT [min]	BIS-NADIR	ST20 [min]	ST10 [min]
1	1.38	49.67	1.27	1.38
2	1.53	49.61	1.33	1.53
3	1.87	49.65	1.38	1.87
4	1.27	40.98	1.18	2.42
5	2.02	49.71	1.42	2.02
6	1.78	49.56	1.40	1.78
7	1.92	49.74	1.45	1.92
8	1.65	49.61	1.38	1.65
9	1.30	44.04	1.20	2.10
10	2.02	49.57	1.43	2.02
11	2.10	49.79	1.52	2.10
12	2.03	49.53	1.45	2.03
13	1.83	49.62	1.43	1.83
mean	1.75	48.54	1.37	1.89
std.dev	0.29	2.75	0.11	0.27
min.	1.27	40.98	1.17	1.38
max.	2.10	49.79	1.52	2.42

Table 5.15: *Performance indexes for the induction phase obtained for each patient of the tuning dataset with the MISO MPC control system.*

Patient	TTp [min]	BIS-NADIRp	TTn [min]	BIS-NADIRn
1	0.47	48.56	1.05	50.08
2	0.48	49.63	0.80	50.08
3	0.48	49.72	0.78	50.09
4	0.47	49.23	0.72	50.02
5	0.55	49.64	1.02	50.09
6	0.52	49.60	0.83	50.06
7	0.58	49.77	1.00	50.06
8	0.55	49.69	0.88	50.03
9	0.48	49.57	0.78	50.04
10	0.50	48.97	1.05	50.08
11	0.73	49.85	1.32	50.06
12	0.53	49.24	1.13	50.28
13	0.53	49.69	0.85	50.06
mean	0.53	49.47	0.94	50.08
std.dev	0.07	0.37	0.17	0.06
min.	0.47	48.56	0.72	50.02
max.	0.73	49.85	1.32	50.28

Table 5.16: *Performance indexes for the maintenance phase obtained for each patient of the tuning dataset with the MISO MPC control system.*

	TT [min]	BIS-NADIR	ST20 [min]	ST10 [min]
mean	1.91	49.40	1.46	1.91
std.dev	0.24	0.40	0.13	0.24
min.	1.37	47.89	1.13	1.37
max.	2.67	49.86	1.93	2.67

Table 5.17: *Induction phase performance indexes obtained with the MISO MPC control system on the 500 perturbed models generated starting from the nominal model of the thirteenth patient of the tuning dataset to simulate intra-patient variability.*

	TTp [min]	BIS-NADIRp	TTn [min]	BIS-NADIRn
mean	0.55	49.82	0.86	50.09
std.dev	0.02	0.08	0.06	0.03
min.	0.50	49.36	0.68	50.03
max.	0.62	49.95	1.05	50.27

Table 5.18: *Maintenance phase performance indexes obtained with the MISO MPC control system on the 500 perturbed models generated starting from the nominal model of the thirteenth patient of the tuning dataset to simulate intra-patient variability.*

	TT [min]	BIS-NADIR	ST20 [min]	ST10 [min]
mean	1.13	44.23	1.27	1.95
std.dev	0.15	4.38	0.62	0.78
min.	0.83	31.46	0.78	0.95
max.	2.23	49.81	3.27	3.78

Table 5.19: *Induction phase performance indexes obtained with the MISO MPC control system on the population of 500 patients used to simulate inter-patient variability.*

	TTp [min]	BIS-NADIRp	TTn [min]	BIS-NADIRn
mean	0.53	49.38	1.03	50.14
std.dev	0.04	0.33	0.09	0.09
min.	0.35	46.69	0.82	49.83
max.	0.75	49.95	1.40	50.61

Table 5.20: *Maintenance phase performance indexes obtained with the MISO MPC control system on the population of 500 patients used to simulate inter-patient variability.*
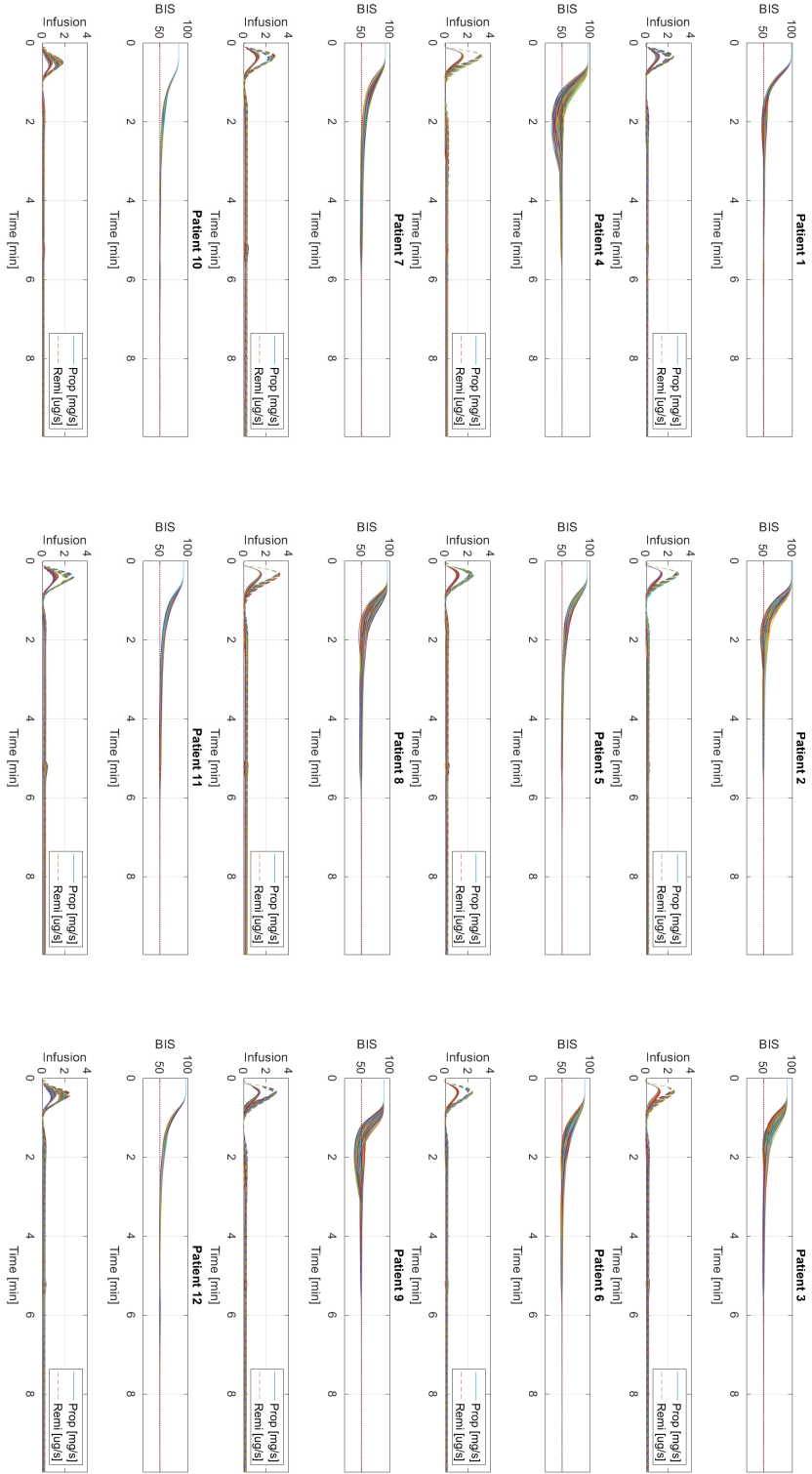
Figure 5.20: *Induction phase responses obtained with the MISO MPC control system on the 500 perturbed models generated starting from the nominal model of each patient of the tuning dataset to simulate intra-patient variability.*
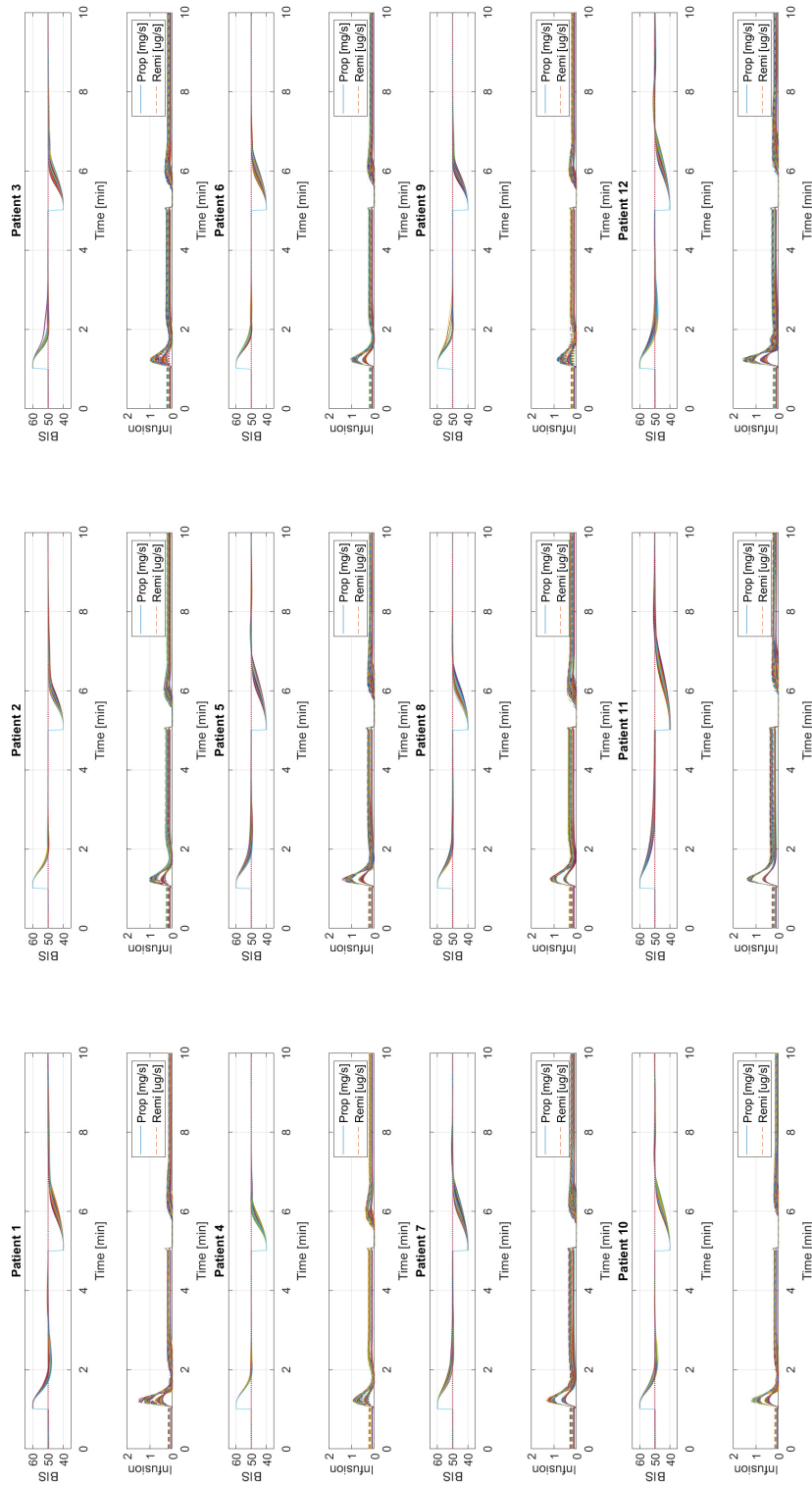
Figure 5.21: *Maintenance phase responses obtained with the MISO MPC control system on the 500 perturbed models generated starting from the nominal model of each patient of the tuning dataset to simulate intra-patient variability.*
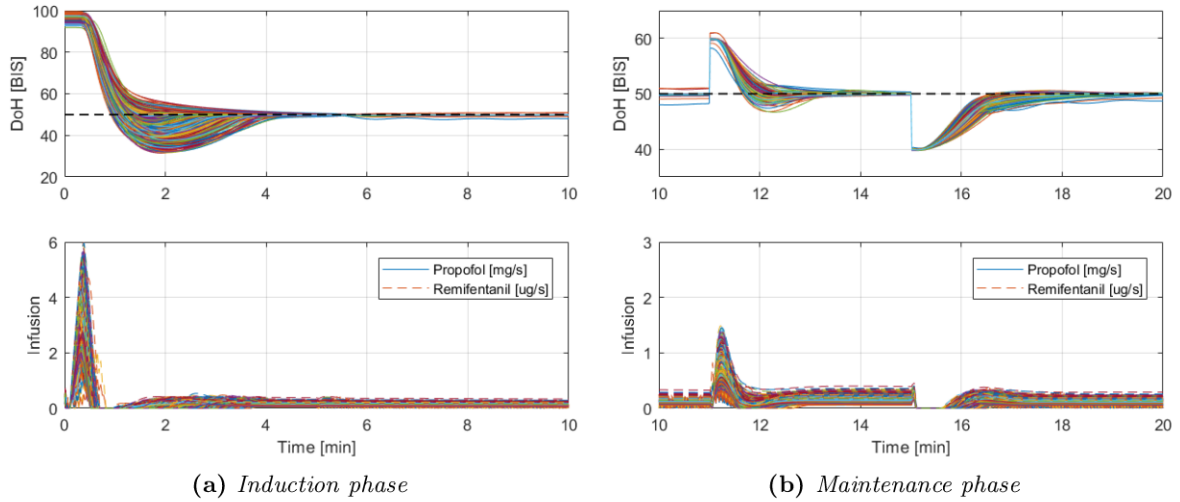
<table>
<tr><td>(a) Induction phase</td><td>(b) Maintenance phase</td></tr>
</table>

Figure 5.22: *Responses obtained with the MISO MPC control system on the population of 500 patients used to simulate inter-patient variability.*

end, the developed control scheme can be modified to handle the particular control scenario where the remifentanil infusion, $u_r(t)$, is manually controlled by the anesthesiologist and, thus, it is kept on a fixed value for long time intervals. To do so, it is necessary to compute the resulting ratio K at each sampling time, since it will change dynamically due to the modifications in the propofol infusion rate. For this, $u_p(t)$ and the fixed value of $u_r(t)$ are used, obtaining the ratio as $K = \frac{u_r(t)}{u_p(t)}$. Once the actual ratio between the two drugs is obtained, it is necessary to recompute the formula from (5.9) (this action needs to be repeated at each sampling time) and finally obtaining the $Y_r(k)$ using (5.10). Thus, an optimal reference signal for the propofol infusion that takes into account the effect of remifentanil can be determined. The remaining steps of the control algorithm remain unchanged. The simulation example for this control scenario is shown in Figure 5.23, where the average patient with a sample fixed value of remifentanil equal to $u_r(t) = 0.25$ μg/s is considered. From the obtained result it can be observed that the modified control architecture is able to properly handle this particular situation. Nevertheless, this approach requires a significant modification of the control architecture and involves the additional retuning of the whole system for best performance.

5.5   Event-based MPC for propofol administration

Event-based PID control of DoH was proposed in [96, 97, 99]. Simulation studies showed that this approach delivers a noise-free control action, reduces the number of control system computations and replicates the anaesthesiologist way of actuation. These findings were also confirmed by the results obtained in the in-vivo experiments presented in Chapter 4.
Event-based MPC controllers are significantly less investigated in the context of closed-loop anesthesia. A preliminary study was presented in [136]. Therein, a virtual band on the actuator was imposed and it was taken into account in the optimization procedure. Consequently, the controlled process was updated in an asynchronous way. The system was verified on one representative patient proving the feasibility of such a method. However, event-based
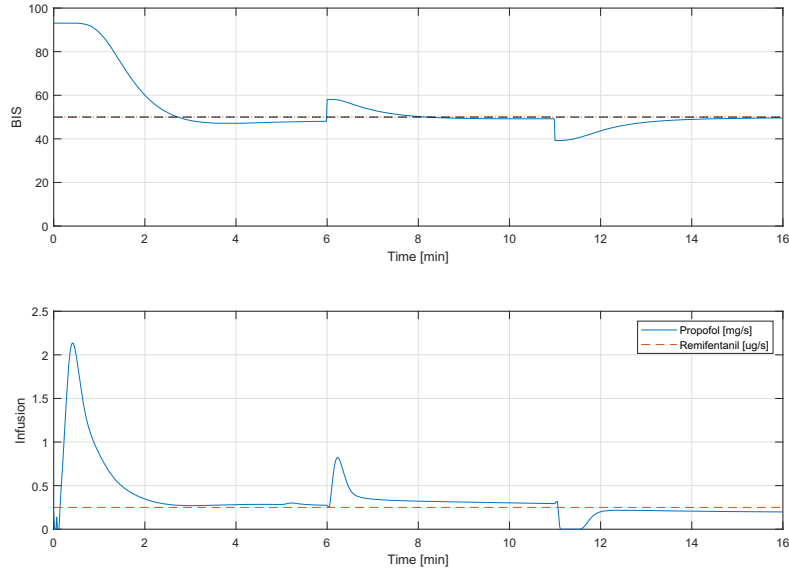
Figure 5.23: *Response obtained for the thirteenth patient of the tuning dataset using the MISO MPC control system with the remifentanil infusion rate fixed to 0.25 µg/s.*

predictive control with sensor dead-band sampling has never been applied to the anaesthesia control problem. Taking into account these aspects and the possible benefits, in this section an event-based MPC control system with dead-band sampling is proposed and evaluated. The whole system is based on that presented in Section 5.1. In the proposed event-based approach, the control action is updated with a higher frequency when the controlled variable goes outside the established tolerance. This provides a safety measure that assures that the required performance is obtained. On the contrary, when the controlled variable remains withing the defined band, the control action is updated with a lower frequency, thus limiting the control effort. Therefore, the event-based system works with a variable sampling rate, by adapting the controller invocation to the patient BIS, that is, by adapting the control effort (propofol infusion rate) to achieve the desired clinical requirements. With this working principle, the control system mimics the anaesthesiologist way of actuation, keeping all the advantages of the closed-loop control at the same time.

5.5.1   Control system architecture

The proposed control scheme, shown in Figure 5.24, has been implemented using the idea introduced in [146] and it has been adapted to the context of anesthesia control. It consists of three main components: an event generator, a controller structure and an external predictor. The event generator provides the information for the controller structure when a new control action should be computed due to a new event occurrence. The controller structure consists of a set of feedback GPC controllers, where one of them is selected in accordance with the actual sampling period (time elapsed between two consecutive events). Moreover, the external predictor (composed of $\tilde{P}$, $\tilde{H}^{-1}$ and F_d blocks) is used to compensate the nonlinear element of the patient model, making possible to exploit a linear MPC such as the GPC algorithm. The

external predictor is the same described in Section 5.1. In this scheme, the controlled variable $y(t)$ is the BIS signal, which is monitored continuously with a sampling time T_{base} and the control variable $u(t)$ is the propofol infusion rate, which is updated with a variable sampling time T_f. In such a way, the new control action is computed by the selected controller when a new event is generated.

The proposed architecture operates using the following working principle:

- The BIS signal process output is monitored within a constant sampling period T_{base} at the event generator block, while the control signal update is obtained at an event occurrence time instant and applied to the infusion pump with a variable sampling period T_f, that is, in an asynchronous way.
- T_f is defined as a set of multiple values of T_{base} and results in $T_f = fT_{base}$, $f \in [1, n_{max}]$. Additionally, $T_f \leq T_{max}$, being $T_{max} = n_{max}T_{base}$ the highest sampling period, which is selected to provide a minimum performance for safety reasons.
- For the anaesthesia process T_{base} and T_{max} are defined taking into account clinical practice and specifications.
- Once the control signal is sent to the infusion pump at time instant t, the DoH process state is checked at the event generator block within the base period T_{base}. The event generator block verifies if the controlled variable meets some specific condition and for this the BIS signal is used. When the condition is satisfied, a new event is triggered with resulting sampling period T_f and a new control signal is calculated by the controller. If no events occur, the controlled process is updated in any case after a t_{max} time interval to assure the minimum performance.
- Following the introduced working principle, the controller will compute the control signal using a variable sampling period T_f. Due to this, a set of predictive feedback controllers will be used, each of them designed for a specific sampling period $T_f = fT_{base}, f \in [1, n_{max}]$. Moreover, to avoid adverse bumps during controller commutations, signals resampling techniques are applied.

To implement the proposed control architecture, a set of controllers is designed, one for any possible sampling rate T_f. Each GPC controller of the set is implemented and designed using the linear part of the model P, that is discretized for any sampling rate T_f. The GPC algorithm is the same presented in Section 5.1. The GPC tuning parameters are: the minimum and maximum prediction horizons N_1^f and N_2^f, the control horizon N_u^f, the future error scaling index δ^f, and the control weighting factors λ^f where ^{f} indicates a specific sampling rate. Taking into account that there is no time delay in the process, the value of N_1^f is set to 0 and, consequently, the resulting prediction horizon will be referred as $N^f = N_2^f$ for simplicity. The GPC algorithm provides the future control actions $u^f(t), u^f(t+1), ..., u^f(t+N_u^f-1)$ that will drive the controlled variable $y^f(t+j)$ close to desired reference $w(t+j)$.

The constraints on the control action that need to be considered are related to the physical limitations and clinical recommendation in drug administration. The physical minimum infusion rate is 0 mg/s and represents the non-infusion of the drug. However, following a safety measure applied in the clinical practice, a minimum nonzero baseline infusion u_b should be used. This baseline infusion is used to avoid null values for the drug infusion system even if the value of the BIS is below the desired reference. The baseline infusion for propofol is therefore set to $u_b = 6$ mg/kg/h according to Roberts manual infusion scheme [120]. As regards the maximum infusion rate, in the induction phase, it is set to 6.67 mg/s. For the maintenance phase the maximum infusion rate is set to 4.00 mg/s, that is typically used in

the clinical practice for the considered type of the surgery. Moreover, the slew-rate infusion pump limitations are directly included in the vector Δu of the control action increments. Also these constraints are defined for each anaesthesia phase separately to match the performance requirements. For the induction phase, they are set to have $-1 \leqslant \Delta \mathbf{u} \leqslant 1 \ [mg/s]$ and for the maintenance phase $-2 \leqslant \Delta \mathbf{u} \leqslant 2$ mg/s.

In the proposed control system, the decision on when new events are triggered is managed by the event generator block shown in Figure 5.25. This element considers two conditions and when one of them is met, a new event is triggered. When a new event is generated, the current value of $\tilde{y}(t)$ is send to the control structure with variable sampling rate, forming the y^f vector and a new control value is computed (propofol infusion rate). The first condition is used to monitor the BIS signal and exploits the dead-band sampling method [146], generating a new system event when the absolute value between two variables is bigger than a established interval β. The condition can be formalized as:

$$|r(t) - y(t)| > \beta, \qquad (5.12)$$

and detects when the process output, $y(t) = BIS(t)$, differs from the desired set-point $r(t)$, more than a specific threshold β. Note that the controlled variable is $\tilde{y}(t)$; however, it is more natural for the anaesthesiologist to use the BIS values, as the threshold for its allowable range is clearly defined, being this the main reason for using this signal for event generation. The second complementary condition is a safety measure, used for minimum performance requirements and is a time-based condition. In this case, the maximum time interval between two consecutive events (between two control signals computation), is given by t_{max}, that is,

$$t - t_{last} \geq t_{max}, \qquad (5.13)$$

where t_{last} refers to the time instant when the last event was triggered. Both criteria are verified with the shortest sampling time T_{base}. However, the events are triggered with a variable rate T_f. Finally, the events occurrence will determine the feedback-loop sampling time T_f that will produce the control signal updates in an asynchronous way [146]. Due to this, to execute the GPC algorithm, the past samples of the process output and of the control signal needs to be accessible for each sampling rate T_f. For this, a resampling and reconstruction techniques must be applied for corresponding signals.

- Resampling - Following the introduced working principle, the controller structure block gets the new information from the controlled process only when a new event is triggered. The received data is accumulated in the controller structure element and is resampled to create a base vector y^b that includes the previous samples of the controlled variable with T_{base} rate. This procedure is accomplished by applying a linear interpolation technique among two consecutive signal values. Then, the obtained signal is sampled with the T_{base} frequency and stored. In fact, the $y^b(k)$ vector is created with $k = 0, T_{base}, 2T_{base}, 3T_{base}, \ldots$. After that step, the required samples with past information need to be provided with the new sampling rate T_f, that creates a new vector y^f of past values sampled with T_f rate. Finally, the y^f vector contains the past process data sampled with actual sampling rate T_f and that information is used to compute the next value of the control signal.

- Reconstruction - This procedure is applied to the control signal and is executed in the opposite direction than for the controlled variable. In the proposed scheme, the control

T_{base}	β	n	N^1	N_u^1	λ^1	T_d	T_r
1	5	10	24	2	14.4	47.3	24.6

Table 5.21: *Tuning parameters of the event-based SISO MPC control system for T_{base} sampling rate.*

signal values are always saved with a T_{base} sampling rate and stored as the u^b vector. In the first step, the required past values are calculated and then the update of u^b is performed. For the new sampling rate T_f, the past information is calculated using u^b and accumulated in temporary vector u_p^f. Subsequently, the u_p^f and y^f vectors are used to feed the GPC algorithm and to compute the new control signal $u^f(T_f) = u^b(k)$. Finally, the u^b vector is updated by keeping the control action constant among two successive system events.

There are three parameters that are related to the event-based mechanism and that have influence over the control performance: they are the dead-band sampling threshold β, and the T_{base} and t_{max} sampling rates. In the analyzed system, T_{base} has been selected as 1 s and matches the BIS monitor data rate. Then, t_{max} has been set to 10 s (that is, n=10) because of safety reasons, as this ensures the minimum performance as shown in Section 5.2. Indeed, it was shown that the sampling period of 10 s is the maximum value that allows the clinical requirements to be met in terms of accuracy and disturbance compensation capability in the presence of measurement noise. Additionally, the value of β has been fixed to 5. With this threshold, with dead-band sampling and for a BIS reference set to 50, the event-based control system working interval is BIS=50±5, being inside the desired tolerance for the desired BIS range between 40 and 60 with the necessary safety margins.

Moreover, it is necessary to design the set of GPC controllers to assure the performance defined by the clinical requirements. For this, the GPC parameters need to be tuned. The tuning is performed for maintenance and induction phase separately, applying a two degree-of-freedom approach, that is, dividing the tuning procedure into two stages [138]. At the first stage, the GPC controllers from the set and the F_d filter are designed. During this procedure the parameters N^f, N_u^f, λ^f, and T_d (related, respectively, to the prediction horizon, the control horizon, the control signal weighing factor and the F_d filter time constant) are obtained with the optimization-based procedure described in Section 2.2.1. In particular Problem 2.2 is defined with N^f, N_u^f, λ^f, and T_d as the θ vector and it is solved by means of GA with a population of 50 elements and by stopping the optimization when the relative change in the cost function value over the last 50 iterations is less than 0.001. The tuning procedure is performed applying the design rule for event-based GPC from [146], where the tuning of GPC controller for T_{base} sampling time is used to derive tuning parameters of the remaining controllers from the set. The second tuning stage is focused on the set-point following task and in this case the optimization is simply executed to determine an adequate value of the F_r filter time constant T_r whereas all the remaining parameters are kept the same as for maintenance phase. Additionally, the defined control system constraints were active in both stages of tuning procedure. The resulting control system parameters are summarized in Table 5.21.
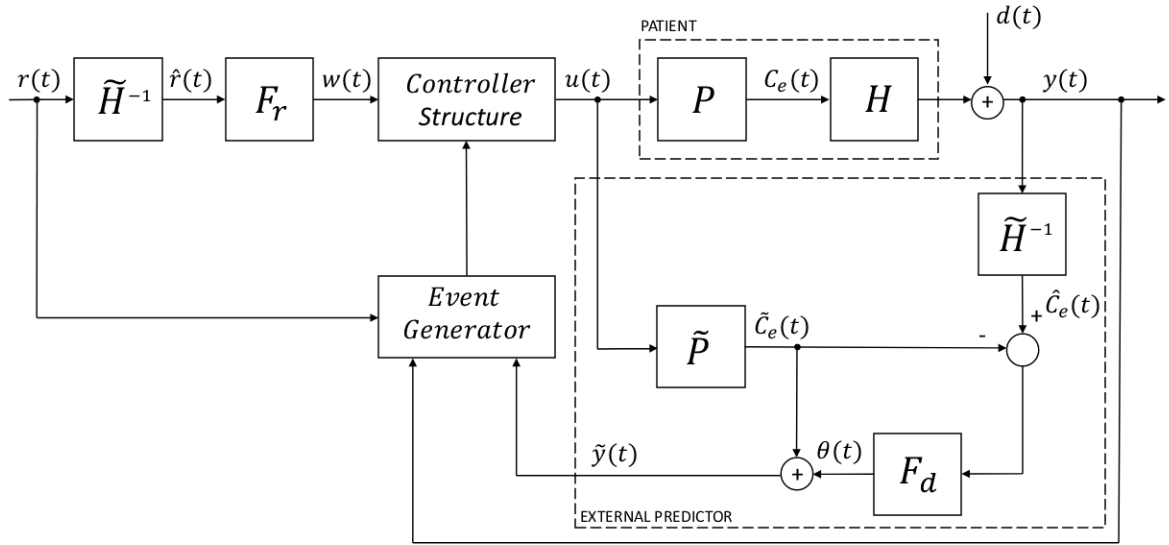
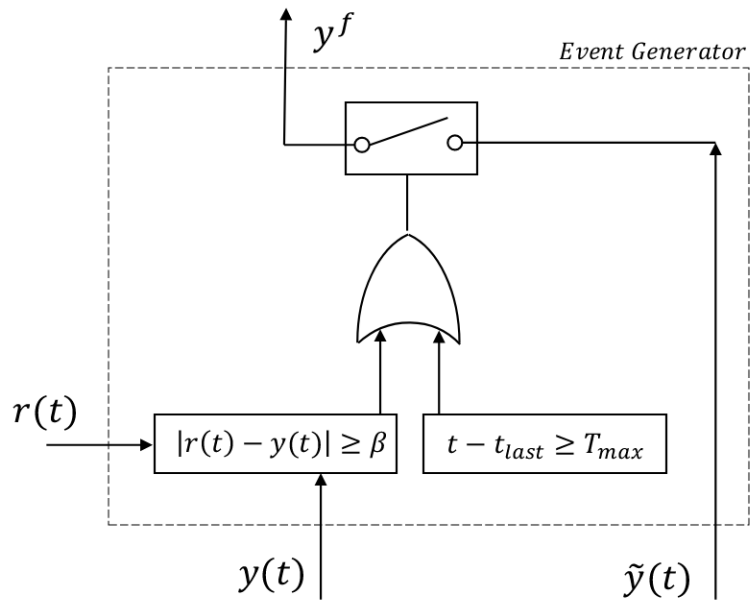**Figure 5.24:** *Schematic representation of the event-based SISO MPC control system for propofol administration.*

Figure 5.25: *Implementation details of the event generator block employed in the event-based SISO MPC control system.*

5.5.2   Simulation results

The performance of the proposed event-based control system is evaluated in simulation to verify that the clinical specifications are met. Simulations have a duration of 20 min and include both the anesthesia induction and maintenance phases. The induction phase starts at minute 0 when the BIS set-point $r(t)$ is changed from 100 to the desired value of 50. Once the BIS target is obtained, the maintenance phase begins. During this phase the ability of the control system to reject disturbances is assessed. To simulate the occurrence of a disturbance on the BIS due to surgical stimuli, the double step disturbance profile shown in Figure 1.6 is used. The effect of noise is also considered. The noise signal shown in Figure 1.9, which has been extracted from real clinical data, is added to the BIS. The simulations are performed on the tuning dataset of Table 2.1. In these first simulations, a perfect knowledge of the linear element of the patient model ($\tilde{P} = P$) is assumed. As regards the Hill function, the average parameters of Table 1.3 are used instead of the patient's specific ones ($\tilde{H} \neq H$).

To better show the behavior of the event-based control system the first simulation is performed on the average patient of the dataset. The results obtained are shown in Figure 5.26. The top plot shows the BIS signal, the middle plot shows the propofol infusion rate and the bottom plot shows the behavior of the event generator. In particular, the presence of a vertical line indicates the generation of an event, while its height represent the resulting sampling rate. From the BIS plot it is possible to observe that the clinical specifications are satisfied. Indeed, during the induction phase the BIS reaches the target value in approximately 2 min and during the maintenance phase the BIS is kept close to the target despite the presence of noise and of the double step disturbance. By observing the events plot it appears that the controller generates more events, and thus a shorter sampling rate, in those phases where the BIS is far from the target value. For example, during the induction phase, and between minute 15 and minute 16 when the positive step disturbance occurs and the BIS tends to rise, and between minute 16 and minute 18 when the negative step disturbance occurs and the BIS tends to drop. On the contrary, when the BIS remains close to the target value, less events are generated, with a consequent longer sampling period. For example, between minute 8 and minute 11 the maximum admissible sampling rate of 10 s is always selected because the BIS remains close to the target value. The resulting propofol infusion profile is not affected by the presence of residual noise and it resembles the control action typically performed by an anesthesiologist. Indeed, the propofol bolus performed in the induction phase is common in clinical practice and the infusion rate remains constant for long periods of time when the BIS is close to the target. However, the controller promptly responds to significant deviations of the BIS signal from the set-point value.

The simulation is then performed on all the patients of the tuning dataset. The results regarding the induction phase are shown in Figure 5.27a. The BIS target is always reached in less than 4 min for each patient of the dataset without undesired undershoots. Only for one patient the BIS falls slightly below 40. This is due to the presence of noise and it is not significant from a clinical point of view. Once the BIS has reached the target it is properly maintained within the recommended range from 40 to 60 despite the presence of noise. The results regarding the maintenance phase are shown in Figure 5.27b. The positive step disturbance occurring at minute 11 is promptly compensated by the controller without causing undershoots. Only for one patient the BIS drops below 40 but it remains above the threshold of 30. Also the negative step is properly compensated.

The event-based control system performance is compared with the classical time-based GPC

controller proposed in Section 5.1, which has been designed to handle the noise in the predictive DoH control system. The performance indexes used for the comparison are the IAE, the IAU, and the TV that are calculated as shown in Section 1.3.3. The TV index is a measure of the control effort and it has been previously used to compare an event-based PID controller with its time-based counterpart [99]. From the anaesthesia process point of view, it is desired to reduce control signal changes especially taking into account the noisy characteristic of the BIS signal used as feedback information. Finally, the total number of events generated is also considered. The results obtained for each patient of the dataset are shown in Table 5.22. It is worth noting the significant reduction in the number of control signal updates (denoted in the table as events) provided by the event-based controller with respect to the classic time-based controller. In the classic controller they are equal to the simulation time because they are synchronously generated and they match the sampling period that is equal to 1 s. With the event-based controller the number of control signal updates is reduced from a minimum of 39.3% up to a maximum of 62.2%, with an average reduction of about 54.3%. This is not paid off with a reduction of the control performance as indicated by the IAE. Indeed, with the event-based controller there is a small average IAE increase of 11.7% with respect to the time-based controller. However, this has no relevant deleterious effects on the performance from a clinical point of view. Concurrently, the total amount of drug used (IAU) and the TV are reduced, on average, of 2.1% and of 6.8%, respectively. This indicates that the control action is less subject to unnecessary variations introduced by noise.

A robustness analysis with respect to inter-patient and intra-patient variability is also performed. As regards the inter-patient variability the method described in Section 2.2.1 has been applied. The parameters of the Hill function have been generated by considering the statistical properties given in [28]. As for the simulation on the tuning dataset, P is set equal to $\tilde{P}$ and $\tilde{H}$ is selected as the average Hill function. The simulation results regarding the induction phase are shown in Figure 5.28a. For each of the 500 patients the BIS target value is reached in less than 3 min and the undershoot always remains above the BIS value of 30, thus confirming the satisfactory results obtained on the tuning dataset. The simulation results regarding the maintenance phase are shown in Figure 5.28b. For each of the 500 patients the double step disturbance is properly compensated without causing undershoots of the BIS below the value of 30 and rises of the BIS above the value of 70. As before, the performance is then compared with that of the classic time-based controller and the results are shown in Table 5.23. Also in this case the event-based controller provides a reduction of the number of events, of the TV and of the IAU at the expense of a slightly greater IAE.

As regards the intra-patient variability, the robustness of the controller with respect to the mismatches of the linear part of the model is assessed. To this end, the method described in Section 2.2.1 has been applied with the statistical properties of the PK model given in [25] to generate 500 perturbed models P for each patient of the tuning dataset, while $\tilde{P}$ is determined by using the average parameters values. So, in this case, there are mismatches both in the linear part of the model ($\tilde{P} \neq P$) and in the Hill function model ($\tilde{H} \neq H$). As an illustrative example, the set-point responses for the 500 perturbed models of the average patient of the dataset are shown in Figure 5.29a. Also in presence of intra-patient variability, the BIS target value is reached in less than 3 min and the undershoot always remains above the BIS value of 30. The load disturbance responses for the same set of perturbed models are shown in Figure 5.29b. Also in this case the double step disturbance is properly compensated without undershoots of the BIS below the value of 30 and rises of the BIS above the value of 70. The same results obtained with the perturbed models of the average patient
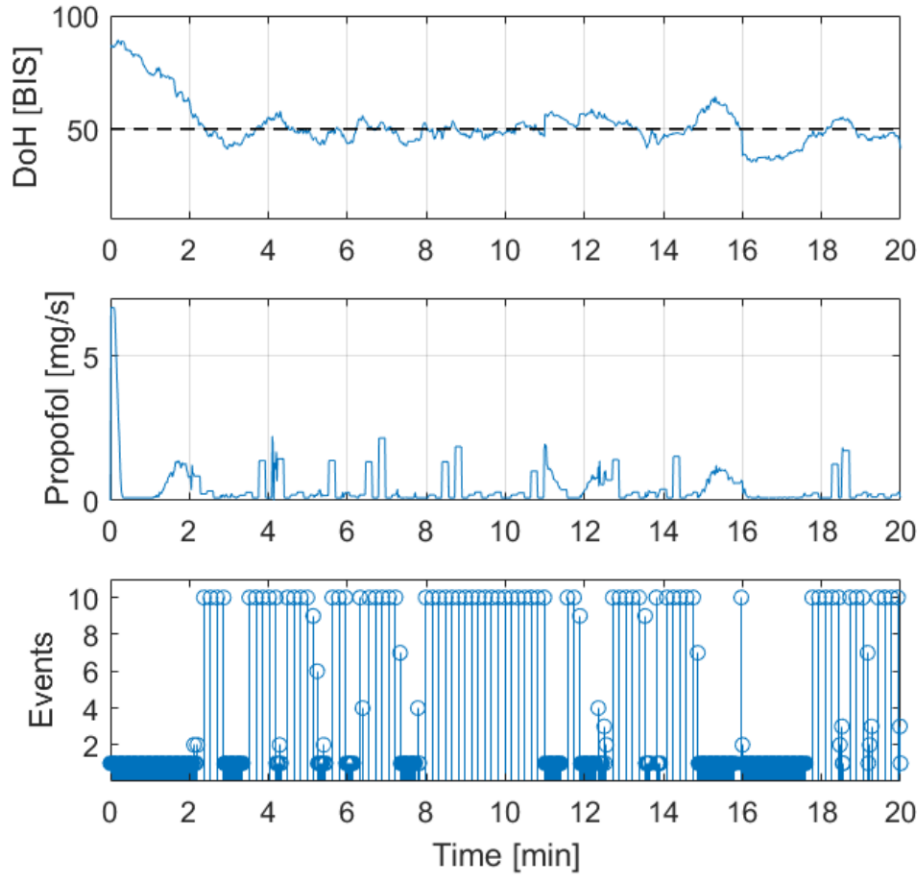
Figure 5.26: *Response obtained for the thirteenth patient of the tuning dataset using the event-based SISO MPC control system.*

are obtained also for the perturbed models of the others patients of the design dataset as shown in Figure 5.30 for the induction phase and in Figure 5.31 for the maintenance phase. Also in case of intra-patient variability, when the performance is compared with that of the classic time-based controller, it appears that the event-based controller provides a reduction of the number of events, of the TV and of the IAU that is paid by a slightly greater IAE, as shown in Table 5.24. It should be highlighted that the obtained results are important from the clinical practice standpoint since propofol overdosing can lead to undesired effects on the patient in the form of arterial hypotension and post-operative delirium. In light of these possible problems, it is advantageous to obtain the desired clinical effect (the DoH level) by using a control technique that ensure the correct dose.

5.6   Conclusions

In this chapter a novel MPC methodology for DoH control that uses the compensation of the nonlinear part of the process and an external predictor to fully exploit a GPC algorithm has been presented. Initially, a SISO control scheme that exploits the BIS as feedback variable and the propofol infusion rate as control variable has been presented. The control structure is based on an individualized patient model, where saturation and slew rate constraints of

(a) *Induction phase* **(b)** *Maintenance phase*
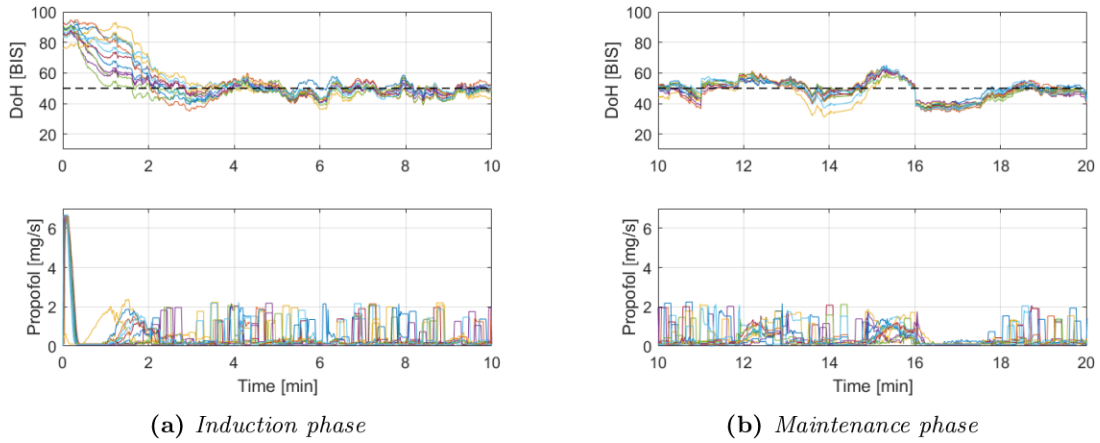
Figure 5.27: *Responses obtained for each patient of the tuning dataset with the event-based SISO MPC control system.*

(a) *Induction phase* **(b)** *Maintenance phase*
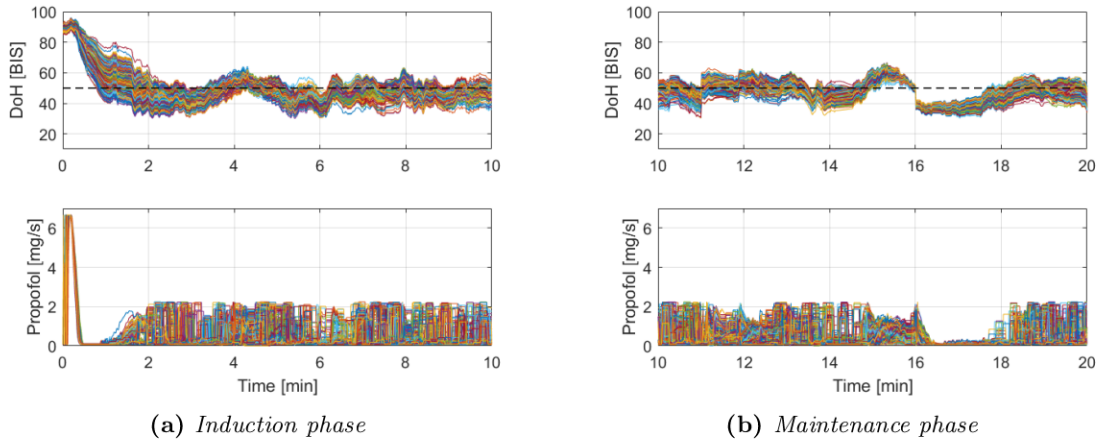
Figure 5.28: *Responses obtained with the event-based SISO MPC control system on the population of 500 patients used to simulate inter-patient variability.*

(a) *Induction phase* **(b)** *Maintenance phase*

Figure 5.29: *Responses obtained with the event-based SISO MPC control system on the 500 perturbed models generated starting from the nominal model of the thirteenth patient of the tuning dataset to simulate intra-patient variability.*

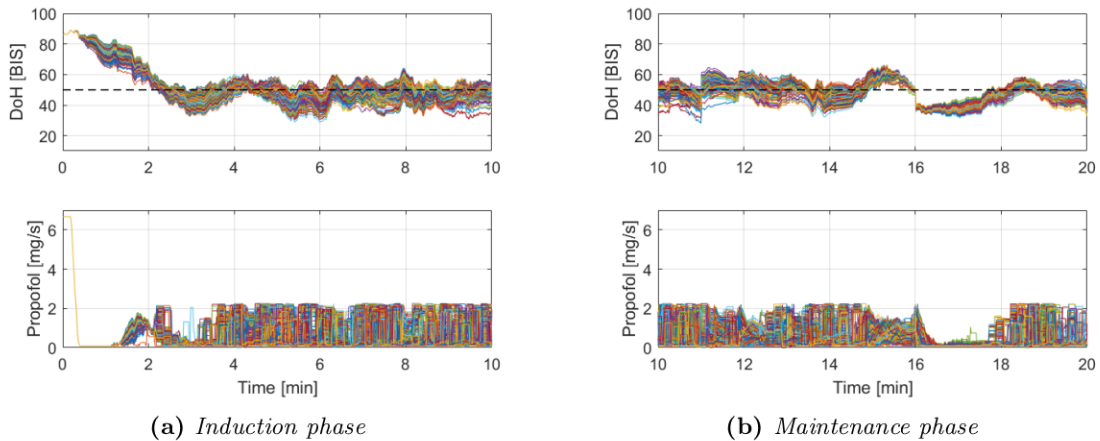| Patient	IAE[-]$*10^3$			IAU[mg]			TV[-]			Events[-]		
	TB	**EB**	**Δ [%]**	**TB**	**EB**	**Δ [%]**	**TB**	**EB**	**Δ [%]**	**TB**	**EB**	**Δ [%]**
1	6.49	7.60	17.1	543.7	516.1	-5.1	117.4	115.2	-1.8	1200	574	-52.2
2	8.06	9.15	13.6	563.6	557.8	-1.0	113.4	114.6	1.0	1200	637	-47.0
3	8.07	8.83	9.3	682.2	678.3	-0.6	118.5	101.7	-14.2	1200	501	-58.3
4	5.86	6.95	18.6	549.3	539.9	-1.7	109.4	87.8	-19.7	1200	517	-57.0
5	5.97	6.93	15.9	419.9	405.8	-3.4	86.2	90.5	4.9	1200	566	-52.9
6	7.53	8.70	15.6	637.9	619.3	-2.9	113.0	99.5	-11.9	1200	580	-51.7
7	6.71	7.28	8.5	575.1	555.5	-3.4	114.1	98.9	-13.3	1200	530	-55.9
8	7.54	8.62	14.3	663.2	658.4	-0.7	115.6	100.0	-13.4	1200	534	-55.5
9	10.19	11.56	13.4	566.6	566.4	-0.1	98.9	89.3	-9.8	1200	729	-39.3
10	7.78	8.17	4.9	516.0	504.4	-2.3	78.5	73.8	-5.9	1200	555	-53.8
11	5.69	5.67	-0.4	450.1	437.4	-2.8	94.1	95.2	1.1	1200	454	-62.2
12	5.45	6.02	10.3	451.0	440.0	-2.4	76.2	79.5	4.4	1200	469	-60.9
13	6.93	7.72	11.3	579.8	576.4	-0.6	110.4	99.7	-9.7	1200	484	-59.7
mean	-	-	**11.7**	-	-	**-2.1**	-	-	**-6.8**	-	-	**-54.3**

Table 5.22: *Comparison of the performance indexes obtained on the tuning dataset with the time-based (TB) and with the event-based (EB) SISO MPC control system. The Δ value refers to the percentage change of the index taking as reference the time-based system.*

	IAE [-]$*10^3$	IAU [mg]	TV [-]	Events [-]
Classic	6.30	459.2	91.0	1200
EB	7.68	443.9	87.3	599
Δ	21.8	-3.3	-4.3	-50.13

Table 5.23: *Comparison of the mean values of the performance indexes obtained on the population of 500 patients used to simulate inter-patient variability with the time-based (TB) and with the event-based (EB) SISO MPC control system. The Δ value refers to the percentage change of the index taking as reference the time-based system.*

	IAE [-]$*10^3$	IAU [mg]	TV [-]	Events [-]
TB	7.18	551.4	101.1	1200
EB	8.12	538.7	94.8	567
Δ	13.1	-1.9	-4.9	-52.8

Table 5.24: *Comparison of the mean values of the performance indexes obtained on the 6500 perturbed models used to simulate intra-patient variability with the time-based (TB) and with the event-based (EB) SISO MPC control system. The Δ value refers to the percentage change of the index taking as reference the time-based system.*

Figure 5.30: *Induction phase responses obtained with the event-based SISO MPC control system on the 500 perturbed models generated starting from the nominal model of each patient of the tuning dataset to simulate intra-patient variability.*
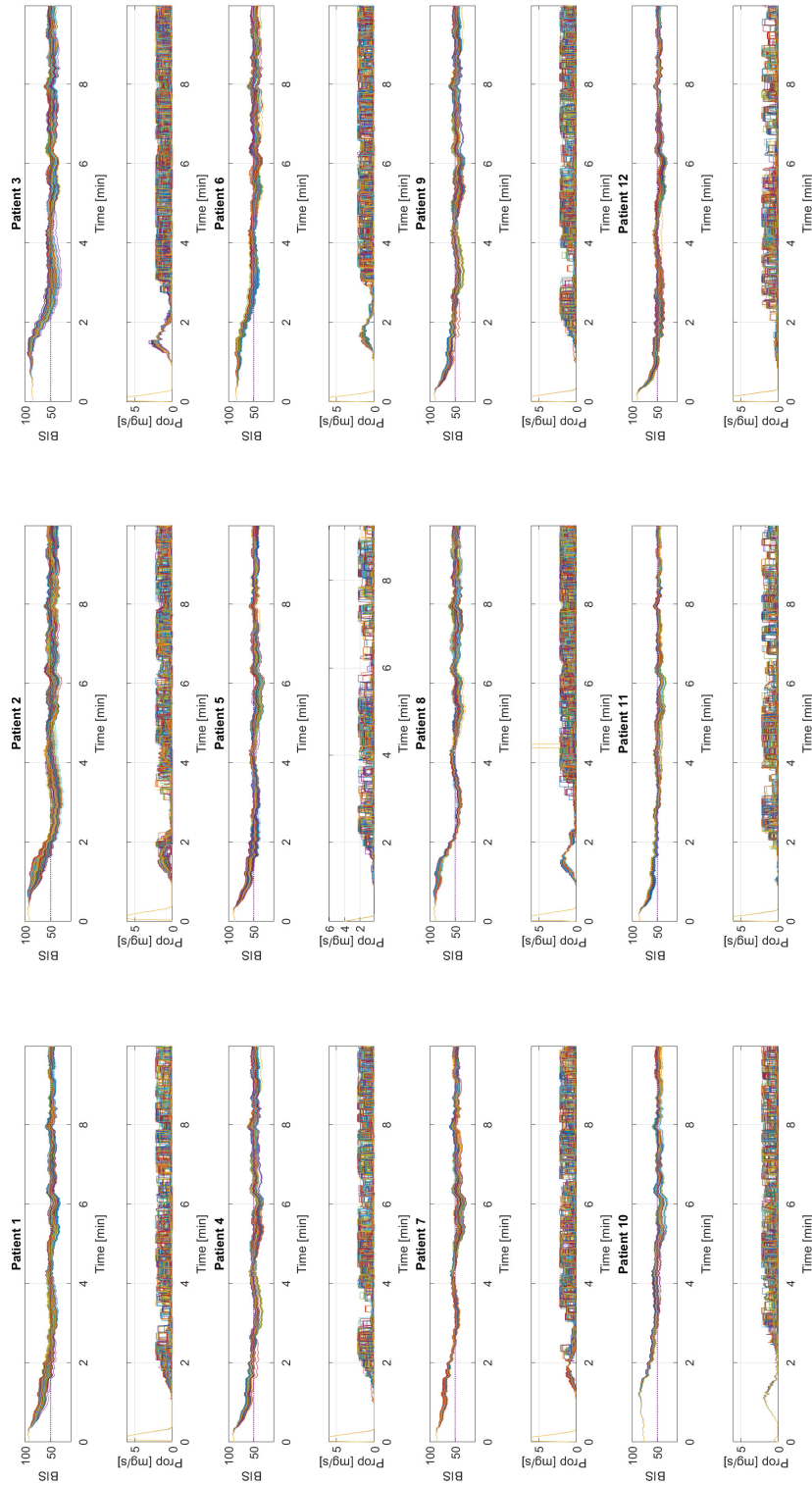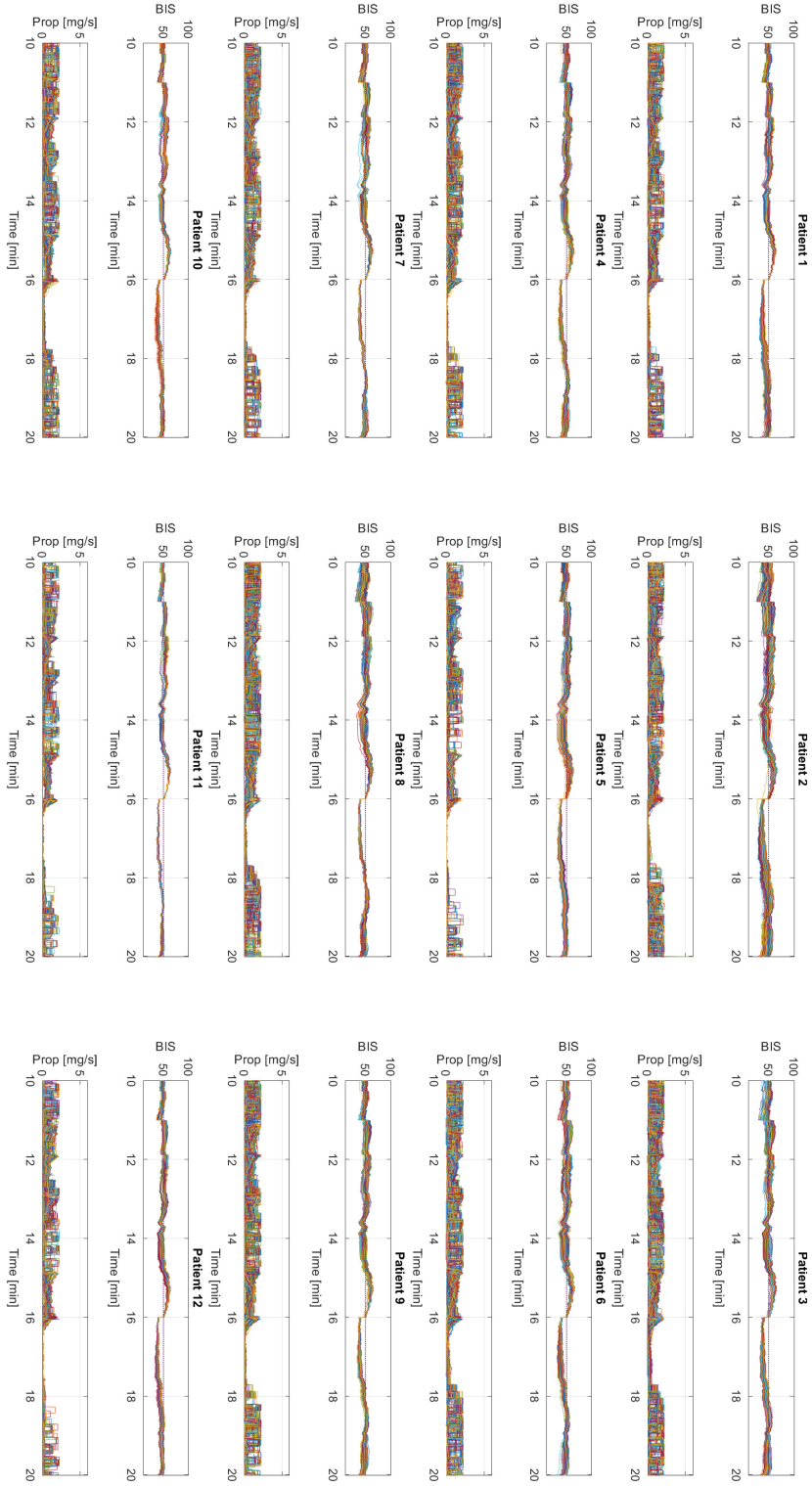
Figure 5.31: *Maintenance phase responses obtained with the event-based SISO MPC control system on the 500 perturbed models generated starting from the nominal model of each patient of the tuning dataset to simulate intra-patient variability.*

the control signal are taken into account. The tuning procedure of the overall control scheme has been performed by exploiting the optimization based approach. The developed control structure is characterized by low complexity and low computational effort, so that it can be easily deployed to standard hardware and software platforms. The control system has been tested through an extensive simulation study, considering inter- and intra-patient variability and by comparing it with other control schemes previously presented in the literature. The obtained results show that this new MPC approach provides a satisfactory performance for this challenging process. Moreover, typical process constrains like control signal saturation and infusion pump slew rate have been considered into the optimization procedure. All these features allowed the developed control structure to obtained better performance than the PID based approach used for comparison. Additionally, the proposed control structure was evaluated for a typical disturbances in DoH in anaesthesia, related to surgical interventions. These disturbance profiles were used in several previous works and and its effect on controller can be used for comparison purposes with other control systems.

The performance degradation due to the noise presence in the control loop has been analyzed. To assure a proper noise handling, an additional filter in the feedback loop has been included. However, its presence requires the retuning of the overall control system. A simulation study, considering a representative set of virtual patients has been used to test different noise characteristics and sampling periods. The obtained results confirmed that clinical requirements can be satisfied if the noise issue is explicitly considered during the design stage.

The control system has been tested in an in-vivo study on four patients undergoing elective plastic surgery. The control system performed well and the performance was compatible with the clinical practice. However, the experimental results pointed out the importance of considering also the administration of remifentanil.

To this end, the control system has been extended to the MISO case for propofol and remifentanil coadministration. The PK/PD interaction model has been used to decouple the drugs synergistic effect for control purposes. The obtained results have demonstrated that, also in the MISO case, the proposed control structure gives a satisfactory performance despite inter- and intra-patient variability. Moreover, the proposed approach could also be useful to provide a hybrid control system architecture that enables the manual control of the remifentanil, providing optimal control of the propofol taking into account the interaction between the two drugs.

The SISO approach has also been extended with an event-based GPC algorithm with sensor deadband to reduce the variability of the control signal. The proposed system provides a reduction of the number of control signal changes despite the presence of process noise and unmeasurable disturbances. The performance of the analyzed control system has been evaluated using an in-silico study. In realistic conditions, it was possible to reduce the number of control signal changes of about 55% on average. On the other side, the control system performance is only 11% less than in the classical time-based framework. Moreover, the proposed event-based approach was able to reduce the amount of the drug used of about 2.1% on average. Taking into account these results, the developed event-based predictive control architecture on the one hand is able to meet the clinical requirements and on the other hand it can reduce significantly the influence of the noise simultaneously saving the control resources (quantity of administrated drug). Additionally, the execution of control actions is similar to the anesthesiologist actuation so that it is likely that this kind of controllers can be more accepted in the clinical practice where the anesthesiologist acts as a supervisor.

Chapter 6

Influence of opioid-hypnotic balance: in-silico study

The experimental results presented in Chapters 3 and 4 have demonstrated the effectiveness of the MISO control approach first proposed in [93], that is based on the introduction of a ratio that links the infusion rates of propofol and remifentanil. A similar approach has also been proposed in [81] and promising results regarding its effectiveness have been obtained in an in-vivo experiment performed on two patients [82]. However, the potentialities of this approach have been only partly exploited in the clinical experiments presented in the aforementioned chapters of this thesis. Indeed, only an opioid/hypnotic ratio equal to 2 have been considered while the proposed controllers have been designed to properly operate on the whole range from 0.5 to 15.

The clinical reasons that motivated the choice of using the ratio equal to 2 have been discussed in Section 2.2.2. This value has not been changed during the clinical experiments performed with the aim to better understand the results obtained. In fact, the arbitrary modification of this parameter made by the anesthesiologist would have introduced a confounding factor which would have made the interpretation of the obtained results difficult. Indeed, the modification of the opioid/hypnotic balance produces significant clinical effects.

The possibility for the anesthesiologist to regulate this parameter could represent a great step towards the implementation of the anesthesiologist-in-the-loop paradigm. This would give the possibility to the anesthesiologist to adapt the system behavior according to clinical needs that are not known by the controller, thus merging the benefits of closed-loop controllers to the knowledge and experience of clinical practitioners. This could contribute in reducing the mistrust that anesthesiologists might have with respect to control solutions that completely exclude manual interventions from the control loop. Moreover, recently, the attention in the development of closed-loop systems for anesthesia is moving toward the combined control of DoH and hemodynamic variables, as pointed out in Section 2.1.

In this chapter, the effect of the regulation of opioid/hypnotic balance is investigated in simulation. This is made possible by a recently proposed open source patient simulator that provides a realistic simulation environment to effectively perform in-silico validations of closed-loop controllers for anesthesia [49]. The features of this innovative tool have been already presented in Section 1.3.2. The availability of these tools is of fundamental importance since useful clinical insights can be obtained without any risks for patients safety. Both the time-based PID MISO control system of Section 3.1.1 and the event-based MISO control

145

system of Section 4.1.1 are considered and the results obtained are presented [110].

6.1 PID-based MISO control scheme

The regulation of opioid-hypnotic balance is fundamental in TIVA since it has a significant impact on DoH and hemodynamics. Therefore, when a fully automated control system for anesthesia is developed, this aspect must be considered. In the PID-based control scheme for propofol and remifentanil coadministration summarized in Section 2.2.2, the opioid-hypnotic balance is handled by imposing a ratio between the infusion rates of these two drugs. By changing this value, the anesthesiologist can choose the most suitable balance for each patient and for each phase of surgery. The aim of this section is to evaluate and discuss the benefits that this solution can bring in the clinical practice. In order to do so, the proposed solution has been tested in simulation by using the open source patient simulator introduced in Section 1.3.2. It implements both anesthetic and hemodynamic variables and takes into account their interaction.

In this context, propofol and remifentanil infusion rates are considered as inputs of the simulator. The dopamine, SNP and atracurium inputs of the simulator are not considered and they are set equal to zero. In the simulator, the Schnider model described in Section 1.2.2 is used for propofol and the Minto model described in Section 1.2.2 is used for remifentanil. Their combined effect on BIS is modeled with the model described in Section 1.2.2. The tuning dataset shown in Table 2.2 has been considered to perform the simulations. The simulator also includes the possibility to simulate disturbances on the BIS caused by surgical stimulation. Here, the double step disturbance profile, shown in Figure 1.6, has been considered.

The control system architecture considered here is the second one described in Section 2.2.2, with the discretized PID controller. The PID tuning considered is that shown in Table 3.1. A schematic view of the control loop, with the simulator, is shown in Figure 6.1.

The opioid-hypnotic balance can be modified by selecting a value of the ratio in the range from 0.5 to 15. By selecting a lower ratio, the BIS target is obtained with a higher propofol concentration and a lower remifentanil concentration, thus increasing the hypnotic component over the analgesic component of anesthesia. This situation is desirable in case of moderate painful stimulation or in case of concomitant use of loco-regional analgesics as this allows the reduction of the infused dose of remifentanil, thus reducing opioid-induced side-effects. On the contrary, by selecting a higher ratio, the BIS target is obtained with a lower propofol concentration and a higher remifentanil concentration, thus increasing the analgesic component over the hypnotic component of anesthesia. This configuration is indicated for surgical phases that involve strong painful stimulation but, consequently, it increases the risk of opioid-induced side-effects. The default value of ratio in the proposed control scheme has been set equal to 2, as explained in Section 3.1.1. The simulation has been performed by setting a target BIS value of 50. The baseline values before drug administration for MAP and CO have been set to 90 mmHg and 5 l/min respectively. The simulation results for anesthesia induction performed on the tuning dataset are shown in Figure 6.2 where the opioid-hypnotic ratio is set equal to 2. The PID controller rapidly drives the BIS to the target value of 50 without causing undershoot below the value of 40 for all thirteen patients of the tuning dataset. As regards the hemodynamic variables, the CO remains inside the recommended bounds for all the patients while the MAP drops below the lower bound of 65 mmHg in two out of thirteen patients, namely patients 8 and 10. The RASS varies between -4 in patient 1 and -6 in patient

8, thus indicating a slight underdosing and overdosing of analgesic respectively. Although potentially problematic MAP and RASS situations only occur in 2 out of 13 patients, they must be appropriately managed by the control system. The proposed control solution manages this issue by means of the ratio value. In Figure 6.3a the setpoint response for patient 1 and patient 8 is shown. These two patients show different behaviors, indeed, patient 8 appears to be more sensitive to remifentanil since it shows a RASS value below the target and shows hypotension. Conversely, patient 1 appears to be less sensitive to remifentanil since it shows a RASS value above the target and a reduce lowering of MAP with respect to baseline. Hence, it is appropriate to decrease the ratio for patient 8 and increase it for patient 1 in order to reach the same BIS target with less or more remifentanil, respectively. Figure 6.3b shows the setpoint response for patient 1 and patient 8 obtained by setting the ratio to 2.5 and 1.3, respectively. By doing so, both patients reach the RASS target without showing hypotensive episodes.

The ratio can also be changed by the anesthesiologist during the course of anesthesia according to the observed response. In order to better clarify this aspect, a simulation that comprises the setpoint response and the disturbance rejection response for patient 8 has been performed and the results are shown in Figure 6.4. In this example, anesthesia is induced with a ratio equal to 2. Then, at time 200 s the anesthesiologist observes that MAP is below the recommended value of 65 mmHg and RASS is below the target value of -5. Hence, he/she decides to lower the ratio from 2 to 0.8 in order to reduce the opioid-induced side-effects on MAP. At time 300 s the BIS settles at the setpoint value. Thus, the anesthesiologist decides to perform the gain-scheduling. By doing so the tuning parameters for disturbance rejection are selected. At time 400 s there is a disturbance on the BIS due to surgical stimulation that is compensated by the controller. At time 500 s the anesthesiologist decides to increase the ratio from 0.8 to 1.5 in order to keep a suitable analgesic coverage. The black dashed line represents the response that would have been obtained without changing the ratio from 2 to 0.8 at time 200 s. Notice that this would have caused hypotension and an excessively low RASS value. The black dash-dotted line represents the response that would have been obtained without changing the ratio from 0.8 to 1.5 at time 500 s, which would have caused a rise of the RASS above the target value. It is worth noting that the changes in the ratio value do not affect the BIS value.

In conclusion, the introduction of the open source patient simulator presented in [49] allows the performance of control systems to be analyzed also with respect to these important aspects. The simulation performed on all the thirteen patients of the tuning dataset, with the recommended opioid-hypnotic ratio of 2, shows that the system achieves the target BIS without violating the lower bound of MAP in eleven out of thirteen patients. In the two remaining patients the MAP falls slightly below the lower bound of 65 mmHg, thus indicating a generally good behavior with respect to hemodynamics. The RASS is slightly above the desired target in only one out of thirteen patients, thus indicating a good analgesic coverage. These results have also been confirmed experimentally in Section 3.1, where none of the ten patients enrolled show clinical signs of inadequate analgesia or hemodynamic instability. However, in the simulation performed on the considered tuning dataset, two patients, namely patient 1 and patient 8, show opposite behaviors in response to remifentanil administration. The simulations performed on these two patients by changing the ratio value have shown the importance of a control system that offers the possibility to modify this parameter to adapt to the characteristics of each patient. The simulation performed on patient 8 for both anesthesia induction and disturbance rejection has also shown the usefulness of giving to the
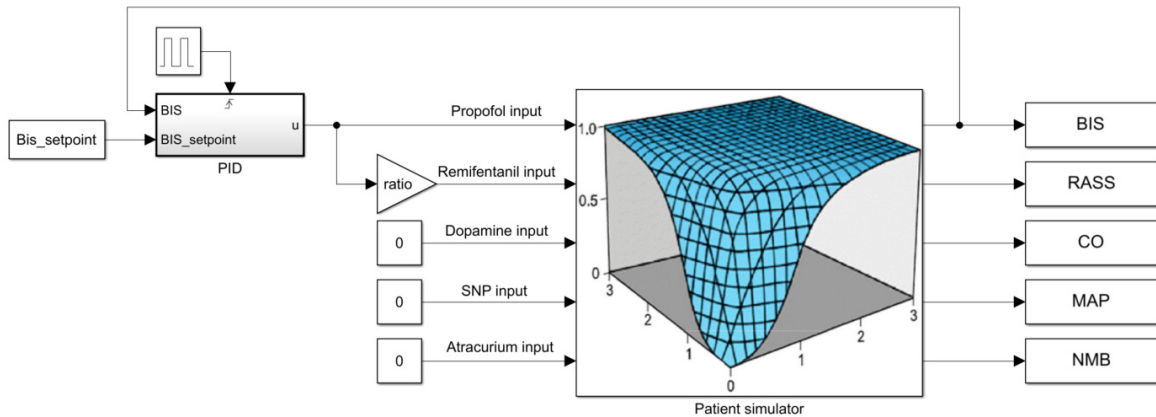
Figure 6.1: *Schematic representation of the PID-based MISO control loop employed to evaluate the influence of the opioid-hypnotic balance. This figure has been adapted from [49].*

anesthesiologist the possibility to regulate the ratio during anesthesia depending on the different situations that may occur.

Despite the good results obtained in simulation, it is important to underline that the situations considered can be simplistic compared to those that can occur in clinical practice. Indeed, there are other aspects to consider for the regulation of the opioid-hypnotic balance, such as the phase of anesthesia, the type of surgical procedure and the physiological response to stimulation. There may also be situations in which the patient shows hemodynamic instability even in the presence of reduced doses of drugs or for particular surgical procedures that affect the cardiovascular system. In these cases the use of drugs active on hemodynamics, such as vasopressors, is essential. In this sense the possibility to select the opioid-hypnotic ratio can help the anesthesiologist to manage patient's hemodynamics but it might not be sufficient to ensure hemodynamic stability. In this simulation, analgesia is represented by the RASS since other more specific measurements are not available yet. Moreover, the blunting effect of remifentanil on surgical stimulation affecting the DoH is not considered since the disturbance profile employed acts on the BIS with the same magnitude regardless of the remifentanil concentration. Since the simulator is open source, the modeling of these effects can be implemented in a future version when more sophisticated models will become available.

6.2   Event-based MISO control scheme

In this section, the event-based control scheme for propofol and remifentanil coadministration presented in Section 2.2.2 is evaluated on the open source patient simulator. In particular, the same test configuration proposed in Section 6.1 for the PID-based controller is proposed here for the event-based controller. Indeed, also the control architecture here considered has MISO structure where the opioid-hypnotic balance can be adjusted by means of the ratio value. Since the event-based control architecture has been specifically designed to deal with the presence of noise on the BIS signal, the real noise signal profile shown in Figure 1.9 has been added to the simulator to make the simulation more realistic and to better evaluate the filtering effect of the event-based controller.

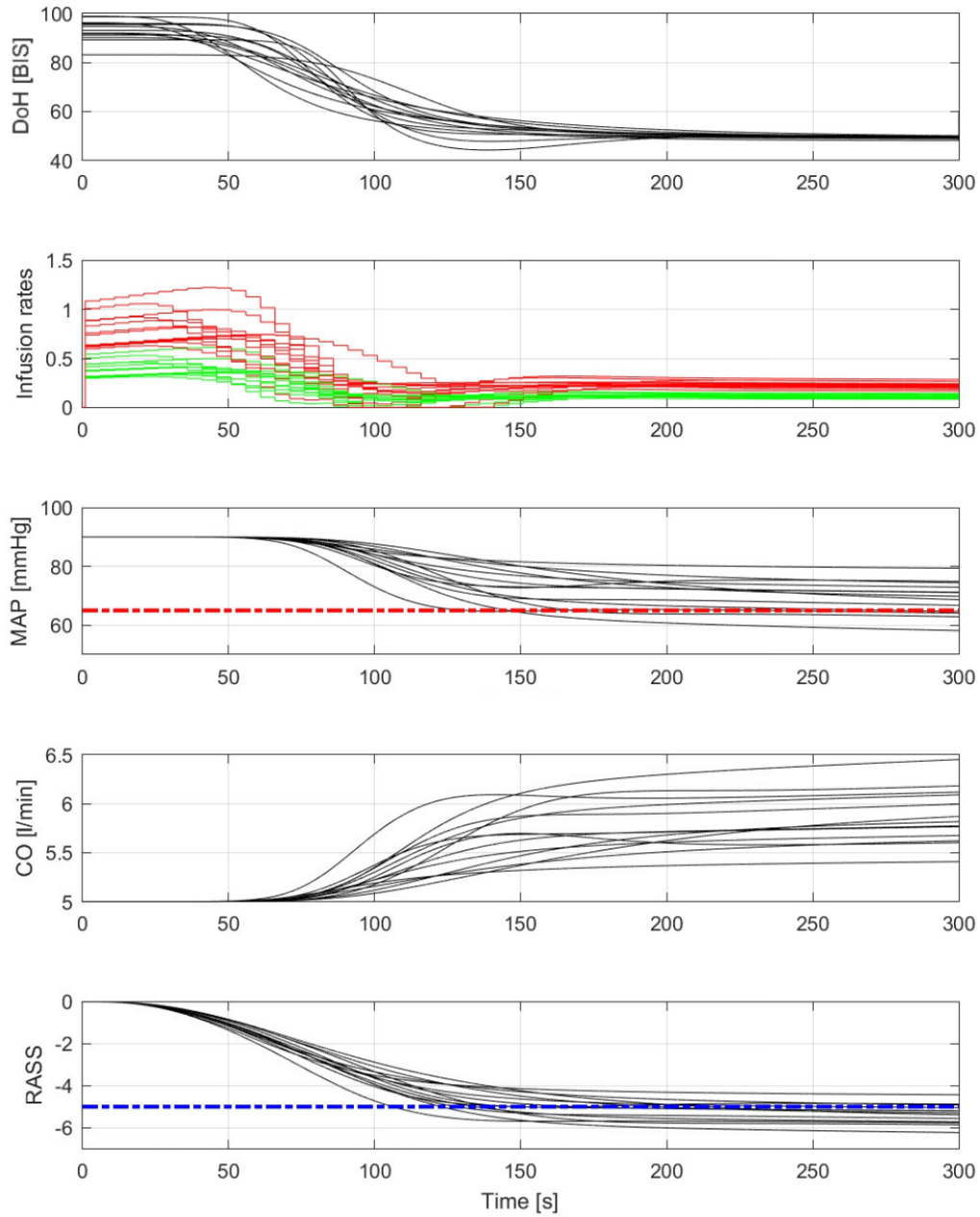**Figure 6.2:** *Induction phase responses obtained on the thirteen patients of the tuning dataset with the PID-based MISO controller with ratio=2. Infusion rates are expressed in mg/kg/min for propofol (green solid line) and μg/kg/min for remifentanil (red solid line). The red horizontal dash-dotted line represents the MAP lower safety bound of 65 mmHg. The blue horizontal dash-dotted line represents the RASS target of -5.*

(a) *Ratio=2*   (b) *Ratio=2.5 (patient 1), ratio=1.3 (patient 8)*

Figure 6.3: *Induction phase responses obtained on patient 1 (solid line) and patient 8 (dashed line) of the tuning dataset with the PID-based MISO controller with different values of ratio. Infusion rates are expressed in mg/kg/min for propofol (green solid line) and μg/kg/min for remifentanil (red solid line). The red horizontal dash-dotted line represents the MAP lower safety bound of 65 mmHg. The blue horizontal dash-dotted line represents the RASS target of -5.*
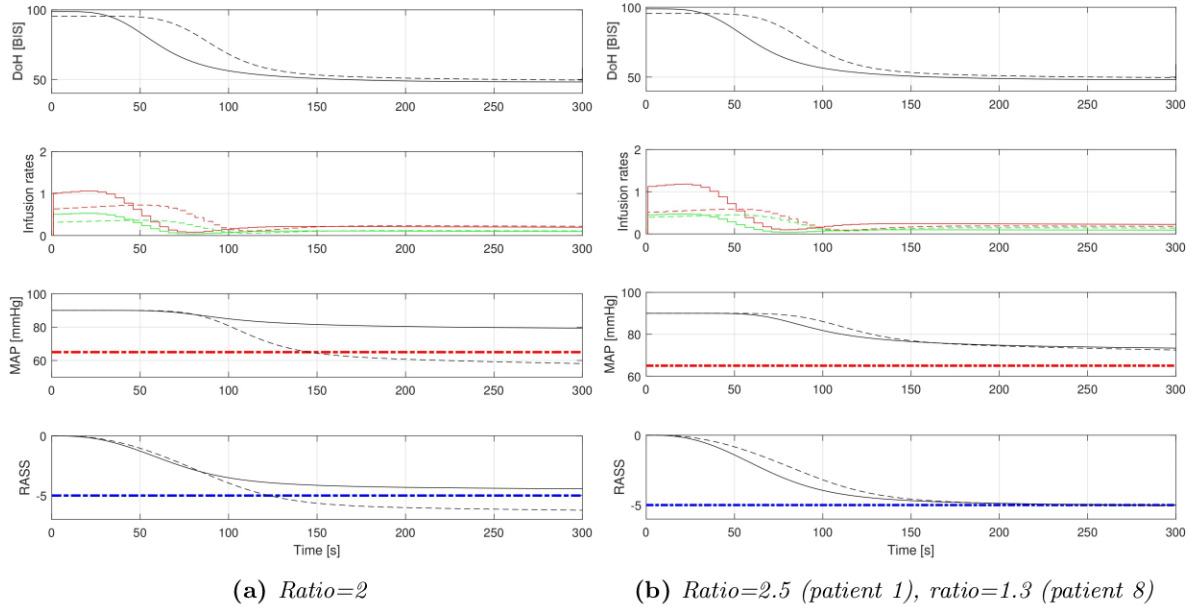
A schematic representation of the overall control architecture considered, with the simulator, is shown in Figure 6.5.

As in Section 6.1, the simulations have been performed on the tuning dataset of Table 2.2. The simulations have been performed by choosing 50 as BIS target. The simulation scenario has a duration of 42 min and it is structured as follows. At the beginning of the simulation the controller is tuned with the set of tuning parameters optimized for the induction phase. At minute 5 the induction phase is considered to be finished, thus the bumpless switching mechanism is activated to tune the controller with the set of tuning parameters optimized for the maintenance phase. Then, this tuning is kept until the end of the simulation. During the maintenance phase the double step disturbance profile shown in Figure 1.6 is applied. In particular, at minute 10 a surgical disturbance is applied to the BIS signal. In particular, the disturbance is a positive step of amplitude 10. This disturbance lasts till minute 25, where it is stopped, that is, a negative step of amplitude -10 is applied to the BIS signal.

Simulation results performed with a fixed opioid-hypnotic ratio equal to 2 are shown in Figure 6.6. The control system is able to rapidly drive the BIS to the reference value of 50 without causing relevant undershoot episodes for every considered patient. Concerning the hemodynamic variables, the CO is kept inside the recommended values in every patient. For this reason, this variable will be omitted in further considerations. In 11 out of 13 patients the MAP values drops below the safety value of 65 $mmHg$ for most of the time of the simulation. As regards the RASS, for every patient it varies between -5 and -8. This behavior indicates that the dosage of remifentanil is slightly higher than required. These potentially dangerous MAP and RASS behaviors must be handled by the control system. The proposed solution consists of manually modifying the ratio value in order to always infuse an adequate
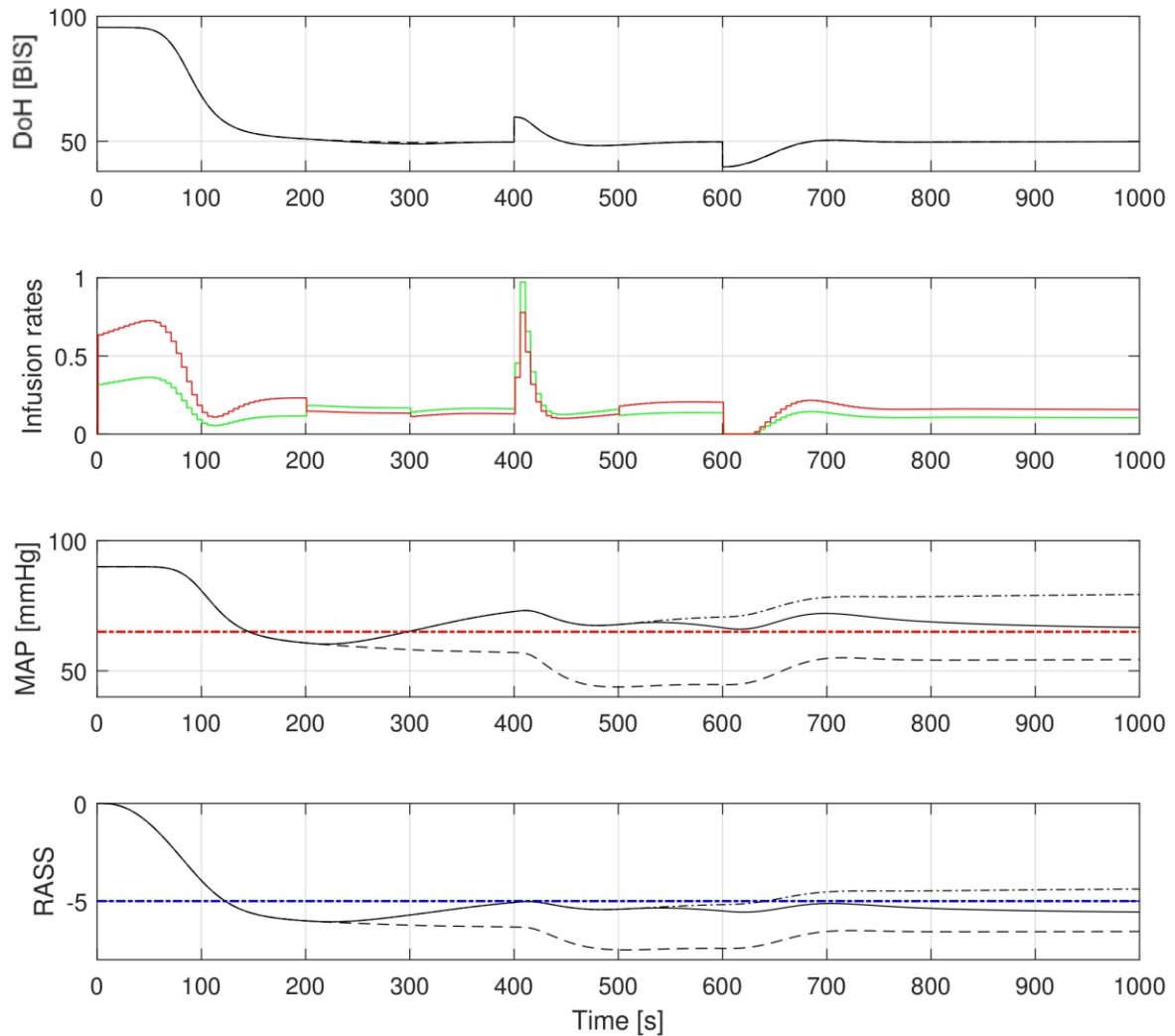
Figure 6.4: *Response obtained for patient 8 of the tuning dataset with the PID-based MISO controller. At time 200 s the ratio is switched from 2 to 0.8 and at time 500 s the ratio is switched from 0.8 to 1.5. Infusion rates are expressed in mg/kg/min for propofol (green solid line) and µg/kg/min for remifentanil (red solid line). The red horizontal dash-dotted line represents the MAP lower safety bound of 65 mmHg. The blue horizontal dash-dotted line represents the RASS target of -5. For BIS, MAP and RASS the black solid line represents the response obtained by switching the ratio, the black dashed line represents the response obtained with ratio=2 and the dash-dotted line represents the response obtained without switching the ratio from 0.8 to 1.5 at time 500 s.*

propofol-remifentanil balance.

To further analyze this strategy, patient 11 is considered as a single example. In Figure 6.7a, it is possible to see the response of this patient. Despite the BIS signal is always inside the appropriate interval from 40 to 60, the patient seems to be sensitive to remifentanil since it has the RASS and MAP values below the target. As said before, this means that the amount of administered remifentanil is too high. Thus, it is sensible to decrease the ratio in order to reduce the remifentanil effect. In Figure 6.7b, the simulation response of patient 11, obtained by switching the ratio, is presented. At the beginning, the anesthesia is induced with a ratio equal to 2. After performing the gain scheduling, at minute 7, the anesthesiologist decreases the ratio to 1.5 since the RASS trend is decreasing. In fact, the presence of a surgical disturbance applied to the BIS signal tends to decrease the MAP and RASS, so that the anesthesiologist decides to change the ratio to 0.9 in order to maintain an adequate level of sedation. This value is maintained until minute 27, where an increment of the hemodynamic variables can be noticed since the disturbance expired some minutes before. Accordingly, the anesthesiologist performs a last ratio change to 1.8, to keep the variables at their recommended values. Note that, every time the ratio is changed, the PIDplus proportional gain changes accordingly to the tuning rule of Table 2.7. Looking at the infusion rates of Figure 6.7a and 6.7b, it is possible to notice the effect of the ratio switching. In particular, in the third zone, the gap between the green and red solid lines is much reduced. In conclusion, it is sensible to underline that, despite the ratio changing, the BIS signal of the two cases is about the same. For the sake of completeness, in Figure 6.8, the simulation results obtained for every patient by switching the ratio are presented. Moreover, in Table 6.1, it is possible to see, for all patients, at which time the ratio has been changed and its new value. It is worth stressing that every anesthetic and hemodynamic variable is inside its recommended value.

From the simulation performed for each of the 13 patients, with a fixed opioid-hypnotic ratio equal to 2, the control system meets the requirements concerning the BIS signal. On the other hand, in the majority of the cases, the MAP and RASS fall below the desired thresholds resulting in hypotension and excessive infusion of remifentanil. However, the simulations carried out on the same patients, by modifying the ratio value, have shown encouraging results since both MAP and RASS achieve their recommended values. Moreover, the option to change the opioid-hypnotic balance according to the state of each patient is the added value of the described control solution and could bring further advantages to the anesthesia practice. It is important to underline that the simulations performed are simple compared to the situations that can occur during a surgical procedure. In fact, there are other aspects that should be considered for the regulation of the propofol-remifentanil balance. Concerning the filtering action of the event-based controller, in Figure 6.9 it is possible to see how the event generator filters the noise reducing the control effort. This allows the excitement of the actuators to be reduced so that they do not follow detrimental variations of the BIS signal due to the presence of noise. Moreover, it can be recalled that there are not significant differences between an event-based controller and a standard PID controller in terms of BIS performance since the two signals present a very similar trend [99].

6.3   Conclusions

In this chapter the influence of opioid-hypnotic balance has been tested through simulations using an in-silico approach thanks to a recently devised open source patient simulator
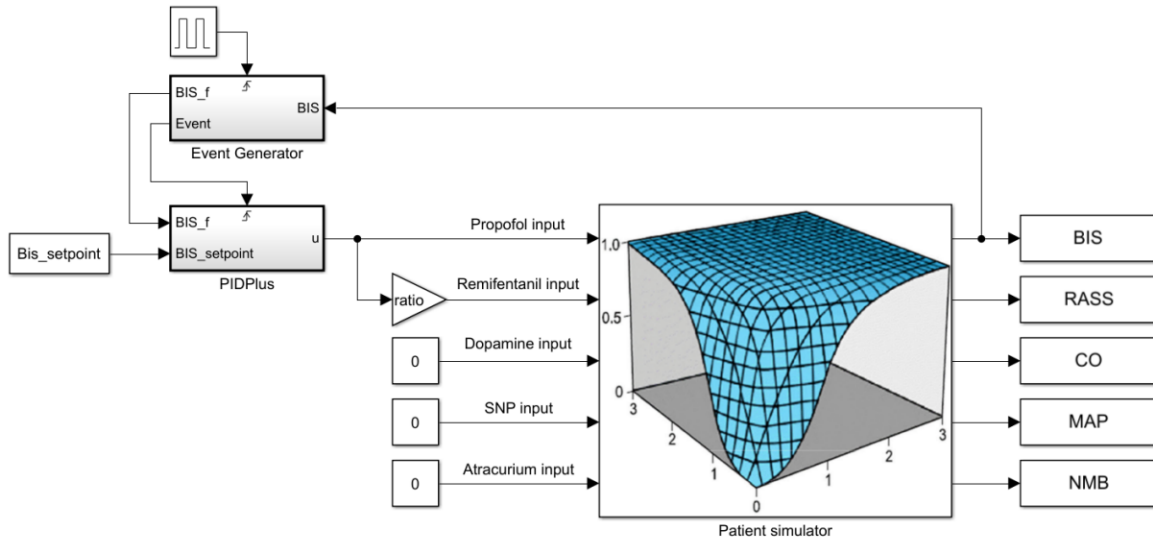
Figure 6.5: *Schematic representation of the event-based PID MISO control loop employed to evaluate the influence of the opioid-hypnotic balance. This figure has been adapted from [49].*

	1st Change		2nd Change		3rd Change		4th Change	
Id	Time [min]	Value	Time [min]	Value	Time [min]	Value	Time [min]	Value
1	10	1.6	25	3	-	-	-	-
2	2	1	5	1.5	10	1	25	2
3	4	1.6	10.5	1.2	25	2	-	-
4	2.5	1.3	11	1	17	1.5	-	-
5	10	1.2	25	2.5	-	-	-	-
6	6	1.5	10	1.2	25	2.2	-	-
7	6	1.5	10	1	25	2	-	-
8	2.5	1	11	0.8	25	1.3	-	-
9	10	1.4	25	2.2	-	-	-	-
10	2.5	1.2	11	1	25	1.6	-	-
11	7	1.5	10	0.9	27.5	1.8	-	-
12	10	1.1	25	2.5	-	-	-	-
13	2.5	1.2	11	1	25	1.6	-	-

Table 6.1: *Timeline of the ratio changes performed on the thirteen patients of the tuning dataset with the event-based PID MISO controller. The simulation started with a baseline value of ratio=2 for all patients. Note that blank cells denote that no further changes have been done.*

Figure 6.6: *Responses obtained on the thirteen patients of the tuning dataset with the event-based PID MISO controller with ratio=2. Green solid line: propofol infusion rate expressed in mg/kg/min. Red solid line: remifentanil infusion rate expressed in µg/kg/min. Magenta dashed line: BIS target. Red dashed lines: MAP safety limits. Cyan dashed lines: CO safety limits. Blue dashed line: RASS target.*
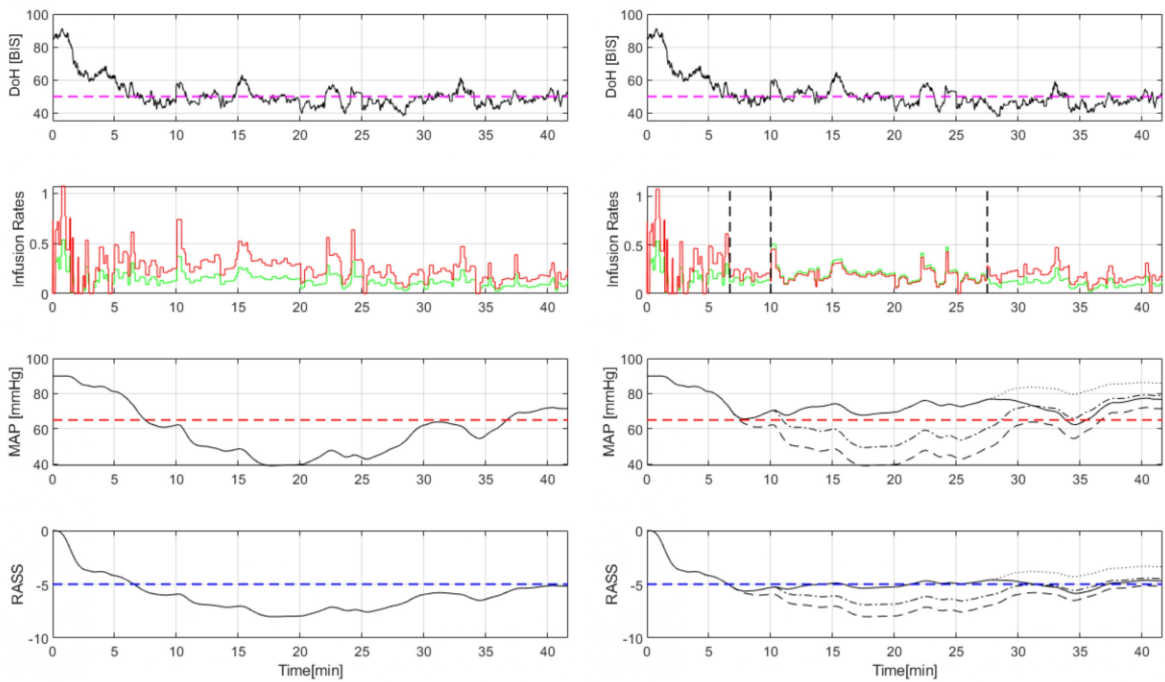
(a) *Fixed ratio.* **(b)** *Variable ratio.*

Figure 6.7: *Responses obtained for patient 11 of the tuning dataset with the event-based PID MISO controller. Green solid line: propofol infusion rate expressed in mg/kg/min. Red solid line: remifentanil infusion rate expressed in μg/kg/min. Magenta dashed line: BIS target. Red dashed line: MAP safety limit. Blue dashed line: RASS target. In the left plot a constant ratio equal to 2 is used. In the right plot black vertical dashed lines indicates the time instants when ratio changing occurs. For MAP and RASS the black solid line represents the response obtained by switching the ratio. Black dashed line: ratio = 2. Black dash-dotted line: ratio = 1.5. Black dotted line: ratio = 0.9.*
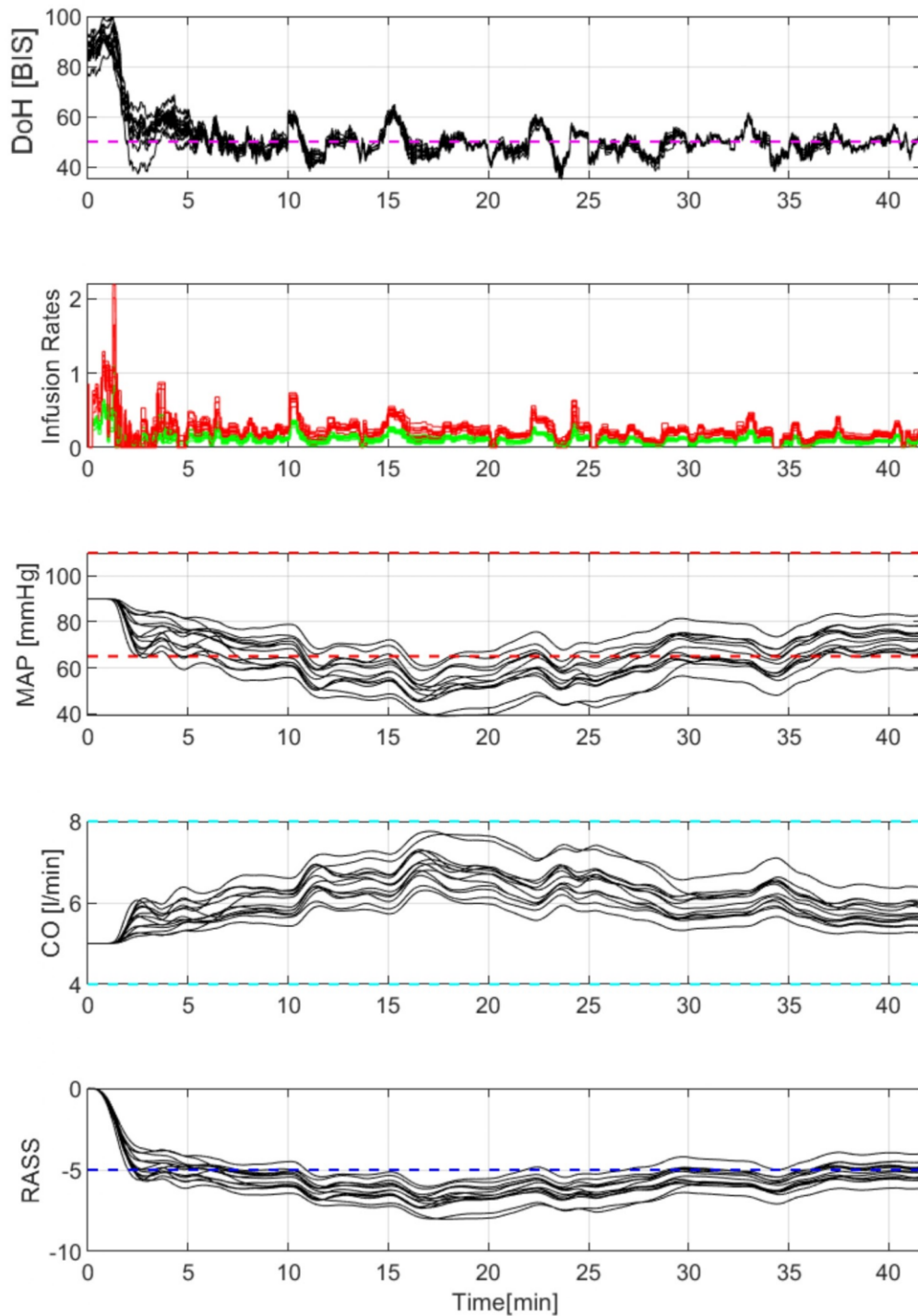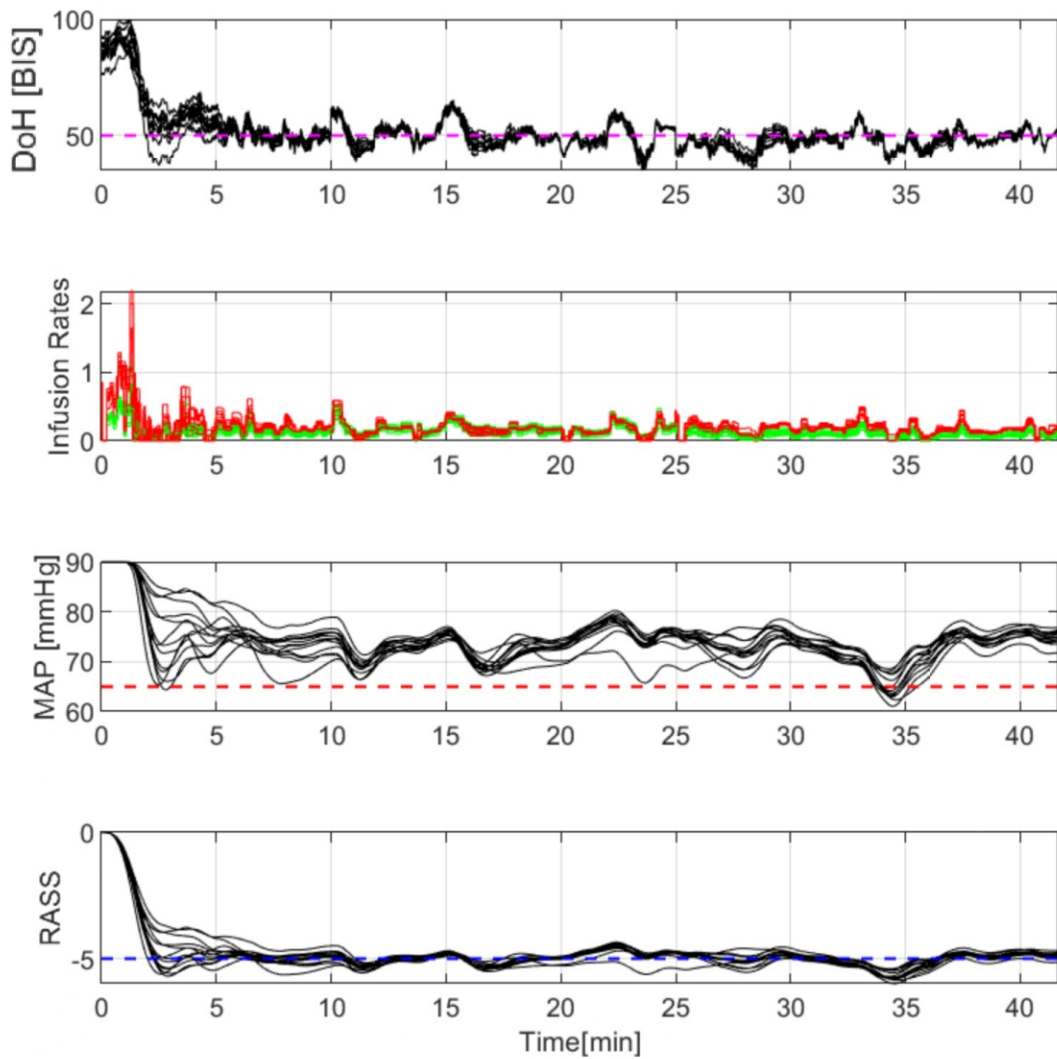
Figure 6.8: *Responses obtained on the thirteen patients of the tuning dataset with the event-based PID MISO controller by changing the ratio during the surgical procedure. Green solid line: propofol infusion rate expressed in mg/kg/min. Red solid line: remifentanil infusion rate expressed in μg/kg/min. Magenta dashed line: BIS target. Red dashed line: MAP safety limit. Blue dashed line: RASS target.*
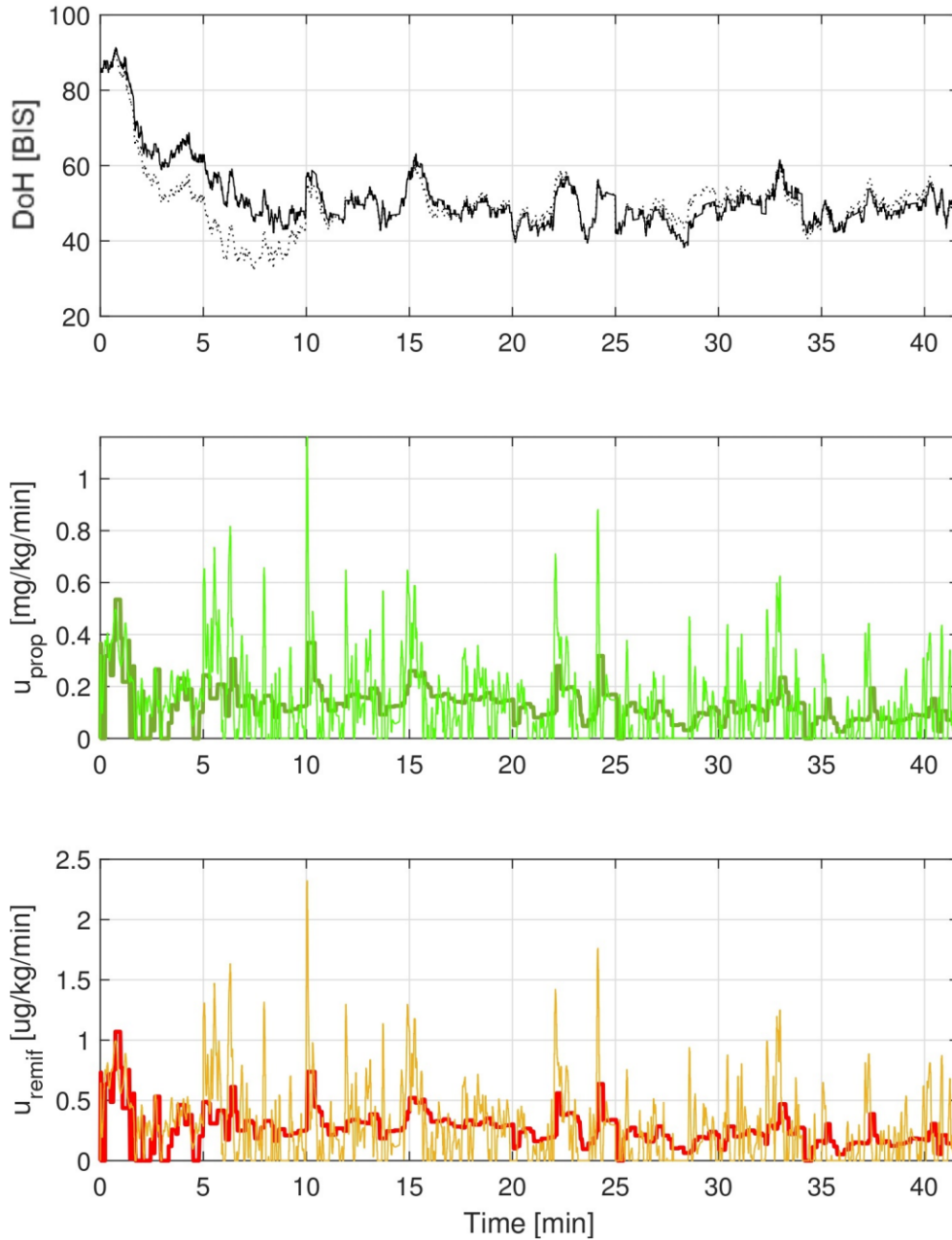
Figure 6.9: *Responses obtained for patient 11 of the tuning dataset with ratio changing. The solid black line represents the BIS trend obtained with the event-based PID MISO controller. The dotted black line represents the BIS obtained with the standard time-based PID MISO controller. Infusion rates represented with a dark green and red solid lines result from the event-based PID MISO controller, whereas, the green and orange solid lines represent the infusion rates that result from the standard time-based PID MISO controller.*

that implements the interactions between anesthetic drugs, hemodynamics and analgesic coverage.

The PID-based MISO control scheme for propofol and remifentanil coadministration has been first considered. In the proposed solution, the opioid-hypnotic balance can be manually adjusted by the anesthesiologist during the time course of anesthesia. Simulation results have shown the importance of this parameter that allows the anesthesiologist to select the most appropriate opioid-hypnotic ratio depending on the patient and on the specific phase of anesthesia. Hence, the possibility to select the ratio can help the anesthesiologist to better manage the combination of patient's DoH, analgesia and hemodynamics.

The event-based MISO control scheme for propofol and remifentanil coadministration has been then assessed. The event-based controller confirms its satisfactory behavior in both controlling anesthesia and filtering the noise that affects the BIS signal. In the proposed solution, during the surgical procedure, the propofol-remifentanil balance can be manually regulated by the anesthesiologist in order to deal with the patients characteristics and their response to drugs infusion. Therefore, the option to modify the opioid-hypnotic ratio can help the anesthesiologist to suitably handle DoH, analgesia and hemodynamics at the same time, resulting in a reduction of intra-operative and post-operative side effects.

Giving the anesthesiologist the opportunity to adjust the opioid/hypnotic balance in an easy and intuitive way can be a great step forward for the introduction of these systems in the routine clinical practice. The satisfactory results obtained in this in-silico study suggest that this approach is ready to be safely tested in-vivo.

Chapter 7

Individualized PID tuning for anesthesia maintenance

As already pointed out is Chapter 1, one of the main challenges in the design of closed-loop system for automatic anesthesia regulation is represented by the great amount of variability in the clinical response to drug administration. This limits the benefits of using complex control architectures. For this reason many control solutions based on simple PID controllers have been proposed. Indeed, reducing the effect of variability is critical and provides a suitable alternative to the implementation of more complex control solutions, as highlighted in [147]. To this end, robust PID control strategies have been proposed, and their feasibility has been demonstrated [85, 92, 148, 149]. All the solutions summarized in Section 2.2 are based on this approach. Hence, to deal with variability, the PID controllers have been tuned with a population-based optimization technique. They employ a set of tuning parameters that is suitable for every patient. Another approach consists in providing personalized controllers. This method relies on the use of controllers that are specifically tuned for each patient, or for groups of them who exhibit similar characteristics in response to drug administration. The methodology proposed in this chapter is based on this latter approach. Indeed, a novel optimization-based PID tuning methodology that exploits the covariates of linear PK models, i.e., the demographic data of the patient, to obtain a patient-individualized tuning is presented. The proposed approach provides an optimal set of tuning parameters for each combination of covariates, thus providing an individualization of the controller dynamics based on the demographic data of the patient. The advantages of this approach in reducing the detrimental effects of inter-patient and intra-patient variability are analyzed. In particular, it is interesting to understand whether a tuning of the PID controller that takes into account the covariates of the PK model can provide some advantage despite the presence of the non-linear PD. To this end, the results obtained in simulation with the new individualized tuning are compared with those obtained by using an optimized population-based tuning [111, 112]. It is worth noting that the methodology proposed in this chapter has been considered only for the maintenance phase of anesthesia. This choice has been made because the induction phase of anesthesia is highly influenced by the presence of the Hill function, that introduces a strong nonlinear behavior for BIS values lower than 40 or greater than 60, while, in the range from 40 to 60, the Hill function behaves approximately like a constant gain. Hence, during the maintenance phase when the BIS remains mostly inside the range from 40 to 60, the dynamic behavior of the patient is less affected by the nonlinearity, and the proposed

individualized tuning could provide more benefits. On the contrary, to provide individualized control solutions for the induction phase of anesthesia nonlinear control methodologies are proposed in Chapter 8.

7.1   Individualized PID tuning for propofol administration

In this section, the SISO control architecture for propofol administration with the BIS as feedback variable, shown in Figure 2.2, is considered. The proposed tuning methodology exploits the covariates of the Schnider PK model for propofol shown in Table 1.1, i.e., the demographic data of the patient, to obtain a patient-individualized tuning of the PID controller, that is in form 2.7. A conditional integration anti-windup strategy has also been implemented.

7.1.1   Controller tuning

The proposed tuning methodology adjust the PID parameters according to the patient's demographic data. In other words, their knowledge provides information about the system's dynamics that can be explicitly exploited in the tuning of the controller. The optimization-based individualized tuning approach derives from that described in Section 2.2.1, but here the optimization problem (5.7) is considered. Hence, it is a minimization problem of the IAE for a specific patient. Once the patient's age, weight, height and gender are known, the PK/PD linear model is constructed by using the Schnider model, shown in Table 1.1, and the model of Vanluchene, shown in Table 1.3, is used for the Hill function. The obtained model is then used to simulating the response to the double-step disturbance profile shown in Figure 1.6, thus obtaining the IAE. The optimization problem 5.7 is then solved by means of a PSO algorithm, eventually obtaining the set of optimal PID parameters that minimizes the IAE for that specific combination of age, weight, height and gender. The PSO algorithm is set with a swarm size of 100 particles and the optimization is stopped when the relative change in the best IAE value over the last 50 iterations is less than 0.001.

To verify how the PID parameters change according to patient demographics, a sample population has been generated, and for each individual, the optimal PID parameters have been calculated with the proposed methodology. For each gender, an individual of the population is characterized by the quadruple (A, H, W, G), where A stands for age, H for height W for weight and G for gender, and the entire population is the set $\{(A, H, W, G) \,|\, A = 20 + 10i; H = 150 + 5j; W = 50 + 5k; i, j, k \in \mathbb{N}_0; i \leq 7; j, k \leq 8; G \in \{F, M\}\}$ where F and M stand for female and male, respectively. The population covariates cover the following ranges, $age \in [20, 90]$ in steps of 10 years, $height \in [150, 190]$ cm in steps of 5 cm and $weight \in [50, 90]$ kg in steps of 5 kg, and for each combination of the above, there are both a female and a male individual. The optimal PID parameters obtained for each individual of the sample population are shown in Figure 7.1 where it is possible to observe that the optimal tuning parameters change significantly across the considered domain. To quantify the amount of change, the coefficient of variation (CV) is calculated for each parameter. For the given population/sample, CV is defined as:

$$CV = \frac{\sigma}{|\mu|} \cdot 100 [\%], \tag{7.1}$$
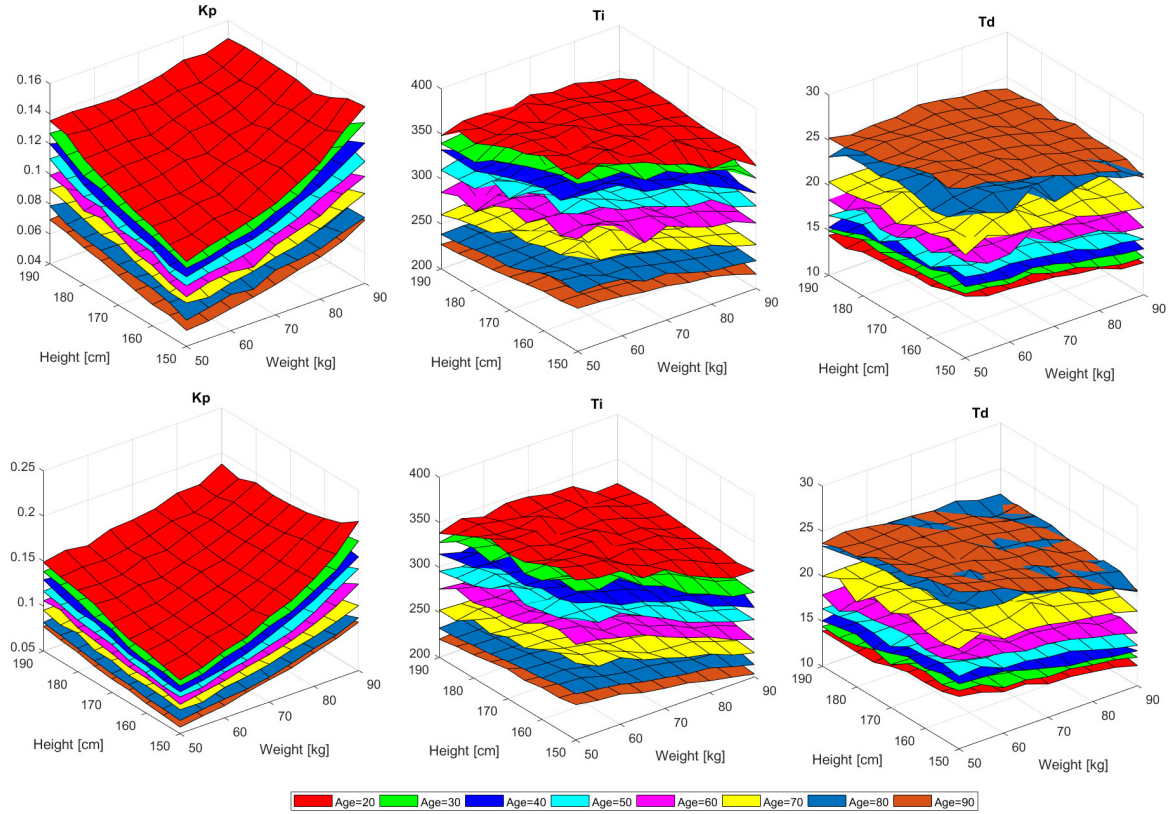
Figure 7.1: *Trends of the individualized PID parameters obtained for the sample population. The parameters for males are shown in the top row while the parameters for females are shown in the bottom row.*

where σ is the standard deviation and μ is the average. For males it results $CV_{K_p} = 22.40\%$, $CV_{T_i} = 15.44\%$ and $CV_{T_d} = 20.86\%$, while for females it results $CV_{K_p} = 25.28\%$, $CV_{T_i} = 15.28\%$ and $CV_{T_d} = 20.02\%$. The CVs are similar for both genders and the tuning parameter that shows the largest variability is the proportional gain K_p. Further, note that all the parameters show a monotonic behavior with respect to age (with the exception of T_d which shows a slight overlap for 80 and 90 years old individuals), see Figure 7.1. In particular, K_p and T_i decrease as age increases, while T_d increases as age increases. Note that K_p also shows a clear increasing trend with respect to height and weight. Finally, T_i and T_d show less noticeable trends with respect to weight and height, and they decrease slightly as the weight increases and remain almost unchanged as the height varies. The same considerations apply to both males and females.

7.1.2   Simulation results

In this section the results obtained by testing the individualized tuning in simulation are reported. These results are compared with those obtained by employing the population-based PID tuning methodology proposed in Section 2.2.1 in order to understand the improvements that an individualized tuning brings with respect to a population-based approach. The tuning procedure proposed in Section 2.2.1 has been applied to the control structure here considered

and the following population-based tuning parameters have been obtained: $K_p = 0.2$ mg/s, $T_i = 386$ s, $T_d = 14$ s. The simulation has been performed by simulating the maintenance phase of anesthesia in order to obtain a tuning suitable to reject disturbances, and therefore a fair comparison. The reference signal $r(t)$ is initially set equal to 50, the input and the states of the system are initialized as the equilibrium input and the corresponding equilibrium states such that $BIS(t) = 50$. Further, the integrator of the PID controller is preloaded to a value such that the control action in absence of tracking error equals the above-mentioned equilibrium input. Then, the double-step disturbance profile shown in Figure 1.6 is applied. Initially, the controllers have been tested on the tuning dataset shown in Table 2.1. Note that the population-based PID tuning considered for the sake of comparison has been obtained by minimizing the worst-case scenario over the above-mentioned dataset, while the individualized tuning is obtained by considering the values of the parameters of the Hill function described by the model of Vanluchene. The responses obtained in simulation with both tuning methods are shown in Figure 7.2. To better highlight the differences in the responses to the positive step disturbance obtained with the two different tunings, a comparison between the mean, minimum and maximum values of performance indices TTp and BIS-NADIRp is shown in Figure 7.5a. Note that the TTp obtained with the individualized tuning is slightly longer than the one obtained with the population-based tuning. In particular, the individualized tuning shows a mean TTp of 17.8 s while the population based tuning shows a mean TTp of 14.1 s. Nevertheless, the TTp obtained with the individualized tuning remains clinically acceptable as the maximum value is 23.3 s. Furthermore, the higher TTp values obtained with the individualized tuning are counterbalanced by a reduction in the BIS-NADIRp. In particular, the population-based tuning shows a mean BIS-NADIRp value of 47.5 against the 48.9 obtained with the individualized tuning. This difference is even more evident if the minimum values are considered. Indeed, with the individualized tuning, a minimum BIS of 48.3 is reached against the minimum BIS of 45.8 obtained with the population-based tuning. The individualized tuning also shows a reduction in the variability of the BIS-NADIRp. Indeed, with the population-based tuning, a range of 3.0 is obtained among the 13 patients against a range of 1.0 obtained with the individualized tuning.

The behavior of the two different tuning approaches has been tested with respect to intra-patient variability. To this end, the method described in Section 2.2.1 has been applied with the statistical properties of the PK model given in [25], and for each of the perturbed models the response to disturbance has been simulated. It is worth stressing that the individualized tuning procedure is still performed on the nominal model, hence the tuning parameters are the same for each one of the 500 perturbed models generated for each patient of the tuning dataset. As an illustrative example, the responses obtained for the 500 perturbed models related to the thirteenth patient of the tuning dataset are shown in Figure 7.3. The mean value, minimum value, maximum value and range for each one of the thirteen patients of the tuning dataset are shown in Figure 7.5c. Even in the presence of intra-patient variability, the results obtained with the perturbed population shows similarity with those achieved on the nominal tuning dataset. In particular, the individualized tuning achieves higher values of the BIS-NADIRp, thus reducing the undershoot, at the cost of an increased value of the TTp with respect to the population-based tuning. As regards TTn and BIS-NADIRn, the same considerations made for the tuning dataset remain valid also for this more general case. Note that the individualized tuning achieves a reduction in the variability of BIS-NADIRp.

The behavior of the two different tuning approaches with respect to inter-patient variability has finally been assessed by applying the method described in Section 2.2.1. The parameters

Figure 7.2: *Maintenance phase responses obtained with the PID controller for propofol admin- istration on the thirteen patients of the tuning dataset. Black solid line: population-based tuning. Green solid line: individualized tuning.*

of the Hill function have been generated by considering the statistical properties given in [28]. The individualized tuning has been performed for each one of the 500 generated patients by considering the nominal parameters of the Hill function shown in Table 1.3. The responses obtained are shown in Figure 7.4. Even for a wider random population the same considerations made on the tuning dataset still apply. In particular, with the individualized tuning, an increase of the BIS-NADIRp index is obtained simultaneously reducing its variability, at the cost of an increased TTp index. Also in this case the TTn and BIS-NADIRn indices do not show significant differences between the two different tunings. The TTp and BIS-NADIRp indices obtained with both tuning methods are also shown in Figure 7.5b in order to facilitate the comparison. In particular, the minimum value of the BIS-NADIRp obtained with the population based tuning is 39.2 while a value of 45.6 is achieved with the individualized tuning. Conversely, the maximum value of the TTp index goes from 17.8 s with the population-based tuning to 28.9 s with the individualized tuning. However, with both tunings, the responses obtained meet the control specifications and are acceptable in clinical practice, even in the presence of inter-patient variability.

7.1.3   Discussion

The proposed individualized tuning provided a satisfactory control performance on the considered benchmark dataset. The individualized-tuning performed well in both the cases of intra-patient variability and inter-patient variability, always guaranteeing the fulfillment of the control specifications. In order to better understand the advantages and disadvantages that an individualized tuning can provide, the results obtained have been compared with those obtained with a population-based tuning. This comparison showed that the individu-
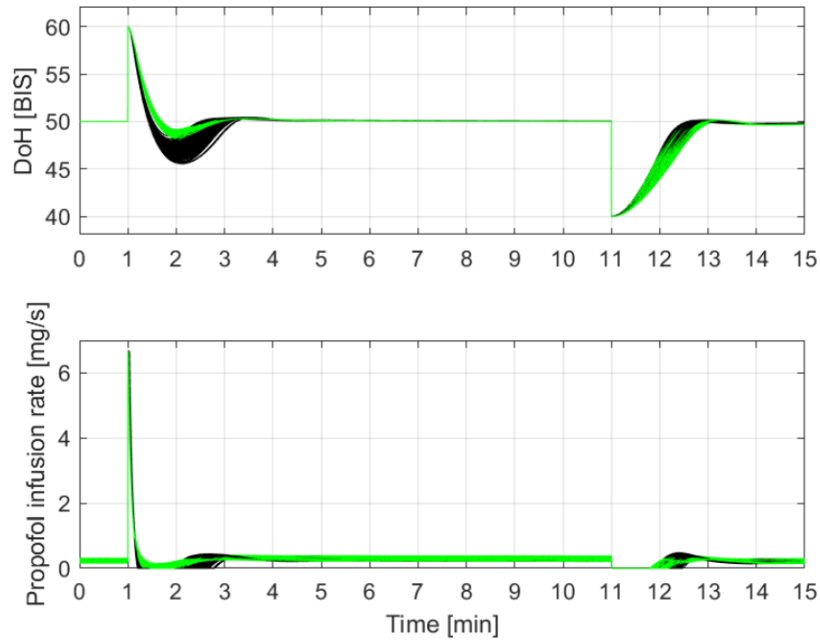
Figure 7.3: *Maintenance phase responses obtained with the PID controller for propofol administration on the 500 perturbed models generated starting from the nominal model of the thirteenth patient of the tuning dataset. Black solid line: population-based tuning. Green solid line: individualized tuning.*
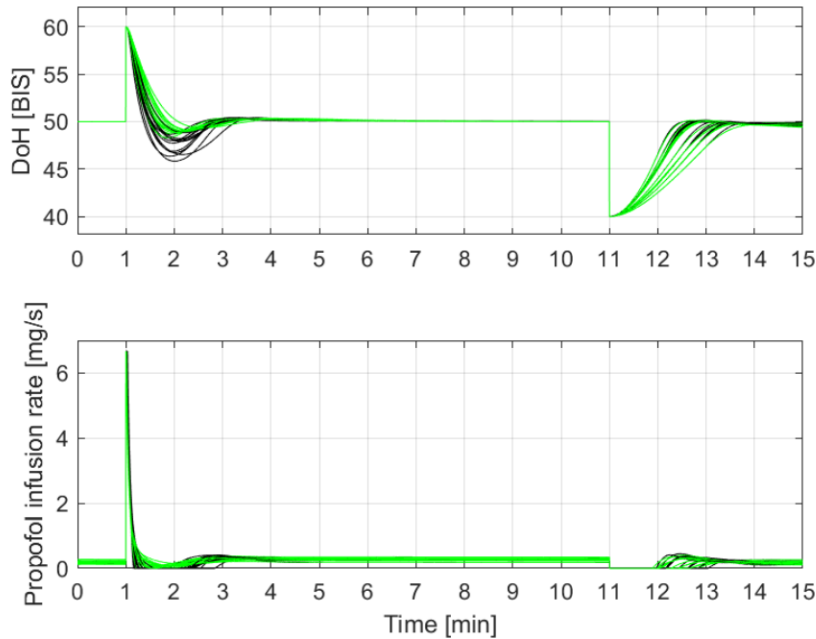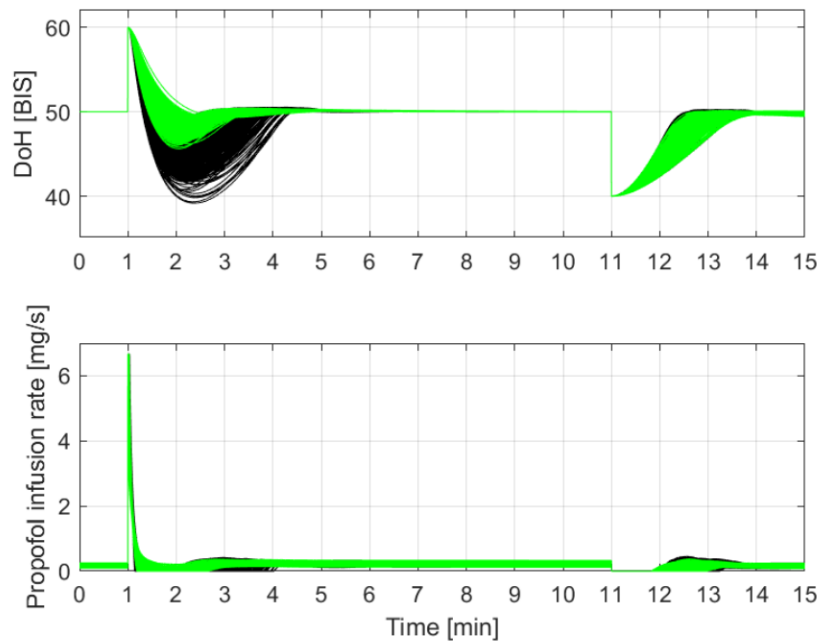

Figure 7.4: *Maintenance phase responses obtained with the PID controller for propofol administration on the population of 500 patients used in order to simulate inter-patient variability. Black solid line: population-based tuning. Green solid line: individualized tuning.*

(a) *Tuning dataset*

(b) *Inter-patient variability*
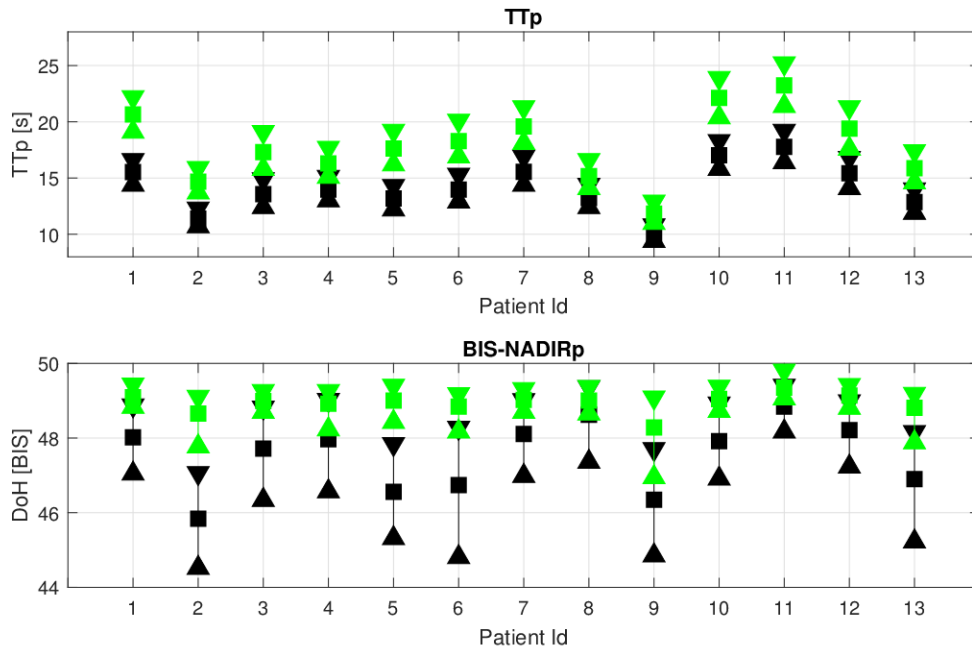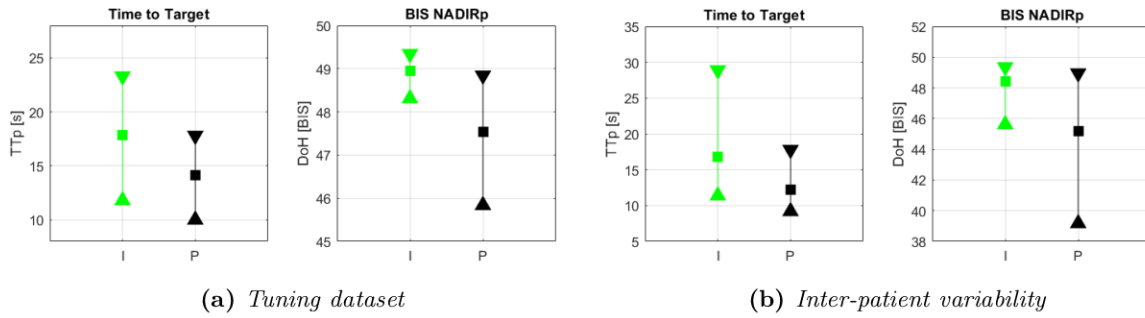
(c) *Intra-patient variability*

Figure 7.5: *Comparison of mean, minimum and maximum values of maintenance phase performance indexes obtained with the PID controller for propofol administration.* ■ *: mean value,* ▲ *: minimum value,* ▼ *: maximum value. Individualized tuning (I: green line), population-based tuning (P: black line).*

alized tuning can effectively reduce the undershoot resulting from the rejection of a positive step disturbance, by reducing also its variability. This is consistently observed in all the tests carried out, and it is particularly evident especially in the case of inter-patient variability. Indeed, the minimum value of BIS-NADIRp reached with the population-based tuning is equal to 39.2, hence slightly below the lower BIS bound imposed by the control specification, while with the individualized tuning this value is equal to 45.6, hence well above the lower limit. Also the variability of BIS-NADIRp is significantly reduced, with the amplitude of the range of observed values dropping from 9.8 with the population based tuning to 3.7 with the individualized tuning. The reduction of the effect of variability achieved with the individualized tuning gives greater robustness with respect to BIS undershoot. However, this increase in robustness is paid for with a reduction in the controller bandwidth, which translates in an increase of the TTp index. As for the reduction of the undershoot, this is consistently observed in all tests, and it is especially evident in the case of inter-patient variability, with the maximum observed TTp values increasing from 17.8 s with the population-based tuning to 28.9 s with the individualized tuning. Also the variability in the TTp index increases with the individualized tuning, and the amplitude of the range of observed values increases from 8.6 s with the population-based tuning to 17.5 s with the individualized tuning. Hence, the population-based tuning is less sensitive to the effect of variability with respect to the time to target. It is worth stressing that, despite these different behaviors, both tunings guarantee the fulfillment of the control specifications, thus constituting two valid alternatives. The lower undershoot achieved with the individualized tuning makes it preferable in those situations and for those individuals where even slight overdosing should be avoided, for example, for patients with a high tendency to hypotension. On the other hand, the fastest disturbance rejection provided by the population-based tuning could be more suitable to reduce the risk of intraoperative awareness in situations where the patient is subject to strong surgical stimulation. In this work the individualization of the controller has been considered only for the maintenance phase of anesthesia since the induction phase of anesthesia is highly influenced by the presence of the Hill function, which introduces a strong nonlinear behavior. The individualization of the parameters relies on the knowledge of patient's demographic data that are not related to the parameters of the Hill function, but only affects the dynamics of the linear PK model.

7.2   Individualized PID tuning for propofol and remifentanil coadministration

In this section, the individualized tuning approach is extended to the MISO control scheme for propofol and remifentanil coadministration presented in Section 2.2.2. In particular, it is interesting to understand whether the patient-individualized design can provide an improved robustness also in the MISO case. Here, the tuning methodology exploits the covariates of the Schnider and Minto PK model for propofol and remifentanil, respectively, to obtain a patient-individualized tuning of the PID controller, that is in form 2.7. A conditional integration anti-windup strategy has also been implemented.

7.2   Individualized PID tuning for propofol and remifentanil coadministration

7.2.1   Controller tuning

The tuning methodology proposed in Section 7.1 for the SISO case is here extended to the MISO case. In particular, the same optimization problem 5.7, based on the IAE, is considered and it is solved with a PSO algorithm that is set with a swarm size of 100 particles. The optimization ends when the relative change in the best IAE value over the last 50 iterations is less than 0.001. Once the patient's age, weight, height and gender are known, the PK/PD linear models for propofol and remifentanil are constructed by using the Schnider and Minto models, shown in Table 1.1 and 1.2, respectively. For the nonlinear interaction model, the values shown in Table 1.4 are considered. This model is then used to run the optimization procedure by simulating the response to the double-step disturbance profile shown in Figure 1.6, thus obtaining the set of optimal PID parameters that minimizes the IAE for that specific patient. Hence, with this approach, the set of tuning parameters is calculated for each patient, thus providing an individualization of the PID parameters based on the demographic data of the patient. The tuning procedure must be performed separately for each value of the infusions ratio since the system dynamics depends on this parameter. The ratios 0.5, 2, 5 and 15 have been chosen as representative values.

7.2.2   Simulation results

In this section the results obtained in simulation with the individualized tuning methodology are presented and they are compared with those obtained by using the population-based tuning methodology shown in Table 2.4. All the simulations have been performed by considering only the maintenance phase of anesthesia. The reference signal $r(t)$ is set equal to 50. Propofol and remifentanil infusion rates and the state of the system are initialized at the equilibrium corresponding to $BIS(t) = 50$. Further, the integrator of the PID controller is preloaded to a value such that the control action in absence of tracking error equals the above-mentioned equilibrium input. Then, the double-step disturbance profile shown in Figure 1.6 is applied.

Initially the two approaches have been tested on the tuning dataset shown in Table 2.2. Note that the population-based PID tuning has been obtained by minimizing the worst-case scenario over the above-mentioned dataset, while the individualized tuning is obtained by considering the values of the parameters of the nonlinear interaction function shown in Table 1.4. The responses obtained in simulation with both tuning methods for each considered value of the ratio are shown in Figure 7.6. The two tunings exhibit different behaviors for the rejection of the positive step disturbance, while they do not show significant differences for rejection of the negative step. This behavior is expected because, in order to compensate for the BIS rise due to the positive step, the controller reacts by increasing the drugs infusion rate with a dynamics that is imposed by the PID controller. On the other hand, to compensate for the drop in BIS due to the end of the disturbance action, the controller reacts by setting the drug flow to zero (due to the saturation imposed by the fact that it is impossible to remove the drug from the patient). Thus, the increase of the BIS is mainly dominated by patient dynamics over which the PID controller has no control. Hence, TTn and BIS-NADIRn are practically identical with both tunings and therefore they are not shown in this comparison. To better highlight the differences in the responses to the positive step disturbance obtained with the two different tunings, a comparison between the mean, minimum and maximum values of performance indices TTp and BIS-NADIRp is shown in Figure 7.7. For each value

of ratio, the patient-individualized tuning reduces the undershoot, as observable from the minimum values of BIS-NADIRp obtained. In particular, the individualized-tuning shows an average BIS-NADIRp of 48 while the population-based tuning shows an average BIS-NADIRp of 46. The patient-individualized tuning also provides a reduction in the variability of the BIS-NADIRp, as it is possible to notice by analyzing the minimum values of BIS-NADIRp. Indeed, with the population-based tuning the minimum BIS-NADIRp is 42 for every value of the ratio, while for the individualized tuning it is around 46 with ratio 0.5 and 2, 45 with ratio 5, and 43 with ratio 15. This reduction of the BIS-NADIRp of the individualized tuning is obtained at the expense of a slightly longer TTp. However, the maximum TTp obtained with the patient-individualized tuning never exceeds 30 s which is perfectly acceptable in the clinical practice.

The behavior of the two different tuning approaches has been tested with respect to intra-patient variability. To this end, the method described in Section 2.2.1 has been applied with the statistical properties of the Schnider PK model given in [25] and of the Minto PK model given in [27], and for each of the perturbed models the response to disturbance has been simulated. It is worth stressing that the individualized tuning procedure is still performed on the nominal model, hence the tuning parameters are the same for each one of the 500 perturbed models generated for each patient of the tuning dataset. The responses obtained in simulation with both tuning methods for each value of ratio for patient thirteen are shown in Figure 7.9 as an example. The perturbed response for the other patients of the dataset are not shown for the sake of brevity but similar results have been obtained. The mean value, minimum value, maximum value and range for each of the thirteen patients of the dataset, and for each value of ratio, are shown in Figure 7.10. Even in the presence of intra-patient variability, the results obtained with the perturbed population are similar to those achieved on the dataset of the thirteen nominal patients. In particular, the individualized tuning achieves higher values of the BIS-NADIRp and reduces its variability. This is obtained at the cost of an increased value of TTp compared to the one obtained with the population-based tuning.

The behavior of the two different tuning approaches with respect to inter-patient variability has finally been assessed by applying the method described in Section 2.2.1. The parameters of the Hill function have been generated by considering the statistical properties given in [28, 29, 30]. The individualized tuning has been performed for each one of the 500 generated patients by considering the nominal parameters of the Hill function shown in Table 1.3. The individualized tuning has been performed for each one of the 500 generated patients by considering the nominal parameters of the nonlinear interaction model. The responses obtained in simulation with both tuning methods for each value of ratio considered are shown in Figure 7.11. The mean value, minimum value, maximum value and range for each of the thirteen patients of the tuning dataset, and for each value of ratio considered, are shown in Figure 7.8. Even for a larger population, the same results obtained for the thirteen patients of the sample dataset remain valid and in particular, the reduction of the undershoot achieved with the individualized tuning is even more evident. Indeed, with the individualized tuning, the minimum value of BIS-NADIRp never drops below 44, while with the population-based tuning the minimum value of BIS-NADIRp is 38. Again, the reduction of the undershoot obtained with the individualized tuning is obtained at the expense of a longer TTp with respect to the one obtained with the population-based tuning. However, the maximum TTp obtained with the individualized tuning never exceeds 35 s, thus always remaining below the clinically acceptable threshold.

(a) *Ratio 0.5*

(b) *Ratio 2*

(c) *Ratio 5*

(d) *Ratio 15*

Figure 7.6: *Maintenance phase responses obtained with the PID controller for propofol and remifentanil coadministration on the thirteen patients of the test population with different values of ratio. Black solid line: population-based tuning. Green solid line: individualized tuning.*
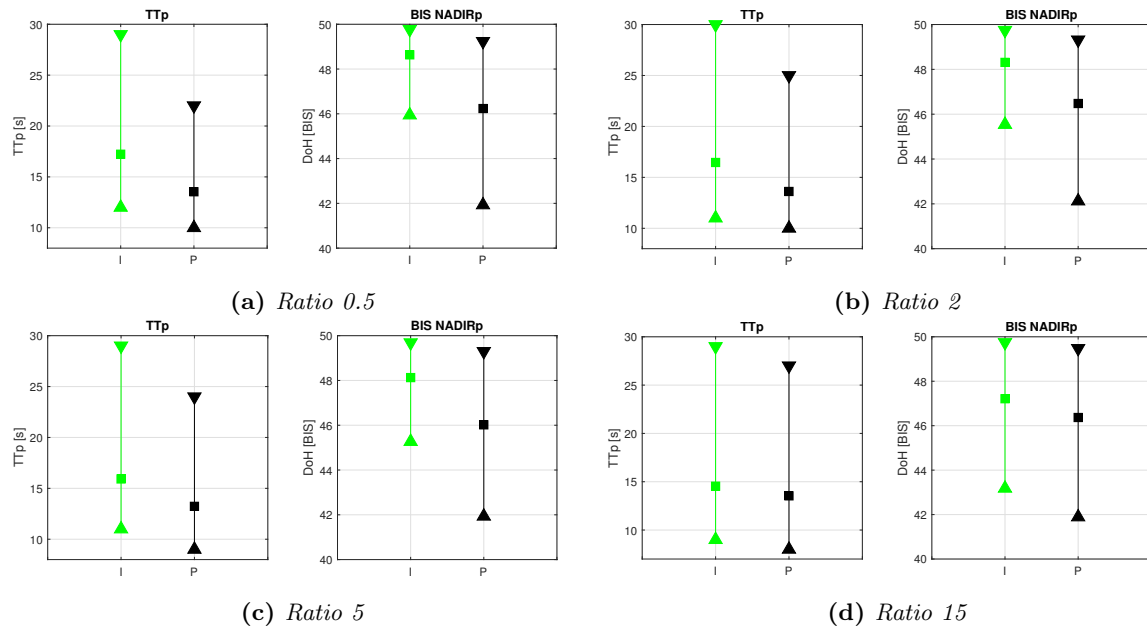
Figure 7.7: *Comparison of mean, minimum and maximum values of maintenance phase performance indexes obtained with the PID controller for propofol and remifentanil coadministration on the thirteen patients of the test population with the individualized tuning (I: green line) and with the population-based tuning (P: black line). ■ : mean value, ▲ : minimum value, ▼ : maximum value.*
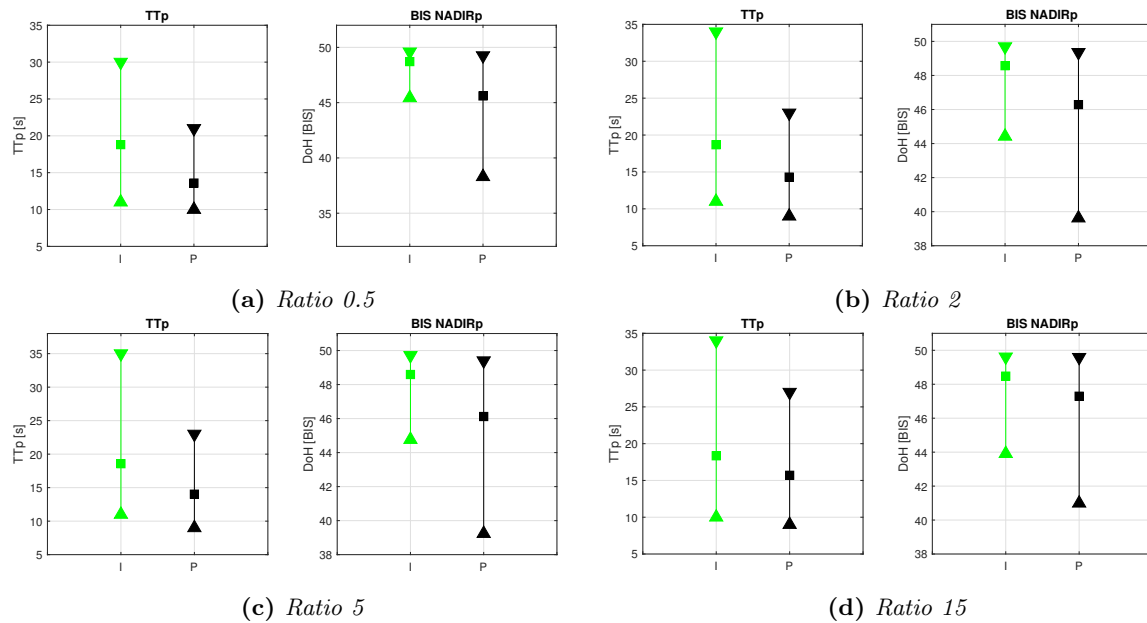
Figure 7.8: *Comparison of mean, minimum and maximum values of maintenance phase performance indexes obtained with the PID controller for propofol and remifentanil coadministration on the population of 500 patients used to simulate inter-patient variability with the individualized tuning (I: green line) and with the population-based tuning (P: black line). ■ : mean value, ▲ : minimum value, ▼ : maximum value.*

(a) *Ratio 0.5*

(b) *Ratio 2*

(c) *Ratio 5*

(d) *Ratio 15*
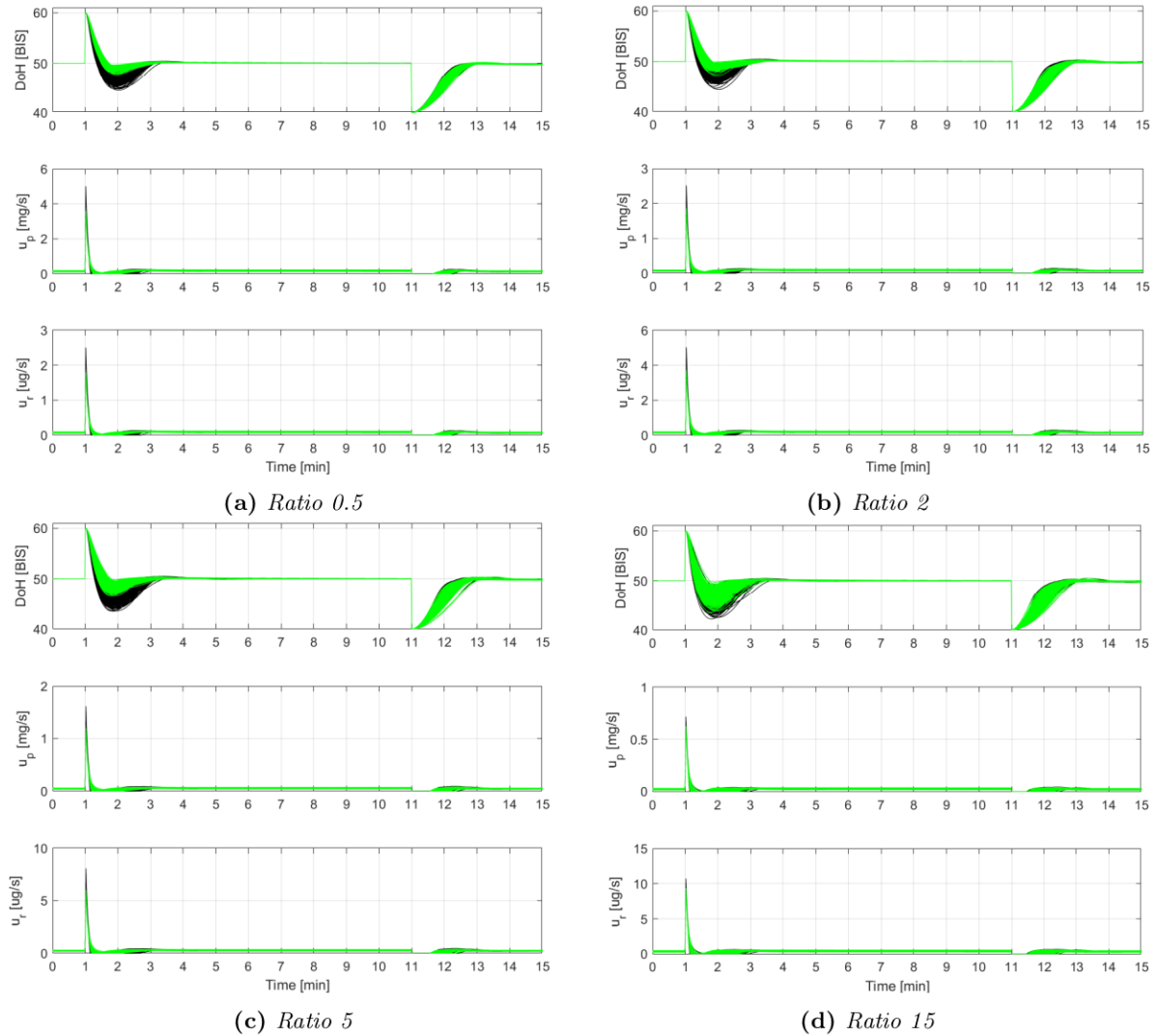
Figure 7.9: *Maintenance phase responses obtained with the PID controller for propofol and remifentanil coadministration on the 500 perturbed models generated from the nominal model of the thirteenth patient of the tuning dataset with different values of ratio. Black solid line: population-based tuning. Green solid line: individualized tuning.*

(a) *Ratio 0.5*

(b) *Ratio 2*

(c) *Ratio 5*

(d) *Ratio 15*
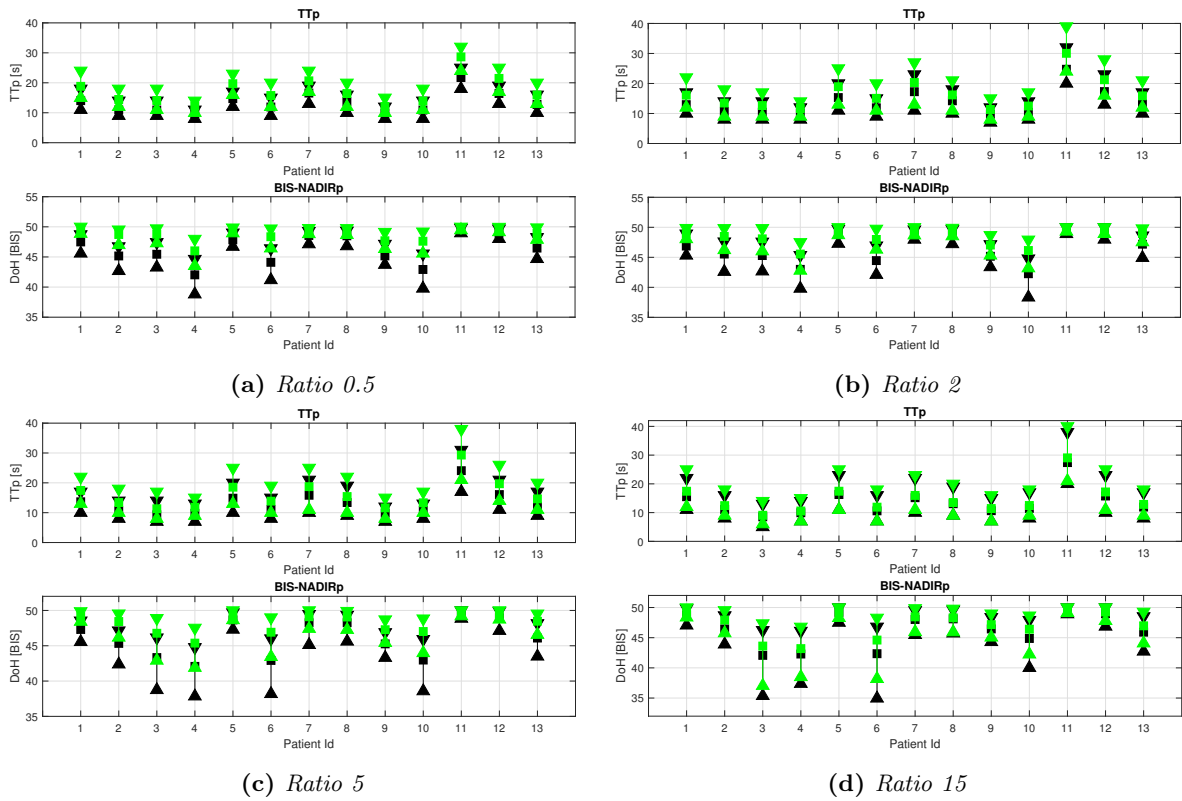
Figure 7.10: *Comparison of mean, minimum and maximum values of maintenance phase per-formance indexes obtained with the PID controller for propofol and remifentanil coadministration for each of the thirteen patients of the test dataset subjected to intra-patient variability with the individualized tuning (green line) and with the population-based tuning (black line). ■ : mean value, ▲ : minimum value, ▼ : maximum value.*

(a) *Ratio 0.5*
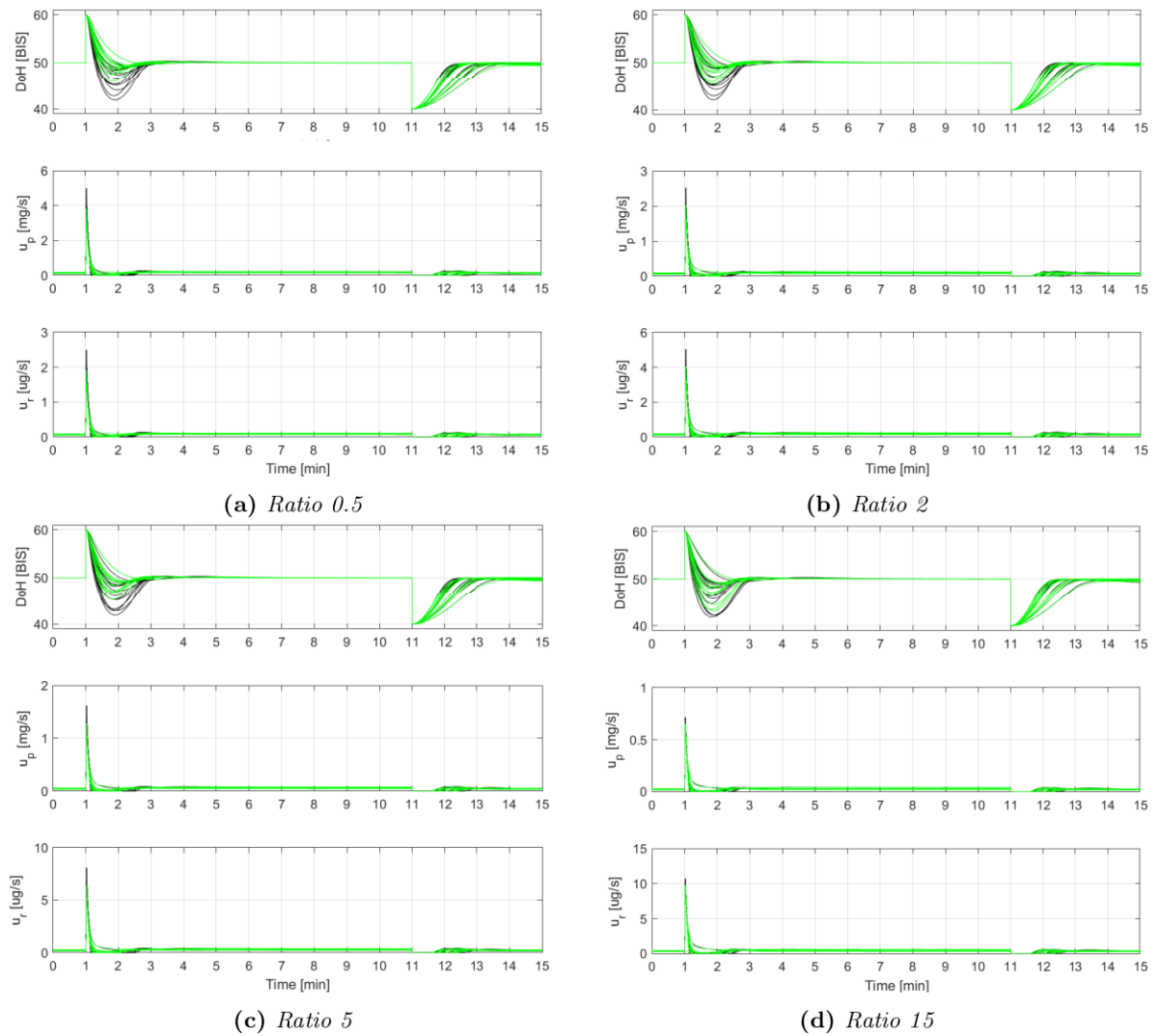
(b) *Ratio 2*

(c) *Ratio 5*

(d) *Ratio 15*
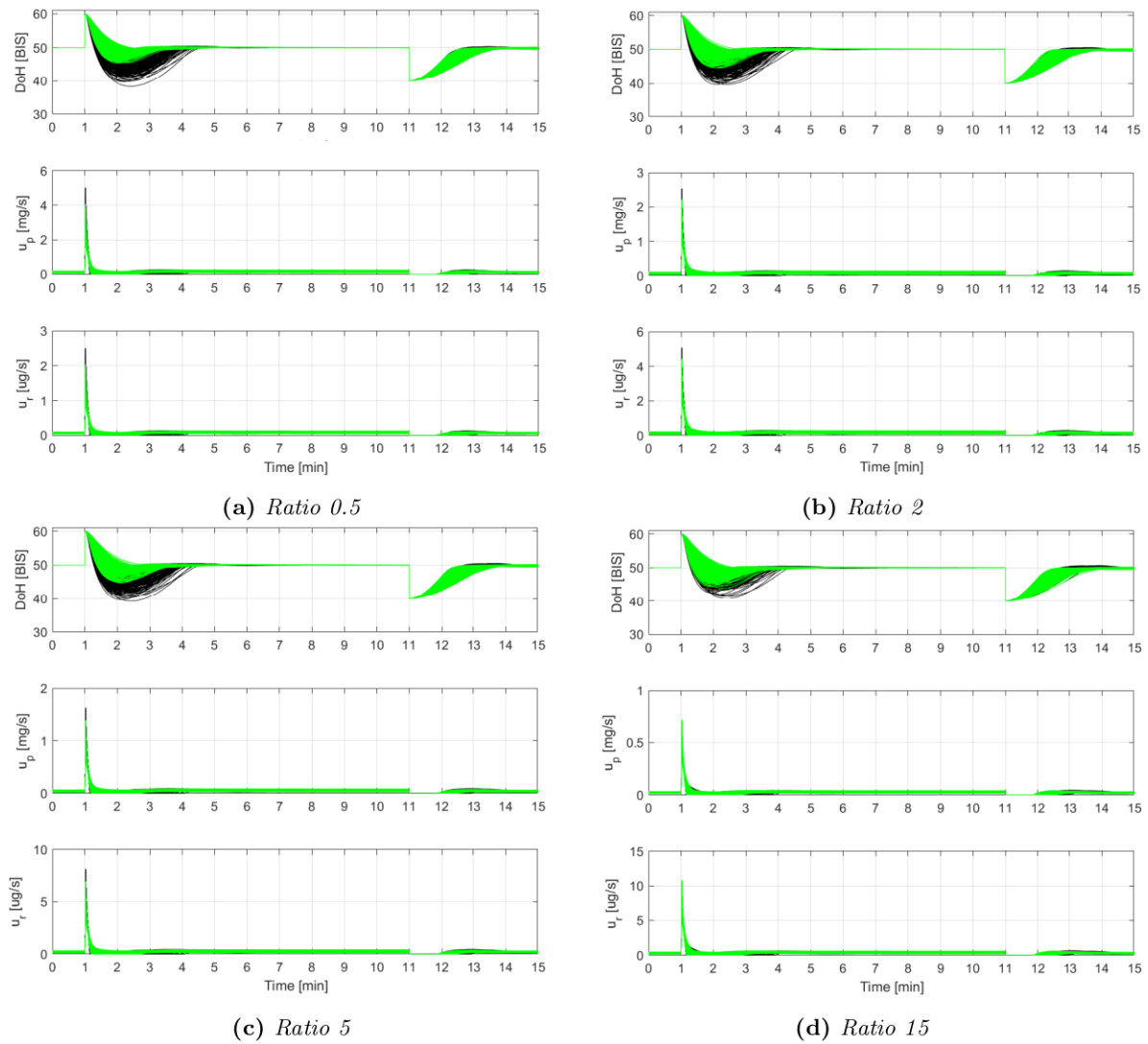
Figure 7.11: *Maintenance phase responses obtained with the PID controller for propofol and remifentanil coadministration on the population of 500 patients randomly generated to test inter-patient variability with different values of ratio. Black solid line: population-based tuning. Green solid line: individualized tuning.*

7.2.3   Discussion

The obtained simulation results suggest that the patient-individualized tuning approach provides satisfactory control performance for every value of ratio considered. In particular, it performs well on the tuning dataset and it shows a good robustness with respect to both intra-patient variability and inter-patient variability, by always guaranteeing the fulfillment of the control specifications. When compared with a population-based tuning, it shows its effectiveness in reducing the effect of variability on BIS undershoot. Indeed, in all the simulations performed, the individualized tuning provides a reduction of the maximum undershoot, which is represented by the minimum value of BIS-NADIRp and of the variability range of the undershoot, which is represented by the difference between the maximum and the minimum values of BIS-NADIRp. This increased robustness to undershoot is counterbalanced by a reduction of the controller bandwidth that translates into an increment of the TTp. In all the simulations performed with the individualized tuning, the increment of the mean value of TTp is limited, while it is more evident if the maximum value of TTp is considered. The lower undershoot achieved with the individualized tuning makes it preferable in those situations and for those individuals where even slight overdosing should be avoided, for example, for patients with a high tendency to hypotension. On the other hand, the fastest disturbance rejection provided by the population-based tuning could be more suitable to reduce the risk of intraoperative awareness in situations where the patient is subject to strong surgical stimulation. In any case, with both tunings the control specifications are always fulfilled. The simulation results obtained confirm that the approach presented in Section 7.1 for the control of propofol alone remains valid also for the case of propofol and remifentanil coadministration. Indeed, similar trends are observed and the considerations regarding the TTp and the BIS-NADIRp are the same for both the SISO and the MISO cases. The BIS remains mainly inside the range from 40 to 60, where the nonlinear interaction approximately behaves like a constant gain matrix. Hence, during the maintenance phase, the dynamic of the PK/PD model of the patient is less affected by the nonlinear behavior. The proposed approach allows the full exploitation of the knowledge of patient's demographic data and it is straightforwardly implementable in the clinical practice since these data are always available. Finally, it is worth clarifying that, although the ratio values considered in this paper are limited, the same results obtained applies for all values in the considered range, from 0.5 to 15. The particular values selected have been chosen as representative examples, 0.5 and 15 being the extrema while 2 and 5 are commonly used values in the clinical practice.

7.3   Conclusions

In this chapter a patient-individualized PID tuning approach has been presented. It is applicable to both SISO and MISO control schemes and it allows the controller parameters to be individualized on the basis of the patient's demographic data. The proposed approach allows the knowledge of all the patient's measurable demographic data to be exploited and it is straightforwardly implementable in the clinical practice since covariates are easily measurable. Thus, it represents a step forward in the implementation of personalized medicine solutions. The maintenance phase of anesthesia has been considered in order to minimize the effect of the nonlinearity introduced by the Hill function, which is particularly significant in the induction phase, since its parameters do not depend on patient's demographic data. The individualized tuning has been tested in simulation on the tuning dataset and its behavior with

respect to intra-patient and inter-patient variability has been investigated. The controller has given satisfactory results always guaranteeing the fulfillment of the control specifications. The results obtained in simulation with the individualized controllers have been compared with those obtained with PID controllers tuned with a population-based methodology. The individualized controllers have shown an improved robustness with respect to intra-patient and inter-patient variability, at the cost of a slight decrement of the bandwidth. This translates into an increase in the amount of time required to reject positive disturbances, which however remains within acceptable limits. Both tunings perform well in simulation and represent therefore viable alternatives for the tuning of PID controllers to be employed in the clinical practice, thus allowing the anesthesiologist to choose the most suitable controller for a specific patient and/or surgical procedure.

Chapter 8

Optimization-based strategies for anesthesia induction

Anesthesia induction represents a critical phase in clinical practice and it is particularly demanding for the anesthesiologist. Indeed, propofol must be carefully dosed to rapidly drive patients into a state of unconsciousness. A quick loss of consciousness facilitates airway instrumentation, thus ensuring patient's safety. It also prevents patients from feeling anxiety and discomfort due to pain on propofol injection. However, this should not be obtained at the expense of a propofol overdose as it can lead to severe complications, like hypotension and post-operative delirium. In the clinical practice of TIVA, anesthesia is generally induced by administering a bolus of propofol. The dose is chosen based on mathematical models and clinical guidelines that take into account the physical characteristics of the patient. However, the clinical effect of this initial bolus strongly depends on the variability that each patient shows in response to drug administration. This difficulty in drug dosing, combined with the fact that it is necessary to deal with the delicate procedure of airway instrumentation, makes anesthesia induction a demanding task for the anesthesiologist. Hence, the assistance provided by computerized systems can bring several benefits in this phase. When TCI is used the anesthesiologist selects a desired plasma or effect site concentration of propofol and the system aims to achieve it by delivering an appropriate infusion profile. It is a bolus-like profile that is calculated by exploiting a PK/PD model of the patient. The use of TCI helps the anesthesiologist in dosing the drug. However, it is an open-loop system and, thus, it is susceptible to unavoidable model uncertainties. On the contrary, closed-loop systems can compensate for uncertainties. However, their design is particularly challenging, especially as regards the induction phase, as they must be able to guarantee a fast set-point tracking with limited overshoot despite the high variability in drug response and the presence of nonlinearities.

In [150], an input-output inversion-based control solution has been proposed, while in [151] an Explicit Reference Governor scheme has been developed to formally guarantee overshoot prevention. Although these solutions have provided promising results, one of the reasons that limits the use of this type of systems is represented by the fact that their behavior deviate from what is the clinical practice of using a propofol bolus. This implies that the induction might result too slow to be acceptable in some clinical practices and for some kind of patients. Furthermore, this difference from standard clinical practice can create distrust in clinicians. In an attempt to overcome this issue, new optimization-based feedforward control approaches
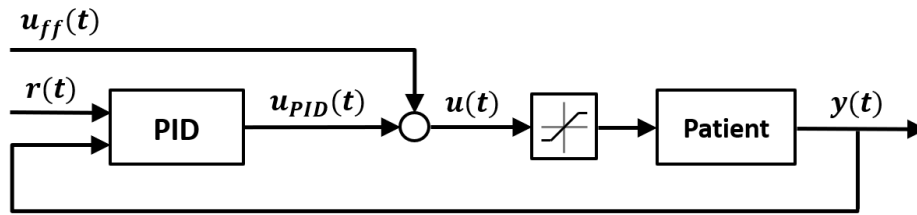
Figure 8.1: *Schematic representation of the control architecture with the optimized feedforward bolus.*

specifically designed for the induction phase of BIS-guided propofol anesthesia are proposed [113, 114, 115]. The results obtained are summarized in this chapter.

8.1 Optimized feedforward control

The approach proposed in this section is based on the use of an optimization strategy to determine the initial propofol bolus to induce anesthesia. The optimized bolus aims to minimize the induction time and it is used as a feedforward action together with a specifically tuned PID controller. More in details, the optimization objective is to minimize the transition time of the BIS from the initial value E_0 to its target range from 40 to 60. In particular, the time required for the BIS to drop below 60 has been minimized since it has been shown that, in general, BIS values below this threshold are associated with a reduced risk of awareness during endotracheal intubation [37]. This objective is constrained by the fact that it is necessary to avoid large undershoots of the BIS. Indeed, they could be harmful for the patient health. The method provides an infusion profile similar to the one commonly used in clinical practice to rapidly induce anesthesia (i.e. an initial bolus followed by a continuous infusion). The initial bolus is provided by a feedforward action that is calculated by taking into account the nominal patient model. In case of perfect knowledge of the model, the feedforward action alone would be sufficient to drive the BIS to the target range in a minimum time. However, because of unavoidable model uncertainties, a feedback PID controller is included in the control scheme. Thus, the main idea is to combine the ability to provide a personalized drug infusion offered by TCI systems with the advantages of continuous adjustment and reduction of variability in the response offered by closed-loop systems.

8.1.1 Control system architecture

The system architecture is shown in Figure 8.1 where $u_{ff}(t)$ is the feedforward action, while $u_{PID}(t)$ is the output of the PID controller. The overall control action $u(t)$ is obtained as the sum of these two actions and it represents the propofol infusion rate expressed in mg/s. This value is bounded between the minimum value of 0 mg/s and maximum value, u_M, of 6.67 mg/s. The reference value for the BIS is denoted as $r(t)$, while $y(t)$ is the measured BIS value.

Feedforward action

The feedforward action is calculated by means of an optimization procedure. This procedure is carried out before the beginning of anesthesia induction. It is based on the offline simulation of the patient's response to drug infusion. The latter is obtained by exploiting the nominal PK/PD propofol model, described in Section 1.2.2, with the aim to provide a personalized drug infusion. In particular, for the linear part the Schnider model, shown in Table 1.1, is used. For the Hill function the Vanluchene model, shown in Table 1.3, is used. The parameter E_0 of the Hill function can be obtained by measuring the baseline BIS value before drug administration.

The feedforward action can bring significant benefits in terms of performance as it explicitly takes into account the nonlinearity of the Hill function. In particular, as it is possible to verify from Equation 1.6, the Hill function has an initial *plateau*. Thus, a low drug concentration in the effect site compartment has almost no effect on the BIS. The effect becomes visible only when the concentration in the effect-site compartment reaches a sufficiently high value. Therefore, especially during the initial stages of induction, the states of the system 1.1 cannot be determined from the BIS. This is particularly detrimental for a feedback controller since, during the first moments of induction, the feedback signal is not very informative, thus limiting the bandwidth achievable by the controller without risking instability.

In the following, the procedure for computing the feedforward control action is presented. First, consider the linear model 1.1 and its state-space representation 1.4 with the BIS signal as nonlinear output (1.6):

$$y(t) = BIS(t) = h(x(t)) = f(C_e(t)), \tag{8.1}$$

where the output function $h : \mathbb{R}^4 \to \mathbb{R}$ is such that $h([q_1, q_2, q_3, C_e]^T) = f(C_e)$. If all parameters appearing in 1.1 are nonzero, then system (1.1) is asymptotically stable by vii) of Theorem 2.10 of [152]. In fact, by defining p as $[1, 1, 1, V_1 k_{10}/k_{1e}]^T$ and r as $[0, 0, 0, -k_{e0} V_1 k_{10}/k_{1e}]^T$, condition $0 = A^T p + r$ is satisfied. Then, being A non-singular, system 1.1 is asymptotically stable. Hence, for a constant input $u(t) = u_0$, by the final value theorem, the state converges to a constant, namely:

$$\lim_{t \to \infty} x(t) = \left[\frac{u_0}{k_{10}}, \frac{k_{12} u_0}{k_{10} k_{21}}, \frac{k_{13} u_0}{k_{10} k_{31}}, \frac{u_0 k_{1e}}{V_1 k_{10} k_{e0}} \right]^T,$$

and the BIS signal converges to $f(\frac{u_0 k_{1e}}{V_1 k_{10} k_{e0}})$. Because of the large time constants in 1.1, due to slow drug diffusion in fat tissues, steady state is not reached during normal surgical procedures. A feedforward control is computed such that, at time $\hat{t}$, corresponding to the end of the induction phase, the BIS signal reaches a desired value y_0, which is set equal to 50, and can be maintained constant for all $t \geq \hat{t}$ with a suitable choice of the infusion rate. To this end, set $g(y_0) = \frac{V_1 k_{e0}}{k_{1e}} f^{-1}(y_0)$ and note that, if $y(\hat{t}) = h(x(\hat{t})) = y_0$ and $(\forall t \geq \hat{t}) \, q_1(t) = g(y_0)$ then $(\forall t \geq \hat{t}) \, y(t) = y_0$. That is, $g(y_0)$ is the drug mass in the primary compartment that allows the BIS signal to be maintained on the desired target value y_0. In the induction phase, the feedforward infusion u that brings system 1.1, from the initial rest condition $x(0) = 0$, to a state $x(\hat{t})$, such that $h(x(\hat{t})) = y_0$, $q_1(\hat{t}) = g(y_0)$ is computed. During this phase, the BIS value must always be above a given safety threshold $BIS_{\min}$, that is set equal to 40. Moreover, to minimize time-to-target, the control u must minimize

$\bar{t} = \min\{t \in \mathbb{R} : (\forall \tau \in [t, \hat{t}]) \, BIS(\tau) \le y_0\}$, that is the time after which the BIS value is kept below the target value y_0. In practice, since a discrete-time controller is used, the feedforward control signal is constant between sampling times. Let $T \in \mathbb{R}$ be a positive constant that represents the sampling period. Assume that the continuous-time control signal $u : \mathbb{R} \to \mathbb{R}$ is obtained by applying a zero-order hold filter (ZOH) to a discrete-time input $u_d : \mathbb{Z} \to \mathbb{R}$, that is:

$$u(t) = u_d(k) \quad t \in [kT, (k+1)T],$$

and set the sampled state $x^*(k) = x(kT)$ and the sampled output $y^*(k) = y(kT)$. Functions x^*, y^* satisfy the difference equation:

$$\begin{aligned} x^*(k+1) &= A_T x^*(k) + B_T u_d(k) \\ y^*(k) &= h(x^*(k)), \end{aligned} \tag{8.2}$$

with $A_T = e^{AT}$, $B_T = \int_0^T e^{A\tau} B d\tau$. Define the set of admissible final induction states as:

$$\mathcal{F}(y_0) = \left\{ [q_1, q_2, q_3, C_e]^T \in \mathbb{R}^4 : f(C_e) = y_0, q_1 = g(y_0) \right\}.$$

In other words, $\mathcal{F}(y_0)$ is composed of those states $[q_1, q_2, q_3, C_e]$ such that the BIS output corresponds to the required target value y_0 and the drug mass in the primary compartment allows maintaining the BIS output constant. The overall goal of the induction phase is to perform a transition of system 8.1 from an initial equilibrium condition $x^*(0) = 0$, in which no drug is present in any compartment, to set $\mathcal{F}(y_0)$. At all times, the BIS signal must be greater than or equal than a safety threshold BIS_{min} and the input signal has to be positive and remain below an assigned threshold. The control must minimize the time-to-target, that is the time after which the BIS signal is below threshold y_0. More precisely, the problem at hand is the following one.

$$\min_{0 < \bar{k} \le \hat{k}} \bar{k} \tag{8.3a}$$

$$\text{s.t. } 0 \le u_d(k) \le u_M \qquad\qquad k = 0, \dots, \hat{k} \tag{8.3b}$$

$$x^*(k+1) = A_T x^*(k) + B_T u_d(k) \qquad\qquad k = 0, \dots, \hat{k} - 1 \tag{8.3c}$$

$$x_4^*(k) \ge f^{-1}(BIS_{min}) \qquad\qquad k = 0, \dots, \hat{k} \tag{8.3d}$$

$$x_4^*(k) \le f^{-1}(y_0) \qquad\qquad k = \bar{k}, \dots, \hat{k} \tag{8.3e}$$

$$x^*(0) = 0 \tag{8.3f}$$

$$x^*(\hat{k}) \in \mathcal{F}(y_0), \tag{8.3g}$$

where x_4^* denotes the $4th$ component of x^* and f is defined as in 1.6. In Problem 8.3, $\hat{k}$ is a number of samples such that $\hat{t} = \hat{k}T$ is the overall duration of the induction phase. Constraint 8.3b represents input limitations. Constraint 8.3c guarantees that x^* is a solution of 8.2, condition 8.3d guarantees that the calculated BIS signal does not fall below BIS_{min} at all times. Condition 8.3e states that the calculated BIS signal must be below threshold y_0 at all samples greater than or equal to $\bar{k}$. Condition 8.3f states that the drug initial concentration is zero in all compartments. Finally, condition 8.3g guarantees that at final sample $\hat{k}$ the state belongs to set $\mathcal{F}(y_0)$. Problem 8.3 can be solved by bisection as a sequence of linear programming problems. Initially, $\bar{k} = \hat{k}$ is set and the feasibility of Problem 8.3b-

8.3g is checked. Since all constraints are linear with respect to variables $u_d(k)$, $k = 1, \ldots, \bar{k}$, feasibility can be tested by a standard linear programming solver. For instance, GUROBI (Gurobi Optimization, LLC) [153] has been used in this implementation. Note that, if the problem is feasible for a given value of $\bar{k}$, it is feasible also for larger values of $\bar{k}$. This is due to the fact that $\bar{k}$ appears only in constraint 8.3e, which becomes less restrictive if $\bar{k}$ is increased. If this problem is not feasible for $\bar{k} = \hat{k}$, then also Problem 8.3 is not feasible. Otherwise, $\bar{k}$ is halved and the feasibility test is repeated. This procedure is repeated until the minimum value of $\bar{k}$ that satisfies the feasibility of Problem 8.3 is found. This corresponds to the optimal value of $\bar{k}$.

In our tests, the solution u_d of Problem 8.3 is composed of the following four phases (see Figure 8.2). In the following, $0 \leq k_1 \leq k_2 \leq k_3$ are appropriate samples that separate the different phases.

1. $u_d(k) = u_M$ for $0 \leq k \leq k_1$,
2. $u_d(k)$ is monotone non increasing for $k_1 \leq k \leq k_2$,
3. $u_d(k) = 0$ for $k_2 \leq k \leq k_3$,
4. $u_d(k) > 0$ for $k_3 < k \geq \hat{k}$.

Initially, the drug infusion rate saturates to the maximum allowed value u_M. Clinically, this corresponds to administering an initial drug bolus. Then, the infusion rate decreases to 0 and remains zero up to sample k_3. Finally, the infusion rates becomes positive again. This last phase corresponds to the beginning of the maintenance phase.

Determination of the reference signal and the feedforward control

For $k \geq \hat{k}$, the feedforward control u_d is such that $(\forall k \geq \hat{k})\ q_1^*(k) = \frac{V_1 k_{e0}}{k_{1e}} f^{-1}(y_0)$. Then, u_d is computed from 8.2. It corresponds to the infusion rate u_d that keeps q_1^*, C_e (and therefore the BIS signal) constant. Note that u_d is bounded. In fact, the transfer function $T_{u,q_1}(s)$ of continuous-time system 1.1 from u to q_1 is:

$$T_{u,q_1}(s) = \frac{k_{e0}\ (k_{21} + s)\ (k_{31} + s)}{b(s)},$$

where $b(s)$ is an Hurwitz polynomial of degree 3. Since $T_{u,q_1}(s)$ has relative degree 1 and is minimum-phase, by [154], the zeros of the discretized transfer function $T_{u_d,q_1^*}(z)$ from u_d to q_1^* approach $e^{-k_{21}T}, e^{-k_{31}T}$ as T approaches 0, so that $T_{u,q_1}(z)$ is minimum-phase for sufficiently small values of T. In the closed-loop control system shown in Figure 8.1, the reference signal $r(t)$ is obtained by applying a zero-order hold to discrete-time signal:

$$r_d(k) = \begin{cases} h(x^*(k)) & \text{if } k \leq \hat{k} \\ y_0 & \text{if } k > \hat{k}. \end{cases}$$

The feedforward control u_{ff} is obtained by applying a zero-order hold to:

$$u_{ff,d}(k) = \begin{cases} u_d(k) & \text{if } k \leq \hat{k}_2 \\ 0 & \text{if } k > \hat{k}_2. \end{cases}$$

That is, the part of signal u_d that corresponds to the maintenance phase is set to zero. In this way, only the feedforward action for the induction phase is actually implemented in the

controller and the maintenance phase is totally managed by the feedback controller. This choice has been made because the purpose of the feedforward action is to determine the optimal bolus to be administrated to the patient. In the proposed architecture, the task of maintaining the BIS at the target value can be fully achieved by the integral action of the PID controller. This also makes sense because the feedforward action is calculated by considering only the patient dynamics and by neglecting the dynamics of the PID controller which is negligible during the early phases of induction but it gradually becomes relevant, thus making the feedforward action calculated for the maintenance phase less accurate. An example of the overall feedforward action, of the employed bolus-like feedforward action $u_{ff}(t)$ and of the determined reference signal $r(t)$ is shown in Figure 8.3.

Feedback controller

At the end of the first part of the feedforward action, the concentration of drug in the effect site compartment has reached a value such that the Hill function is out of its *plateau* and it is close to its point of maximum slope. Therefore, the feedback action plays a key role to compensate for variability. The feedback controller consists of an output filtered PID controller in the form 2.6 that has been tuned with the optimization-based approach presented in Section 2.2.1. In particular, a PSO algorithm has been employed to minimize the IAE in the worst-case simulated step response (where both the feedforward and the feedback control actions are applied) on the tuning dataset of Table 2.1. The PSO algorithm was run with a swarm size of 100 particles. Optimization ended when the relative change in the best IAE value over the last 50 iterations was less than 0.001. The IAE was evaluated by performing a numerical simulation of the response of each patient to drug infusion with a discretization step equal to 0.1 s. The resulting tuning parameters are $K_p = 0.16$ mg/s, $T_i = 476$ s and $T_d = 13$ s. Finally, T_f has been fixed equal to 0.7 s as in [92]. An anti-windup back calculation method has also been implemented, where the value of the tracking time constant has been selected as the square root of the product of the integral and derivative time constants.

8.1.2 Simulation results

In this section, results obtained for the proposed control methodology are shown. These results are compared with those obtained by employing the PID controller proposed in [92], and summarized in Section 2.2.2. The control system has been initially tested on the tuning dataset already used to tune the PID controller. Then a much wider population obtained by means of a Monte Carlo method is considered.
Both controllers have been tested with a BIS set-point value of 50. For the control system with the PID controller alone, a step set-point change is applied, while for the feedforward/feedback controller the reference signal $r(t)$ is employed.
As a first illustrative result, the responses for both controllers for the average patient of the tuning dataset are plotted in Figure 8.4 where the control variable $u(t)$ and the BIS value $y(t)$ are shown. It appears that the initial bolus provided by the feedforward controller causes a rapid drop in the BIS and a more pronounced and longer lasting undershoot than the PID that, on the other hand, provokes almost no undershoot. The performance indexes obtained are shown in Table 8.1. The feedforward/feedback controller reduces TT of 25.8% with respect to the PID controller. This is achieved at the cost of a lower BIS-NADIR associated with a longer lasting period of BIS below the target value highlighted by higher values of
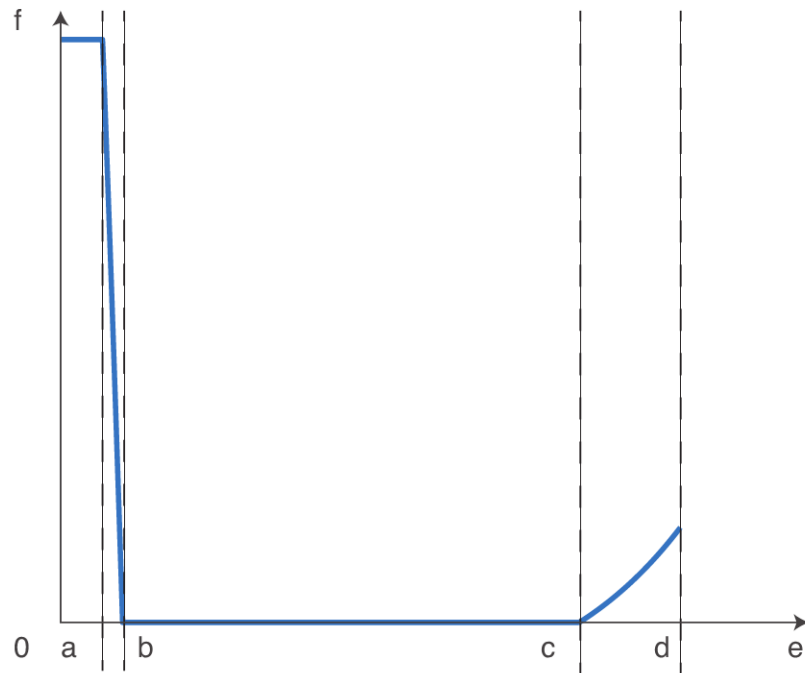
Figure 8.2: *Typical structure of optimal infusion rate u_d.*
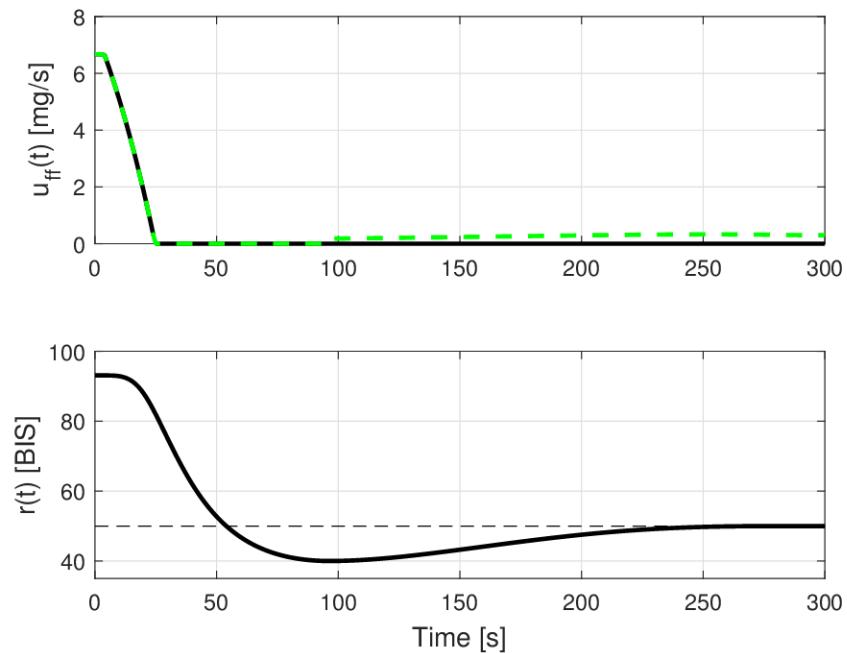
Figure 8.3: *The overall feedforward action (green dashed line), the feedforward action $u_{ff}(t)$ actually employed in the controller (black solid line) and the reference signal $r(t)$ calculated for a 38 years old female patient, 169 cm, 65 kg.*

ST10 and ST20. However, the undershoot value obtained with the feedforward is acceptable as BIS-NADIR values up to 30 are common in clinical practice and are not considered harmful to the patient health as discussed in Section 1.3.2.

The same test performed on the average patient has then been performed on the whole tuning dataset. The feedforward actions $u_{ff}(t)$ and reference signals $r(t)$ for each patient are shown in Figure 8.6. The different shapes of $u_{ff}(t)$ and $r(t)$ show that the feedforward action accounts both for the pharmacokinetics parameters variability and for the variability in E_0. The bolus doses obtained for each patient of the tuning dataset, expressed in mg/kg, are shown in Table 8.2. Note that their values are in accordance with the clinical practice. The responses obtained are shown in Figure 8.5 together with those obtained with the PID controller alone. It is possible to notice that the same behavior obtained for the average patient is also obtained on the whole tuning dataset. Indeed, on each of the thirteen patients, by using the feedforward/feedback controller, there is an average reduction in TT of 26.7% compared to the PID controller and an increase in settling times due to a greater undershoot of the BIS. However for none of the thirteen patients there is an excessive suppression of the BIS level, that always remains above 30. A comparison between the mean, minimum and maximum values of performance indexes is shown in Figure 8.9a.

To evaluate the robustness of the controller with respect to intra-patient variability the method described in Section 2.2.1 has been applied with the statistical properties of the PK model given in [25] and the set-point response has been simulated for each of these perturbed models. It is worth stressing that feedforward action $u_{ff}(t)$ and the reference signal $r(t)$ are the same for each of the 500 perturbed models generated for each patient of the tuning dataset as they are calculated by taking into account the values of the nominal model. Therefore, the variability is managed by the feedback controller. For the sake of readability only results related to the average patient of the tuning dataset are shown in Figure 8.7 where it is possible to notice that the variability introduced in the model is properly managed by the feedback controller. Similar behavior is also obtained for all other patients in the test population. The mean, minimum and maximum values for each patient of the tuning dataset, obtained with the Monte Carlo simulation, are shown in Figure 8.9c where they are also compared with those obtained with the PID controller. Even in the presence of intra-patient variability the TT values obtained with the feedforward controller are always lower than those of the PID controller and the BIS-NADIR never drops below 30.

Finally, to validate the robustness with respect to inter-patient variability the method described in Section 2.2.1 is applied. The parameters of the Hill function have been generated by considering the statistical properties given in [28]. For each generated patient the feedforward action $u_{ff}(t)$ and the reference signal $r(t)$ have been calculated. The set-point responses are shown in Figure 8.8, the performance indexes obtained are shown in Table 8.3 and the comparison of the mean, minimum and maximum values of performance indexes with respect to the PID is shown in Figure 8.9b. It appears that, even in the case of inter-patient variability, the use of the devised feedforward controller is able to provide an average improvement of 23.4% of the TT at the expense of a slight worsening of the indices relating to the settling time and undershoot. Indeed, the BIS-NADIR always remains above 30, therefore it never reaches critical values.
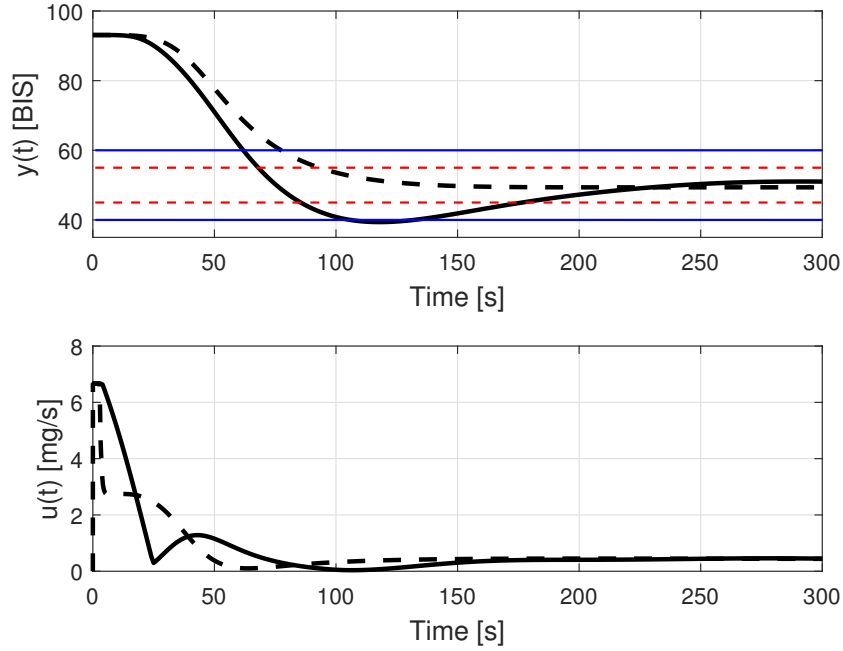
Figure 8.4: *Induction phase response for the thirteenth patient of the tuning dataset obtained with the feedforward controller (black solid line) and with the PID controller (black dashed line). The blue horizontal solid lines delimit the interval of BIS values between 40 and 60 and the red horizontal dashed lines delimit the interval of BIS values between 45 and 55.*

	Feedforward	PID
TT $[s]$	69	93
ST10 $[s]$	177	93
ST20 $[s]$	132	77
BIS − NADIR	39.38	49.33

Table 8.1: *Induction phase performance indexes for the thirteenth patient of the tuning dataset obtained with the feedforward controller and with the PID controller.*

Patient	1	2	3	4	5	6	7	8	9	10	11	12	13
Bolus [mg/kg]	2.07	2.24	1.95	1.37	1.74	1.62	1.37	1.44	1.41	1.50	1.28	1.92	1.62

Table 8.2: *Propofol boluses doses administered by the feedforward action $u_{ff}(t)$ for each patient of the tuning dataset.*
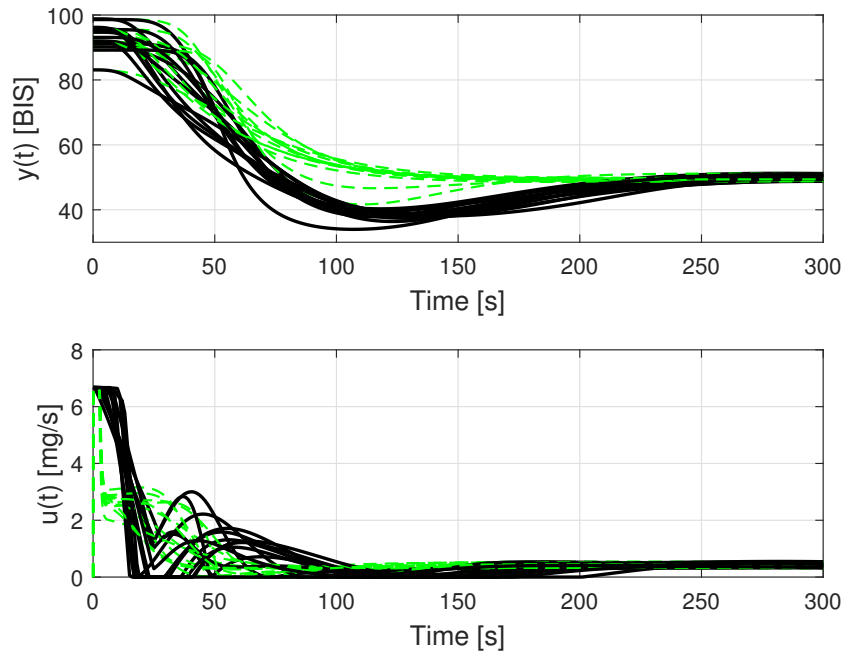
Figure 8.5: *Induction phase responses for each patient of the tuning dataset. Black solid line: optimized feedforward control. Green dashed line: PID controller.*
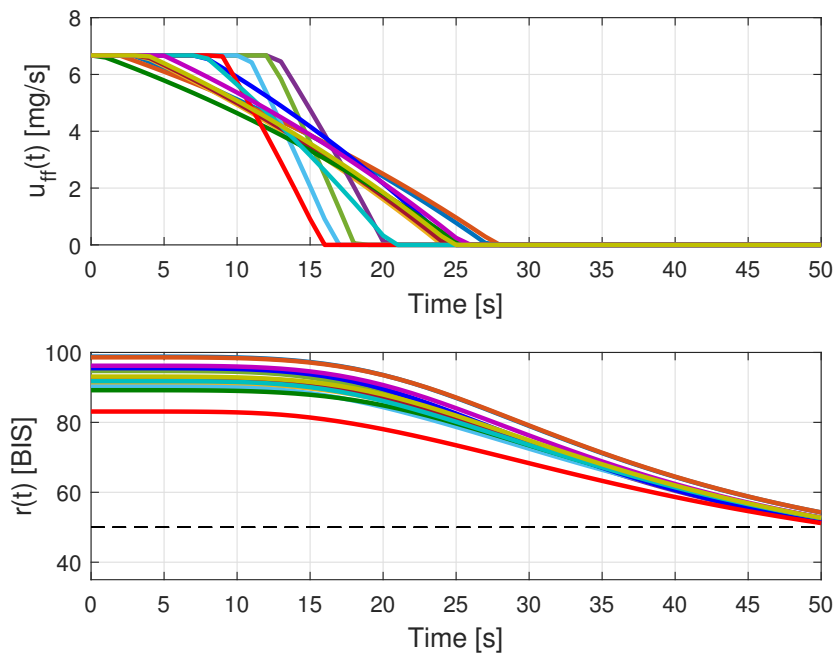
Figure 8.6: *Feedforward actions $u_{ff}(t)$ and reference signals $r(t)$ calculated for each patient of the tuning dataset.*
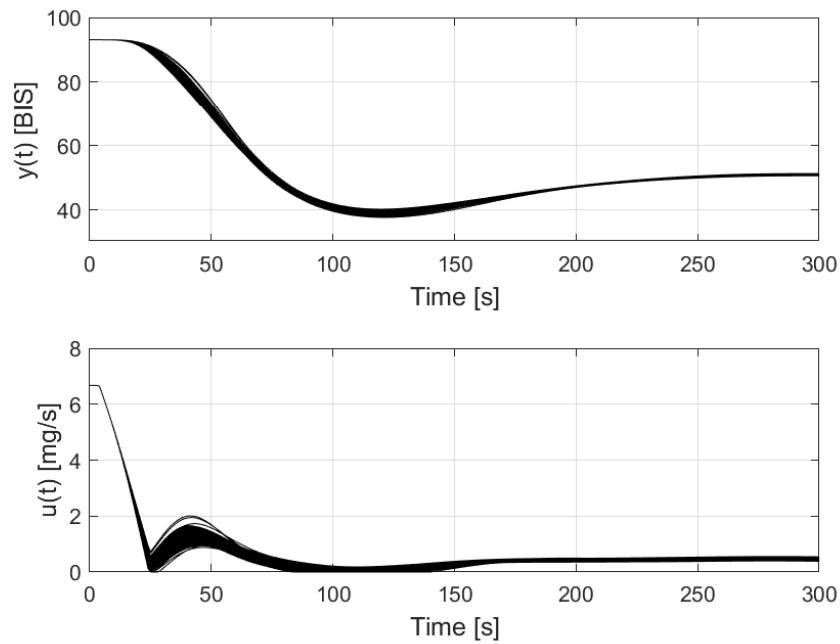
Figure 8.7: *Induction phase responses obtained with the optimized feedforward control on the thirteenth patient of the tuning dataset subjected to intra-patient variability.*
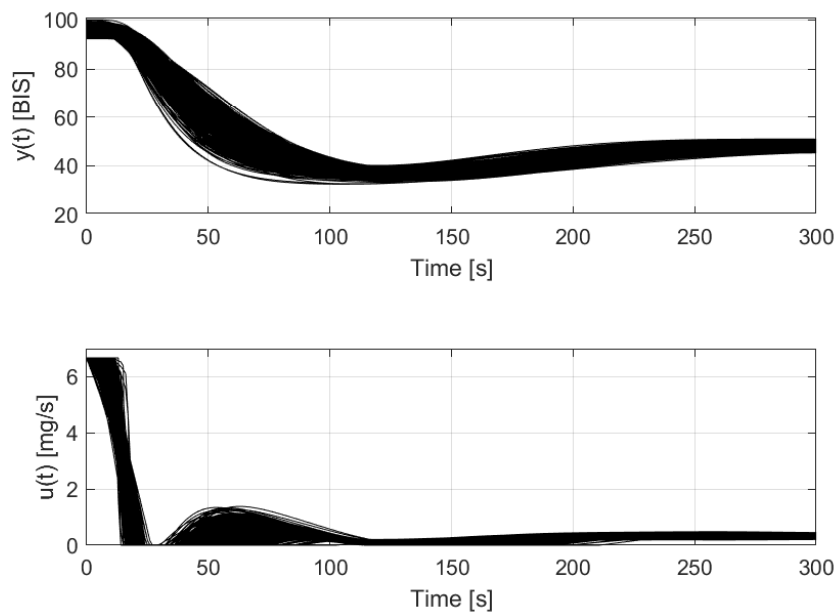
Figure 8.8: *Induction phase responses obtained with the optimized feedforward control on a population of 500 patients used to simulate inter-patient variability.*

(a) *Tuning dataset*

(b) *Inter-patient variability*

(c) *Intra-patient variability*
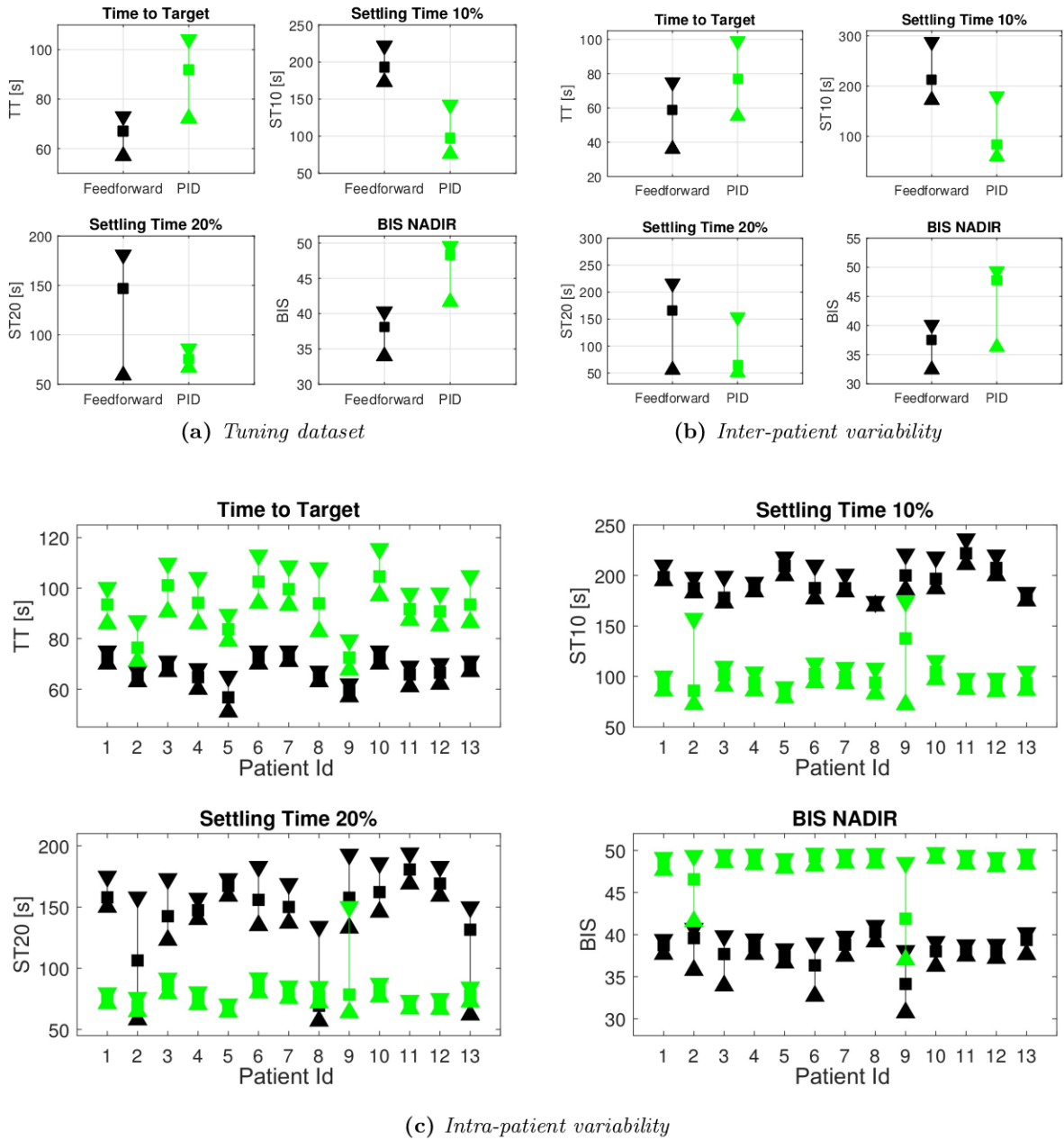
Figure 8.9: *Comparison of mean, minimum and maximum values of induction phase performance indexes obtained with the optimized feedforward control. ■ : mean value, ▲ : minimum value, ▼ : maximum value. Black line: optimized feedforward control; green line: PID controller.*

	FF/FB			**PID**		
	mean	**min.**	**max.**	**mean**	**min.**	**max.**
TT [s]	59	36	75	77	55	99
ST10 [s]	213	172	288	83	59	180
ST20 [s]	166	56	216	64	51	154
BIS − NADIR	37.53	32.44	40.13	47.76	36.31	49.33

Table 8.3: *Mean, minimum and maximum values of induction phase performance indexes obtained with the optimized feedforward control and with the PID controller on the population of 500 patients used to simulate inter-patient variability.*

8.1.3 Discussion

The proposed feedforward/feedback control system allows the achievement of the typical target required by the anesthesiologist, that is, a short anesthesia induction time avoiding excessive BIS undershoots even in the presence of inter-patient and intra-patient variability. This is achieved through a bolus, which is consistent with the clinical practice. In particular, by comparing the results obtained with those of the optimized PID controller proposed in [92], it appears that the feedforward controller allows an average reduction of 26.7% of the time-to-target on the considered test population. This reduction of time implies less stress for the patient who will lose consciousness more quickly. Moreover, from the anesthesiologist point of view, it allows to quickly secure patient's airways. The reduction of the induction time is obtained at the cost of an increase in the undershoot value, which in any case always remains within acceptable values. By observing the propofol doses provided by the feedforward action, the risk of overdosing is reduced. Indeed, in the manual practice a bolus dose of 2 mg/kg is usually administered to healthy patients during the induction phase and the doses provided by the feedforward action of the controller range from 1.28 mg/kg to 2.24 mg/kg, therefore they are consistent with those commonly used. The increase in the undershoot, in turn, causes an increase in the settling time. In fact, the value of the BIS tends to remain below the target value for a longer time than that which occurs for the PID. However, this value still remains within acceptable limits, as the BIS always returns inside the optimal range from 40 to 60 in less than 4 min. Hypnosis values slightly deeper than necessary may also be desirable in this phase as they allow blunting the stimulation due to airway instrumentation, thus preventing undesirable increases in the BIS value during this operation, with the consequent risk of awareness. Finally, it is worth noting that the calculation of the feedforward action is carried out offline based on the nominal model of the patient, before induction and not during the operation of the control system. This allows the use of the usual sampling period.

8.2 Optimized reference signal

The solution proposed in this section shares the same goals of that presented in Section 8.1. The difference is that, here, the initial bolus is obtained by applying a reference command input. The aim consists of taking the dynamics of the PID controller into account during the determination of the optimized feedforward control action to improve the robustness of the system. More specifically, also in this case, the optimization objective is to minimize the transition time of the BIS from the initial value E_0 to the target range below 60.

8.2.1 Control system architecture

The feedback control loop shown in Figure 2.2 is considered. The objective of the proposed design methodology is to determine $r(t)$ in order to generate a control action $u(t)$ that brings $y(t)$ to the target value by minimizing the transition time.

To obtain the reference signal $r(t)$, the feedforward action $u^*(t)$ must be calculated first. It is determined by following the same procedure presented in Section 8.1 for the calculation of $u_{ff}(t)$. Here the constraint $BIS_{\min}$ of Problem 8.3 is set equal to 50. Hence, optimization procedure is applied to calculate the optimal open-loop bolus $u^*(t)$ required to bring the theoretical patient BIS level $y^*(t)$ from E_0 to 50 without undershoot. Since the parameters of the model employed in the optimization procedure depend on patient's demographic data the resulting optimized feedforward bolus $u^*(t)$ is personalized. An example of the feedforward action $u^*(t)$ and of the corresponding theoretical output trajectory $y^*(t)$ obtained on the nominal model is shown in Figure 8.10. Then $u^*(t)$ is used to determine the corresponding optimized reference command input $r(t)$, which is obtained by dynamic inversion of the PID controller in the form 2.4. By doing so, in the nominal case, when $r(t)$ is given as input to the PID controller the resulting control action $u(t)$ is equal to $u^*(t)$. Since there are unavoidable model uncertainties, the actual control action $u(t)$ will be different from the theoretical one $u^*(t)$, as the PID controller will act in order to compensate for them. An example of the reference signal $r(t)$ is shown in Figure 8.11.

With the proposed technique, the tuning of the PID controller plays a key role since the reference signal depends on the controller dynamics. Although in the nominal case the obtained control variable is obviously the same optimized feedforward bolus as in Section 8.1, the approach proposed here is expected to add robustness and to make the performance of the overall control system less dependent on the tuning of the PID controller itself. In order to investigate this aspect, two different sets of PID tuning parameters have been considered. Both of them have been obtained with the optimization-based approach presented in Section 2.2.1. The first set of PID parameters is the one presented in Table 2.3 for the induction phase. The second set of PID parameters has been obtained by performing the optimization-based approach but also considering the presence of the reference command $r(t)$ in the optimization. The optimization problem has been solved with a PSO algorithm with a swarm size of 100 particles. Optimization ended when the relative change in the best IAE value over the last 50 iterations was less than 0.001. The IAE was evaluated by performing a numerical simulation of the response of each patient to drug infusion with a discretization step equal to 0.1 s. The solution is $K_p = 0.05$ mg/s, $T_i = 288$ s and $T_d = 23$ s. This represents an optimal combination of tuning parameters for the whole feedforward/feedback system since $r(t)$ depends on K_p, T_i and T_d. The performance obtained with this latter tuning can be considered as the best performance achievable with this control solution since it has been shown that the design of both the feedback and feedforward part plays a key role in achieving the required performance and therefore using a combined approach gives a significant advantage [155]. For the sake of brevity, in the rest of this section these two tuning sets will be referred to as tuning 1 and tuning 2, respectively.

For discrete-time implementation, the following form of the PID controller is used (see eq. (1.39) of [156])

$$u^*(k+1) - u^*(k) = K_1 e(k) + K_2 e(k-1) + K_3 e(k-2),\qquad(8.4)$$
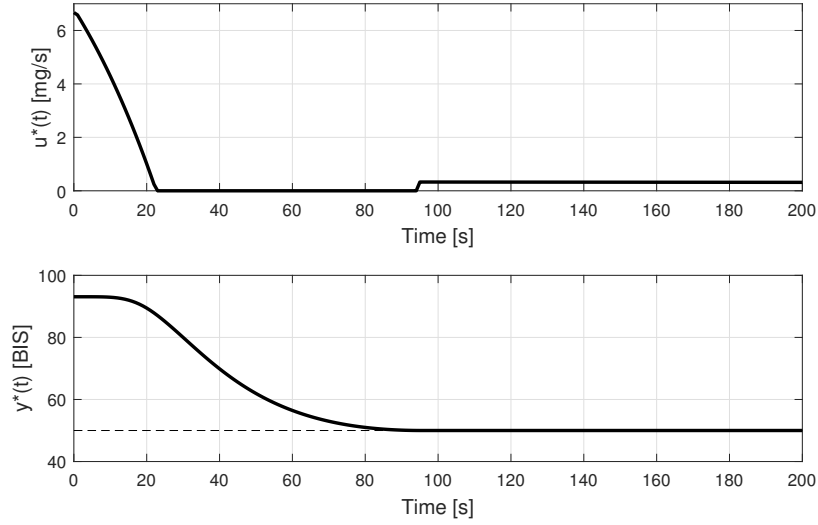
Figure 8.10: *Optimized feedforward action $u^*(t)$ and expected output trajectory $y^*(t)$ calculated for a 38 years old female patient, 169 cm, 65 kg.*
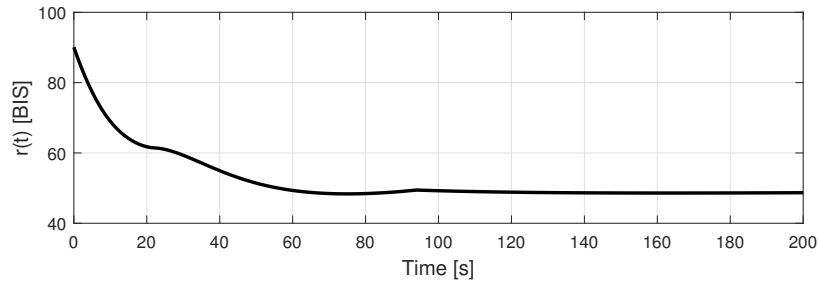
Figure 8.11: *Reference signal $r(t)$ obtained by inversion of the optimal feedforward bolus $u^*(t)$ by considering a PID controller with $K_p = 0.06$ mg/s, $T_i = 333$ s and $T_d = 34$ s.*

where $e(k) = r(k) - y^*(k)$ and

$$
\begin{aligned}
K_1 &= K_p \left(1 + \frac{T_s}{T_i} + \frac{T_d}{T_s} \right) \\
K_2 &= -K_p \left(1 + 2\frac{T_d}{T_s} \right) \\
K_3 &= K_p \frac{T_d}{T_s}.
\end{aligned}
$$

By solving 8.4 with respect to $r(k)$, the obtained r is the solution of

$$r(k) = y^*(k) + K_1^{-1} \left(u^*(k+1) - u^*(k) + K_2(y^*(k-1) - r(k-1)) + K_3(y^*(k-2) - r(k-2)) \right)$$
$$r(-1) = r(-2) = E_0.$$

The numerical solution of this difference equation gives the reference signal r.

8.2.2 Simulation results

In this section, simulation results obtained for the proposed control methodology are shown and compared with those obtained by employing the PID controller proposed in [92], which is summarized in Section 2.2.2, with a step reference input and the optimized feedforward bolus proposed in Section 8.1. For the sake of clarity, in the rest of this section it is indicated as (a) the control scheme with PID controller and a step reference signal, (b) the control system with a feedforward bolus and a feedback PID controller, (c) the novel control system with the determined reference input and the PID controller with tuning 1 and (d) the novel control system with the determined reference input and the PID controller with tuning 2. All the control systems have been initially tested on the tuning dataset of Table 2.1 and then on a much wider population obtained by means of a Monte Carlo method, in order to evaluate the controllers robustness to intra-patient and inter-patient variability.

A comparison between mean, minimum and maximum values of the performance indexes obtained on the tuning dataset is shown in Figure 8.12a. It can be observed that with all the feedforward strategies it is possible to reduce the TT with respect to the PID controller. In particular, there is a reduction of TT of 27% with (b), of 15% with (c) and of 9% with (d). However, the significant reduction in TT obtained with (b) is achieved at the expense of a significant increase in the undershoot with a consequent increment of the settling times ST10 and ST20 with respect to (a). On the other hand (c) shows only a slight increment in the minimum value of undershoot with a consequent increment in the maximum values of the settling times but the mean values remain close to that of (a). Conversely, with (d) there is a reduction also the minimum value of undershoot and the maximum values of the settling times with respect to (a).

In order to evaluate the robustness of the controller to intra-patient variability the method described in Section 2.2.1 has been applied with the statistical properties of the PK model given in [25] and the set-point response has been simulated for each of these perturbed models. By doing so each controller has been tested on a set of 6500 perturbed models and the comparison between the obtained mean, minimum and maximum values of the performance indexes is shown in Figure 8.12b. The same considerations made with the tuning dataset hold true even in case of intra-patient variability. With respect to the nominal situation there is a decrease in the BIS NADIR minimum values for each controller but it never falls below 30 thus ensuring patient's safety.

To validate the robustness with respect to inter-patient variability the method described in Section 2.2.1 is applied. The parameters of the Hill function have been generated by considering the statistical properties given in [28]. A comparison between the obtained mean, minimum and maximum values of the performance indexes is shown in Figure 8.12c. Even in presence of inter-patient variability the feedforward strategies are still able to reduce the TT with respect to the PID controller. In particular there is a reduction of TT of 23% with (b), of 12% with (c) and of 10% with (d). Even in this case the significant reduction of TT obtained with (b) is accompanied by a significant increase in the undershoot with a consequent lengthening of the settling times ST10 and ST20. Conversely, (c) and (d) are able also to reduce the undershoot and to shorten the settling times ST10 and ST20 with respect to (a). In particular, with (c) and (d) the BIS NADIR never falls below the lower threshold of the recommended range from 40 to 60. It is wort stressing that even with (a) and (b) the BIS NADIR never falls below 30, hence guaranteeing patient's safety even in presence of inter-patient variability.

(a) *Tuning dataset*　　**(b)** *Intra-patient variability*　　**(c)** *Inter-patient variability*
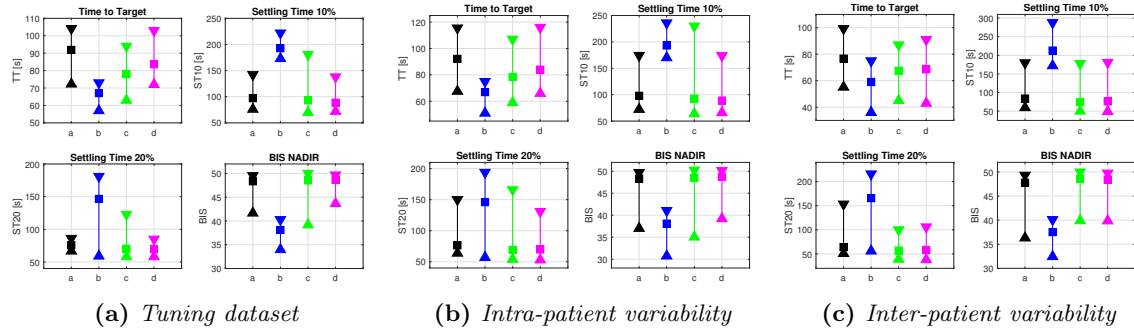
Figure 8.12: *Comparison of mean, minimum and maximum values of induction phase performance indexes obtained with the optimized reference signal.* ■ *: mean value,* ▲ *: minimum value,* ▼ *: maximum value. (a) PID controller, (b) optimized feedforward control, (c) optimized reference with tuning 1, (d) optimized reference with tuning 2.*

8.2.3 Discussion

The proposed reference input design methodology provided satisfactory control performance when tested in simulation on the considered benchmark dataset. This approach provides a satisfactory performance even in presence of both intra-patient and inter-patient variability. In particular, it always guarantees the fulfillment of the control specifications, thus a fast anesthesia induction time without causing an excessive suppression of the BIS. In order to better understand the advantages and disadvantages that the proposed control solution can provide, the results obtained have been compared with those obtained with an optimally tuned PID controller and with those obtained with an optimal feedforward bolus strategy. When tested on a benchmark dataset of 13 patients the proposed solution is able to reduce the TT required for anesthesia induction with respect to the PID controller without causing excessive undershoots of the BIS value that in fact remain comparable to those of the PID controller. Indeed, the undershoot remains limited both in its amplitude, as shown by the BIS NADIR, and in its duration, as shown by the settling times ST10 and ST20. The shortest induction time TT is obtained with the optimized feedforward bolus but at expense of a larger undershoot. Although the undershoot never reaches critical values this situation is not desirable for every patient and for all clinical procedures. Hence, the proposed reference input design method can provide a good alternative to the feedforward bolus when it is desirable to reduce as much as possible the induction time without causing excessive suppression of the BIS. These evaluations hold true even in case of intra-patient and inter-patient variability. It is also interesting to observe the behavior of the two different tuning set of the PID parameters that have been considered with the proposed reference command input. In particular the tuning 2 shows a reduced variability of the performance indexes on the dataset of 13 patients even in presence of intra-patient variability with respect to tuning 1. This difference is then no longer present when the control solutions are tested on the large population of 500 patients used to assess the inter-patient variability. Indeed in this case approximately the same performance is obtained with both the tuning sets. The difference in performance on the 13 patient dataset is justified by the fact that tuning 2 has been performed by considering the dataset itself, so this may have constituted a performance bias. The same consideration also applies to the case of intra-patient variability as the perturbed models were obtained starting from the nominal models of the same dataset of 13 patients. In the simulation on a

larger population of 500 patients for inter-patient variability, however, this bias effect is not present as both controllers are tested for the first time on a new dataset. This shows the effectiveness of the proposed solution in making the performance of the control system less dependent on the PID calibration as its dynamics is taken into account during the inversion of the feedforward signal.

8.3   Optimized robust feedforward/feedback control

In this section an optimized robust feedforward/feedback control strategy is proposed. It shares the same theoretical approach of Section 8.1 but it aims to avoid the occurrence of undershoot. This is achieved by taking into account the variability of the response to propofol administration during the calculation of the optimized feedforward bolus in such a way to provide a robust control action that avoids undershoots. In order to still guarantee a sufficiently fast response, the first part of induction is managed in open loop, while the last part is managed by an optimally tuned PID controller that compensates for variability and that smoothly drives the BIS to the target value. More in detail, the control action is divided in two parts, a feedforward action, that acts alone in the first phase of anesthesia induction, and a feedback PID action that concludes the induction. The feedforward action is given by an optimized bolus of propofol that is determined by taking into account the uncertainty of the nonlinear PD model for the effect of propofol on BIS. In particular, the bolus is obtained as the solution of a constrained minimum-time control problem in order to minimize the induction time of anesthesia while preventing the undershoot of the BIS level. Thus the patient's safety is ensured by avoiding side-effects due to drug overdosing. The PID controller is then used in order to compensate for the deviation of the BIS from the theoretical behavior caused by the effect of variability.

8.3.1   Control system architecture

The control objective consists of minimizing the anesthesia induction time by mimicking the infusion profile commonly used in the clinical practice to rapidly induce hypnosis while avoiding undershoot. Low BIS values should be avoided, especially in elderly patients, since they could provoke serious side-effects such as arterial hypotension and post-operative delirium. The feedforward/feedback control loop introduced in Section 8.1 is considered, here the feedforward and the feedback actions act at separate time intervals. The control scheme considered is shown in Figure 8.13, where the pathways of the feedforward and of the feedback actions are highlighted. The measured BIS value is indicated as $BIS(t)$ and $u_{ff}(t)$ is the feedforward action, while $u_{PID}(t)$ is the output of the PID controller. The overall control action $u(t)$ is obtained by adding these two actions and it represents the propofol infusion rate expressed in mg/s. This value is bounded between 0 mg/s and 6.67 mg/s. The BIS target value is denoted as $BIS_{sp}(t)$ and $e(t)$ is the control error calculated as $e(t) = BIS(t) - BIS_{sp}(t)$. The BIS target value is set at a constant value of 50, hence $BIS_{sp}(t) = 50$. In Section 8.1, both the feedforward and the feedback part of the control scheme work together since the beginning of induction, thus the system always works in feedback. Here, on the contrary, at the beginning of induction the system works in open-loop, indeed $u(t) = u_{ff}(t)$ for $t < 80$ s. After this time interval the loop is closed by the PID controller which completes the induction phase in feedback by smoothly driving $BIS(t)$ to the desired target $BIS_{sp}(t) = 50$. The value $t < 80$ s has been chosen on the basis of the observed time to peak effect after a

propofol bolus injection, as reported in [26]. By doing so, the PID starts to act only when the effect of the bolus on the BIS has already been observed. This control choice has been done to account for the initial *plateau* of the Hill function, as already pointed out in Section 8.1.1. This means that a low drug concentration C_e has almost no effect on the BIS. The effect becomes visible only when C_e reaches a sufficiently high value. Therefore, especially during the initial stages of induction, the BIS does not carry enough information about the actual state of the system. This aspect can be detrimental for a feedback controller and it limits the bandwidth that the controller can have without risking instability. For this reason, the feedforward controller is applied alone in open loop during the first phase of anesthesia induction. Thus, the BIS measure is ignored and the controller exploits the knowledge of the PK/PD model that is included in the feedforward action $u_{ff}(t)$. When the peak-effect is reached, the C_e is sufficiently high to exit the Hill function plateau, thus the BIS signal is more informative and then the loop is closed by the PID controller, which compensates for the deviation observed in the actual response with respect to the one predicted by the theoretical PK/PD model.

As already mentioned, the whole control scheme is composed by the combination of a feedforward and a feedback control action, hence the overall performance of the control system depends on the design of both actions. The feedforward action $u_{ff}(t)$ is calculated as explained in Section 8.1, but here Problem 8.3 is solved by requiring that the final BIS remains bounded inside the range from 40 to 80. The value of 40 has been chosen since it is the lower bound of the suggested BIS range while 80 has been chosen since BIS values below this threshold are usually associated with loss of consciousness and sedation. Thus the resulting $u_{ff}(t)$ guarantees that the patient quickly looses consciousness, thus preventing the onset of anxiety and pain, while ensuring to avoid undershoots of the BIS value below the recommended value of 40. It is worth noting that in Section 8.1 the model uncertainty has not been taken into account and the calculation of $u_{ff}(t)$ relies only on the nominal model. On the contrary, here, the uncertainty of the PK/PD model reported in [25, 28] has been considered when solving Problem 8.3. An example of the optimized feedforward bolus and of the corresponding BIS output is shown in Figure 8.14 where it is possible to observe the effect that uncertainty has on system's response. Indeed, by applying the control input shown in the bottom plot the system response can vary inside the yellow patch shown in the top plot. It can also be observed that, despite the variability, the response remains always bounded inside the desired range from 40 to 80. The great amount of uncertainty in the patient response suggests the need of a feedback controller in order to compensate for it and drive the BIS to the target value. Here, an optimally tuned PID controller has been employed as feedback controller. The PID controller is implemented in the form 2.6. An anti-windup back calculation method has also been implemented, where the value of the tracking time constant has been selected as the square root of the product of the integral and derivative time constants. The PID tuning parameters are those of Table 2.3 for the induction phase.

8.3.2 Simulation results

In this section, simulation results obtained for the proposed control methodology are shown and compared with those obtained by employing the PID controller proposed in [92], which is summarized in Section 2.2.2, and with the optimized feedforward bolus proposed in Section 8.1. For the sake of clarity, in the rest of this section (a) indicates the control scheme with PID controller only, (b) indicates the control system with a feedforward bolus proposed
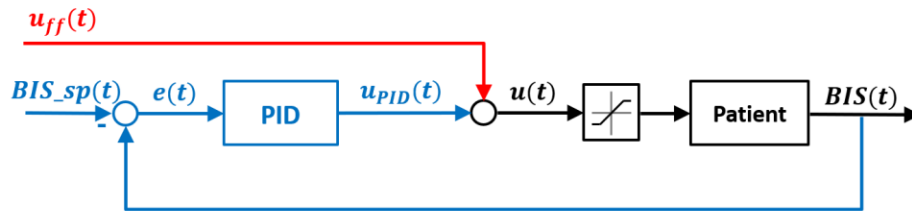
Figure 8.13: *Schematic representation of the feedforward/feedback control loop. The feedforward part is highlighted in red while the feedback part is highlighted in blue.*
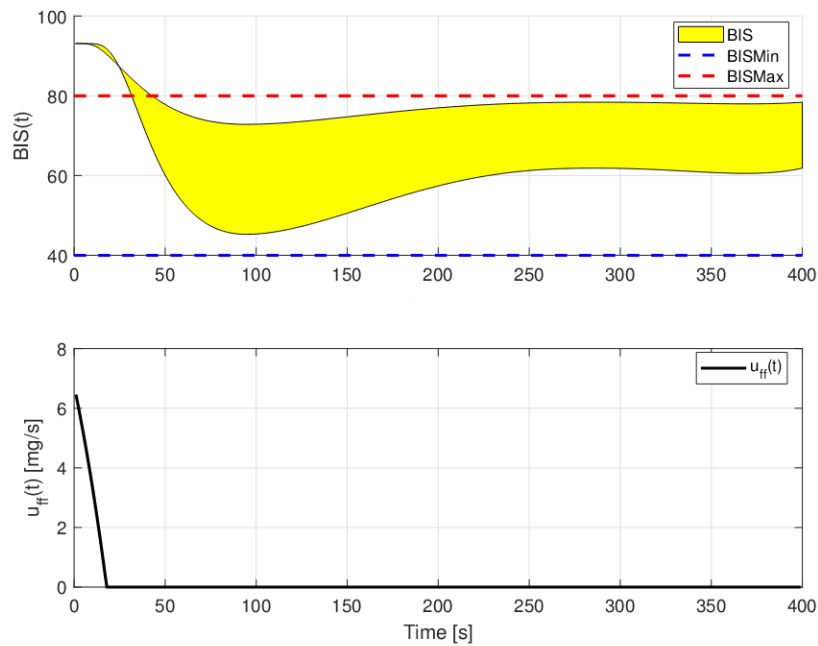
Figure 8.14: *Optimized feedforward action $u_{ff}(t)$ and expected output trajectory $BIS(t)$ subject to variability calculated for a 38 years old female patient, 169 cm, 65 kg.*

in Section 8.1 and (c) indicates the new feedforward/feedback control system proposed in this paper. All the control systems have been initially tested on the tuning dataset of Table 2.1 and then on a much wider population obtained by means of a Monte Carlo method, in order to evaluate the controllers robustness to intra-patient and inter-patient variability.

The anesthesia induction response has been first simulated on the tuning dataset. The responses obtained with the PID controller and with the proposed feedforward/feedback controller are shown in Figure 8.15 where it is possible to observe the differences between the two control strategies. In particular, the PID controller acts by giving a continuous infusion during indicatively the first 50 s. At this time interval it is possible to observe that the BIS is decreasing and the PID controller can only counteract by reducing, and eventually stopping the propofol infusion, but the amount of drug that eventually causes undershoot of the BIS value by that moment has already been injected and the controller can no longer remove it from patient body. With the new feedforward/feedback control strategy, the optimal feedforward bolus is given during the first 10-20 s of anesthesia. Then the infusion is stopped in order to give time to the feedforward bolus to act on the BIS. At 80 s, the PID controller starts working and the BIS is smoothly driven to the target value of 50.

A comparison between mean, minimum and maximum values of the performance indexes is shown in Figure 8.16a. It can be observed that with (c) it is possible to obtain a BIS-NADIR which is always close to 50, hence there is no undershoot. This is obtained at the expense of a longer TT which, however, remains acceptable as it is around 3 min and in any case it enters the recommended BIS range from 40 to 60 (ST20) in about 2.5 min which is a range of time fully compatible with the clinical practice. The system (c) also improves the values of ST10 and ST20 with respect to (b), which shows longer settling times due to a more pronounced undershoot. The controller (a) shows better performance in terms of TT, ST10 and ST20 that is obtained at the cost of a larger undershoot (which in any case remains above the recommended value of 40) with respect to (c).

In order to evaluate the robustness of the controller to intra-patient variability the method described in Section 2.2.1 has been applied with the statistical properties of the PK model given in [25] and the set-point response has been simulated for each of these perturbed models. By doing so each controller has been tested on a set of 6500 perturbed models and the comparison between the obtained mean, minimum and maximum values of the performance indexes is shown in Figure 8.16b. The same considerations made with the nominal dataset hold true even in case of intra-patient variability. It is worth noting that for the controller (c) the BIS-NADIR always remains close to 50 and the performance with respect to TT, ST10 and ST20 is not worsened, thus indicating that the proposed control solution is robust with respect to intra-patient variability.

Finally, in order to validate the robustness with respect to inter-patient variability, the method described in Section 2.2.1 is applied. The parameters of the Hill function have been generated by considering the statistical properties given in [28]. A comparison between the obtained mean, minimum and maximum values of the performance indexes is shown in Figure 8.16c. Also in this case the controller (c) demonstrates its robustness by keeping the BIS-NADIR always close to 50 without compromising the other performance indices that always remain inside clinically acceptable ranges.
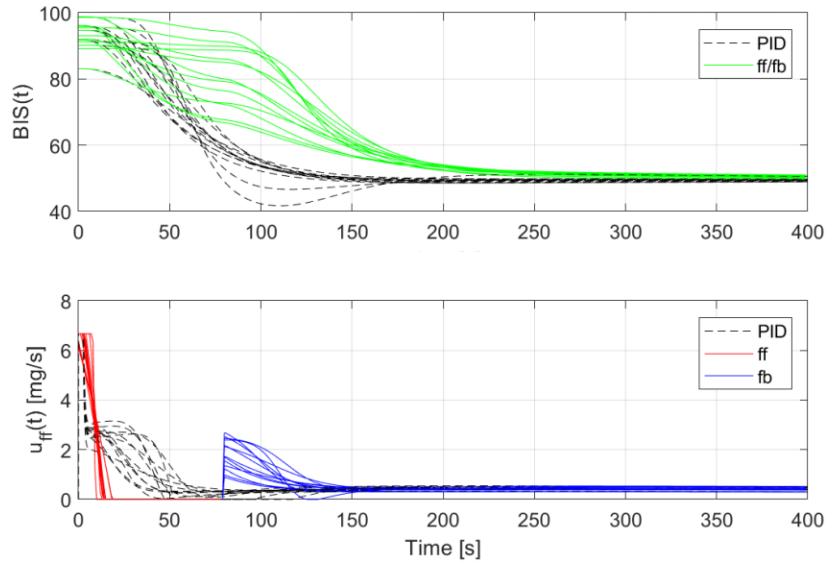
Figure 8.15: *Set-point responses for the thirteen patients of the tuning dataset obtained wit the PID controller and with the feedforward/feedback controller. In the bottom plot it is possible to observe the optimized feedforward action (solid red line) and the feedback action (solid blue line).*

(a) *Tuning dataset* **(b)** *Intra-patient variability* **(c)** *Inter-patient variability*
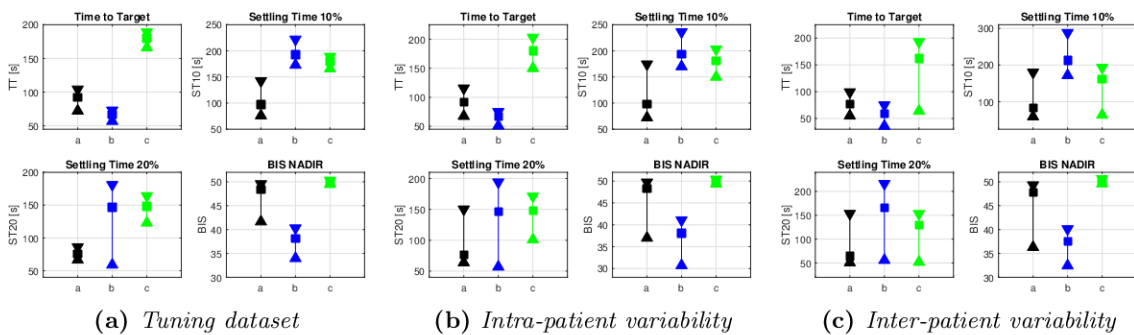
Figure 8.16: *Comparison of mean, minimum and maximum values of induction phase performance indexes obtained with the feedforward/feedback controller on the thirteen patients of the tuning dataset.* ■ *: mean value,* ▲ *: minimum value,* ▼ *: maximum value. (a) PID controller, (b) feedforward bolus, (c) feedforward/feedback controller.*

8.3.3 Discussion

The proposed feedforward/feedback controller provided satisfactory performance when tested in simulation on the considered tuning dataset. The proposed approach provides a remarkable performance even in presence of intra-patient and inter-patient variability. In particular, the fulfillment of the control specifications is always guaranteed. Anesthesia is always induced in less than 3 min without causing any undershoot of the BIS. The results obtained have been compared with those obtained with a PID controller optimally tuned for anesthesia induction and with those obtained with the optimal feedforward bolus strategy proposed in Section 8.1. This comparison allows the differences of the proposed feedforward/feedback controller with respect to the other control solutions to be highlighted. In particular (b) has been designed to obtain the fastest possible induction in those cases where an undershoot of the BIS up to 30 is admissible. It is most suited for those situations in which deep hypnosis must be reached as fast as possible, however this solution could be inadvisable for some patients. On the other hand, (c) has been designed to obtain the fastest possible induction time without causing undershoot. It is most suited for those situations in which BIS undershoot must be avoided, for example in elderly patients. Hence, these two control solutions can provide the anesthesiologist with two alternatives that both mimic the clinical practice of the propofol bolus for anesthesia induction. Although good performance is achieved with PID, it deviates from what is done in clinical practice with the initial propofol bolus. Furthermore, since the nonlinearity of the response is handled with a linear controller, the undershoot can be further reduced only by considerably reducing the controller bandwidth thus causing a significant lengthening of the TT, ST10 and ST20 which may not be acceptable for all clinical situations. The new proposed method, on the other hand, combines the advantages of a nonlinear controller, which exploits the knowledge of the model in the first instants of induction when the effect of nonlinearity is predominant, with the advantages of a simple linear PID controller, which has been tuned with an optimization procedure and it provides an overall satisfactory performance.

8.4 Conclusions

In this chapter new optimization-based feedforward/feedback control approaches specifically designed for the induction phase of BIS-guided propofol anesthesia have been presented. The proposed solutions share the same rationale, where the feedforward action consists of a propofol bolus optimized according to the patient's physical characteristics. The aim is of minimizing the induction time while avoiding excessive suppression of DoH. The feedback controller corrects the bolus dose on the basis of the measured BIS to compensate for unavoidable variability in patient's response to propofol administration. Simulation results show that these methodologies can reduce the induction time of anesthesia with respect to a standard PID controller without causing excessive BIS undershoot and properly managing uncertainty. In particular, in Section 8.1, a new feedforward control strategy has been proposed. The feedforward action is personalized for each patient and it mimics the infusion profile commonly used in clinical practice, thus making the system behavior intuitive for anesthesiologists. In order to cope with intra-patient and inter-patient variability the control system is equipped also with a PID feedback controller, whose parameters have been tuned by means of an optimization procedure. Simulation results where the method has been applied to a large number of patients models have demonstrated the robustness of the approach. The control system

proposed in this section aims to provide a solution that is particularly suitable when it is necessary to perform induction of anesthesia as fast as possible while preventing propofol overdosing.

In Section 8.2 a new reference input design strategy has been presented. The proposed solution is a modification of that proposed in Section 8.1 as it explicitly takes into account the dynamics of the feedback PID controller in the calculation of the feedforward action. Promising results have been obtained in simulation since the proposed control solution has always guaranteed the fulfillment of the control specifications even in presence of intra-patient and inter-patient variability. The comparative analysis carried out with an optimally tuned PID controller and with the optimal feedforward bolus of Section 8.1 shows that this solution can provide a valid intermediate alternative. In fact, it is particularly suitable when it is desired to reduce the induction time obtainable with the PID controller without however causing a BIS suppression level such as that of the optimal feedforward bolus.

In Section 8.3 an optimized feedforward/feedback controller has been proposed. It is based on that proposed in Section 8.1 but it has been modified by taking into account the model uncertainty in the computation of the feedforward control action. The first phase of anesthesia induction is performed in open loop and the feedback loop is closed with a PID controller only when the peak effect of the feedforward action is reached. Promising results have been obtained in simulation since the proposed feedforward/feedback controller has always guaranteed the fulfillment of the design specifications even in presence of intra-patient and inter-patient variability. In particular, the robustness shown with respect to the undershoot is remarkable. The proposed feedforward/feedback controller is particularly suited for those situation and for those patients in which anesthesia should be rapidly induced but undershoot must be avoided.

In conclusion, the encouraging results obtained in simulation with all the proposed control strategies suggest that they are suitable to be clinically tested on real patients. Their introduction in the clinical practice could be relevant since it is, in fact, important to diversify the control strategies available to the anesthesiologist so he/she can choose the most appropriate one according to his/her preferences and clinical expertise, type of surgery and patient characteristics.

Conclusions

In this thesis new developments and clinical experiments regarding closed-loop anesthesia have been presented. In Chapter 3 the clinical performance of the PID-based MISO control scheme described in Section 2.2.2 has been experimentally assessed. The control scheme has been specifically modified to implement it in the control software, described in Section 2.2.3, for run time operation. In particular, problems related to the BIS filtering and to the actuators driving signals have been tackled. After the successfully implementation of the PID-based controller in the control software, an in-vivo experiment on ten patients has been performed. The control system demonstrated its ability to satisfactory handle all anesthesia phases and to fulfill all clinical specifications for all the patients enrolled. Manual interventions from the anesthesiologist were never required. The results have also been compared to those obtained with manually controlled anesthesia to verify the applicability of the proposed control solution in the clinical practice. This comparison has shown that the behavior of the control system is sensible and consistent with the clinical practice, thus suggesting that it can be safely used in the operating room. Then, a modified version of the PID-based MISO control scheme has been proposed. It has been obtained by considering specific requirements related to the clinical practice that are relevant for the anesthesiologist. In particular, a feedforward induction sequence that comprises a bolus of propofol followed by a bolus of remifentanil has been added to the PID control action at the beginning of the induction phase. Moreover, nonzero baseline infusions of propofol and remifentanil are administered in the maintenance phase if the administered doses drop below safety thresholds. The effectiveness of this modified version has been assessed in-vivo on ten patients and the results have been compared with those of the original controller. The results obtained suggest that the proposed changes are a significant step toward the integration of the system into the clinical practice and provide measurable clinical advantages for the patients. A higher number of patients, specifically forty-two patients, have been enrolled with the modified version of the controller to further assess its clinical performance. The patients enrolled had a wide range of physical characteristics and were scheduled for procedures that greatly varied in length, body location, and level of painful stimulation. Even on this wider population, the control system showed satisfactory clinical performance during both the induction and maintenance phases for all the patients enrolled, thus demonstrating its robustness. Moreover, the control system has demonstrated satisfactory clinical performance concerning BIS, hemodynamic stability, analgesic coverage, drug consumption, emergence time, and quality of post-operative recovery. Then, an experiment has been performed on nine patients to evaluate the performance of the modified control system in terms of its ability to deal with issues that may arise during its practical use in a clinical setting. In particular, the aim was to assess the performance of the control system when additional drug boluses are manually administered by the anesthesiologist, and when different brands and models of syringe pumps are used as actuators. Results demonstrate that

the control system can handle these practical issues and it is therefore suitable to be used in the clinical practice. Moreover, the possibility for the anesthesiologist to intervene with manual boluses, if deemed as appropriate, represents a step toward the implementation of collaborative control strategies and the direct inclusion of the anesthesiologist in the control loop.

In Chapter 4 the clinical performance of the event-based MISO control scheme described in Section 2.2.2 has been experimentally assessed. The controller has been tested on fourteen patients and its performance has been compared with the standard time-based PID controller. The obtained results show that the design objective of providing noise-free infusion profiles that mimic those used by the anesthesiologist is achieved. The behavior of the resulting control system is intuitive, thus making it easier for the anesthesiologist to supervise. Moreover, the event-based control action reduces the control effort on the actuators with respect to standard time-based control. To better verify and validate this aspect, the results obtained with the event-based controller have been compared with those obtained with manually controlled anesthesia. The comparison with manual practice suggests that the system can be well integrated in clinical anesthesia.

In Chapter 5 a novel MPC methodology for anesthesia control has been proposed. By compensating the nonlinear part of the process and by using an external predictor, it fully exploits a GPC algorithm. The developed control structure is characterized by low complexity and low computational effort, so that it can be easily implemented on standard hardware and software platforms. First, the case for propofol only administration has been considered. The obtained results show that this new MPC approach provides a satisfactory performance. The performance degradation due to BIS noise has been analyzed. To assure a proper noise handling, an additional filter in the feedback loop has been included. However, its presence requires the retuning of the overall control system. A simulation study has been used to test different noise characteristics and sampling periods. The obtained results confirmed that clinical requirements can be satisfied if the noise issue is explicitly considered during the design stage. The clinical performance of the GPC controller has been experimentally evaluated on four patients. The control system performed well with respect to the clinical practice. However, the experimental results pointed out the importance of also considering the administration of remifentanil. To this end, the control system has also been extended to the case of propofol and remifentanil coadministration. The obtained simulation results have demonstrated that, also in this case, the proposed control structure gives a satisfactory performance. Moreover, the proposed approach could also be useful to provide a hybrid control system architecture that enables the manual control of the remifentanil, providing optimal control of the propofol considering the interaction between the two drugs. The control system for propofol only administration has also been extended with an event-based GPC algorithm with sensor deadband to reduce the residual noise in the control action. The obtained simulation results show that the controller meets the clinical requirements, reduces the influence of noise simultaneously reducing the quantity of drug administered with respect to the standard GPC controller. Additionally, the obtained infusion profile is similar to those of manually controlled anesthesia, thus improving the consistency of the controller behavior with the clinical practice.

In Chapter 6 the open-source simulator proposed in [49] has been used to validate the performance of the PID-based MISO control scheme described in Section 2.2.2 when the opioid-hypnotic balance is dynamically changed during anesthesia. Indeed, the control scheme gives the possibility to the anesthesiologist to manually adjust the opioid-hypnotic balance during

the time course of anesthesia. The obtained simulation results have shown the importance of this parameter that allows the anesthesiologist to select the most appropriate value depending on the patient, on the specific phase of anesthesia and on other clinical considerations. The simulator has also been used to validate the performance of the event-based PID MISO control scheme, described in Section 2.2.2, when the opioid-hypnotic balance is dynamically adjusted. To further assess the filtering capabilities of the event-based approach the simulator has been extended by including the possibility of simulating realistic noise on the BIS signal. The obtained results confirm the importance of regulating the opioid-hypnotic balance and confirm the good filtering properties of the event-based approach. Simulation results suggest that this approach for the dynamical regulation of the opioid-hypnotic balance is ready to be safely tested in-vivo.

The design of new control solutions oriented at providing a personalization of the controller based on the physical characteristics of each patient has also been investigated. In this context, in Chapter 7 a novel tuning methodology that optimizes the PID tuning parameters according to patient's demographic data has been developed. The methodology focuses on the maintenance phase of anesthesia, and it has been tested in simulation for the case of propofol only administration. The obtained results show that this methodology reduces the effect of variability on control performance with respect to a previously proposed population based PID tuning. Then, the personalized PID tuning has been extended by considering both propofol and remifentanil administration. The performance has been assessed in simulation and the good results obtained when propofol only is considered are confirmed also in this case. Also in this context, in Chapter 8 an optimized feedforward control strategy for anesthesia induction has been developed. It consists in providing an optimized induction bolus of propofol. It aims to minimize the induction time while avoiding BIS undershoots. The optimization is performed for each patient by taking into account demographic data, so that the resulting bolus is personalized. A feedback PID controller is also included in the control scheme. It corrects the bolus based on the measured BIS to compensate for the unavoidable uncertainty in the response of each patient to drug administration. Simulation results have shown that this methodology reduces the induction time of anesthesia with respect to a standard PID controller without causing excessive BIS undershoots. To increase the robustness of the solution proposed a reference (command) input design strategy has been proposed. It explicitly considers the dynamics of the feedback PID controller in the calculation of the feedforward propofol bolus. The simulation results confirm the improved robustness of the proposed approach. Moreover, an optimized feedforward/feedback control strategy has been proposed. It considers uncertainty in the computation of the feedforward propofol bolus. The first phase of anesthesia induction is performed in open loop. The feedback loop is then closed when the peak effect of the feedforward bolus is reached. Simulation results have demonstrated a remarkable robustness with respect to BIS undershoot. Thus, it is particularly suitable for those situations and for those patients in which anesthesia should be quickly induced but undershoot must be avoided.

Future work should focus on the clinical validation of the control solution of which only simulation results have been presented in this thesis. Indeed, they have been extensively validated in simulation and the results obtained suggest that they are ready to be safely employed for in-vivo studies. In particular, as regards the GPC, the clinical performance of the MISO controller should be experimentally assessed to compare the results with those of propofol only administration. Then, the effectiveness of the event-base architecture should

be experimentally evaluated. The influence of the dynamic regulation of the opioid-hypnotic balance should also be experimentally assessed. Finally the clinical effectiveness of the individualized PID tuning for anesthesia maintenance and of the optimization-based strategies for anesthesia induction should be experimentally evaluated.

Future steps in the development of automatic control in clinical anesthesia should focus on the development of MIMO control architectures that exploit the latest progresses in analgesia monitoring. For example, the use of the Conox monitor (Fresenius Kabi, Bad Homburg, DE) should be investigated as it provides two indexes, qCON and qNOX, for hypnosis and analgesia, respectively [22]. This could represent a step toward the decoupled regulation of propofol and remifentanil, thus moving from MISO to MIMO control paradigm.

For future developments of closed-loop anesthesia, the anesthesiologist-in-the-loop issue also plays a key role [6]. This thesis provided contributions in this context but much work still needs to be done.

Finally, the clinical experiments are providing a significant amount of recorded data such as EEG measurements, hemodynamic data and drugs infusion rates. These data constitute a rich database that could be useful for the development of machine learning techniques with the aim to introduce new features to improve control systems performance.

Appendix

The ACTIVA control software has been designed to safely and easily test the developed control solutions in the operating room. The block diagram of its overall architecture is shown in Figure 8.17. The software has been entirely developed in Matlab by following the object-oriented programming paradigm, thus making it modular and flexible. In particular, it has been designed by separating the hardware-dependent parts from the hardware-independent parts. The **Main** contains the management logic and it is hardware-independent. The **Drivers** are hardware-dependent because they contain all the specific commands to communicate with the medical devices and with the operating system.

More in details, the **Main** is divided in:

- **Control cycle**: it is a cyclic task that is executed at the frequency of 1 Hz. It contains all the functionality required to execute the control algorithm.
- **Auxiliary features**: manages the asynchronous routines to manage system initialization, the interactive GUI functionalities and the safety features.

The main control cycle executes the following sequential tasks:

- *Data reading*: the data message is read from the monitor through RS-232 protocol. This part of the code manages all the exceptions that can arise during serial reading/writing operations and it checks for the monitor status and message integrity.
- *Control action calculation*: the control action is calculated according to the controller selected (manual control, PID, PIDPlus or GPC). The controller type is selected by the user by means of a menu placed on the GUI. All the auxiliary features like gain scheduling, minimum infusions, boluses and ratio variations are also taken into account.
- *Actuators driving*: the calculated control actions, which are infusion rates, are sent to the infusion pumps through RS-232 protocol. This part of the code manages all the exceptions that can arise during serial reading/writing operations and it checks for the pumps status.
- *GUI update*: the GUI plots and indicators are updated.
- *Data recording*: the control system's logs are written on .csv files.

The **Drivers** are:

- *Monitor Driver*: contains all the commands and features to communicate with the Dräger Infinity Delta monitor.
- *Pump Driver*: contains all the commands and features to communicate with the infusion pumps. Two drivers have been implemented, one for the Graseby 3500 and one for the Alaris GH and they are selected according to the pump model that is selected by the user by means of a menu placed on the GUI.
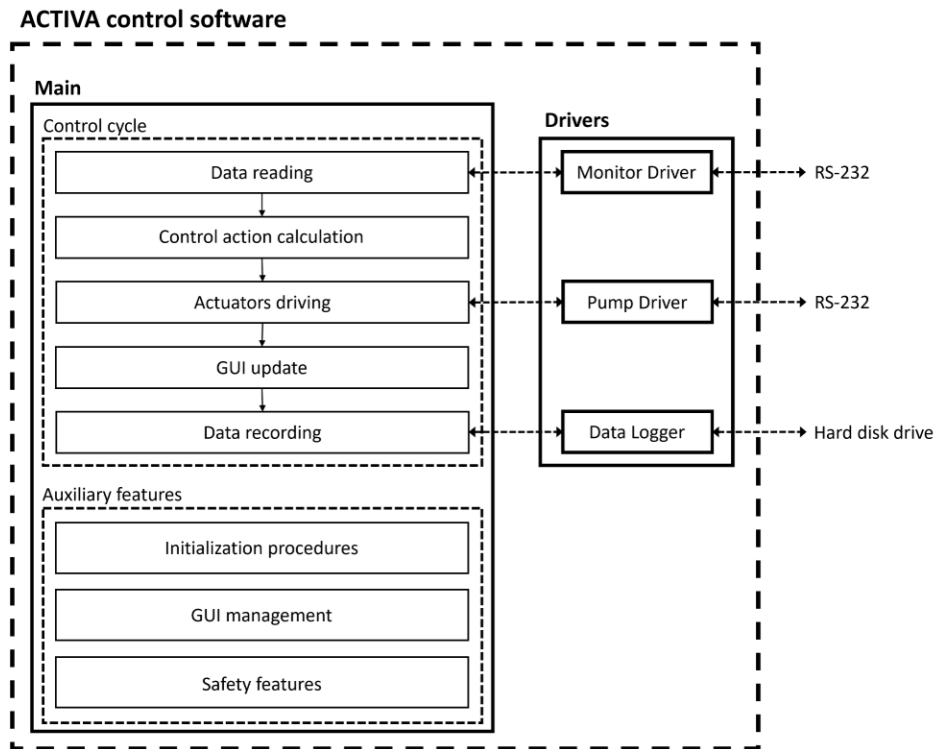
Figure 8.17: *Block diagram of the ACTIVA control software architecture.*

- *Data Logger*: contains all the commands and features to write control system's logs on the .csv files. It is hardware-dependent because it contains commands that change according to the operating system.

The only part of the control software that changes when different controllers are used is the *Control action calculation*. In particular, according to the controller type selected by the user different control routines are called according to the following switching mechanism:

```
1  % Check the controller type selected by the user
2  % Systema is a global variable that stores system information
3  switch Systema.ctrl_type
4      case 0 % Manual control
5          % Calculate the control actions according to the
               infusion rates selected by the user on the GUI
6          % Patient is a global variable that stores patient
               information
7          u_prop = (Systema.manual_propofol_infusion*Patient.
               weight)/CONSTANTS.PROPOFOL_DILUTION;
8          u_rem = (Systema.manual_remifentanil_infusion*Patient.
               weight*CONSTANTS.HOURS_TO_MINUTES_CONVERSION)/
               CONSTANTS.REMIFENTANIL_DILUTION;
9      case 1 % PID controller
10         PID_controller_routine
11     case 2 % Modified PID controller
```

```
12              Modified_PID_controller_routine
13          case 3 % Event-based PID controller
14              PID_Plus_controller_routine
15          case 4 % GPC controller
16              GPC_Propofol_controller_routine
17          otherwise
18              % Safety measure. The control actions are set to zero if
                    the controller type is not selected
19              u_prop = CONSTANTS.MINIMUM_ADMISSIBLE_PROPOFOL_INFUSION;
20              u_rem = CONSTANTS.
                    MINIMUM_ADMISSIBLE_REMIFENTANIL_INFUSION;
21  end
```

If the PID controller is selected the following routine is used:

```
1  % PID_controller_routine
2
3  % Infusion rates lower saturation set to zero
4  u_prop_min = CONSTANTS.MINIMUM_ADMISSIBLE_PROPOFOL_INFUSION;
5  u_rem_min = CONSTANTS.MINIMUM_ADMISSIBLE_REMIFENTANIL_INFUSION;
6
7  % Control actions calculation
8  % Controller.controller is an object of the class
       PID_variable_ratio_reset
9  [u_prop,u_rem] = Controller.controller.take_control_step(
       BIS_to_controller,Systema.set_point,Flags.gain_scheduling,
       u_prop_min,CONSTANTS.MAXIMUM_ADMISSIBLE_PROPOFOL_INFUSION,
       u_rem_min,CONSTANTS.MAXIMUM_ADMISSIBLE_REMIFENTANIL_INFUSION,
       Systema.ratio,reset_int,CONSTANTS.TS,CONSTANTS.
       PROPOFOL_DILUTION,CONSTANTS.REMIFENTANIL_DILUTION);
```

The PID controller is implemented in the following class:

```
1  classdef PID_variable_ratio_reset < handle
2  % PROPERTRIES
3      % VARIABLE PROPERTRIES
4      properties (GetAccess=private)
5          sum_e
6          e_before
7          u_prop_old
8          u_rem_old
9          u_filusc
10          u_filusc1
11          xk_fd
12          y7
13          y6
14          y5
15          y4
16          y3
```

```
17          y2
18          y1
19          u_der
20          cont
21          sat
22          i
23          init
24      end
25
26 % METHODS
27      methods
28          function obj = PID_variable_ratio_reset()
29          % Constructor method
30              obj.i = 0;
31              obj.cont = 0;
32              obj.e_before = 0;
33              obj.sum_e = 0;
34              obj.u_filusc = 0;
35              obj.u_filusc1 = 0;
36              obj.y7 = 0;
37              obj.y6 = 0;
38              obj.y5 = 0;
39              obj.y4 = 0;
40              obj.y3 = 0;
41              obj.y2 = 0;
42              obj.y1 = 0;
43              obj.sat = 0;
44              obj.u_prop_old = 0;
45              obj.u_rem_old = 0;
46              obj.xk_fd = 0;
47              obj.init = true;
48          end
49
50
51          function [u_prop,u_rem] = take_control_step(obj,y,sp,gs,
               u_prop_min,u_prop_max,u_rem_min,u_rem_max,ratio,reset
               ,Ts,dilution_prop,dilution_rem)
52          % Control actions calculation.
53          % INPUTS:
54          %   y = current BIS value
55          %   sp = current BIS set-point value
56          %   gs = gain scheduling flag
57          %   u_prop_min = lower bound for propofol infusion rate
58          %   u_prop_max = upper bound for propofol infusion rate
59          %   u_rem_min = lower bound for remifentanil infusion
               rate
60          %   u_rem_max = upper bound for remifentanil infusion
```

```
              rate
61     %    ratio = remifentanil/propofol ratio
62     %    reset = flag to reset the PID integral action
63     %    Ts = sampling period
64     %    dilution_prop = propofol dilution in mg/ml
65     %    dilution_rem = remifentanil dilution in ug/ml
66     % OUTPUTS:
67     %    u_prop = propofol infusion rate in ml/h
68     %    u_rem = remifentanil infusion rate in ml/h
69
70         % Initialization
71         if obj.init
72             obj.i = 0;
73             obj.cont = 0;
74             obj.e_before = 0;
75             obj.sum_e = 0;
76             obj.u_filusc = 0;
77             obj.u_filusc1 = y;
78             obj.y7 = y;
79             obj.y6 = y;
80             obj.y5 = y;
81             obj.y4 = y;
82             obj.y3 = y;
83             obj.y2 = y;
84             obj.y1 = y;
85             obj.sat = 0;
86             obj.u_prop_old = 0;
87             obj.u_rem_old = 0;
88             obj.xk_fd = 0;
89             obj.init = false;
90         end
91
92         % Moving average filter
93         obj.u_filusc = obj.y7*0.125+obj.y6*0.125+obj.y5
                *0.125+obj.y4*0.125+obj.y3*0.125+obj.y2*0.125+obj
                .y1*0.125+y*0.125;
94         BISf = obj.u_filusc;
95         obj.y7 = obj.y6;
96         obj.y6 = obj.y5;
97         obj.y5 = obj.y4;
98         obj.y4 = obj.y3;
99         obj.y3 = obj.y2;
100        obj.y2 = obj.y1;
101        obj.y1 = y;
102
103        % Control error calculation
104        e_now = obj.u_filusc - sp;
```

```
105
106                  % Gain scheduling
107                  % Induction
108                  if ~gs
109                      Kp = 0.01504*ratio^(-0.4266)-0.001895;
110                      Ti = 2.800942872321284e+02;
111                      Td = 33.246408139299504;
112                      Kp_o = 0.04532*ratio^(-0.3579)-0.01067;
113                      Ti_o = 1.718280748380050e+02;
114                      Td_o = 19.014777832998607;
115                      % Set gain scheduling index
116                      if obj.i == 2
117                          obj.i = 1;
118                      end
119                  % Maintenance
120                  else
121                      Kp_o = 0.01504*ratio^(-0.4266)-0.001895;
122                      Ti_o = 2.800942872321284e+02;
123                      Td_o = 33.246408139299504;
124                      Kp = 0.04532*ratio^(-0.3579)-0.01067;
125                      Ti = 1.718280748380050e+02;
126                      Td = 19.014777832998607;
127                      % Set gain scheduling index
128                      if obj.i == 0
129                          obj.i = 1;
130                      end
131                  end
132
133                  % Integral action calculation
134                  % Antiwindup
135                  if obj.sat == 0
136                      e_int = e_now;
137                  else
138                      e_int = 0;
139                  end
140                  % Reset
141                  if reset == 0
142                      int_e = ((e_int + obj.e_before)*Ts)/2;
143                      u_Ti = (int_e + obj.sum_e)*1/Ti;
144                      obj.sum_e = obj.sum_e + int_e;
145                  else
146                      obj.sum_e = 0;
147                      u_Ti = 0;
148                  end
149                  obj.e_before = e_int;
150
151                  % Derivative action
```

```
152         obj.u_der = (((obj.u_filusc - obj.u_filusc1)/Ts)*Td)
                ;
153         obj.u_filusc1 = obj.u_filusc;
154         % Filter on the derivative action
155         % Induction
156         if gs == 1
157             xk1_fd = 0.8601*obj.xk_fd+0.4650*obj.u_der;
158             u_Td = 0.2797*obj.xk_fd+0.0699*obj.u_der;
159             obj.xk_fd = xk1_fd;
160         else
161         % Maintenance
162             xk1_fd = 0.7676*obj.xk_fd+0.4419*obj.u_der;
163             u_Td = 0.4648*obj.xk_fd+0.1162*obj.u_der;
164             obj.xk_fd = xk1_fd;
165         end
166
167         % Control action
168         u_prop = Kp*(e_now + u_Ti + u_Td);
169         u_rem = u_prop*ratio;
170
171         % Bumpless switching mechanism
172         if (obj.i == 1)
173             utot = Kp_o*obj.sum_e/Ti_o;
174             obj.sum_e = utot*Ti/Kp;
175             u_Ti = obj.sum_e/Ti;
176             u_prop = Kp*(e_now + u_Ti + u_Td);
177             u_rem = u_prop*ratio;
178             if gs == 2
179                 obj.i = 2;
180             else
181                 obj.i = 0;
182             end
183         end
184
185         % Conversion in ml/h
186         u_prop = (u_prop/dilution_prop)*3600;
187         u_rem = (u_rem/dilution_rem)*3600;
188
189         % Saturations
190         if u_prop<u_prop_min || u_prop>u_prop_max || u_rem<
              u_rem_min || u_rem>u_rem_max
191             obj.sat = 1;
192         else
193             obj.sat = 0;
194         end
195         if u_prop < u_prop_min
196             u_prop = u_prop_min;
```

```
197                end
198                if u_prop > u_prop_max
199                    u_prop = u_prop_max;
200                end
201                if u_rem < u_rem_min
202                    u_rem = u_rem_min;
203                end
204                if u_rem > u_rem_max
205                    u_rem = u_rem_max;
206                end
207
208                % Update the control action every 5 s
209                if Ts == 1
210                    if obj.cont+1 == 5 || obj.u_prop_old == 0
211                        obj.cont = 0;
212                        obj.u_prop_old = u_prop;
213                        obj.u_rem_old = u_rem;
214                    else
215                        u_prop = obj.u_prop_old;
216                        u_rem = obj.u_rem_old;
217                        obj.cont = obj.cont+1;
218                    end
219                end
220            end
221        end
222 end
```

If the modified PID controller is selected the following routine is used:

```
1  % Modified_PID_controller_routine
2
3  % Condition for baseline infusions
4  if (BIS_to_controller >= CONSTANTS.BIS_DEADBAND_LOWER_THRESHOLD)
5      u_prop_min = CONSTANTS.MINIMUM_ADMISSIBLE_PROPOFOL_INFUSION;
6      u_rem_min = CONSTANTS.
          MINIMUM_ADMISSIBLE_REMIFENTANIL_INFUSION;
7      if (Data.ce_p <= Systema.baseline_propofol_concentration)
8          u_prop_min = (Systema.baseline_propofol_infusion*Patient
              .weight)/CONSTANTS.PROPOFOL_DILUTION;
9      end
10     if (Data.ce_r <= Systema.baseline_remifentanil_concentration
          )
11         u_rem_min = (Systema.baseline_remifentanil_infusion*
              Patient.weight*CONSTANTS.HOURS_TO_MINUTES_CONVERSION)
              /CONSTANTS.REMIFENTANIL_DILUTION;
12     end
13 else
14     u_prop_min = CONSTANTS.MINIMUM_ADMISSIBLE_PROPOFOL_INFUSION;
```

```
15      u_rem_min = CONSTANTS.
           MINIMUM_ADMISSIBLE_REMIFENTANIL_INFUSION ;
16  end
17
18  % Control actions calculation
19  % Controller.controller is an object of the class
       PID_variable_ratio_reset
20  [u_prop , u_rem] = Controller.controller.take_control_step(
       BIS_to_controller , Systema.set_point , Flags.gain_scheduling ,
       u_prop_min , CONSTANTS.MAXIMUM_ADMISSIBLE_PROPOFOL_INFUSION ,
       u_rem_min , CONSTANTS.MAXIMUM_ADMISSIBLE_REMIFENTANIL_INFUSION ,
       Systema.ratio , reset_int , CONSTANTS.TS , CONSTANTS.
       PROPOFOL_DILUTION , CONSTANTS.REMIFENTANIL_DILUTION ) ;
```

If the PIDPlus controller is selected the following routine is used:

```
1  % PID_Plus_controller_routine
2
3  % Current propofol infusion rate
4  u_sat = (Data.propofol_rate*CONSTANTS.PROPOFOL_DILUTION)/
      CONSTANTS.HOURS_TO_SECONDS_CONVERSION ;
5
6  % Event-based filter
7  % Controller.Eb_Filter_sp and Controller.Eb_Filter_dist are
      objects of the class event_based_filter
8  % Event-based filter for the induction phase
9  [yf_sp , ev_sp] = Controller.Eb_Filter_sp.take_control_step(
      BIS_to_controller , CONSTANTS.TS ) ;
10  % Event-based filter for the maintenance phase
11  [yf_dist , ev_dist] = Controller.Eb_Filter_dist.take_control_step(
      BIS_to_controller , CONSTANTS.TS ) ;
12
13  % Select the output of the filter for induction or maintenance
      according to the value of Flags.gain_scheduling
14  if Flags.gain_scheduling
15      yf = yf_dist ;
16      ev = ev_dist ;
17  else
18      yf = yf_sp ;
19      ev = ev_sp ;
20  end
21
22  % Condition for baseline infusions
23  if (yf >= CONSTANTS.BIS_DEADBAND_LOWER_THRESHOLD)
24      u_prop_min = CONSTANTS.MINIMUM_ADMISSIBLE_PROPOFOL_INFUSION ;
25      u_rem_min = CONSTANTS.
           MINIMUM_ADMISSIBLE_REMIFENTANIL_INFUSION ;
26      if (Data.ce_p <= Systema.baseline_propofol_concentration)
```

```
27          u_prop_min = (Systema.baseline_propofol_infusion*Patient
                .weight)/CONSTANTS.PROPOFOL_DILUTION;
28      end
29      if (Data.ce_r <= Systema.baseline_remifentanil_concentration
           )
30          u_rem_min=(Systema.baseline_remifentanil_infusion*
                Patient.weight*CONSTANTS.HOURS_TO_MINUTES_CONVERSION)
                /CONSTANTS.REMIFENTANIL_DILUTION;
31      end
32  else
33      u_prop_min = CONSTANTS.MINIMUM_ADMISSIBLE_PROPOFOL_INFUSION;
34      u_rem_min = CONSTANTS.
            MINIMUM_ADMISSIBLE_REMIFENTANIL_INFUSION;
35  end
36
37  % Control actions calculation
38  % Controller.PidPlus_sp and Controller.PidPlus_dist are objects
        of the class PIDPlus_variable_ratio_reset
39  [u_prop_sp,u_rem_sp] = Controller.PidPlus_sp.take_control_step(
        yf,Systema.set_point,ev,u_sat,Systema.ratio,u_prop_min,
        u_rem_min,reset_int,CONSTANTS.TS);
40  [u_prop_dist,u_rem_dist] = Controller.PidPlus_dist.
        take_control_step(yf,Systema.set_point,ev,u_sat,Systema.ratio
        ,u_prop_min,u_rem_min,reset_int,CONSTANTS.TS);
41
42  % Select the output of the PIDPlus controller for induction or
        maintenance according to the value of Flags.gain_scheduling
43  if Flags.gain_scheduling
44      u_prop = u_prop_dist;
45      u_rem = u_rem_dist;
46  else
47      u_prop = u_prop_sp;
48      u_rem = u_rem_sp;
49  end
50
51  % Conversion in ml/h
52  u_prop = (u_prop/CONSTANTS.PROPOFOL_DILUTION)*CONSTANTS.
        HOURS_TO_SECONDS_CONVERSION;
53  u_rem = (u_rem/CONSTANTS.REMIFENTANIL_DILUTION)*CONSTANTS.
        HOURS_TO_SECONDS_CONVERSION;
54
55  % Saturations
56  if u_prop<u_prop_min
57      u_prop=u_prop_min;
58  end
59  if u_prop>CONSTANTS.MAXIMUM_ADMISSIBLE_PROPOFOL_INFUSION
60      u_prop=CONSTANTS.MAXIMUM_ADMISSIBLE_PROPOFOL_INFUSION;
```

```matlab
61  end
62  if u_rem<u_rem_min
63      u_rem=u_rem_min;
64  end
65  if u_rem>CONSTANTS.MAXIMUM_ADMISSIBLE_REMIFENTANIL_INFUSION
66      u_rem=CONSTANTS.MAXIMUM_ADMISSIBLE_REMIFENTANIL_INFUSION;
67  end
```

The event-based filter is implemented in the following class:

```matlab
1   classdef event_based_filter < handle
2   % PROPERTRIES
3       % VARIABLE PROPERTRIES
4       properties (GetAccess=private)
5           init
6           ev_k1
7           tw_k1
8           t_k1
9           ys_k1
10          y_k1
11          ie_k1
12          e_k1
13          yf_e
14          Di
15          Tmax
16      end
17
18  % METHODS
19      methods
20          function obj = event_based_filter(Di,Tmax)
21          % Constructor method
22          % Inputs:
23          %   Di = event generation threshold
24          %   Tmax = event generation timeout
25              obj.init = true;
26              obj.ev_k1 = 0;
27              obj.tw_k1 = 0;
28              obj.t_k1 = 0;
29              obj.ys_k1 = 0;
30              obj.y_k1 = 0;
31              obj.ie_k1 = 0;
32              obj.e_k1 = 0;
33              obj.yf_e = 0;
34              obj.Di = Di;
35              obj.Tmax = Tmax;
36          end
37
38          function [yf,ev] = take_control_step(obj,y_k,Ts)
```

```matlab
39          % Event-based filtering
40          % INPUTS:
41          %   y_k = current BIS value
42          %   Ts = sampling period
43          % OUTPUTS:
44          %   yf = filtered BIS value
45          %   ev = flag to indicate if an event is triggered
46
47          % Initialization
48          if obj.init
49              obj.init = false;
50              obj.tw_k1 = 0;
51              obj.t_k1 = 0;
52              obj.ev_k1 = 0;
53              obj.ys_k1 = 0;
54              obj.y_k1 = 0;
55              obj.ie_k1 = 0;
56              obj.e_k1 = 0;
57              obj.yf_e = y_k;
58          end
59
60
61          if obj.ev_k1==1 % If an event occurred in the
                previous sampling instant
62              tw_k = 0;
63              obj.tw_k1 = 0;
64              obj.t_k1 = 1;
65              ys_k = 0;
66              obj.ys_k1 = 0;
67              obj.y_k1 = y_k;
68              ie_k = 0;
69              obj.ie_k1 = 0;
70              obj.e_k1 = y_k - obj.yf_e;
71          else
72              tw_k = (Ts*obj.t_k1) + obj.tw_k1;
73              obj.tw_k1 = tw_k;
74              obj.t_k1 = 1;
75              ys_k = (Ts*obj.y_k1) + obj.ys_k1;
76              obj.ys_k1 = ys_k;
77              obj.y_k1 = y_k;
78              ie_k = (Ts*obj.e_k1) + obj.ie_k1;
79              obj.ie_k1 = ie_k;
80              obj.e_k1 = y_k - obj.yf_e;
81          end
82          if tw_k~=0
83              ym_k = ys_k/tw_k;
84          else
```

```
85                    ym_k = y_k;
86                end
87
88                % Condition for event generation
89                if (abs(ie_k) > obj.Di) || (tw_k > obj.Tmax-2)
90                    ev = 1;
91                    obj.ev_k1 = ev;
92                    yf = ym_k;
93                    obj.yf_e = yf;
94                else
95                    ev = 0;
96                    obj.ev_k1 = ev;
97                    yf = obj.yf_e;
98                end
99            end
100       end
101 end
```

The PIDPlus controller is implemented in the following class:

```
1  classdef PIDPlus_variable_ratio_reset < handle
2  % PROPERTRIES
3      % VARIABLE PROPERTRIES
4      properties (GetAccess=private)
5          init
6          ev_k1
7          y_k1
8          tw_k1
9          t_k1
10         ud_k1
11         uder_k1
12         uint_k1
13         A_kp
14         B_kp
15         C_kp
16         Ti
17         Td
18     end
19
20 % METHODS
21     methods
22         function obj = PIDPlus_variable_ratio_reset(A_kp,B_kp,
               C_kp,Ti,Td)
23         % Constructor method
24         % INPUTS:
25         %   A_kp, B_kp, C_kp = coefficients to calculate the
               proportional gain Kp according to the value of ratio
26         %   Ti = integral time constant
```

```matlab
27          %    Td = derivative time constant
28              obj.init = true;
29              obj.A_kp = A_kp;
30              obj.B_kp = B_kp;
31              obj.C_kp = C_kp;
32              obj.Ti = Ti;
33              obj.Td = Td;
34              obj.ev_k1 = 0;
35              obj.y_k1 = 0;
36              obj.tw_k1 = 0;
37              obj.t_k1 = 0;
38              obj.ud_k1 = 0;
39              obj.uder_k1 = 0;
40              obj.uint_k1 = 0;
41          end
42
43          function [u_propofol,u_remifentanil] = take_control_step
               (obj,y_k,r_k,ev,u_sat,ratio,u_prop_min,u_rem_min,
               reset,Ts)
44          % Control actions calculation.
45          INPUTS:
46          %   y_k = event-based filtered BIS
47          %   r_k = current BIS setpoint value
48          %   ev = flag to indicate if an event is triggered
49          %   u_sat = current propofol infusion rate
50          %   ratio = remifentanil/propofol ratio
51          %   u_prop_min = lower bound for propofol infusion rate
52          %   u_rem_min = lower bound for remifentanil infusion
               rate
53          %   reset = flag to reset the PIDPlus integral action
54          %   Ts = sampling period
55          OUTPUTS:
56          %   u_propofol = propofol infusion rate in mg/s
57          %   u_remifentanil = remifentanil infusion rate in ug/s
58
59              % Initialization
60              if obj.init
61                  obj.init = false;
62                  obj.y_k1 = y_k;
63                  obj.tw_k1 = 0;
64                  obj.t_k1 = 0;
65                  obj.ev_k1 = 0;
66                  obj.ud_k1 = 0;
67                  obj.uder_k1 = 0;
68                  obj.uint_k1 = 0;
69              end
70
```

```matlab
71              % Calculation of the proportional gain Kp according
                    to the ratio value
72              Kp = obj.A_kp*ratio^(obj.B_kp)+obj.C_kp;
73
74              if obj.ev_k1==1 % If an event occurred in the
                    previous sampling instant
75                  tw_k = 0;
76                  obj.tw_k1 = 0;
77                  obj.t_k1 = 1;
78              else
79                  tw_k = (Ts*obj.t_k1) + obj.tw_k1;
80                  obj.tw_k1 = tw_k;
81                  obj.t_k1 = 1;
82              end
83
84              if ev==1 % If an event is triggered by the event-
                    generator
85                  % Derivative action calculation
86                  if tw_k>0
87                      ud_k = (y_k - obj.y_k1)/tw_k;
88                      obj.ud_k1 = ud_k;
89                  else
90                      ud_k = obj.ud_k1;
91                  end
92                  uder_k = ud_k*obj.Td;
93                  obj.uder_k1 = uder_k;
94                  % Integral action calculation
95                  uint_k = obj.uint_k1 + (u_sat-obj.uint_k1)*(1-
                        exp(-tw_k/obj.Ti));
96              else
97                  uder_k = obj.uder_k1;
98                  uint_k = obj.uint_k1;
99              end
100
101             % Control error calculation
102             e_k = y_k - r_k;
103
104             % Control actions calculation
105             uprop_k = Kp*(e_k+uder_k);
106             if reset
107                 uint_k = 0;
108             end
109             u_k = uprop_k + uint_k;
110             obj.ev_k1 = ev;
111             obj.y_k1 = y_k;
112             obj.uint_k1 = uint_k;
113             u_propofol = u_k;
```

```
114              u_remifentanil = u_propofol*ratio;
115          end
116      end
117 end
```

If the GPC controller is selected the following routine is used:

```
1  % GPC_Propofol_controller_routine
2
3  % Propofol infusion rate lower saturation set to zero
4  u_prop_min = CONSTANTS.MINIMUM_ADMISSIBLE_PROPOFOL_INFUSION;
5
6  % Control action calculation
7  % Controller.GPC_Propofol is an object of the class GPC_Propofol
8  [u_prop] = Controller.GPC_Propofol.take_control_step(
     BIS_to_controller,Systema.set_point,Flags.gain_scheduling,
     u_prop_min);
9
10 % Conversion in ml/h
11 u_prop = (u_prop/CONSTANTS.PROPOFOL_DILUTION)*CONSTANTS.
     HOURS_TO_SECONDS_CONVERSION;
12
13 % Manually controlled remifentanil infusion rate
14 % Conversion in ml/h
15 u_rem = (Systema.manual_remifentanil_infusion*Patient.weight*
     CONSTANTS.HOURS_TO_MINUTES_CONVERSION)/CONSTANTS.
     REMIFENTANIL_DILUTION;
16
17 % Saturations
18 if u_prop<CONSTANTS.MINIMUM_ADMISSIBLE_PROPOFOL_INFUSION
19     u_prop=CONSTANTS.MINIMUM_ADMISSIBLE_PROPOFOL_INFUSION;
20 end
21 if u_prop>CONSTANTS.MAXIMUM_ADMISSIBLE_PROPOFOL_INFUSION
22     u_prop=CONSTANTS.MAXIMUM_ADMISSIBLE_PROPOFOL_INFUSION;
23 end
24 if u_rem<CONSTANTS.MINIMUM_ADMISSIBLE_REMIFENTANIL_INFUSION
25     u_rem=CONSTANTS.MINIMUM_ADMISSIBLE_REMIFENTANIL_INFUSION;
26 end
27 if u_rem>CONSTANTS.MAXIMUM_ADMISSIBLE_REMIFENTANIL_INFUSION
28     u_rem=CONSTANTS.MAXIMUM_ADMISSIBLE_REMIFENTANIL_INFUSION;
29 end
```

The GPC controller is implemented in the following class:

```
1  classdef GPC_Propofol < handle
2  % PROPERTRIES
3      % VARIABLE PROPERTRIES
4      properties (GetAccess=private)
5          init
```

```
 6          matrix_initialization
 7          N
 8          Nu
 9          lambda
10          Tf
11          Tfr
12          Tn
13          y_t
14          Du_t1
15          u_km1
16          na
17          nb
18          nu
19          options
20          Nq
21          T
22          Aq2_1
23          Aq2_2
24          u_nb
25          CeP_na
26          r_km1
27          CePf_ref_km1
28          thetaf_km1
29          theta_km1
30          bis_km1
31          bisf_km1
32          Q
33          F
34          GP
35          G
36          Hq
37          C50
38          gamma
39          E0
40          Emax
41          A
42          B
43          Fr_num
44          Fr_den
45          Fd_num
46          Fd_den
47          Fn_num
48          Fn_den
49          Umin_sp
50          Umin_dist
51          Umax_sp
52          Umax_dist
```

```
53              DUmin_sp
54              DUmin_dist
55              DUmax_sp
56              DUmax_dist
57              Du_past
58              u_past
59              Ts
60              cont
61              u_k_old
62          end
63
64
65  % METHODS
66      methods
67          function obj = GPC_Propofol(N,Nu,lambda,Tf,Tfr,Tn)
68          % Constructor method
69          % INPUTS:
70          %   N = prediction horizon
71          %   Nu = control horizon
72          %   lambda = control effort weight
73          %   Tf = time constant of the model mismatch filter
74          %   Tfr = time constant of the setpoint filter
75          %   Tn = time constant of the noise filter
76              obj.init = true;
77              obj.matrix_initialization = false;
78              obj.N = N;
79              obj.Nu = Nu;
80              obj.lambda = lambda;
81              obj.Tf = Tf;
82              obj.Tfr = Tfr;
83              obj.Tn = Tn;
84              obj.C50 = 4.92;
85              obj.gamma = 2.69;
86              obj.E0 = 100;
87              obj.Emax = 100;
88              obj.Umin_sp = 0;
89              obj.Umin_dist = 0;
90              obj.Umax_sp = 6.67;
91              obj.Umax_dist = 4;
92              obj.DUmin_sp = -1;
93              obj.DUmin_dist = -0.4;
94              obj.DUmax_sp = 1;
95              obj.DUmax_dist = 0.4;
96              obj.options = optimset('Display','off','LargeScale',
                    'off');
97              obj.cont = 0;
98              obj.u_k_old = 0;
```

```
 99              obj.y_t = [];
100              obj.Du_t1 = [];
101              obj.u_km1 = [];
102              obj.na = [];
103              obj.nb = [];
104              obj.nu = [];
105              obj.Nq = [];
106              obj.T = [];
107              obj.Aq2_1 = [];
108              obj.Aq2_2 = [];
109              obj.u_nb = [];
110              obj.CeP_na = [];
111              obj.r_km1 = [];
112              obj.CePf_ref_km1 = [];
113              obj.thetaf_km1 = [];
114              obj.theta_km1 = [];
115              obj.bis_km1 = [];
116              obj.bisf_km1 = [];
117              obj.Q = [];
118              obj.F = [];
119              obj.GP = [];
120              obj.G = [];
121              obj.Hq = [];
122              obj.A = [];
123              obj.B = [];
124              obj.Fr_num = [];
125              obj.Fr_den = [];
126              obj.Fd_num = [];
127              obj.Fd_den = [];
128              obj.Fn_num = [];
129              obj.Fn_den = [];
130              obj.Du_past = [];
131              obj.u_past = [];
132              obj.Ts = [];
133          end
134
135      function model_initialization(obj,Ts,Age,Height,Weight,
             Gender)
136      % Initialize the GPC controller
137      % INPUTS:
138      %   Ts = sampling period
139      %   Age = patient age
140      %   Height = patient height
141      %   Weight = patient weight
142      %   Gender = patient gender
143
144          obj.Ts = Ts;
```

```matlab
145
146             % Filters calculation
147             Fr_sysd = c2d(tf(1,[obj.Tfr 1]),Ts);
148             [temp_1, temp_2] = tfdata(Fr_sysd);
149             obj.Fr_num = temp_1{1,1};
150             obj.Fr_den = temp_2{1,1};
151             if obj.Fr_num(1)==0
152                 obj.Fr_num = obj.Fr_num(1,2:end);
153             end
154             Fd_sysd = c2d(tf(1,[obj.Tf 1]),Ts,'tustin');
155             [temp_1, temp_2] = tfdata(Fd_sysd);
156             obj.Fd_num = temp_1{1,1};
157             obj.Fd_den = temp_2{1,1};
158             if obj.Fd_num(1)==0
159                 obj.Fd_num = obj.Fd_num(1,2:end);
160             end
161             Fn_sysd = c2d(tf(1,[obj.Tn 1]),Ts);
162             [temp_1, temp_2] = tfdata(Fn_sysd);
163             obj.Fn_num = temp_1{1,1};
164             obj.Fn_den = temp_2{1,1};
165             if obj.Fn_num(1)==0
166                 obj.Fn_num = obj.Fn_num(1,2:end);
167             end
168
169             % Patient model calculation
170             [PKmodelP, CPmodelP] = obj.sim_Propofol(Age,Height,
                    Weight,Gender);
171             % Converting LTI to TF representation of linear part
172             [numPK,denPK] = tfdata(PKmodelP,'v');
173             [numCP,denCP] = tfdata(CPmodelP,'v');
174             % Continous time system
175             Gnumc = conv(numCP,numPK);
176             Gdenc = conv(denCP,denPK);
177             delay = 0; % Continous time delay
178             obj.gpc_matrix_calculation(Gnumc,Gdenc,delay,Ts);
179             [~,obj.na] = size(obj.F);
180             [~,obj.nb] = size(obj.GP);
181             [~,obj.nu] = size(obj.G);
182             obj.matrix_initialization = true;
183         end
184
185         function [u_k] = take_control_step(obj,bis_k,r_k,gs,Umin
                )
186         % Control action calculation
187         % INPUTS:
188         %   bis_k = current value of the BIS
189         %   r_k = current BIS set-point value
```

```
190          %    gs = gain scheduling flag
191          %    Umin = lower bound of propofol infusion rate
192
193          coder.extrinsic('quadprog')
194          coder.extrinsic('optimset')
195
196
197          % Initialization
198          if obj.init
199              obj.init = false;
200              obj.y_t = zeros(obj.na,1);
201              obj.Du_t1 = zeros(obj.nb,1);
202              obj.Du_past = zeros(5,1);
203              obj.u_past = zeros(5,1);
204              obj.u_km1 = 0;
205              obj.Nq = ones(obj.nu,1);
206              obj.T = tril(ones(obj.nu));
207              obj.Aq2_1 = eye(obj.nu);
208              obj.Aq2_2 = -eye(obj.nu);
209              obj.u_nb = zeros(obj.nb+1,1);
210              obj.CeP_na = zeros(obj.na-1,1);
211              obj.r_km1 = r_k;
212              obj.CePf_ref_km1 = 0;
213              obj.theta_km1 = 0;
214              obj.thetaf_km1 = 0;
215              obj.bis_km1 = bis_k;
216              obj.bisf_km1 = bis_k;
217          end
218
219
220          if gs % Constraints for maintenance phase
221              Umax = obj.Umax_dist;
222              DUmin = obj.DUmin_dist;
223              DUmax = obj.DUmax_dist;
224          else  % Constraints for induction phase
225              Umax = obj.Umax_sp;
226              DUmin = obj.DUmin_sp;
227              DUmax = obj.DUmax_sp;
228          end
229
230          % Reference filter
231          CeP_ref_km1 = obj.C50*((obj.r_km1-obj.E0)/(obj.E0-
                 obj.r_km1-obj.Emax))^(1/obj.gamma);
232          CePf_ref_k = -obj.Fr_den(2)*obj.CePf_ref_km1 + obj.
                 Fr_num*CeP_ref_km1;
233
234          % BIS filter
```

```
235        bisf_k = -obj.Fn_den(2)*obj.bisf_km1 + obj.Fn_num*
               obj.bis_km1;
236        CeP_bis_k = obj.C50*((bisf_k-obj.E0)/(obj.E0-bisf_k-
               obj.Emax))^(1/obj.gamma);
237
238        % Model simulation
239        CeP_model_k = obj.B*obj.u_nb - obj.A(:,2:end)*obj.
               CeP_na;
240
241        % Model mismatch
242        theta_k = CeP_bis_k-CeP_model_k;
243
244        % Model mismatch filtering
245        thetaf_k = -obj.Fd_den(2)*obj.thetaf_km1 + obj.
               Fd_num(2)*obj.theta_km1 + obj.Fd_num(1)*theta_k;
246        y_k = thetaf_k+CeP_model_k;
247
248        obj.y_t = circshift(obj.y_t,1);
249        obj.y_t(1) = y_k;
250        w = ones(obj.N,1)*CePf_ref_k;
251        f = (obj.F*obj.y_t)+(obj.GP*obj.Du_t1);
252        Du_k = 0;
253        fq = -obj.G'*(w-f);
254        Aq = [];
255        bq = [];
256        Aq1_1 = obj.T;
257        bq1_1 = obj.Nq*Umax-obj.Nq*obj.u_km1;
258        Aq1_2 = -obj.T;
259        bq1_2 = -obj.Nq*Umin+obj.Nq*obj.u_km1;
260        Aq=[Aq; Aq1_1; Aq1_2];
261        bq=[bq; bq1_1; bq1_2];
262        bq2_1 = obj.Nq*DUmax;
263        bq2_2 = -obj.Nq*DUmin;
264        Aq = [Aq;obj.Aq2_1;obj.Aq2_2];
265        bq = [bq;bq2_1;bq2_2];
266
267        % Unconstrained solution
268        tempDu = obj.Q*(w-f);
269
270        % Control action calculation
271        temp = quadprog(obj.Hq,fq,Aq,bq,[],[],[],[],tempDu,
               obj.options);
272        if ~isempty(temp)
273            Du_k = temp(1);
274        else
275            Du_k = obj.u_km1*-1;
276        end
```

```matlab
277                u_k = obj.u_km1+Du_k;
278                if u_k<0
279                    u_k = 0;
280                end
281                obj.u_km1 = u_k;
282                obj.Du_t1 = circshift(obj.Du_t1,1);
283                obj.Du_t1(1) = Du_k;
284                obj.Du_past = circshift(obj.Du_past,1);
285                obj.Du_past(1) = Du_k;
286                obj.u_past = circshift(obj.u_past,1);
287                obj.u_past(1) = u_k;
288                obj.u_nb = circshift(obj.u_nb,1);
289                obj.u_nb(1) = u_k;
290                obj.CeP_na = circshift(obj.CeP_na,1);
291                obj.CeP_na(1) = CeP_model_k;
292                obj.r_km1 = r_k;
293                obj.CePf_ref_km1 = CePf_ref_k;
294                obj.theta_km1 = theta_k;
295                obj.thetaf_km1 = thetaf_k;
296                obj.bisf_km1 = bisf_k;
297                obj.bis_km1 = bis_k;
298
299                % Update the control action every 5 s
300                if obj.Ts==1
301                    if (obj.cont+1 == 5) || (obj.u_k_old == 0)
302                        obj.cont = 0;
303                        u_k = mean(obj.u_past);
304                        obj.u_k_old = u_k;
305                    else
306                        u_k = obj.u_k_old;
307                        obj.cont = obj.cont+1;
308                    end
309                end
310            end
311
312        function [PKmodelP, CPmodelP] = sim_Propofol(obj,Age,
                Height,Weight,Gender)
313        % Calculate patient PK/PD model
314        % INPUTS:
315        %   Age = patient age
316        %   Height = patient height
317        %   Weight = patient weight
318        %   Gender = patient gender
319        % OUTPUTS:
320        %   PKmodelP = state-space PK model
321        %   CPmodelP = state-space PD model
322
```

```
323             if Gender == 1
324                 %lean body mass (James Formula for Men)
325                 lbm = 1.1*Weight - 128*(Weight/Height)^2;
326             else % 2 per donne
327                 %lean body mass (James Formula for Women)
328                 lbm = 1.07*Weight - 148*( Weight / Height )^2;
329             end
330             %Volume of the compartments [L]
331             Vc = 4.27;
332             V2 = 18.9 - 0.391*(Age - 53);
333             V3 = 238;
334             %Clearance of compartments [L/s]
335             Cl1 = 1.89 + 0.0456*(Weight - 77) - 0.0681*(lbm -
                    59) + 0.0264*(Height - 177);
336             Cl2 = 1.29 - 0.024*(Age - 53);
337             Cl3 = 0.836;
338             %Transfer Rate of Drug [1/s]
339             % N.B. kij transfer rate from i to j
340             k10 = Cl1 / Vc / 60;
341             k12 = Cl2 / Vc / 60;
342             k13 = Cl3 / Vc / 60;
343             k21 = Cl2 / V2 / 60;
344             k31 = Cl3 / V3 / 60;
345             k41 = 0.459 / 60;
346             ke0  = k41;
347             % State space pharmacokinetic model (PK)
348             % State Matrix
349             Assp =[-(k10+k12+k13)  k21    k31;
350                       k12          -k21     0;
351                       k13           0  -k31];
352             % Input Matrix
353             Bssp = [ 1; 0; 0 ];
354             % Output Matrix
355             Cssp = [ 1 0 0 ] / Vc;
356             % Feedthrough Matrix
357             Dssp = 0;
358             PKmodelP = ss(Assp,Bssp,Cssp,Dssp);
359             % State space compartmental model (CP)
360             k1e = ke0;
361             %State Matrix
362             Aecp = -ke0;
363             %Input Matrix
364             Becp = k1e;
365             %Output Matrix
366             Cecp = 1;
367             Decp = 0;
368             CPmodelP = ss(Aecp,Becp,Cecp,Decp);
```

```
369        end
370
371        function gpc_matrix_calculation(obj,Gnumc,Gdenc,delay,Ts
              )
372        % Calculate the matrixes for the GPC controller
373        % INPUTS:
374        %   Gnumc = numerator of patient PK/PD model
375        %   Gnumc = denominator of patient PK/PD model
376        %   delay = process delay
377        %   Ts = sampling period
378
379            % A and B polynomials calculation
380            sysd = c2d(tf(Gnumc,Gdenc),Ts);
381            [temp1, temp2] = tfdata(sysd);
382            obj.B = temp1{1,1};
383            if obj.B(1)==0
384                obj.B=obj.B(1,2:end);
385            end
386            obj.A = temp2{1,1};
387            obj.na = length(obj.A);
388            obj.nb = length(obj.B);
389            % Dynamic matrix calculation
390            obj.G = zeros(obj.N,obj.Nu);
391            [g,~] = stepz(obj.B,obj.A,obj.N);
392            for k=1:obj.Nu
393                obj.G(k:end,k) = g(1:end-k+1);
394            end
395            % Free response matrices calculation
396            At = conv([1 -1],obj.A);
397            XXB = 1;
398            nbb = length(XXB);
399            div_no = obj.N+delay;
400            E_temp = zeros(div_no,1);
401            F_temp = zeros(div_no,obj.na);
402            for k=1:div_no
403                if k==1
404                    E_temp(k) = At(1);
405                    temp = (-1*At(1)*At)+[XXB zeros(1,length
                        (At)-nbb)];
406                    F_temp(k,:) = temp(2:length(temp));
407                else
408                    E_temp(k) = F_temp(k-1,1);
409                    temp = -1*F_temp(k-1,1)*At+[F_temp(k
                        -1,:) 0];
410                    F_temp(k,:) = temp(2:length(temp));
411                end
412            end
```

```matlab
                        E = zeros(div_no,div_no);
                        e = E_temp';
                        for k=1:div_no
                            E(k,1:k) = e(1:k);
                        end
                        EB=[];
                        for k=1:div_no
                            EB(k,:) = conv(E(k,:),obj.B);
                        end
                        obj.GP=[];
                        obj.F=[];
                        for n=1:obj.N
                            for m=1:n
                                GM(n,m) = EB(n+delay,n-m+1);
                                 if (delay+obj.nb>1)
                                     for l=1:delay+obj.nb-1
                                         obj.GP(n,l) = EB(n+delay,n+l);
                                     end
                                 end
                            end
                            for m=1:obj.na
                                obj.F(n,m) = F_temp(delay+n,m);
                            end
                        end
                        % K matrix calculation
                        I = eye(obj.Nu);
                        obj.Q = inv(obj.G'*obj.G+obj.lambda*I)*obj.G';
                        % K = Q(1,:);
                        obj.Hq=obj.G'*obj.G+obj.lambda*I;
            end
        end
end
```

Bibliography

[1] J. Yanase and E. Triantaphyllou. A systematic survey of computer-aided diagnosis in medicine: past and present developments. *Expert Systems with Applications*, 138:112821, 2019.

[2] M. Diana and J. Marescaux. Robotic surgery. *British Journal of Surgery*, 102(2):15–28, 2015.

[3] W. H. Chang and Y. H. Kim. Robot-assisted therapy in stroke rehabilitation. *Journal of Stroke*, 15(3):174, 2013.

[4] J. Sápi, L. Kovács, D. A. Drexler, P. Kocsis, D. Gajári, and Z. Sápi. Tumor volume estimation and quasi-continuous administration for most effective bevacizumab therapy. *PloS one*, 10(11):0142190, 2015.

[5] L. Kovács, B. Benyó, J. Bokor, and Z. Benyó. Induced L2-norm minimization of glucose-insulin system for type I diabetic patients. *Computer Methods and Programs in Biomedicine*, 102(2):105–118, 2011.

[6] M. Ghita, M. Neckebroek, C. Muresan, and D. Copot. Closed-loop control of anesthesia: survey on actual trends, challenges and perspectives. *IEEE Access*, 8:206264–206279, 2020.

[7] C. Zaouter, A. Joosten, J. Rinehart, M. M. R. F. Struys, and T. M. Hemmerling. Autonomous systems in anesthesia: where do we stand in 2020? A narrative review. *Anesthesia & Analgesia*, 130(5):1120–1132, 2020.

[8] E. Brogi, S. Cyr, R. Kazan, F. Giunta, and T. M. Hemmerling. Clinical performance and safety of closed-loop systems: a systematic review and meta-analysis of randomized controlled trials. *Anesthesia & Analgesia*, 124(2):446–455, 2017.

[9] L. Pasin, P. Nardelli, M. Pintaudi, M. Greco, M. Zambon, L. Cabrini, and A. Zangrillo. Closed-loop delivery systems versus manually controlled administration of total IV anesthesia: a meta-analysis of randomized clinical trials. *Anesthesia & Analgesia*, 124(2):456–464, 2017.

[10] M. R. Blayney. Procedural sedation for adult patients: an overview. *Continuing Education in Anaesthesia, Critical Care & Pain*, 12(4):176–180, 2012.

[11] S. Bibian, C. R. Ries, M. Huzmezan, and G. A. Dumont. Introduction to automated drug delivery in clinical anesthesia. *European Journal of Control*, 11:535–557, 2005.

[12] M. Tramer, A. Moore, and H. McQuay. Propofol anaesthesia and postoperative nausea and vomiting: quantitative systematic review of randomized controlled studies. *British Journal of Anaesthesia*, 78(3):247–255, March 1997.

[13] I. J. Rampil. A primer for EEG signal processing in anesthesia. *Anesthesiology*, 89:980–1002, 1998.

[14] T. J. Gan, P. S. Glass, A. Windsor, F. Payne, C. Rosow, P. Sebel, and P. Manberg. Bispectral index monitoring allows faster emergence and improved recovery from propofol, alfentanil, and nitrous oxide anesthesia. *Anesthesia*, 87(4):808–815, 1997.

[15] P.S. Glass, M. Bloom, L. Kearse, C. Rosow, P. Sebel, and P. Manberg. Bispectral analysis measures sedation and memory effects of propofol, midazolam, isoflurane, and alfentanil in healthy volunteers. *Anesthesiology*, 86(4):836–847, 1997.

[16] M. M. R. F. Struys, L. Versichelen, G. Byttebier, E. Mortier, A. Moerman, and G. Rolly. Clinical usefulness of the bispectral index for titrating propofol target effect-site concentration. *Anaesthesia*, 53(1):4–12, 1998.

[17] C. Rosow and P. J. Manberg. Bispectral index monitoring. *Anesthesiology Clinics of North America*, 19(4):947–966, 2001.

[18] M. M. R. F. Struys, H. Vereecke, A. Moerman, E. W. Jensen, D. Verhaeghen, N. De Neve, F. J. E. Dumortier, and E. P. Mortier. Ability of the bispectral index, autoregressive modelling with exogenous input-derived auditory evoked potentials, and predicted propofol concentrations to measure patient responsiveness during anesthesia with propofol and remifentanil. *Anesthesiology*, 99(4):802–812, 2003.

[19] S. S. Liu. Effects of bispectral index monitoring on ambulatory anesthesia: a meta-analysis of randomized controlled trials and a cost analysis. *Anesthesiology*, 101(2):311–315, 2004.

[20] T. Zikov, S. Bibian, G. A. Dumont, M. Huzmezan, and C. R. Ries. Quantifying cortical activity during general anesthesia using wavelet analysis. *IEEE Transactions on Biomedical Engineering*, 53(4):617–632, 2006.

[21] L. S. Prichep, L. D. Gugino, E. R. John, R. J. Chabot, B. Howard, H. Merkin, M. L. Tom, S. Wolter, L. Rausch, and W. J. Kox. The patient state index as an indicator of the level of hypnosis under general anaesthesia. *British journal of anaesthesia*, 92(3):393–399, 2004.

[22] E. W. Jensen, J. F. Valencia, A. Lopez, T. Anglada, M. Agusti, Y. Ramos, R. Serra, M. Jospin, P. Pineda, and P. Gambus. Monitoring hypnotic effect and nociception with two EEG-derived indices, qCON and qNOX, during general anaesthesia. *Acta Anaesthesiologica Scandinavica*, 58(8):933–941, 2014.

[23] M. Gruenewald, C. Ilies, J. Herz, T. Schoenherr, A. Fudickar, J. Höcker, and B. Bein. Influence of nociceptive stimulation on analgesia nociception index (ANI) during propofol-remifentanil anaesthesia. *British journal of Anaesthesia*, 110(6):1024–1030, 2013.

[24] R. Edry, V. Recea, Y. Dikust, and D. I. Sessler. Preliminary intraoperative valida-tion of the nociception level index: a noninvasive nociception monitor. *Anesthesiology*, 125(1):193–203, 2016.

[25] T. W. Schnider, C. F. Minto, P. L. Gambus, C. Andresen, D. B. Goodale, S. L. Shafer, and E. J. Youngs. The influence of method of administration and covariates on the pharmacokinetics of propofol in adult volunteers. *Anesthesiology*, 88:1170–1182, 1998.

[26] T. W. Schnider, C. F. Minto, S. L. Shafer, P. L. Gambus, C. Andresen, D. B. Goodale, and E. J. Youngs. The influence of age on propofol pharmacodynamics. *Anesthesiology*, 90(6):1502–1516, 1999.

[27] C. F. Minto, T. W. Schnider, T. D. Egan, E. Youngs, H. J. Lemmens, P. L. Gambus, V. Billard, J. F. Hoke, K. H. Moore, D. J. Hermann, and K. T. Muir. Influence of age and gender on the pharmacokinetics and pharmacodynamics of remifentanil. *Anesthesiology*, 86:10–23, 1997.

[28] A. L. G. Vanluchene, H. Vereecke, O. Thas, E. P. Mortier, S. L. Shafer, and M. M. R. F. Struys. Spectral entropy as an electroencephalographic measure of anesthetic drug effect. a comparison with bispectral index and processed midlatency auditory evoked response. *Anesthesiology*, 101:34–42, 2004.

[29] T. W. Bouillon, J. Bruhn, L. Radulescu, C. Andresen, T. J. Shafer, C. Cohane, and S. L. Shafer. Pharmacodynamic interaction between propofol and remifentanil regard-ing hypnosis, tolerance of laryngoscopy, bispectral index, and electroencephalographic approximate entropy. *Anesthesiology*, 100(6):1353–1372, 2004.

[30] S. E. Kern, G. Xie, J. L. White, and T. D. Egan. Opioid-hypnotic synergy. *Anesthesi-ology*, 100:1373–1381, 2004.

[31] M. M. R. F. Struys, T. De Smet, J. I. B. Glen, H. E. M. Vereecke, A. R. Absalom, and T. W. Schnider. The history of target-controlled infusion. *Anesthesia & Analgesia*, 122(1):56–69, 2016.

[32] K. Leslie, O. Clavisi, and J. Hargrove. Target-controlled infusion versus manually-controlled infusion of propofol for general anaesthesia or sedation in adults. *Cochrane database of systematic reviews*, 2008.

[33] J. B. Glen. The development of 'Diprifusor': a TCI system for propofol. *Anaesthesia*, 53(1):13–21, April 1998.

[34] A. R. Absalom, J. I. B. Glen, G. J. C. Zwart, T. W. Schnider, and M. M. R. F. Struys. Target-controlled infusion: a mature technology. *Anesthesia & Analgesia*, 122(1):70–78, 2016.

[35] I. Iselin-Chaves, R. Flaishon, P. S. Sebel, S. Howell, T. J. Gan, J. Sigl, B. Ginsberg, and P. S. Glass. The effect of the interaction of propofol and alfentanil on recall, loss of consciousness, and the bispectral index. *Anesthesia & Analgesia*, 87:949–955, 1998.

[36] B. Guignard, C. Menigaux, X. Dupont, D. Fletcher, and M. Chauvin. The effect of remifentanil on the bispectral index change and hemodynamic responses after orotra-cheal intubation. *Anesthesia & Analgesia*, 90:161–167, 2000.

[37] A. Ekman, M. L. Lindholm, C. Lennmarken, and R. Sandin. Reduction in the incidence of awareness using BIS monitoring. *Acta Anaesthesiologica Scandinavica*, 48(1):20–26, 2004.

[38] J. Bruhn, T. W. Bouillon, and S. L. Shafer. Bispectral index (BIS) and burst suppression: revealing a part of the BIS algorithm. *Journal of Clinical Monitoring and Computing*, 16(8):593–596, 2000.

[39] M. Soehle, A. Dittmann, R. K. Ellerkmann, G. Baumgarten, C. Putensen, and U. Guenther. Intraoperative burst suppression is associated with postoperative delirium following cardiac surgery: a prospective, observational study. *BMC Anesthesiology*, 15(1):61, 2015.

[40] M. L. Lindholm, S. Traff, F. Granath, S. D. Greenwald, A. Ekbom, C. Lennmarken, and R. H. Sandin. Mortality within 2 years after surgery in relation to low intraoperative bispectral index values and preexisting malignant disease. *Anesthesia & Analgesia*, 108(2):508–512, 2009.

[41] C. M. Ionescu, R. De Keyser, B. C. Torrico, T. De Smet, M. M. R. F. Struys, and J. E. Normey-Rico. Robust predictive control strategy applied for propofol dosing using BIS as a controlled variable during anesthesia. *IEEE Transactions on Biomedical Engineering*, 55(9):2161–2170, September 2008.

[42] K. Soltesz. *On automation in anesthesia*. PhD thesis, Lund University (S), 2013.

[43] G. A. Dumont, A. Martinez, and J. M. Ansermino. Robust control of depth of anesthesia. *International Journal of Adaptive Control and Signal Processing*, 23(5):435–454, 2009.

[44] J. O. Hahn, G. A. Dumont, and J. M. Ansermino. Robust closed-loop control of hypnosis with propofol using WAV$_{CNS}$ index as the controlled variable. *Biomedical Signal Processing and Control*, 7(5):517–524, 2012.

[45] D. Copot, M. Neckebroek, and C. M. Ionescu. Hypnosis regulation in presence of saturation, surgical stimulation and additional bolus infusion. *IFAC-PapersOnLine*, 51(4):84–89, 2018.

[46] T. Neff, J. Fischer, S. Fehr, O. Baenziger, and M. Weiss. Start-up delays of infusion syringe pumps. *Pediatric Anesthesia*, 11(5):561–565, 2001.

[47] E. Sarraf and J. E. Mandel. Time-delay when updating infusion rates in the graseby 3400 pump results in reduced drug delivery. *Anesthesia & Analgesia*, 118(1):145–150, 2014.

[48] C. M. Ionescu, D. Copot, and R. De Keyser. Anesthesiologist in the loop and predictive algorithm to maintain hypnosis while mimicking surgical disturbance. In *IFAC 20th World Congress*, pages 15080–15085, Toulouse, France, July 2017.

[49] C. M. Ionescu, M. Neckebroek, M. Ghita, and D. Copot. An open source patient simulator for design and evaluation of computer based multiple drug dosing control for anesthetic and hemodynamic variables. *IEEE Access*, 9:8680–8694, 2021.

[50] M. M. R. F. Struys, T. De Smet, S. Greenwald, A. R. Absalom, S. Bingé, and E. P. Mortier. Performance evaluation of two published closed-loop control systems using bispectral index monitoring. A simulation study. *Anesthesiology*, 100(3):640–647, 2004.

[51] R. G. Bickford. Automatic electroencephalographic control of general anesthesia. *Electroencephalography and Clinical Neurophysiology*, 2(1-4):93–96, 1950.

[52] D. R. Westenskow, A. M. Zbinden, D. A. Thomson, and B. Kohler. Control of end-tidal halotane concentration: Part A: anaesthesia breathing system and feedback control of gas delivery. *British Journal of Anaesthesia*, 58(5):555–562, 1986.

[53] H. Schwilden, H. Stoeckel, and J. Schuttler. Closed-loop feedback control of propofol anaesthesia by quantitative EEG analysis in humans. *British Journal of Anaesthesia*, 62(3):290–296, 1989.

[54] K. Soltesz, J. Hahn, T. Hägglund, G. A. Dumont, and J. M. Ansermino. Individualized closed-loop control of propofol anesthesia: a preliminary study. *Biomedical Signal Processing and Control*, 8(6):500–508, 2013.

[55] T. De Smet, M. M. R. F. Struys, S. Greenwald, E. P. Mortier, and S. L. Shafer. Estimation of optimal modeling weights for a bayesian-based closed-loop system for propofol administration using the bispectral index as a controlled variable: a simulation study. *Anesthesia & Analgesia*, 105(6):1629–1638, 2007.

[56] B. L. Moore, T. M. Quasny, and A. G. Doufas. Reinforcement learning versus proportional-integral-derivative control of hypnosis in a simulated intraoperative patient. *Anesthesia & Analgesia*, 112(2):350–359, 2011.

[57] R. Padmanabhan, N. Meskin, and W. M. Haddad. Closed-loop control of anesthesia and mean arterial pressure using reinforcement learning. *Biomedical Signal Processing and Control*, 22:54–64, 2015.

[58] A. R. Absalom, N. Sutcliffe, and G. N. Kenny. Closed-loop control of anesthesia using bispectral index: performance assessment in patients undergoing major orthopedic surgery under combined general and regional anesthesia. *Anesthesiology*, 96(1):67–73, 2002.

[59] A. R. Absalom and G. N. Kenny. Closed-loop control of propofol anaesthesia using bispectral index: performance assessment in patients receiving computer-controlled propofol and manually controlled remifentanil infusions for minor surgery. *British Journal of Anaesthesia*, 90(6):737–741, 2003.

[60] N. Liu, T. Chazot, A. Genty, A. Landais, A. Restoux, K. McGee, P. A. Laloë, B. Trillat, L. Barvais, and M. Fischler. Titration of propofol for anesthetic induction and maintenance guided by the bispectral index: closed-loop versus manual control: a prospective, randomized, multicenter study. *The Journal of the American Society of Anesthesiologists*, 104(4):686–695, 2006.

[61] G. D. Puri, B. Kumar, and J. Aveek. Closed-loop anaesthesia delievery system (CLADS) using bispectral index; a performance assessment study. *Anaesthesia and Intensive Care*, 35:357–362, 2007.

[62] K. Van Heusden, G. A. Dumont, K. Soltesz, C. L. Petersen, A. Umedaly, N. West, and J. M. Ansermino. Design and clinical evaluation of robust PID control of propofol anesthesia in children. *IEEE Transactions on Control Systems Technology*, 22(2):491–501, 2013.

[63] K. van Heusden, K. Soltesz, E. Cooke, S. Brodie, N. West, M. Görges, J. M. Ansermino, and G. A. Dumont. Optimizing robust PID control of propofol anesthesia for children: design and clinical evaluation. *IEEE Transactions on Biomedical Engineering*, 66(10):2918–2923, 2019.

[64] M. M. R. F Struys, T. De Smet, L. F. M. Versichelen, S. Van de Velde, R. Van den Broecke, and E. P. Mortier. Comparison of closed-loop controlled administration of propofol using bispectral index as the controlled variable versus standard practice controlled administration. *Anesthesiology*, 95(1):6–17, 2001.

[65] T. De Smet, M. M. R. F. Struys, M. Neckebroek, K. Van den Hauwe, S. Bonte, and E. P. Mortier. The accuracy and clinical feasibility of a new bayesian-based closed-loop control system for propofol administration using the bispectral index as a controlled variable. *Anesthesia & Analgesia*, 107(4):1200–1210, 2008.

[66] T. M. Hemmerling, S. Charabati, C. Zaouter, C. Minardi, and P. A. Mathieu. A randomized controlled trial demonstrates that a novel closed-loop propofol system performs better hypnosis control than manual administration. *Canadian Journal of Anesthesia*, 57(8):725–735, 2010.

[67] Y. Sawaguchi, E. Furutani, G. Shirakami, M. Araki, and K. Fukuda. A model-predictive hypnosis control system under total intravenous anesthesia. *IEEE Transactions on Biomedical Engineering*, 55(3):874–887, 2008.

[68] M. Neckebroek, C. M. Ionescu, K. Van Amsterdam, T. De Smet, P. De Baets, J. Decruyenaere, R. De Keyser, and M. M. R. F. Struys. A comparison of propofol-to-BIS post-operative intensive care sedation by means of target controlled infusion, bayesian-based and predictive control methods: an observational, open-label pilot study. *Journal of Clinical Monitoring and Computing*, 33(4):675–686, 2019.

[69] B. L. Moore, L. D. Pyeatt, V. Kulkarni, P. Panousis, K. Padrez, and A. G. Doufas. Reinforcement learning for closed-loop propofol anesthesia: a study in human volunteers. *The Journal of Machine Learning Research*, 15(1):655–696, 2014.

[70] J. A. Mendez, A. Marrero, J. A. Reboso, and A. Leon. Adaptive fuzzy predictive controller for anesthesia delivery. *Control Engineering Practice*, 46:1–9, 2016.

[71] J. A. Mendez, A. Leon, A. Marrero, J. M. Gonzalez-Cava, J. A. Reboso, J. I. Estevez, and J. F. Gomez-Gonzalez. Improving the anesthetic process by a fuzzy rule based medical decision system. *Artificial Intelligence in Medicine*, 84:159–170, 2018.

[72] C. M. Ionescu, I. Nascu, and R. De Keyser. Lessons learned from closed loops in engineering: towards a multivariable approach regulating depth of anaesthesia. *Journal of Clinical Monitoring and Computing*, 28(6):537–546, 2014.

[73] M. Janda, A. Schubert, J. Bajorat, R. Hofmockel, G. F. E. Noeldge-Schomburg, B. P. Lampe, and O. Simanski. Design and implementation of a control system reflecting the level of analgesia during general anesthesia. *Biomedizinische Technik/Biomedical Engineering*, 58(1):1–11, 2013.

[74] T. M. Hemmerling, E. Arbeid, M. Wehbe, S. Cyr, R. Taddei, and C. Zaouter. Evaluation of a novel closed-loop total intravenous anaesthesia drug delivery system: a randomized controlled trial. *British Journal of Anaesthesia*, 110(6):1031–1039, 2013.

[75] C. Zaouter, T. Hemmerling, R. Lanchon, E. Valoti, A. Remy, S. Leuillet, and A. Ouattara. The feasibility of a completely automated total IV anesthesia drug delivery system for cardiac surgery. *Anesthesia & Analgesia*, 123:885–893, 2017.

[76] T. M. Hemmerling, E. Salhab, G. Aoun, S. Charabati, and P. A. Mathieu. The analgoscore: a novel score to monitor intraoperative pain and its use for remifentanil closed-loop application. In *2007 IEEE International Conference on Systems, Man and Cybernetics*, pages 1494–1499, 2007.

[77] C. C. Peñaranda, F. D. Casas Arroyave, F. J. Gómez, P. A. Pinzón Corredor, J. M. Fernández, M. Velez Botero, J. D. Bohórquez Bedoya, and C. Marulanda Toro. Technical and clinical evaluation of a closed loop TIVA system with SEDLine spectral density monitoring: multicentric prospective cohort study. *Perioperative Medicine*, 9(1):1–11, 2020.

[78] C. M. Ionescu, R. De Keyser, and M. M. R. F. Struys. Evaluation of a propofol and remifentanil interaction model for predictive control of anesthesia induction. In *2011 50th IEEE Conference on Decision and Control and European Control Conference*, pages 7374–7379, 2011.

[79] I. Nascu, C. M. Ionescu, I. Nascu, and R. De Keyser. Evaluation of three protocols for automatic DoA regulation using propofol and remifentanil. In *2011 9th IEEE International Conference on Control and Automation (ICCA)*, pages 573–578, 2011.

[80] K. Soltesz, G. A. Dumont, K. van Heusden, T. Hägglund, and J. M. Ansermino. Simulated mid-ranging control of propofol and remifentanil using EEG-measured hypnotic depth of anesthesia. In *2012 IEEE 51st IEEE Conference on Decision and Control (CDC)*, pages 356–361, 2012.

[81] F. N. Nogueira, T. Mendonça, and P. Rocha. Controlling the depth of anesthesia by a novel positive control strategy. *Computer Methods and Programs in Biomedicine*, 114(3):87–97, 2014.

[82] F. N. Nogueira, T. Mendonça, and P. Rocha. Positive state observer for the automatic control of the depth of anesthesia - clinical results. *Computer Methods and Programs in Biomedicine*, 171:99–108, 2019.

[83] N. Liu, T. Chazot, S. Hamada, A. Landais, N. Boichut, C. Dussaussoy, B. Trillat, L. Beydon, E. Samain, and D. I. Sessler. Closed-loop coadministration of propofol and remifentanil guided by bispectral index: a randomized multicenter study. *Anesthesia & Analgesia*, 112(3):546–557, 2011.

[84] K. van Heusden, J. M. Ansermino, and G. A. Dumont. Robust MISO control of propofol-remifentanil anesthesia guided by the NeuroSENSE monitor. *IEEE Transactions on Control Systems Technology*, 26(5):1758–1770, 2017.

[85] N. West, K. van Heusden, M. Görges, S. Brodie, A. Rollinson, C. L. Petersen, G. A. Dumont, J. M. Ansermino, and R. N. Merchant. Design and evaluation of a closed-loop anesthesia system with robust control and safety system. *Anesthesia & Analgesia*, 127(4):883–894, 2018.

[86] A. Savoca and D. Manca. Control strategies in general anesthesia administration. In *Control Applications for Biomedical Engineering Systems*, pages 299–324. Academic Press, 2020.

[87] A. Savoca, K. van Heusden, D. Manca, J. M. Ansermino, and G. A. Dumont. The effect of cardiac output on the pharmacokinetics and pharmacodynamics of propofol during closed-loop induction of anesthesia. *Computer Methods and Programs in Biomedicine*, 192:105406, 2020.

[88] A. Joosten, V. Jame, B. Alexander, T. Chazot, N. Liu, M. Cannesson, J. Rinehart, and L. Barvais. Feasibility of fully automated hypnosis, analgesia, and fluid management using 2 independent closed-loop systems during major vascular surgery: a pilot study. *Anesthesia & Analgesia*, 128(6):88–92, 2019.

[89] A. Joosten, J. Rinehart, A. Bardaji, P. Van der Linden, V. Jame, L. Van Obbergh, B. Alexander, M. Cannesson, S. Vacas, N. Liu, H. Slama, and L. Barvais. Anesthetic management using multiple closed-loop systems and delayed neurocognitive recovery: a randomized controlled trial. *Anesthesiology*, 132(2):253–266, 2020.

[90] O. Kramer. *Genetic algorithms.* Springer, 2017.

[91] J. Kennedy and R. Eberhart. Particle swarm optimization. In *Proceedings of International Conference on Neural Networks*, volume 4, pages 1942–1948, 1995.

[92] F. Padula, C. Ionescu, N. Latronico, M. Paltenghi, A. Visioli, and G. Vivacqua. Optimized PID control of depth of hypnosis in anesthesia. *Computer Methods and Programs in Biomedicine*, 144:21–35, 2017.

[93] L. Merigo, F. Padula, N. Latronico, M. Paltenghi, and A. Visioli. Optimized PID control of propofol and remifentanil coadministration for general anesthesia. *Communications in Nonlinear Science and Numerical Simulation*, 72:194–212, 2019.

[94] J. Vuyk, M. J. Mertens, E. Olofsen, A. G. L. Burm, and J. G. Bovill. Propofol anesthesia and rational opioid selection determination of optimal EC50-EC95 propofol-opioid concentrations that assure adequate anesthesia and a rapid return of consciousness. *Anesthesiology*, 87(6):1549–1562, 1997.

[95] L. Merigo, F. Padula, A. Pawlowski, S. Dormido, J. L. Guzman, N. Latronico, M. Paltenghi, and A. Visioli. A model-based control scheme for depth of hypnosis in anesthesia. *Biomedical Signal Processing and Control*, 42:216–229, 2018.

[96] L. Merigo, M. Beschi, F. Padula, N. Latronico, M. Paltenghi, and A. Visioli. Event-based control of depth of hypnosis in anesthesia. *Computer Methods and Programs in Biomedicine*, 147:63–83, 2017.

[97] L. Merigo, M. Beschi, F. Padula, and A. Visioli. A noise-filtering event generator for PIDPlus controllers. *Journal of the Franklin Institute*, 355(2):774–802, 2018.

[98] T. Blevins, M. Nixon, and W. Wojsznis. PID control using wireless measurements. In *Proceedings American Control Conference*, pages 790–795, Portland, Oregon, 2014.

[99] L. Merigo, F. Padula, N. Latronico, M. Paltenghi, and A. Visioli. Event-based control tuning of propofol and remifentanil coadministration for general anaesthesia. *IET Control Theory & Applications*, 14(19):2995–3008, 2020.

[100] M. Schiavo, F. Padula, N. Latronico, L. Merigo, M. Paltenghi, and A. Visioli. First experiments of anesthesia control with optimized PID tuning. *IFAC-PapersOnLine*, 53(2):16125–16130, 2020.

[101] M. Schiavo, F. Padula, N. Latronico, L. Merigo, M. Paltenghi, and A. Visioli. Performance evaluation of an optimized PID controller for propofol and remifentanil coadministration in general anesthesia. *IFAC Journal of Systems and Control*, 15:100121, 2021.

[102] M. Schiavo, F. Padula, N. Latronico, M. Paltenghi, and A. Visioli. A modified PID-based control scheme for depth-of-hypnosis control: design and experimental results. *Computer Methods and Programs in Biomedicine*, 219:106763, 2022.

[103] M. Schiavo, F. Padula, N. Latronico, M. Paltenghi, and A. Visioli. On the practical use of a PID-based control scheme for automatic control of general anesthesia. In *2022 IEEE Conference on Control Technology and Applications (CCTA)*, pages 1105–1110, 2022.

[104] M. Schiavo, F. Padula, N. Latronico, M. Paltenghi, and A. Visioli. Experimental results of an event-based PID control system for propofol and remifentanil coadministration. *Control Engineering Practice*, 131:105384, 2023.

[105] A. Pawlowski, M. Schiavo, N. Latronico, M. Paltenghi, and A. Visioli. Linear MPC for anesthesia process with external predictor. *Computers & Chemical Engineering*, 161:107747, 2022.

[106] A. Pawlowski, M. Schiavo, N. Latronico, M. Paltenghi, and A. Visioli. MPC for propofol anesthesia: the noise issue. In *2022 IEEE Conference on Control Technology and Applications (CCTA)*, pages 1087–1092, 2022.

[107] A. Pawlowski, M. Schiavo, N. Latronico, M. Paltenghi, and A. Visioli. Experimental results of an MPC strategy for total intravenous anesthesia. *IEEE Access*, 11:32743–32751, 2023.

[108] A. Pawlowski, M. Schiavo, N. Latronico, M. Paltenghi, and A. Visioli. Model predictive control using MISO approach for drug co-administration in anesthesia. *Journal of Process Control*, 117:98–111, 2022.

[109] A. Pawlowski, M. Schiavo, N. Latronico, M. Paltenghi, and A. Visioli. Event-based MPC for propofol administration in anesthesia. *Computer Methods and Programs in Biomedicine*, 229:107289, 2023.

[110] M. Schiavo, F. Padula, N. Latronico, M. Paltenghi, and A. Visioli. Optimized PID controller for propofol and remifentanil coadministration: influence of opioid-hypnotic balance. *IFAC-PapersOnLine*, 54(15):13–18, 2021.

[111] M. Schiavo, F. Padula, N. Latronico, M. Paltenghi, and A. Visioli. Individualized PID tuning for maintenance of general anesthesia with propofol. *IFAC-PapersOnLine*, 54(3):679–684, 2021.

[112] M. Schiavo, F. Padula, N. Latronico, M. Paltenghi, and A. Visioli. Individualized PID tuning for maintenance of general anesthesia with propofol and remifentanil coadministration. *Journal of Process Control*, 109:74–82, 2022.

[113] M. Schiavo, L. Consolini, M. Laurini, N. Latronico, M. Paltenghi, and A. Visioli. Optimized feedforward control of propofol for induction of hypnosis in general anesthesia. *Biomedical Signal Processing and Control*, 66:102476, 2021.

[114] M. Schiavo, L. Consolini, M. Laurini, N. Latronico, M. Paltenghi, and A. Visioli. Optimized reference signal for induction of general anesthesia with propofol. *IFAC-PapersOnLine*, 54(15):7–12, 2021.

[115] M. Schiavo, L. Consolini, M. Laurini, N. Latronico, M. Paltenghi, and A. Visioli. Optimized robust combined feedforward/feedback control of propofol for induction of hypnosis in general anesthesia. In *2021 IEEE International Conference on Systems, Man, and Cybernetics (SMC)*, pages 1266–1271, 2021.

[116] M. Hosseinzadeh, G. A. Dumont, and E. Garone. Constrained control of depth of hypnosis during induction phase. *IEEE Transactions on Control Systems Technology*, 28(6):2490–2496, 2019.

[117] K. van Heusden, N. West, A. Umedaly, J. M. Ansermino, R. N. Merchant, and G. A. Dumont. Safety, constraints and anti-windup in closed-loop anesthesia. *IFAC Proceedings Volumes*, 47(3):6569–6574, 2014.

[118] M. Yousefi, K. van Heusden, I. M. Mitchell, J. M. Ansermino, and G. A. Dumont. A formally-verified safety system for closed-loop anesthesia. *IFAC-PapersOnLine*, 50(1):4424–4429, 2017.

[119] N. Eskandari, K. van Heusden, and G. A. Dumont. Extended habituating model predictive control of propofol and remifentanil anesthesia. *Biomedical Signal Processing and Control*, 55:101656, 2020.

[120] F. L. Roberts, J. Dixon, G. T. R. Lewis, R. M. Tackley, and C. Prys-Roberts. Induction and maintenance of propofol anaesthesia: a manual infusion scheme. *Anaesthesia*, 43:14–17, 1988.

[121] A. F. Nimmo, A. R. Absalom, O. Bagshaw, A. Biswas, T. M. Cook, A. Costello, S. Grimes, D. Mulvey, S. Shinde, and T. Whitehouse. Guidelines for the safe practice of total intravenous anaesthesia (TIVA). *Anaesthesia*, 74(2):211–224, 2019.

[122] P. R. Hinton. *Statistics explained.* Routledge, 2014.

[123] G. Besch, N. Liu, E. Samain, C. Pericard, N. Boichut, M. Mercier, T. Chazot, and S. Pili-Floury. Occurrence of and risk factors for electroencephalogram burst suppression during propofol-remifentanil anaesthesia. *British Journal of Anaesthesia*, 107(5):749–756, 2011.

[124] B. A. Fritz, P. L. Kalarickal, H. R. Maybrier, M. R. Muench, D. Dearth, Y. Chen, K. E. Escallier, A. B. Abdallah, N. Lin, and M. S. Avidan. Intraoperative electroencephalogram suppression predicts postoperative delirium. *Anesthesia & Analgesia*, 122(1):234, 2016.

[125] H. C. Lee, H. G. Ryu, Y. Park, S. B. Yoon, S. M. Yang, H. W. Oh, and C. W. Jung. Data driven investigation of bispectral index algorithm. *Scientific Reports*, 9(1):1–8, 2019.

[126] M. Hosseinzadeh, K. van Heusden, M. Yousefi, G. A. Dumont, and E. Garone. Safety enforcement in closed-loop anesthesia. a comparison study. *Control Engineering Practice*, 105:104653, 2020.

[127] M. Yousefi, K. van Heusden, N. West, I. M. Mitchell, J. M. Ansermino, and G. A. Dumont. A formalized safety system for closed-loop anesthesia with pharmacokinetic and pharmacodynamic constraints. *Control Engineering Practice*, 84:23–31, 2019.

[128] R. S. Twersky, B. Jamerson, D. S. Warner, L. A. Fleisher, and S. Hogue. Hemodynamics and emergence profile of remifentanil versus fentanyl prospectively compared in a large population of surgical patients. *Journal of Clinical Anesthesia*, 13(6):407–416, 2001.

[129] A. Krieger and E. N. Pistikopoulos. Model predictive control of anesthesia under uncertainty. *Computers and Chemical Engineering*, 71:699–707, 2014.

[130] S. Ntouskas and H. Sarimveis. A robust model predictive control framework for the regulation of anesthesia process with propofol. *Optimal Control Applications and Methods*, 42(4):965–986, 2021.

[131] I. Naşcu, R. Oberdieck, and E. N. Pistikopoulos. An explicit hybrid model predictive control strategy for intravenous anaesthesia. *IFAC-PapersOnLine*, 48(20):58–63, 2015.

[132] I. Naşcu, R. Oberdieck, and E. N. Pistikopoulos. Explicit hybrid model predictive control strategies for intravenous anaesthesia. *Computers and Chemical Engineering*, 106:814–825, 2017.

[133] H. Chang, A. Krieger, A. Astolfi, and E. N. Pistikopoulos. Robust multi-parametric model predictive control for LPV systems with application to anaesthesia. *Journal of Process Control*, 24(10):1538–1547, 2014.

[134] I. Naşcu and E. N. Pistikopoulos. Modeling, estimation and control of the anaesthesia process. *Computers and Chemical Engineering*, 107:318–332, 2017.

[135] E. F. Camacho and A. C. Bordons. *Model predictive control.* Springer science and business media, 2013.

[136] A. Pawlowski, L. Merigo, J. L. Guzman, and A. Visioli. Event-based GPC for depth of hypnosis in anesthesia for efficient use of propofol. In *3rd International Conference on Event-Based Control, Communication and Signal Processing (EBCCSP)*, 2017.

[137] D. Ingole and M. Kvasnica. FPGA implementation of explicit model predictive control for closed loop control of depth of anesthesia. *IFAC-PapersOnLine*, 48(23):483–488, 2015.

[138] A. Pawlowski, L. Merigo, J. L. Guzmán, S. Dormido, and A. Visioli. Two-degree-of-freedom control scheme for depth of hypnosis in anesthesia. *IFAC-PapersOnLine*, 51(4):72–77, 2018.

[139] A. Pawlowski, J. L. Guzmán, J. E. Normey-Rico, and M. Berenguel. Improving feedforward disturbance compensation capabilities in generalized predictive control. *Journal of Process Control*, 22(3):527–539, 2012.

[140] M. J. Khodaei, N. Candelino, A. Mehrvarz, and N. Jalili. Physiological closed-loop control (PCLC) systems: Review of a modern frontier in automation. *IEEE Access*, 8:23965–24005, 2020.

[141] W. M. Haddad, K. Y. Volyanskyy, J. M. Bailey, and J. J. Im. Neuroadaptive output feedback control for automated anesthesia with noisy EEG measurements. *IEEE Transactions on Control Systems Technology*, 19(2):311–326, 2010.

[142] S.Tarbouriech, I. Queinnec, G. Garcia, and M. Mazerolles. Dead-zone observer-based control for anesthesia subject to noisy BIS measurement. *IFAC-PapersOnLine*, 53(2):16191–16196, 2020.

[143] S. Khosravi. *Constrained model predictive control of hypnosis*. PhD thesis, University of British Columbia, 2015.

[144] S. Hall. Real-time projected gradient based NMPC with an application to anesthesia control. Master's thesis, ETH Zurich, 2020.

[145] C. F. Minto, T. W. Schnider, T. G. Short, K. M. Gregg, A. Gentilini, and S. L. Shafer. Response surface model for anesthetic drug interactions. *The Journal of the American Society of Anesthesiologists*, 92(6):1603–1616, 2000.

[146] A. Pawlowski, J. L. Guzmán, J. E. Normey-Rico, and M. Berenguel. A practical approach for generalized predictive control within an event-based framework. *Computers and Chemical Engineering*, 41:52–66, 2012.

[147] K. van Heusden, J. M. Ansermino, and G. A. Dumont. Performance of robust PID and Q-design controllers for propofol anesthesia. *IFAC-PapersOnLine*, 51(4):78–83, 2018.

[148] N. West, G. A. Dumont, K. van Heusden, C. L. Petersen, S. Khosravi, K. Soltesz, A. Umedaly, E. Reimer, and J. M. Ansermino. Robust closed-loop control of induction and maintenance of propofol anesthesia in children. *Pediatric Anesthesia*, 23(8):712–719, 2013.

[149] G. A. Dumont, N. Liu, C. Petersen, T. Chazot, M. Fischler, and J. M. Ansermino. Closed-loop administration of propofol guided by the neurosense: clinical evaluation using robust proportional-integral-derivative design. In *American Society of Anesthesiologists (ASA) Annual Meeting*, page 48, 2011.

[150] F. Padula, C. Ionescu, N. Latronico, M. Paltenghi, A. Visioli, and G. Vivacqua. Inversion-based propofol dosing for intravenous induction of hypnosis. *Communications in Nonlinear Science and Numerical Simulation*, 39:481–494, 2016.

[151] M. Hosseinzadeh, K. van Heusden, G. A. Dumont, and E. Garone. An explicit reference governor scheme for closed-loop anesthesia. In *2019 18th European Control Conference (ECC)*, pages 1294–1299, Naples, Italy, June 2019.

[152] W. M. Haddad, V. S. Chellaboina, and Q. Hui. *Nonnegative and Compartmental Dynamical Systems*. Princeton University Press, 2010.

[153] LLC Gurobi Optimization. Gurobi optimizer reference manual. `http://www.gurobi.com`, 2020.

[154] K. J. Astrom, P. Hagander, and J. Sternby. Zeros of sampled systems. *Automatica*, 20(1):31 – 38, 1984.

[155] S. Piccagli and A. Visioli. PID tuning rules for minimum-time rest-to-rest transitions. *IFAC Proceedings Volumes*, 44(1):5771–5776, 2011.

[156] A. Visioli. *Practical PID Control*, chapter Anti-windup strategies. Springer, 2006.

Glossary of medical terminology

Airway instrumentation refers to the use of medical devices to establish and maintain a patient's airway for breathing purposes.

Analgesia refers to the reduction or absence of pain sensation.

Antiemetic is a drug used to treat nausea and vomiting.

Bispectral Index Scale (BIS) is one of the most widespread and clinically accepted indicator of depth of hypnosis. It is based on the bispectral analysis of a frontal electroencephalogram and it provides an estimation of the depth of hypnosis by means of a dimensionless number which varies from 0 (absence of brain activity) to 100 (patient fully awake). During general anesthesia this index should be kept inside the range 40-60 for most kinds of surgeries.

Blood pressure (BP) refers to the force exerted by circulating blood against the walls of the arteries.

Body mass index (BMI) is a numerical value calculated based on a person's weight and height.

Bolus refers to a single, large drug dose that is administered rapidly to produce a quick and powerful clinical effect.

Bradycardia is a medical condition characterized by an abnormally slow heart rate. It can lead to inadequate blood flow which can cause organs damage.

Burst suppression (BS) refers to a pattern in electroencephalography readings, where bursts of high-frequency activity are followed by periods of electrical silence or suppression. It can be an indicator of anesthetic overdose.

Burst suppression ratio (BSR) is a measure that quantifies the degree of suppression in the electroencephalography readings. It is the ratio of the duration of the suppression period to the total time of the recording.

Cardiac output (CO) refers to the amount of blood pumped by the heart in a minute.

Curare is a drug used to induce paralysis.

Depth of hypnosis (DoH) refers to the level of consciousness and responsiveness of a patient who is undergoing anesthesia.

Diastolic blood pressure (BP$_d$) refers to the lowest level of pressure exerted on the walls of the arteries when the heart is relaxed between beats and refilling with blood.

Electrocautery device is a medical device that uses the heat generated from an electric current to control bleeding during surgery.

Endotracheal tube is a medical device used to maintain a patient's airway during general anesthesia. It consists of a tube that is inserted through the mouth or nose into the trachea.

Ephedrine is a vasopressor drug that can be used to treat hypotension during surgery. It works by stimulating the sympathetic nervous system, which increases heart rate and blood pressure.

Etilefrine is a cardiac stimulant used to treat hypotension during surgery.

Fentanyl is a potent synthetic opioid that is used as analgesic drug.

General anesthesia is a pharmacologically induced, temporary and reversible state that provokes on the patient the inhibition of sensitivity, consciousness, and pain.

Hemostasis refers to the control of bleeding during surgery to prevent excessive blood loss, to maintain a clear surgical field and to reduce the risk of complications.

Hypertension is a medical condition characterized by high blood pressure levels in the arteries. It can lead to damage of the arteries and other organs.

Hypotension is a medical condition characterized by low blood pressure levels in the arteries. It can lead to inadequate blood flow which can cause organs damage.

Infusion pump is a medical device used to deliver intravenous drugs in a controlled manner.

Intubation is a medical procedure in which an endotracheal tube is inserted into a patient's airway through their mouth or nose.

Laryngeal mask is a medical device used to maintain a patient's airway during general anesthesia. It consists of a tube with a cuff that is inserted into the patient's throat and positioned over the larynx.

Lean body mass (LBM) refers to the total weight of a person's body minus the weight of their fat stores.

Mean arterial pressure (MAP) is the average pressure exerted by the blood on the walls of the arteries over the entire cardiac cycle, taking into account both the systolic and diastolic pressures as well as the length of time that the blood spends in each phase. MAP is calculated as the diastolic pressure plus one-third of the difference between the systolic and diastolic pressures.

Mean blood pressure (BP_m) is the average pressure exerted by the blood on the walls of the arteries over the course of one complete cardiac cycle, calculated as the sum of the systolic pressure and twice the diastolic pressure, divided by three. It represents an overall measure of blood pressure in the arteries during a single heartbeat.

Mechanical ventilation refers to the use of a medical device, such as a ventilator, to assist or replace a patient's breathing.

Peripheral oxygen saturation (SpO_2) is a measure of the amount of oxygen being carried in the bloodstream.

Post-operative delirium is a side effect of anesthesia. It is a form of delirium that manifests in patients between one and three days after anesthesia.

Post-operative nausea and vomiting (PONV) is a common side effect of anesthesia. It refers to the feeling of sickness and vomiting that some patients experience after undergoing anesthesia.

Post-operative pain is the pain perceived by the patient after surgery.

Post-operative sedation is a common side effect of anesthesia. It is a residual sedation that affects the patient after the anesthesia emergence phase.

Propofol is a short-acting intravenous hypnotic drug. It has a rapid onset that produces a quick loss of consciousness and a short duration of effect.

Ramsay Agitation Sedation Score (RASS) is a medical scale used to measure the agitation or sedation level of a patient.

Remifentanil is a potent, short-acting intravenous analgesic drug. It acts quickly, with a rapid onset of action and a short duration of effect.

Systolic blood pressure (BP_s) refers to the highest level of pressure exerted on the walls of the arteries when the heart contracts and pumps blood out to the rest of the body.

Tachycardia is a medical condition characterized by an abnormally fast heart rate. It can lead to heart muscle damage and it can increase the risk of bleeding and other complications during surgery.

Total intravenous anesthesia is an anesthesia technique in which drugs are delivered entirely through an intravenous access.

Vasoactive medications are drugs that have an effect on the blood vessels, causing them to either dilate or constrict. They are commonly used in the treatment of hypotension and hypertension.

Vasopressors are drugs that cause the blood vessels to narrow, which increases blood pressure and can improve blood flow to vital organs.

List of abbreviations

BIS: bispectral index scale

BIS-NADIR: lowest observed BIS value

BIS-NADIRn: lowest observed BIS value to negative step disturbance

BIS-NADIRp: lowest observed BIS value to positive step disturbance

BMI: body mass index

BP: blood pressure

BP_d: diastolic blood pressure

BP_m: mean blood pressure

BP_s: systolic blood pressure

BS: burst suppression

BSR: burst suppression ratio

CO: cardiac output

CV: coefficient of variation

DoA: depth of anesthesia

DoH: depth of hypnosis

EEG: electroencephalogram

GA: genetic algorithms

GPC: generalized predictive control

GUI: graphical user interface

HR: heart rate

IAE: integrated absolute error

IAU: integrated absolute value of the control variable

IQR: interquartile range

LBM: lean body mass

MAP: mean arterial pressure

MDAPE: median absolute performance error

MDPE: median performance error

MIMO: multiple-input-multiple-output

MISO: multiple-input-single-output

MPC: model predictive control

NMB: neuromuscular blockade

NRS: numeric rating scale

PC: personal computer

PD: pharmacodynamic

PID: proportional-integral-derivative

PK: pharmacokynetic

PONV: post-operative nausea and vomiting

PSD: power spectral density

PSO: particle swarm optimization

QP: quadratic programming

RASS: Ramsay Agitation Sedation Score

SISO: single-input-single-output

SNP: sodium nitroprusside

SpO_2: peripheral oxygen saturation

SQI: signal quality index

SS: sedation score

ST10: settling time at 10%

ST20: settling time at 20%

TCI: target controlled infusion

TIVA: total intravenous anesthesia

TT: time-to-target

TTn: time-to-target to negative step disturbance

TTp: time-to-target to positive step disturbance

TV: total variation